Multidimensional characterization of potential plant beneficial bacteria for single strain and consortia application on crop plants

Theresa Kuhl-Nagel

Helmholtz Zentrum München,
Deutsches Forschungszentrum für Gesundheit und Umwelt (GmbH),
Institut für Netzwerkbiologie (INET)

Dissertation
an der Fakultät für Biologie der
Ludwig-Maximilian-Universität München
zur Erlangung des akademischen Grad eines
Doktor der Naturwissenschaften
(Dr. rer. nat.)

München, Januar 2022

Erstgutachter:	Prof. Dr. Pascal Falter-Braun
Zweitgutachterin:	Prof. Dr. Kirsten Jung
Dissertation eingereicht am:	13.01.2022
Tag der mündlichen Prüfung:	21.09.2022

Eidesstattliche Erklärung

Ich versichere hiermit an Eides statt, dass die vorgelegte Dissertation von mir selbstständig und ohne unerlaubte Hilfe angefertigt wurde. Des Weiteren erkläre ich, dass ich nicht anderweitig ohne Erfolg versucht habe, eine Dissertation einzureichen oder mich der Doktorprüfung zu unterziehen. Die folgende Dissertation liegt weder ganz, noch in wesentlichen Teilen einer anderen Prüfungskommission vor.

München, den 13.01.2022

Theresa Kuhl-Nagel

Summary

Pollution with mineral fertilizers and chemical pesticides due to anthropogenic activities as well as extreme weather situations caused by climate change put agroecosystems under pressure. Plants live in close association with a plethora of microorganisms, including plant growth-promoting bacteria (PGPB). The interactions of plants and beneficial microbes could be a solution for sustainable agriculture to overcome the previously described hazards. Prerequisites for successful application of PGPB are large culture collections of well characterized strains and a substantial knowledge about the functional plant microbiome. The aim of this thesis was to discover new PGPB from crop plants and to understand plant-microbe as well as microbe-microbe-interactions under different abiotic conditions. The underlying questions were, if the applied bacteria have a beneficial effect on the plant under different abiotic conditions, what their beneficial traits are, and if the microbiome is modulated by the applied bacteria.

In the first part of the thesis these questions were addressed by culture-dependent *in vitro* characterization of selected isolates of a culture collection established throughout this doctoral project. Based on the results microbial consortia were assembled and their effects were assessed after application to wheat plants. The microbial composition of inoculated and non-inoculated wheat plants was characterized under different abiotic conditions using next-generation-sequencing. Results revealed that the wheat microbiome is a rich source of potential PGPB. It was possible to assemble and apply a consortium, which increased root growth under non-drought conditions, whereas the effect was lost under drought stress. Application of the microbial consortia as well as drought stress caused a shift in the microbial composition of wheat. Further analysis of a smaller consortium revealed a conceivable key role of the interaction of five particular isolates for the beneficial effect on root growth.

The second part of the thesis was focused on *Rhodococcus qingshengii* RL1 isolated from rucola (*Eruca sativa* Mill.), as well as *Pseudomonas* sp. SCA7, isolated from wheat. The former represents a rather poorly characterized genus of plant-associated bacteria, while the latter represents a more frequently described genus in the rhizosphere. For both strains a genome-based characterization using whole genome sequencing was performed to elucidate their genomic potential and their roles in the plant microbiome. Both strains revealed a remarkable genomic potential, which could be shown to be translated into functional traits by *in vitro* and *in planta* experiments. SCA7 showed effective antagonistic activities against several plant-pathogens *in vitro* and partly *in planta* and

phylogenetic analysis indicated that the strain belongs to a new *Pseudomonas* species. RL1 was compared to two closely related *Rhodococcus* strains (djl6, BG43) and showed the overall best performance regarding potentially plant beneficial traits, although the strains had many traits in common. Moreover, the phylogenetic analysis revealed the indication for a reclassification of the *R. qingshengii* and *R. erythropolis* clade.

Overall, both approaches, i.e. large scale standardized screening of an unknown culture collection as well as targeted functional tests on promising isolates based on comprehensive genome analysis, were successful and could be used complementary to identify plant beneficial isolates plus characterize them in depth for a safe as well as plant and site specific application. Thus, this work can contribute to pursuing the vision of a targeted application of PGPB in sustainable agriculture as single strains or consortia specifically selected from a broad and well-characterized culture collection according to plant demands in a given habitat.

Zusammenfassung

Landwirtschaftliche Ökosysteme stehen unter starkem Druck durch anthropogene Einflüsse wie Verschmutzung mit mineralischen Düngemitteln und chemischen Pestiziden, ebenso wie durch extreme Wettersituationen verursacht durch den Klimawandel. Pflanzen leben in enger Verbindung mit einer Vielzahl von Mikroorganismen, unter ihnen auch pflanzenwachstumsfördernde Bakterien. Die Interaktion von Pflanzen und nützlichen Bakterien könnte eine mögliche Lösung in der nachhaltigen Landwirtschaft sein, um den oben beschriebenen Problemen zu begegnen. Voraussetzung für die erfolgreiche Anwendung von pflanzenwachstumsfördernden Bakterien sind große Sammlungen von gut charakterisierten Mikroorganismen und fundierte Kenntnisse über das funktionale Pflanzenmikrobiom. Das Ziel dieser Doktorarbeit war es neue pflanzenwachstumsfördernde Bakterien von Nutzpflanzen zu finden und Pflanzen-Mikroorganismen und Mikroorganismen-Mikroorganismen-Interaktionen unter unterschiedlichen abiotischen Bedingungen zu verstehen. Die zugrundeliegenden Fragen waren, ob die angewendeten Bakterien unter unterschiedlichen abiotischen Bedingungen einen positiven Effekt auf die Pflanze haben, was ihre nützlichen Wirkmechanismen sind und ob sich das Mikrobiom der Pflanze nach der Inokulation mit den Bakterien verändert.

Um diese Fragen zu beantworten wurde im ersten Teil der Arbeit eine kulturabhängige *in vitro* Charakterisierung ausgewählter Isolate aus einer Sammlung von Mikroorganismen durchgeführt, welche während dieser Doktorarbeit etabliert wurde. Basierend auf diesen Ergebnissen wurden bakterielle Konsortien zusammengestellt und nach der Inokulation wurde ihr Effekt auf Weizenpflanzen untersucht. Die mikrobielle Zusammensetzung der inokulierten und nicht-inokulierten Weizenpflanzen wurde unter verschiedenen abiotischen Bedingungen mit Hilfe der Next-Generation-Sequencing Technologie untersucht. Die Ergebnisse zeigten, dass das Weizenmikrobiom eine reiche Quelle für potentiell pflanzenwachstumsfördernde Bakterien ist. Eines der zusammengestellten und applizierten Konsortien hatte einen positiven Effekt auf das Wurzelwachstum unter nicht trockengestressten Bedingungen, der unter Trockenstress jedoch nicht mehr nachweisbar war. Sowohl die Inokulation der Pflanze mit den bakteriellen Konsortien, als auch die Anwendung von Trockenstress hatten eine Veränderung der mikrobiellen Zusammensetzung in Weizen zur Folge. Weiterführende Untersuchungen mit einem kleineren Konsortium zeigte, dass die Interaktion von fünf Isolaten möglicherweise eine Schlüsselrolle beim beobachteten positiven Effekt auf das Wurzelwachstum spielt.

Der zweite Teil der Arbeit richtete sich auf die Untersuchung von *Rhodococcus qingshengii* RL1, ein Isolat von Rucola (*Eruca sativa* Mill.), welches eine weniger bekannte Gattung von pflanzenassoziierten Bakterien repräsentiert, und auf *Pseudomonas* sp. SCA7, ein Isolat von Weizen und Vertreter der häufig in der Rhizophäre zu findenden Gattung *Pseudomonas.* Von beiden Stämmen wurde das gesamte Genom sequenziert und charakterisiert, um ihr genetisches Potential und ihre mögliche Rolle im Pflanzenmikrobiom zu beleuchten. Beide Stämme zeigten ein beeindruckendes genetisches Potential, das auch in funktionelle Eigenschaften übertragen wurde, was mit *in vitro* und *in planta* Experimenten nachgewiesen werden konnte. SCA7 zeigte effektive biologische Kontrolle von verschiedenen Pflanzenpathogenen *in vitro* und teilweise *in planta*. Darüber hinaus, impliziert die phylogenetische Analyse, dass der Stamm zu einer neuen *Pseudomonas* Spezies gehört. RL1 wurde mit zwei nah verwandten *Rhodococcus*-Stämmen (djl6, BG43) verglichen und zeigte insgesamt die besten Ergebnisse hinsichtlich potentiell förderlicher Eigenschaften für Pflanzen, obwohl die Stämme auch viele Eigenschaften gemeinsam hatten. Außerdem deutet die phylogenetische Analyse darauf hin, dass die *R. qingshengii* und *R. erythropolis* Gruppe neu klassifiziert werden sollte.

Beide Ansätze, das heißt die breite, standardisierte Selektion aus einer unbekannten Sammlung von Mikroorganismen und die gezielte funktionale Testung vielversprechender Kandidaten basierend auf einer vergleichenden Genomanalyse, waren erfolgreich und ergänzen sich um nützliche Bakterien für Pflanzen zu identifizieren sowie diese für eine sichere, pflanzen- und ortsspezifische Anwendung tiefergehend zu charakterisieren. Somit kann diese Arbeit dazu beitragen, die Vision einer gezielten Anwendung von PGPB in der nachhaltigen Landwirtschaft in Form von einzelnen Stämmen oder Konsortien zu verfolgen, die speziell nach den pflanzlichen Anforderungen in einem bestimmten Lebensraum ausgewählt werden können.

List of Publications

Kuhl T, Rothballer M, Falter-Braun P (in preparation). Assembly and application of a plant growth-promoting consortium on wheat under different abiotic conditions.

Kuhl T, Rodriguez PA, Gantner I, Chowdhury SP, Rosenkranz M, Weber B, Kublik S, Rothballer M, Falter-Braun P (in preparation). Novel *Pseudomonas* species displays plant growth promotion effect in two plant families and induces systemic resistance in Arabidopsis

Kuhl T, Chowdhury SP, Uhl J, Rothballer M (2021). Genome-based characterization of plant-associated *Rhodococcus qingshengii* RL1 reveals stress tolerance and plant-microbe interaction traits. *Frontiers in Microbiology* 12:708605. doi: 10.3389/fmicb.2021.708605

Kuhl T, Felder M, Nussbaumer T, Fischer D, Kublik S, Paul Chowdhury S, Schloter M, Rothballer M. (2019). *De novo* genome assembly of a plant-associated *Rhodococcus qingshengii* strain (RL1) isolated from *Eruca sativa* Mill. and showing plant growth-promoting properties. *Microbiol Resour Announc* 8:e01106-19. https://doi.org/10.1128/MRA.01106-19

List of Posters and oral Presentations

11/2020	Poster presentation at ISME "Unity in Diversity" Online-Conference 2020 Title: Screening of wheat microbiome for beneficial drought stress tolerant bacterial consortium
03/ 2019	Oral presentation at 22. Jahrestagung des AK Biologischer Pflanzenschutz 2019 der Deutschen Phytomedizinischen Gesellschaft (DPG) Title: Characterization of new PGPRs isolated from wheat (*Triticum aestivum*) cultivar "Sonett"
03/2019	Poster presentation at Jahrestagung der Vereinigung für Allgemeine und Angewandte Mikrobiologie (VAAM) 2019 Title: Characterization of *Rhodococcus qingshengii* (RL1) in terms of plant growth promotion and healthy human nutrition

Contents

List of Figures

List of Tables

Abbreviations

AAI	Average aminoacid identity
ACC	1-aminocyclopropane-1-carboxylate
AHL	N-Acyl-Homoserine lactone
AI	Artificial intelligence
ANI	Average nucleotide identity
BG43	*Rhodococcus erythropolis* BG43
CFU	Colony forming unit
djl6	*Rhodococcus qingshengii* djl6
dNTP	Desoxy-nucleoside-tri-phosphate
FISH	Fluorescence *in situ* hybridization
FZB42	*Bacillus velezensis* FZB42
GA4	Gibberellin A4
GA9	Gibberellin A9
GSF30	*Herbaspirillum frisingense* GSF30
GSL	Glucosinolate
IAA	Indole-3-acetic acid
ISR	Induced systemic resistance
K1	Consortium K1
K2	Consortium K2
K3	Consortium K3
K4	Consortium K4
MDS	Multidimensional scaling

NaCl	Sodiumchloride
NB17_5	*Rhodococcus* sp. NB17_5
OD	Optical density
OTU	Operational taxonomic unit
PGP	Plant growth-promoting
PGPB	Plant growth-promoting bacteria
PGPR	Plant growth-promoting rhizobacteria
PGPM	Plant growth-promoting microbes
pH	*pondus hydrogenii* = potential of hydrogen
RFLP	Restriction fragment length polymorphisms
RL1	*Rhodococcus qingshengii* RL1
SCA27_61	*Variovorax* sp. SCA27_61
SCA7	*Pseudomonas* sp. SCA7
SynCom	Synthetic community
VOC	Volatile organic compound

1 Introduction

In recent years, the burden of intensively used mineral fertilizers and chemical pesticides coupled with climate change led to massive soil degradation with dangerous consequences on agriculture (chapter 1.1) (Smith *et al.,* 2016; Reid *et al*., 2021). Plants live in close association with microorganisms (Philippot *et al*., 2013; Vandenkoornhuyse *et al*., 2015), which could provide sustainable solutions via the functional plant microbiome including beneficial bacteria (chapter 1.2). Plant beneficial bacteria evolved traits to survive in the plant habitat, which can also have beneficial effects on plants (Berg, 2009; Compant *et al*., 2019) (chapter 1.3). Therefore, many concepts emerged in recent years on how to include beneficial microbes and the microbial community in sustainable agriculture, ranging from tillage practices to artificial intelligence for development of tailored microbial consortia (Schlaeppi and Bulgarelli, 2015; Bender *et al*., 2016; French *et al*., 2021) (chapter 1.4). For application of tailored microbial consortia large culture collections and good characterized microbes are required (Saad *et al*., 2020). Their application as microbial inoculants in form of single strains or consortia comes with advances and challenges (Berg *et al*., 2021) (chapter 1.5). In this study bacteria were isolated from the important crop plants wheat and rucola (chapter 1.6) to find new plant beneficial bacteria for application using microbiota- as well as genome-based approaches and representatives of the genera *Pseudomonas* and *Rhodococcus* were studied in depth (chapter 1.7).

1.1 Agroecosystems under pressure

Over the past decades, anthropogenic activities, such as intensive use of chemical pesticides and mineral fertilizer, as well as improper soil exploitation coupled with climate change have resulted in immense global soil degradation (Tilman *et al.*, 2002; Bender *et al*., 2016; Smith *et al*., 2016; Reid *et al*., 2021). At the same time human population is rising while arable land is declining (Foley *et al*., 2005). Moreover, agroecosystems are under emerging pressure due to increasing extreme weather situations, such as drought, heat waves and heavy storms with flooding, caused by global climate change. The overall situation has caused loss of soil biodiversity and has created harsh biotic and abiotic conditions for plants and their associated microbes (Tsiafouli *et al*., 2015; Bender *et al*., 2016; Banerjee *et al*., 2019; Hutchins *et al*., 2019). Plants exposed to abiotic stresses are more susceptible to pests and pathogens, while increasing temperatures and elevated global traffic allow pathogens to migrate beyond their original habitat and infect new host plants (Bebber *et al*.,

2014a). Pathogens evolve quickly and can overcome plant defense systems and known biocontrol agents (Bebber *et al*., 2014b). Thus, up to one third of the global harvest is lost due to plant diseases (average of 4 years 2010-2014) (Savary *et al*., 2019). Moreover, the plant microbiome influences food quality (Verginer *et al*., 2010; Thomas *et al*., 2011; Hirt, 2020) and the microbiota of plants and humans share many compositional similarities (Mendes and Raaijmakers, 2015). This led to the hypothesis that the plant microbiome can also impact human health via consumption of e.g. raw fruits and vegetables (Berg and Martinez, 2015; Blum *et al*., 2019). Additionally, pollution with mineral fertilizer and chemical pesticides is a threat for human health. The use of sustainable alternatives could improve food quality by reducing chemical residues remaining on the food and decreasing presence of (opportunistic) human pathogens (Van Overbeek *et al*., 2014; Singh *et al*., 2018; Hirt, 2020). Taken together, the situation generates a need for alternative applications for plant growth promotion and biocontrol in order to protect plants and their associated microbiome against the above mentioned hazards. This will not only lead to better yields and higher biodiversity, but also to healthier products for the consumer.

1.2 Current knowledge on the functional plant microbiome

To improve the situation of agroecosystems in a sustainable way, knowledge about the functional plant microbiome is essential. Plants are associated with a plethora of microorganisms living epi- or endophytically in the belowground or above ground parts of the plant, which fulfill specific functions (Vorholt, 2012; Philippot *et al*., 2013; Rheinhold-Hurek *et al*., 2015; Vandenkoornhuyse *et al*., 2015). The microbial assemblages including bacteria, fungi and archaea associated with the plant are termed plant microbiota (comprising all microorganisms) (Schlaeppi and Bulgarelli, 2015; Compant *et al*., 2019). Together with their accompanying functions this characteristic microbial community, which occupies a reasonable well-defined habitat with distinct physio-chemical properties, forms the plant microbiome (Vandenkoornhuyse *et al*., 2015; Compant *et al*., 2019; Berg *et al*., 2020). Plants and their associated microbes build a functional entity, also called meta-organism or holobiont (Vandenkoornhuyse *et al*., 2015; Simon *et al*., 2019; Berg *et al*., 2021). However, the term “holobiont” is under discussion because important principles of co-evolution, co-selection and stress response were not covered by the original definition (Berg *et al*., 2020). Therefore, in this thesis the term “(plant) meta-organism” will be used to refer to plants and their associated microbes.

The plant microbiota colonizes defined habitats, such as the rhizosphere, phyllosphere or endosphere (inner parts of the plants), and can be actively recruited by the plant from the surrounding environment, like soil, airborne dust or irrigation water (Vorholt, 2012; Compant *et al*., 2019; Berg *et al*., 2021). The phyllosphere comprises the aerial plant habitat *sensu lato* or the leaf surface in relation to the external environment (Vorholt, 2012; Compant *et al*., 2019). The term rhizosphere was coined by Lorenz Hiltner in 1904, who discovered the importance of plant-microbe interactions. The rhizosphere is described as the area around roots influenced by root exudates and inhabited by a specific microbial community (Hiltner, 1904; Hartmann *et al*., 2008). Since then the term was elaborated into three areas endorhizosphere, rhizoplane (root surface) and ectorhizosphere, which have gradually changing physicochemical properties (McNear, 2013; Vandenkoornhuyse *et al*., 2015; Compant *et al*., 2019). Plants influence the rhizosphere mainly via their root system providing unique ecological niches for soil microbiota. For example, rhizodeposits enrich the rhizosphere with root exudates, mucilage and dead cells containing nutrients such as carbon, which are used as energy sources by microorganisms (Philippot *et al*., 2013; Pascale *et al*., 2020). This leads to specific community compositions with lower diversity in the rhizosphere compared to bulk soil (Duran e*t al*., 2018; Compant *et al*., 2019). Moreover, plants influence the rhizosphere by changing soil pH, oxygen level and release of antimicrobial compounds (Philippot *et al*., 2013).

Interestingly, to date there is no clear answer or definition of "the" functional or healthy plant microbiome (Berg *et al*., 2021). Microbial composition and community structures of the plant microbiota under different conditions are intensely investigated with advanced sequencing technologies and multi-omics approaches (Berg *et al*., 2020). This showed that a high diversity and high evenness play a role in a functional plant microbiome when comparing between rhizosphere samples (Hu *et al*., 2016; Berg *et al*., 2021; French *et al*., 2021). In relation to bulk soil these parameters are lower in the rhizosphere, because only distinct microbes are recruited (Berg *et al*., 2021), but bacterial numbers are equally high or higher in the rhizosphere (10^6-10^{10}) (Hirt, 2020). The rhizosphere is dominated by Firmicutes, Bacteroidetes, Proteobacteria and Actinobacteria (Mendes and Raaijmakers, 2015). Moreover, the plant microbiome is influenced by many factors, such as plant developmental stage, plant genetic background, soil properties, diverse agricultural management practices and abiotic or biotic stress conditions (Lebeis *et al*., 2015; Castrillo *et al*., 2017; Compant *et al*., 2019; Chowdhury *et al*., 2019; Kavamura *et al*., 2020). Microbial community

shifts upon a large disease outbreak can lead to the enrichment of plant-protective taxa in the soil, which results in disease-suppressive soils (Berendsen *et al*., 2018; Bakker *et al*., 2020) protecting upcoming generations of plants from the disease. This concept is called the soil-borne legacy (Berendsen *et al*., 2018; Bakker *et al*., 2020). Interestingly, the soil-borne legacy has been observed to be active also against phyllosphere pathogens (Panke-Buisse *et al*., 2015; Berendsen *et al*., 2018). This indicates that signaling between the root microbiome and the root is transduced to the upper plant parts via, e.g. induced systemic resistance (ISR) (see chapter 1.3.5) (Kloepper and Beauchamp 1992, Pieterse *et al*., 2014). Microbial community shifts into unfavorable compositions, such as an increase in Proteobacteria or fungi, can cause an imbalance of the microbial taxa, a so-called dysbiosis (Duran *et al*., 2018; Chen *et al*., 2020), which reduces plant health and leads to disease symptoms without a causal agent (Hamonts *et al*., 2018; Chen *et al*., 2020). Interestingly, this shift in microbial composition towards Proteobacteria is also associated with human diseases (Hall *et al*., 2017). On the other hand, in plants a functional microbial community can prevent fungal growth, so called fungistasis, and prevent detrimental effects (Duran *et al*., 2018; Durán *et al*., 2018; Bakker *et al*., 2020). Thus, the appropriate balance of microbial taxa is very important for a healthy microbiome. Overall, the plant microbiome includes pathogenic as well as beneficial bacteria which are both important to study. In terms of alternative solutions for sustainable agriculture the traits of plant beneficial bacteria are of special interest.

1.3 Traits of Plant Growth Promoting Bacteria (PGPB)

A diverse plant microbiome harbors many different bacterial strains including beneficial bacteria, also called plant growth promoting (rhizo-) bacteria (PGPR or PGPB), with various functional traits (Compant *et al*., 2019). PGPR or PGPB have been classically defined as "free-living plant beneficial bacteria which promote plant health" (Kloepper and Schroth, 1978). Well-characterized PGPB belong for example to the bacterial genera *Arthrobacter, Bacillus, Pseudomonas, Rhizobium*, and *Streptomyces* (Berg, 2009; Pieterse *et al*., 2020; Jaiswal *et al*., 2021; Mohanty *et al*., 2021). The term was extended to plant-growth promoting microbes (PGPM) to also include non-rhizobacterial and fungal plant growth promoters like *Ampelomyces, Coniothyrium,* and *Trichoderma* (Berg, 2009; Schlaeppi and Bulgarelli, 2015; Mohanty *et al*., 2021). Plant beneficial bacteria need to survive difficult environmental conditions to maintain a functional plant meta-organism. Therefore, several traits and mechanisms evolved in bacteria to survive in the plant habitat, whereas their beneficial effect for plants is a secondary effect (Glick, 2012). The beneficial

traits often result in enhanced plant growth based on production of plant hormones, providing nutrients to the plants by solubilizing unavailable soil phosphate, iron acquisition, siderophore production, nitrogen fixation (Glick, 2012) and support the plant e.g. in ion homeostasis (Salas-González *et al*., 2021) (**Figure 1**). Common beneficial traits are presented in the following chapters.

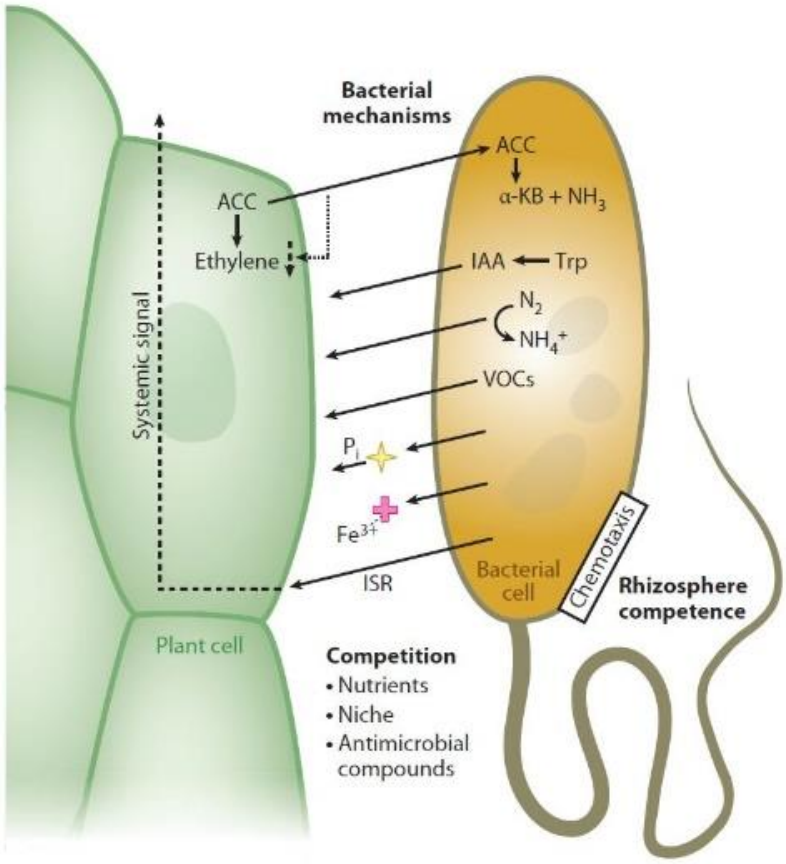

Figure 1: Bacterial plant beneficial traits. Schematic overview of underlying biochemical mechanisms adapted from Bulgarelli *et al.* (2013).

1.3.1 Plant hormone production

Plant-associated bacteria in general can influence root growth, germination, flowering (Panke-Buisse *et al*., 2017) and developmental stages via balancing or producing plant hormones, such as ethylene (chapter 1.3.6), gibberellin (Glick 2014; Kang *et al*., 2014; Salazar-Cerezo *et al*., 2018) or auxins like indole-3-acetic acid (IAA) (Finkel *et al*., 2020). Thus, some plant beneficial bacteria, such as *Azosprillum* spp. or *Bacillus* spp., are able to enhance plant growth and yield by production of gibberellin, which is involved in plant growth and development (Bottini *et al*., 2004; Nagel *et al*., 2018). The role of gibberellin in bacteria is unknown, but the gibberellin produced by bacteria is involved in signaling between plants and microbes (Bottini *et al*., 2004). Some plant-pathogenic

bacteria produce bioactive gibberellin 4 (GA4), which counteracts the jasmonic-acid mediated defense response, thus enabling them to access plants via wounds. Additionally, GA4 has detrimental effects on seedling development. In contrast, beneficial bacteria produce only the precursor of functional gibberellin (= gibberellin 9 (GA9)), which reflects the differential interaction of pathogenic and beneficial bacteria with plants (Nagel and Peters, 2017). Another important plant hormone is IAA, which is one of the best characterized auxins involved in root growth and development (Zhao, 2010). The production of IAA by bacteria, such as the plant beneficial *Azospirillum brasilense* (Hartmann *et al*., 1983) and *Herbaspirillum frisingense* GSF30 (Rothballer *et al*., 2008), can modulate endogenous hormone levels in the plants (Spaepen and Vanderleyden, 2011). This leads to altered root architecture with increased root surface allowing more access to nutrients and water for the plant (Glick, 2012). However, as an excess of IAA can also be detrimental for root and plant development, its production needs to be carefully controlled. Therefore, for example, members of the genus *Variovorax* play a major role balancing auxin production and shaping the microbiome, which influences root growth in *Arabidopsis thaliana* (Finkel *et al*., 2020). Moreover, IAA produced by bacteria loosens plant cell walls, which enhances the release of root exudates providing more nutrients to the bacteria or facilitates endophytic colonization (Glick, 2012). Additionally, IAA can act as a signaling molecule in microorganism (Spaepen and Vanderleyden, 2011).

1.3.2 Biological nitrogen fixation

Biological nitrogen fixation describes the process of reducing atmospheric dinitrogen (N_2) to ammonia (NH_3) and was first described in root-nodule forming rhizobia-legume symbiosis (Hiltner, 1904; Hartmann *et al*., 2008). The process has been demonstrated also for free-living bacteria, such as *Azospirillum* spp. (Hartmann and Hurek, 1988; Döbereiner, 1995; Higdon *et al*., 2020). Bacteria reduce N_2 to NH_3 by the nitrogenase portein complex formed e.g. by canonical or alternative *nif* gene products in various configurations (Higdon *et al*., 2020). Nitrogen fixation can be beneficial for bacteria to survive under nitrogen limited conditions, whereas plants profit from the provided accessible nitrogen in form of ammonia.

1.3.3 Phosphate solubilization

Phosphorus is rather high abundant in the soil. However, most of the phosphorus is present in insoluble forms (Glick, 2012). This is also true for mineral fertilizer containing inorganic phosphorus, which becomes unavailable for the plant soon after application. Phosphate solubilizing

bacteria transform the insoluble phosphate to an accessible form by producing low molecular weight organic acids e.g. gluconic acid (Rodriguez *et al*., 2004; Glick, 2012) and non-specific acid phosphatases (Rodríguez *et al*., 2006). For example, *Azospirillum brasilense* was shown to produce gluconic acid involved in phosphate solubilization (Rodriguez *et al*., 2004). Plants profit strongly from the accessible phosphorus, which makes phosphate-solubilizing bacteria interesting as biofertilizers.

1.3.4 Siderophore production

Insoluble ferric iron (Fe(III)) is common in terrestrial habitats, but unaccessible for microorganisms or plants. Siderophores are secondary metabolites, which are able to chelate insoluble Fe(III) and provide accessible iron for microbial or plant cells (Ahmed and Holmström, 2014). Moreover, siderophores function as biosensors and are involved in bioremediation, plant growth promotion, microbial competition and defense against other microbes e.g. the bacterial plant pathogen *Ralstonia solanacearum* (Ahmed and Holmström, 2014; Gu *et al*., 2020; Pollak and Cordero, 2020). Siderophores produced by *Streptomyces* spp. have been reported to enhance plant growth in rice (Rungin *et al*., 2012) and *Pseudomonas simiae* WCS417 produces the fluorescent siderophore pyoverdine, which enhances plant growth in *Arabidopsis* and is effective against fungal pathogens (Pieterse *et al*., 2020).

1.3.5 Microbe-microbe-interactions and biotic stress protection

The above described beneficial bacterial traits not only provide nutrients or support plant growth, but also allow bacteria to compete with other microbes in the rhizosphere for space and energy sources (Bulgarelli *et al*., 2013). The competition between microbes provides also a beneficial effect for the plant especially when it comes to biotic stress conditions, such as pathogen attack. Here, antagonistic activities (= the inhibition of one microbe by another microbe) of beneficial bacteria against pathogens can protect plants from disease outbreaks and can be exploited for biological control (Johnsson *et al*., 1998; Berg, 2009). Under biotic stress conditions like pathogen attack beneficial bacteria can enhance plant health e.g. by producing active biomolecules like antibiotics (Chowdhury *et al*., 2015a) or volatiles (Netzker *et al*., 2020) against pathogenic bacteria and fungi. In this case the plant microbiome could be seen as part of the first line of defense against pathogens (Mendes *et al*., 2018; Bakker *et al*., 2020). For example, *Bacillus velezensis* FZB42 produces cyclic lipopeptides, such as surfactin, fengycin and bacillomycin D that are active against the pathogen *Rhizoctonia solani*, which is the causative agent of bottom rot in lettuce (Chowdhury

et al., 2015b). Moreover, beneficial bacteria can act antagonistically by competition with other microbes, e.g. for iron by siderophore production (Gu *et al*., 2020, chapter 1.3.4) or by disrupting quorum sensing signals of pathogenic bacteria (Dong *et al*., 2001). Quorum sensing (QS), defining a "minimum behavioral unit as a quorum of bacteria" (Fuqua *et al*., 1994), is often described as bacterial communication to coordinate concerted processes, such as biofilm formation or virulence (Fuqua *et al*., 1994). Quorum sensing molecules and volatiles are also important for crosstalk between microbes and plants (Berg *et al*., 2021). The degradation or interference with quorum sensing molecules can disturb bacterial communication and is called quorum quenching (Dong *et al*., 2001), which was shown for several bacteria. For example, *Pseudomonas segetis* (Rodríguez *et al*., 2020) and *Rhodococcus erythropolis* (Barbey *et al*., 2013) interfere with quorum sensing of the plant pathogen *Pectobacterium atrosepticum*, whereas *Bacillus thuringiensis* reduces virulence of the plant-pathogen *Erwinia carotovora* (now *Pectobacterium carotovora*) via quorum quenching (Dong *et al*., 2004). Many beneficial bacteria can also act indirectly by buffering negative effects of pathogens (Hartman *et al*., 2017) or boosting the plant's defense system, a process also known as ISR (Kloepper and Beauchamp, 1992; Pieterse *et al*., 2014). Bacterial induced ISR puts the plant's immune system in an alerted state to respond quicker and more effectively against pathogen attacks (Van Peer *et al*., 1991; Kloepper and Beauchamp, 1992; Pieterse *et al*., 2014). For example, root-associated *Pseudomonas simiae* WCS417 induced systemic resistance in *Arabidopsis thaliana* against the leaf-infecting plant-pathogenic *Pseudomonas syringae* pv. *tomato* DC3000 (Pieterse *et al*., 1996). Thereby, it triggers the onset of defensive pathways independent from salicylic acid (SA) and accumulation of PR proteins (Pieterse *et al*., 2000; Pieterse *et al*., 2020), which is different from mostly SA-dependent systemic acquired resistance (SAR) (Pieterse *et al*., 2020). ISR depends on the plant hormones jasmonic acid and ethylene (Pieterse *et al*., 2000). The capability to induce systemic resistance was also shown for other beneficial bacteria, such as *Bacillus velezensis* FZB42 (Chowdhury *et al*., 2015a). Taken together, beneficial bacteria show a number of direct as well as indirect mechanisms to protect plants under biotic stresses and their beneficial traits can also become relevant in abiotic stress protection.

1.3.6 Abiotic stress protection

Apart from plant protection against pathogens, the beneficial associations of microbes and plants are of special importance when plants experience abiotic stress (Fahad et al., 2015). Beneficial

bacteria have been shown to support plants also as stress protecting agents under abiotic conditions like salt and drought stress (Berg *et al*., 2013; Kaushal and Wani, 2016; Ahkami *et al*., 2017; Egamberdieva *et al*., 2019), such as the salt tolerant *Azospirillum brasilense* NH, which enhances plant growth in durum wheat (*Triticum durum* var. waha) under saline soil conditions (Nabti *et al*., 2010) or *Bacillus spizizenii* FMH45, which improved salt tolerance and plant growth in tomato plants (Masmoudi *et al*., 2021).

Abiotic stress protecting traits of bacteria become relevant e.g. during high exposure of plants to ethylene. The stress-related plant hormone ethylene can have detrimental effects for the plant in high amounts or during long-term exposure (Glick, 2014; Dubois *et al*., 2018; Tiwari *et al*., 2018). Plant-associated bacteria have developed mechanisms to degrade ethylene or the precursor 1-amino-cyclopropane-1-carboxylate (ACC) by the bacterial enzyme ACC deaminase (*acdS*) (Glick, 2014). Although some pathogenic bacteria use these mechanisms to interfere with the plant defense system (Nascimento *et al*., 2020) it is widely known as an important plant-beneficial trait, e.g. *Variovorax paradoxus* 5C-2 promotes plant growth in *Arabidopsis thaliana* via an ethylene-dependent pathway (Chen *et al*., 2013). This beneficial trait becomes even more relevant in supporting plants under drought or salt stress, as shown for *Achromobacter piechaudii* in drought stressed tomato plants (Mayak *et al*., 2004). Additionally, bacteria can use ACC as a nitrogen (Glick *et al*., 1995; Glick, 2014) or carbon source (Belimov *et al*., 2005). Another adaption and survival strategy to abiotic stress conditions involves so-called osmolytes, which are small, low molecular weight molecules, such as amino acids (proline), amines (glycine, betaine, ectoine) or sugars (trehalose). These molecules accumulate in bacteria supporting the adaption to high salt concentrations and are associated with osmoregulation in bacteria (Bremer and Krämer, 2019). Moreover, the same molecules can be exchanged between microbes and higher organisms, such as plants, and protect plants under osmotic stress (Nabti *et al*., 2014). Osmolytes accumulate in cells under osmotic pressure, protect cellular protein structures and balance the osmotic difference between the cytosol and the environment of the cell (Hartmann *et al*., 2021). PGPB can also support plant growth in contaminated soils by showing pollutant-degrading or bioremediation potential for phytoextraction of heavy-metals from polluted soils (Sessitsch *et al*., 2013; Ma *et al*., 2016b, 2016a; Ahkami *et al*., 2017; Ma, 2019). For example, *Rhodococcus erythropolis* CD 106 improved the degradation of hydrocarbons and plant growth of *Lolium perenne* on a hydrocarbon-polluted soil (Płociniczak *et al*., 2017).

Overall plant-associated bacteria show various traits beneficial for plant growth and health under different conditions, which are interesting for their use in sustainable agriculture and gave raise to several concepts on application presented in the next chapter.

1.4 Microbe-including concepts for sustainable agriculture

The goal of the concepts presented in this chapter is to omit mineral fertilizer and chemical pesticides or to reduce them to a minimal necessary amount in order to get healthier plants and higher yields in a sustainable way. The plant beneficial traits of plant-associated bacteria and the functions of the microbiome described above highlight the PGPB and the microbiome as attractive tools for sustainable agriculture. One of the first biostimulation product based on *Rhizobium* cultures was already developed 1896 by Lorenz Hiltner and colleagues to support leguminous plants in fixing atmospheric nitrogen (Hartmann *et al*., 2008). Since then, the multifaceted interactions of plants and several plant-associated bacteria have been widely studied to understand the underlying molecular mechanisms and to exploit plant beneficial traits for sustainable agriculture (Berg *et al*., 2017; Rodriguez *et al*., 2019; Babin *et al*., 2021; Windisch *et al*., 2021).

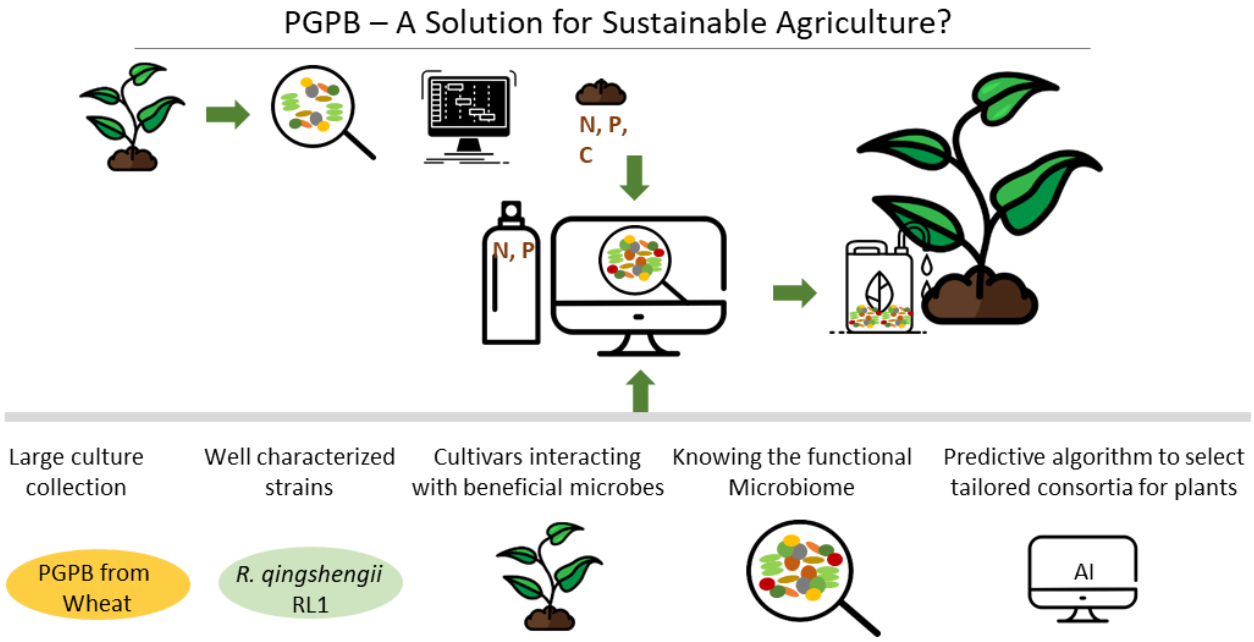

Figure 2: Vision to use PGPB in sustainable agriculture. The illustrated combination of physico-chemical parameter analysis of soil and microbiome analysis could be used to develop tailored consortia for plant beneficial effects. Pre-requisites are large culture collections, well-characterized strains, interacting plant cultivars, knowledge about the functional plant microbiome and a predictive algorithm.

Revolutionizing agriculture with the use of microbes and microbial communities was envisioned by several authors (Schlaeppi and Bulgarelli, 2015; Bender *et al*., 2016; Toju *et al*., 2018; Saad *et al*., 2020; French *et al*., 2021) (**Figure 2**). In this context, the relevance of soil and soil management to manipulate microbial composition and the interaction between soil organisms important for soil functions was emphasized (Bender *et al*., 2016; de Vries and Wallenstein, 2017). For ecological intensification of agriculture, the focus should be on a biological soil engineering approach to stabilize and improve ecosystem functioning (Bender *et al*., 2016). Several practices for changing the soil microbiome in a beneficial way, also termed microbiome engineering, include soil management e.g. reduced tillage, rhizosphere microbiome management by choosing an appropriate plant community and cultivars, as well as the stimulation of soil life e.g. by the application of beneficial soil organisms (including macrofauna) as biocontrol and biofertilizer (Kaul *et al*., 2021). The application of additional components, such as composted cow manure, guano, hair-, and feather-meals (Bradáčová *et al*., 2019), can also improve the microbial community and soil quality.

Inspired by the concept of personalized medicine, where genetic, epigenomic and clinical information about a patient and his disease are taken into account to tailor medication and therapy (Mathur and Sutton, 2017), the concepts on next-generation agriculture or precision microbiome management were developed with customized practices and tools for the individual soil, such as tailored microbial consortia (Schlaeppi and Bulgarelli 2015, French *et al*., 2021). The authors suggest to use microbiome analysis for targeted application of tailored microbial inoculants similar to the application of fertilizer depending on soil nutritional status, which is already common practice today (Schlaeppi and Bulgarelli, 2015). The concept includes plant host, management and microbial biotechnology (French *et al*., 2021). The idea to use microbiome-assisted agricultural practices and PGPM in sustainable agriculture including analysis of the microbiota composition and customize practices was proposed and extended by several authors (Finkel *et al*., 2017; Bakker *et al*., 2020; Saad *et al*., 2020). Design and application of tailored microbial inoculants could follow a detailed framework including thorough analysis of the target field environment and crop of interest, selection of strains from established culture collections based on their individual traits, large-scale production, formulation including compatibility and survival tests, application to the field and evaluation of performance (Saad *et al*., 2020). Therefore, increased scientific research on plant microbiomes coupled with lab-based-experiments and establishment of more systematic culture collections with well characterized strains are required.

The previously described concepts were elaborated for the use of crop core microbiomes, smart farming and artificial intelligence (AI) to improve sustainable agriculture (Toju *et al*., 2018; Kavamura *et al*., 2021). Smart farming describes the application of information and communication technology (ICT) in agriculture to use arable land more efficiently. This benefits the environment as well as species diversity and optimizes complex farming systems (Walter *et al*., 2017). In precision farming autonomous robots can be used for precise application of fertilizers and pesticides. Digital farming generates data to track parameters, such as plant nutritional status, disease symptoms or physico-chemical soil quality using unmanned aerial vehicles (UAVs) (Sugiura *et al*., 2016; Araus and Cairns, 2014). The use of multi-omics diagnostic platforms, inspired by "high-definition medicine" (Torkamani *et al*., 2017), could help to track microbiome changes and community stability to optimize the best time point for application of microbial inoculants (Toju *et al*., 2018). For the assembly of tailored core microbiomes machine learning and AI could help to determine the combination of microbes for the plant (de Souza *et al*., 2020). Standardized methods are required, which facilitate e.g. growth of unculturable organisms using e.g. microbial cell sorting (Song *et al*., 2016) or microfluidic chips, which control density, shape and size of microbial communities (Aleklett *et al*., 2018). Subsequent application to the plant was proposed via soil transplant or automated systems for inoculation e.g. Root Chips (Grossmann *et al*., 2011; Toju *et al*., 2018; French *et al*., 2021).

Alternative ideas to manipulate the plant microbiome include for example the use of root exudate metabolites considering that plants can domesticate microbes for their own advantage (Stringlis *et al*., 2018; Pascale *et al*., 2020). Application of pure compounds instead of compound-producing microbes turned out to be less successful than application of bacteria (Ismail *et al*., 2021). Another option includes the use of genetically modified rhizo-competent strains for PGP traits (Haskett *et al*., 2021). However, this could lead to lower acceptance, limited permission for some countries and bears substantial risks (French *et al*., 2021). In order to find sustainable solutions for agriculture using microbes and microbial communities the knowledge in basic research on harnessing plant microbiomes in sustainable agriculture needs to be expanded (Busby *et al*., 2017). Suggested priorities include the development of model host–microbiome systems for plants, definition of core microbiomes and metagenomes in these model systems, elucidation of rules for synthetic, functionally programmable microbiome assembly, determination of functional mechanisms of

plant-microbiome interactions, and characterization of the interactions of plant genotype, environment, microbiome and soil management (Busby *et al*., 2017).

To achieve the goal of reduced use of chemicals in agriculture and to transfer the knowledge from basic research to application, we need well characterized plant beneficial microbes, large culture collections with microbes to choose from (Saad *et al*., 2020), knowledge about the functional microbiome to improve natural soils accordingly, competent plant cultivars to interact with the beneficial microbes (Compant *et al*., 2019; Rodriguez *et al*., 2019), stable formulations for application of the microbial inoculants (Compant *et al*., 2019; Rodriguez *et al*., 2019) and a computational predictive algorithm based on machine learning (de Souza *et al*., 2020) to select the appropriate microbes.

1.5 Microbial inoculants – challenges and advances

Microbial inoculants are used to supplement the microbiome (Berg *et al*., 2021) with short and long-term effects to improve plant growth and health. Enhanced plant growth of roots and shoots, increased productivity with higher yields in crop plants and/or improved plant health upon application of PGPM are considered as plant beneficial effect (Spaepen *et al*., 2007; Berg, 2009; Berg *et al*., 2021). Modes of action include e.g. (i) hormone balancing (Finkel *et al*., 2020), (ii) provision of nutrients and minerals (Rodriguez *et al*., 2004), (iii) protection against pathogens by competition, production of antimicrobial compounds or induction of systemic resistance (Pieterse *et al*., 2014) and (iv) modulation of the microbiome including temporary microbiome shifts with stabilization or increase of microbial diversity and evenness, compensation of dysbiosis or pathogen-induced modulations as well as targeted shifts toward potential beneficial phyla (Berg *et al*., 2021). A successful microbial inoculant needs to colonize the plant, establish the desired interaction and persist in the environment together with the indigenous microorganisms (Romano *et al*., 2020; French *et al*., 2021).

Microbial inoculants are available as liquid-based formulations, water-dispersible granules, or wettable powders and pellets (Berg, 2009; Herrmann and Lesueur, 2013). Suitable formulations are needed to provide a long shelf-life (long-term viability of cells during storage) ensuring the transfer of sufficient viable cells to the plants in the field (Compant *et al*., 2019; French *et al*., 2021). Finding appropriate formulations is especially difficult for Gram-negative bacteria without spore formation (Mitter *et al*., 2017). Moreover, limited tolerance of bacteria to low humidity often

reduces the viability in the mixture showing the need for new formulations (Compant *et al*., 2019). Additionally, large-scale fermentation processes avoiding contaminations and challenging conditions are needed (Herrmann and Lesueur, 2013). Recently, improved formulations and delivery approaches have been studied for their effective transmission of the bacteria to the plant, such as fertigation, seed inoculation, talc, peat, nanoparticles in macrobeads, application of bacteria during flowering into progeny seeds or use of arbuscular mycorrhizal fungi as vectors (Mitter *et al*., 2017; Bradáčová *et al*., 2019; Compant *et al*., 2019; Novinscak and Filion, 2020; Ujvári *et al*., 2021).

Challenges in the transition from lab to natural systems with varying outcomes and unpredictable results under field conditions discourage farmers from using microbial inoculants instead of mineral fertilizer and chemical pesticides (Vishwakarma *et al*., 2020; French *et al*., 2021). For example, commercially available microbial inoculants recently showed no plant growth promotion in maize (Afanador-Barajas *et al*., 2021). The undesired outcomes of microbial inoculants are mainly based on incompatibility of microorganisms in the mix (Thomloudi *et al*., 2019) or lack of rhizosphere establishment of the inoculum. The latter can be caused by competition with the indigenous microbiome of the plant and a limited survival in the soil because of inappropriate abiotic conditions (Schlaeppi and Bulgarelli, 2015; Finkel *et al*., 2017; Compant *et al*., 2019; French *et al*., 2021; Kavamura *et al*., 2021). Additionally, interactions with mineral fertilizer can sometimes hamper the protecting effect of a microbial inoculant against pathogens (Herrmann and Lesueur, 2013; Berg and Koskella, 2018). Tests for compatibility and dosage can restore the effect of the applied microbes (Berg and Koskella, 2018; Compant *et al*., 2019). Another aspect to consider is that some beneficial traits of the applied microorganisms might not be beneficial under certain conditions, e.g. nitrogen-fixation is not needed, when enough nitrogen is available for the plant or native nitrogen-fixing microbes are already present (Schlaeppi and Bulgarelli, 2015; French *et al*., 2021). In some cases, a specific interaction is required. For example, some antagonistic activities can only emerge upon interaction with other beneficial microbes (De Vrieze *et al*., 2018) or the interaction with the pathogens (Compant *et al*., 2019). Moreover, in order to save energy, plant beneficial microbes can change their genetic regulation undesirably by repressing PGP traits no longer profitable for themselves (Haskett *et al*., 2021). Beside the appropriate formulation also plant cultivars need to be able to interact with the applied microbial inoculum, which was also proposed in previously described concepts for improved agriculture

(Schlaeppi and Bulgarelli, 2015; Bender *et al*., 2016; Toju *et al*., 2018; Rodriguez *et al*., 2019). For example, dwarf wheat cultivars had an altered interaction with the indigenous microbiota, which impacted also functions and network connectedness compared to tall cultivars (Kavamura *et al*., 2020). Keeping these limitations in mind during selection, production and application of microbial inoculants can help to overcome the challenges.

Overall, for acceptance of products by all stakeholders microbial inoculants need to meet several criteria: (i) Safety of application, i.e. strains are sufficiently well-characterized to ensure the absence of human or plant pathogenic traits, (ii) reliable effect, which means that inoculants consistently show yield increases in the field over several seasons and conditions, (iii) simple handling, and (iv) cost-effectiveness (Breakfield *et al*., 2021). Reliable data, proving that the selected inoculum meets the above mentioned requirements as well as application trainings for farmers could further increase confidence in this emerging agrotechnology (Vishwakarma *et al*., 2020).

Despite their limitations microbial inoculants are environmentally friendly, can restore soil diversity, improve ecosystem functions (Bender *et al*., 2016; Wagg *et al*., 2019) and nutrient availability, protect plants against biotic and abiotic stresses, bioremediate toxic substances and attract other beneficial microbes (Molina-Romero *et al*., 2017; Vishwakarma *et al*., 2020). In combination with a reduced amount of mineral fertilizer these advantages allow microbial inoculants to achieve up to the same yield as full mineral fertilization, which was shown in several studies (Angulo *et al*., 2020; Maldonado *et al*., 2020; Scagliola *et al*., 2021). Additionally, the process from discovery to field application is shorter compared to chemical products (Manker, 2020). Therefore, microbial based agricultural products are one of the fastest growing agronomy sectors worldwide (Berg *et al*., 2020) and are predicted to make up 60% of the global crop protection market by 2025. Especially, the market for biocontrol products based on microbial antagonists or microbial derived compounds to fend off harmful organisms (Busson *et al*., 2019), has a predicted value of over 10 billion US dollars by 2025 (Berg *et al*., 2020; French *et al*., 2021). These positive perspectives encourage the search for new PGPB using single strain or consortium based approaches.

1.5.1 Single strains

The plant microbiome acts as a whole and advanced sequencing technologies enabled analysis of the plant microbiota in a holistic approach (Schlaeppi and Bulgarelli, 2015; Marín *et al*., 2021). However, each member of the microbiome is an individual organism with its own functional potential (Marín *et al*., 2021) and functional insights are mainly derived from experiments with a reductionist approach using culturable, well-characterized single strains (Schlaeppi and Bulgarelli, 2015). For example, experiments with tomato plants inoculated with *Pseudomonas azotoformans* or *acdS* gene mutants revealed involvement of the ACC deaminase in crop protection under salt stress (Liu *et al*., 2021) and *Paraburkholderia phytofirmans* PsJN protected *Arabidopsis thaliana* against a pathogenic *Pseudomonas syringae,* showing its ability to induce systemic resistance (Timmermann *et al*., 2017). The thorough characterization of single strains is important because the simple taxonomic affiliation to a certain genus, although it might be frequently associated with plant beneficial traits, does not allow final conclusions about a particular function (Kavamura *et al*., 2021). For example, it has been reported that *Bradyhizobium* spp. from UK showed no nitrogen fixation ability as they were lacking genes for the respective pathway, although the genus is well-known for this trait (Jones *et al*., 2016). An advanced tool to assess the genomic repertoire of a potential PGPM is whole genome sequencing, which allows a genome based characterization in terms of plant beneficial traits for selection of appropriate strains (Levy *et al*., 2018). Moreover, whole genome sequencing can disentangle the complex bacterial phylogeny and possibly identify potent plant beneficial phylogenetic groups (Levy *et al*., 2018). Finally, such thorough analyses allow a reliable discrimination between pathogenic and beneficial strains and ensures that a selected strain does not bear potentially pathogenic traits (Berg, 2009; Hartmann *et al*., 2019). This approach allowed for example the phylogentic separation of plant beneficial *A. brasilense* strains from the opportunistic human pathogen *Roseomonas fauriae* to ensure confidence of farmers when using *A. brasilense* in agricultural practices (Hartmann *et al*., 2019; Levy *et al*., 2018).

Many single strains show more than one mechanism involved in plant growth promotion and biocontrol, such as the model organism *Pseudomonas simiae* WCS417, which produces siderophores and IAA and has antagonistic activities against pathogens (Pieterse *et al*., 2020). Additionally, *Bacillus amyloliquefaciens* GB03 is not only a well-known biocontrol agent (Berg, 2009), but was also able to cause a microbiome shift in tomato plants including a volatile organic compound (VOC) mediated microbiome synchronization of the neighboring plants (Kong *et al*.,

2021). Understanding the dynamics in model organism systems will help to transfer the knowledge to natural systems (Rodriguez *et al*., 2019). Based on the performance of a single strain *in vitro* it cannot always be concluded how it will perform in the field in presence of the diverse members of a plant microbiome. However, many single strains perform successfully in axenic, green house and also field conditions. For example, the inoculation of soy bean with *Bradyrhizobium* increased yield by nitrogen fixation (Cassán *et al*., 2020) and non-pathogenic *Erwinia* sp. strains have been shown to increase phosphate uptake and plant growth of lettuce grown in the field including an optimized effect of the applied fertilizer (Maldonado *et al*., 2020). Single strains also improved yield growth over a long-term period of five years as reported for *Burkholderia cepacia* ISOP5 and *Rhodopseudomonas palustris* ISP-1 on peanut (Wang *et al*., 2021b). One of the best-known examples of a plant growth promoting single strain is *Azospirillum brasilense*, which produces auxin and is sold as biopromoter (Santos *et al*., 2019; Cassán *et al*., 2020). Furthermore, several microbes, such as *Bacillus subtilis* or *Pseudomonas chlororaphis*, to name only a few, reached already successful application as single strain inoculum in the field, especially as commercial biocontrol agents with antagonistic activities against plant pathogens (Johnsson *et al*., 1998; Berg, 2009). These reports show how single strains are already used in sustainable agricultural practices today. However, recently new approaches using SynComs or microbial consortia arise as an alternative to single strain application with certain challenges and advances.

1.5.2 SynComs and microbial consortia

The term “Synthetic communities (SynComs)” describes microbial, typically bacterial, mixtures designed to elaborate the reductionist approach of using single strains by adding more complexity to the system (Marín *et al*., 2021). A similar term often used in this research field is “microbial consortia”. Although these terms are often used as synonyms, the term “SynComs” describes mostly isolates which belong to a culture collection from particular hosts or represent ecological conditions allowing e.g. to mimic the plant microbiome in order to get a deeper inside in multipartite microbe-microbe-plant-interactions (Niu *et al*., 2017; Chen *et al*., 2020; Marín *et al*., 2021). SynComs can have three or more isolates, which are culturable, known and traceable over the course of the experiment (Marín *et al*., 2021). In contrast, the term “microbial consortia” describes microbial mixtures often composed of unrelated strains of bacteria, sometimes combined with beneficial fungi, often used in studies with focus on application (Compant *et al*., 2019). They are not necessarily, but can be, isolated from the same microbial community or same hosts.

The idea to use SynComs or microbial consortia is to multiply the modes of action of single strains by exploiting complementary or synergistic interactions of microbes, increasing functional redundancy and community diversity. Further aims are to ensure presence of at least one functional member under varying abiotic conditions (e.g. temperature, pH or salinity) or inducing metabolite production and transport, which occurs sometimes only upon interaction of certain bacteria (Bradáčová *et al*., 2019; Compant *et al*., 2019; Marín *et al*., 2021). In terms of application, microbial consortia have been used successfully in the field over the years , for various crops, in various countries and in several combinations (Berg, 2009; Compant *et al*., 2019; Santos *et al*., 2019; Cassán *et al*., 2020; Berg *et al*., 2021). For example, plant growth in maize was improved under drought stress upon inoculation of a four-member microbial consortium (Molina-Romero *et al*., 2017). A very successful application is the combination of *Azospirillum brasilense* and *Bradyrhizobium* strains, which increase soy bean yields and are frequently used in South America (Cassán *et al*., 2020). In contrast, the studies with SynComs are basically laboratory or growth chamber based studies which aim to understand the underlying mechanisms of plant-microbe interactions and microbiome modulation (Bai *et al*., 2015; Chen *et al*., 2020; Finkel *et al*., 2020; French *et al*., 2021). Smaller SynComs allow to focus more on the individuals and reveal insights on interactions of the specific members (Bodenhausen *et al*., 2014; Hartman *et al*., 2017; Niu *et al*., 2017), whereas larger SynComs represent the complexity of the microbiome (Finkel *et al*., 2020). In the seminal paper of Bai *et al*. (2015) the authors cultivated representative synthetic microbiota of *Arabidopsis thaliana* and found a close overlap between culturable bacterial species and the sequenced phylogeny as well as a taxonomic overlap between leaf and root microbiota. This strengthened approaches using SynComs trying to mimic the natural microbiota and investigating the dynamics of plant-microbe-interactions under controlled conditions (Duran *et al*., 2018; Finkel *et al*., 2020), considering the role of the microbes (Niu *et al*., 2017; Duran *et al*., 2018; Finkel *et al*., 2020) as well as the role of the plant (Bodenhausen *et al*., 2014; Lebeis *et al*., 2015; Herrera Paredes *et al*., 2018).

Since then many different approaches to select members for SynComs and microbial consortia have been tested. For example, Toju *et al*. (2020) proposed a computational network approach to assemble a SynCom based on members of the core microbiome and found candidates, which prevent pathogen infection (Toju *et al*., 2018, 2020). What was missed in this approach are satellite microbes. Satellite microbes are rare or low abundant taxa only appearing in a reduced number of

sites, but that could play a pivotal role in the plant microbiome (Compant *et al*., 2019). Others chose their candidates based on microbial interaction or correlation networks (Poudel *et al*., 2016; Duran *et al*., 2018; Garrett *et al*., 2018; Kong *et al*., 2018). The microbiota composition depends among other factors on the plant genotype or specific biotic or abiotic conditions (Berendsen *et al*., 2018; Bakker *et al*., 2020; Chen *et al*., 2020; Liu *et al*., 2020). Thus, members of a SynCom or microbial consortium can be selected from plants e.g. exposed to abiotic stress (Jochum *et al*., 2019b; Saad *et al*., 2020), pathogen attack (Berendsen *et al*., 2018) or from dysbiotic mutants (Chen *et al*., 2020). For example, an equal number of strains were randomly picked from wildtype and mutant *Arabidopsis* plants, which represent the respective microbiota composition (Chen *et al*., 2020). After application the dysbiotic community of the *Arabidopsis* mutant caused dysbiosis symptoms in wild type plants (Chen *et al*., 2020). Additionally, a microbial consortium of three strains was assembled based on the three respective, high abundant rhizosphere OTUs, correlating most with pathogen infection and showed biocontrol activity *in planta* (Berendsen *et al*., 2018). Based on this, plant-associated microbes enriched by plant stresses could be assembled to a "DefenseBiome" (Liu *et al*., 2020). In a "drop-out" approach the systematical reduction of the original SynCom allowed conclusions on functions of certain members of the community and identification of keystone taxa (Niu *et al*., 2017; Finkel *et al*., 2020; Moccia *et al*., 2020). A common approach is to choose the bacteria based on their abundance in the natural plant microbiota (or in the culture collection) to represent a simplified natural plant microbiome (Bodenhausen *et al*., 2014; Hartman *et al*., 2017; Niu *et al*., 2017). This approach was successfully extended to assemble the SynCom from a community-based culture collection based on the 20 most abundant OTUs of the natural plant microbiome (Armanhi *et al*., 2018).

A promising and frequently used approach for the selection of SynComs or microbial consortia members is based on their previously known (plant beneficial) functions e.g. derived from *in vitro* experiments (e.g. de Souza *et al*., 2020; Saad *et al*., 2020). The approach was often used in the characterization of single strains (e.g. Majeed *et al*., 2015; Gontia-Mishra *et al*., 2016; Joshi *et al*., 2019; Wang *et al*., 2021a), but has also been elaborated recently for the selection of SynComs and microbial consortia members, mainly with a focus on biocontrol activity (Santhanam *et al*., 2019; Herrera Paredes *et al*., 2018; Hu *et al*., 2016). This could also include testing of direct binary interactions of the bacteria with the plant to identify most promising candidates (Herrera Paredes *et al*., 2018). An improved biocontrol effect of a microbial consortium over single strain application

was shown by the different combinations of eight well-characterized *Pseudomonas* strains applied to infected plants, which revealed the more diverse the community the better it protects the plant against pathogens (Hu *et al*., 2016). The observed effect was most likely related to the increased competition of the community with the pathogen and the production of a larger variety of toxins. Even further, some of these beneficial functions are only shown upon the interaction of the beneficial strains. For example, several strain combinations were tested in a leaf disk assay showing a strong biocontrol effect against the plant-pathogen *Phytophthora infestans*, which was not present in single strain applications (De Vrieze *et al*., 2018). Taken together, the terminology and the optimal assembling strategy for SynComs or microbial consortia can be based on abundance, function and/or interaction, and needs to be verified depending on the hypothesis, the purpose and the experimental set-up.

1.5.3 Methods for verification of microbial inoculants

An important and challenging task is to verify that the observed effects on plant health in growth experiments with PGPM are related to the applied microorganisms. The effectiveness of microbes can be verified by different methodologies depending on the experimental set-up, such as culture-dependent methods, e.g. with selective medium, microscopy (brightfield, electron or fluorescent microscopy), molecular approaches, e.g. PCR-based, DNA probes or next-generation sequencing techniques (Romano *et al*., 2020) as well as biomarkers or fluorescently labelled mutant strains (Marín et al., 2021). A qPCR-based method can be helpful to track biocontrol strains over the course of an experiment (Hernández *et al*., 2020). All methods come with advantages and limitations and are therefore proposed to be used in a combinatorial approach (Romano *et al*., 2020).

Consistent guidelines for microbial inoculant research could improve comparability between the studies and allow large-scale data analyses. These guidelines should cover the vocabulary used for the microbial inoculant (SynCom or microbial consortium) and *in planta* experiments, size of the community (>/= 3 strains) and choice of strains, compatibility of strains, verification of performance of the microbial inoculant, experimental scale (short- or long-term) and the choice of the plant model (Marín *et al*., 2021).

1.6 The plants rucola (*Eruca sativa* Mill.) and wheat (*Triticum aestivum* L.)

Many studies focus on the interaction of bacteria with the model plant *Arabidopsis* (Bodenhausen *et al*., 2014; Bai *et al*., 2015; Finkel *et al*., 2020), whereas, in this thesis, the important crop plants rucola (*Eruca sativa* Mill.) and bread wheat (*Triticum aestivum* L.) were selected to validate results already in terms of application. Additionally, the investigated strains were isolated from these two host plants.

The cruciferous vegetable rucola (synonym arugula, *Eruca sativa* Mill.) belongs to the family *Brassicacea* and is a common leafy green vegetable, mainly eaten raw as salad. This can transmit a range of phytonutrients, including vitamin C or glucosinolates (GSLs) (Bell *et al*., 2017), as well as beneficial microbes (e.g. GSL degrader) or pathogens into the human body (Berg *et al*., 2014; Wassermann *et al*., 2017). GSLs and their degradation products nitriles and isothiocyanates have been investigated for their chemoprotective function awarding rucola an interesting representative of leafy green vegetables (Das *et al*., 2000; Bell *et al*., 2017; Mokhtari *et al*., 2018; Blum *et al*., 2019).

Wheat (*Triticum aestivum* L.) belongs to the major crops worldwide (Savary *et al*., 2019; Kavamura *et al*., 2021) and is responsible for 20% of dietary requirements for calories and protein (Shiferaw *et al*., 2013). At the same time the plant is vulnerable to several plant diseases and extreme weather events such as drought or heat, caused by climate change (Shiferaw *et al*., 2013). PGPM-based consortia can be a sustainable solution and part of a concerted effort to improve adaption of the plant to these challenges. Therefore, they were investigated here, including a more in-depth analysis of two bacterial strains representing the genus *Pseudomonas* and the genus *Rhodococcus* presented in the following chapters.

1.7 The genus *Pseudomonas*

Members of the genus *Pseudomonas* are highly abundant in soil and frequently found in the rhizosphere (Bakker *et al*., 2013). The genus *Pseudomonas* comprising rod-shaped, Gram-negative bacteria with a polar flagellum, includes some of the most potent PGPB (Pieterse *et al*., 2014). One of the potent PGPB is the intensively studied *Pseudomonas simiae* WCS417, which enhances plant growth and increases lateral root formation in the model plant *Arabidopsis thaliana* (Pieterse *et al*., 2020). Additionally, *Pseudomonas fluorescens* SS101 for example can increase *Nicotiana tabacum* biomass via volatile production (Park *et al*., 2015) and *Pseudomonas putida* H-2-3 improves plant

growth under abiotic stress conditions (Kang *et al*., 2014). However, other strains of the species *Pseudomonas putida* have been reported to be human pathogens (Fernández *et al*., 2015). Similarly, *Pseudomonas aeruginosa* shows plant beneficial traits (Steindler *et al*., 2009) and is also an opportunistic human pathogen of immunocompromised patients (Driscoll *et al*., 2007). Some plant-associated *Pseudomonas* cause plant diseases, such as the well-known plant-pathogen *Pseudomonas syringae* (Xin and He, 2013), which has a broad host range. The variant *Pseudomonas syringae* pv. tomato (Pst) strain DC3000 is often used as model organism for plant disease (Xin and He, 2013). On the other hand, members of the same species have been reported as plant beneficial (Passera *et al*., 2019). These findings show that the rhizosphere is a reservoir of potential plant and human pathogens (Mendes *et al*., 2013). Therefore, it is of special importance to discriminate between beneficial and pathogenic bacteria for a safe use of PGPB in agricultural applications (Hartmann *et al*., 2019; Rodriguez *et al*., 2019). In cases where the classification based on the 16S rRNA gene is not sufficient whole genome sequencing comes into use for discriminating between beneficial and pathogenic bacteria, allowing mostly reliable identification (Hartmann *et al*., 2019).

Other plant-associated *Pseudomonas* species have been shown to produce bioactive compounds, such as volatiles (Kai *et al*., 2009; Raza *et al*., 2016; Netzker *et al*., 2020) or secondary metabolites (phenazine: Mavrodi *et al*., 2006; Yu *et al*., 2018; Tagele *et al*., 2019) with antagonistic activities against various plant pathogens, such as *Pseudomonas chlororaphis* MA 432 (Johnsson *et al*., 1998), which is active against several plant-pathogenic fungi and part of a commercial seed coverage biocontrol product. Moreover, plant-associated *Pseudomonas* species can act indirectly via induced systemic resistance (Pieterse *et al*., 2014), such as *Pseudomonas simiae* WCS417 (Pieterse *et al*., 2020). These examples show the high potential of members of the genus *Pseudomonas* to act as PGP or biocontrol agents with a pivotal role in the plant microbiome and permit the careful assessment of the *Pseudomonas* sp. SCA7 isolated from wheat in this thesis. At the same time the examples emphasize the importance of a thorough genetic and functional characterization to discriminate the strains from pathogenic members of the genus *Pseudomonas*.

1.8 The genus *Rhodococcus* (adapted from Kuhl *et al*. (2021))

Further knowledge of the functional repertoire of yet lesser known members of the plant microbiome, such as *Rhodococcus*, is important to understand the role of each member in the plant microbiome. Investigating the modes of interaction with the plant as well as other microbes could

reveal useful traits for an application in specifically demanding agricultural scenarios. The genus *Rhodococcus* comprises Gram-positive, aerobic, non-motile and non-sporulating bacteria belonging to the phylum Actinobacteria. Members of the genus *Rhodococcus* have been isolated from a broad variety of environments including ocean (Lincoln *et al*., 2015), soil (Rückert *et al*., 2015), rhizosphere (Kwasiborski, 2014) and plants (Hong *et al*., 2016; Stevens *et al*., 2017). Several isolates belonging to the genus *Rhodococcus* are resistant to various stresses (Pátek *et al*., 2021), such as heavy-metal stress (Dabrock *et al*., 1994; Weyens *et al*., 2013). Moreover, they are able to degrade and metabolize a large spectrum of xenobiotic, hydrophobic and organic compounds, such as aromatic hydrocarbons, crude-oil (Lincoln *et al*., 2015), nitriles (Kamble *et al*., 2013), quinoline (Gupta, 2019), and polychlorinated biphenyl (PCB) (Pham *et al*., 2015; Ceniceros *et al*., 2017; Gorbunova *et al*., 2020). These traits make the genus *Rhodococcus* interesting for bioremediation applications or decontamination (Leigh *et al*., 2006; Płociniczak *et al*., 2017) and certain enzymes are used in industrial processes, such as nitrile hydratase used to degrade nitriles to amides in the production of acrylamide (Rucká *et al*., 2014; Busch *et al*., 2019).

The phylum Actinobacteria has been shown to be a constitutive part of rhizosphere microbiomes (Bulgarelli *et al*., 2012, 2013; Lundberg *et al*., 2012) and the genus *Rhodococcus* has been frequently reported in metagenomic and microbiome analyses as an established member of plant microbiomes (Francis and Vereecke, 2019; Vereecke *et al*., 2020). Plant-associated *Rhodococcus* have been described as biological control agents as well as plant pathogens. The recently described *Rhodococcus corynebacterioides* PBTS 1 and PBTS2 has been associated with pistachio disease outbreak (Vereecke *et al*., 2020) and *Rhodococcus fascians* D188 is the causal agent of leaf gall disease (Francis *et al*., 2016). However, a mutant of *R. fascians* D188 that lost its virulence plasmid showed PGP properties (Francis *et al*., 2016). Other *Rhodococcus* species showed plant beneficial traits, such as ACC deaminase activity, IAA and siderophore production or phosphate solubilization *in vitro* (Trivedi *et al*., 2007; Abbamondi *et al*., 2016; Murugappan *et al*., 2017; Hasuty *et al*., 2018) and *in planta* (Belimov *et al*., 2001). Two *Rhodococcus* sp. isolates were able to form root nodules involved in nitrogen fixation in *Lotus corniculatus* and *Anthyllis vulneraria* (Ampomah and Huss-Danell, 2011). Several strains of *Rhodococcus erythropolis* are described as biocontrol agents, which antagonizes pathogenic bacteria by disrupting the quorum sensing signals of human pathogenic *Pseudomonas aeruginosa* (Rückert *et al*., 2015) or plant pathogenic *Pectobacterium atrosepticum* (Cirou *et al*., 2007; Barbey *et al*., 2013; Latour *et al*., 2013; Chane

et al., 2019). The plant-associated *R. qingshengii* RL1 was isolated from surface sterilized rucola leaves, whereas the type strain of the species *Rhodococcus qingshengii* djl-6 was isolated from a carbendazim polluted soil (Xu *et al*., 2007). Other members of the species were isolated from arctic sea water (Lincoln *et al*., 2015), weathered serpentine rock (Khilyas *et al*., 2020), polluted rivers (Hasuty *et al*., 2018) or a palm tree rhizosphere (Bala *et al*., 2013). *Rhodococcus qingshengii* S10107 isolated from rhizospheric soil of *Phaseolus vulgaris* possesses nitrogen fixing capacity and improves growth of chick pea plants (Joshi *et al*., 2019). Moreover, *Rhodococcus qingshengii* 100A produces a high amount of IAA *in vitro* (Hasuty *et al*., 2018). These reports indicate that plant-associated *R. qingshengii* isolates may possess traits which facilitate their colonization and survival in plant-associated niches or could be beneficial for the plant. Additionally, to my knowledge RL1 is the first member of the genus *Rhodococcus* isolated from rucola, which additionally warrants a characterization of the new plant-associated isolate RL1.

1.9 Aim of the study

The global need for alternative agricultural solutions is increasing and the beneficial traits of PGPB qualify them as alternative solutions to mineral fertilizer and chemical pesticides. Additionally, PGPB can support plant health under abiotic stress conditions. In order to develop beneficial and tailored microbial inoculants there is a tremendous demand for new well-characterized PGPB to address the specific needs of different crop plants under varying environmental conditions. Therefore, the goal of this thesis was to identify and characterize novel PGP single strains as well as microbial consortia. Moreover, it is critical to advance the understanding of the plant-microbe- and microbe-microbe-interaction dynamics under different abiotic conditions for the future development of microbial inoculants. In order to address this goal, at first the plant beneficial traits of potential candidates will be characterized. The underlying research questions were if applied single strains and microbial consortia can support plant growth under non-drought and drought conditions as well as how the microbial composition changes after application of bacteria. This could reveal important taxa relevant for potentially observed beneficial effects. The first hypothesis was that drought stressed habitats would harbor a high proportion of drought resistant isolates and that among those isolates microbial inoculants could be acquired with beneficial effects on plants under similar drought stress conditions. The second hypothesis was that applied microbial consortia would be more successful in supporting plants compared to single strain application. In order to address these questions and hypotheses two consecutive approaches will be used to characterize the bacteria combining exploratory as well as hypothesis-driven components. In a first approach bacteria from a vast culture collection will be experimentally screened for a set of selected plant beneficial traits. Based on this screening single strains and consortia will be chosen for inoculation. In a second approach the whole genome of two isolates will be sequenced to search for genes potentially involved in plant beneficial traits. The identified traits will be tested in functional analyses to elucidate whether they were actually translated into functions *in vitro* and *in planta*. Both approaches will be evaluated in the next chapters for their contribution to realize the vision of using plant beneficial microbes as sustainable solution for agricultural challenges.

2 Results

In order to address the goal to find and characterize new PGPB the natural microbial composition of two agricultural fields was analyzed to estimate the potential to identify PGPB candidates (chapter 2.1) and a large culture collection was established from the rhizosphere of wheat plants grown on the two fields (chapter 2.2), which was also compared to the natural microbiota (chapter 2.3). In the first approach a selection of isolates was characterized for their plant beneficial and drought stress tolerance related traits as well as for their compatibility with each other *in vitro* (chapter 2.4). Based on these results three different consortia were assembled and applied to wheat plants under drought and non-drought conditions in order to identify plant beneficial consortia (chapter 2.5). Subsequently, in order to understand drought stress induced changes in the plant and its associated microbiota they were further analyzed by differential gene expression analysis (chapter 2.6), bacterial load (chapter 2.7), amplicon based community profiling (chapter 2.8) and co-occurrence network analysis (chapter 2.9). Based on the results, five isolates were selected and applied as single strains and consortia in order to compare their performance (chapter 2.10). In a second approach for in depth characterization of potential PGPB the genomes of the two isolates *Pseudomonas* sp. SCA7 from wheat and *Rhodococcus qingshengii* RL1 from rucola were sequenced and identified plant beneficial as well as stress tolerance traits were subsequently tested in experiments *in vitro* (2.11) and *in planta* (2.12).

2.1 Comparison of natural wheat microbiota in Scheyern and Bernburg

Two agricultural used fields in Scheyern and Bernburg with different environmental conditions sampled after a hot and dry summer period were selected as sampling sites to ensure robustness of the findings (methods 6.1). Their natural wheat microbiota was analyzed to characterize the influence of different environmental parameters on the microbial composition, which was also relevant for a targeted selection of bacterial isolates later in this work.

The 16S rRNA gene amplicon sequencing of twelve root and rhizosphere samples and three soil samples from the two locations Scheyern and Bernburg generated a total of 2,095,955 reads. Merging and filtering resulted in 1,707,789 high-quality sequences with a range of 64,104 to 359,566 sequences per sample and a median of 87,152. Sequences could be assigned to 3263 species-level Operational Taxonomic Units (OTUs; ≥ 97% similarity) applying an abundance

cutoff of 0.01%. 2504 OTUs were allocated to Bernburg samples and 1910 OTUs to Scheyern samples with many overlapping OTUs between the sampling sites.

In order to estimate the differences in the microbial composition different diversity parameters were analyzed. Effective species richness was 78.00 for Scheyern and 80.25 for Bernburg. Scheyern had an evenness of 0.592 and Bernburg of 0.579. The rarefaction curve was asymptotic indicating a sufficient sequencing depth for exploration of bacterial communities. The microbial composition was significantly different between the two sampling sites (**Figure 3A**, p=0.001). The previously grown crops maize and canola had a significant influence on the microbial composition in Bernburg soil (**Figure 3D**, p-value = 0.044), but not when analyzing Bernburg and Scheyern samples with the same pre-crop together (**Figure 3C,** p=0.107). The compartments root (and rhizosphere) and (bulk) soil were not significantly different from each other (**Figure 3B,** p=0.514) and bulk soil samples of Bernburg clustered within root (and rhizosphere) samples.

Root and rhizosphere samples from Scheyern contained 17 phyla dominated by Proteobacteria (34.7%), Actinobacteria (23.5%) and Bacteroidetes (9.3%). In root and rhizosphere samples from Bernburg 19 phyla were identified dominated by Actinobacteria (33.2%), Proteobacteria (20.4%) and Acidobacteria (13.4%) (**Figure 4A**).

The differences in the microbial composition between Scheyern and Bernburg were strongly correlated with the different sampling sites and the different previously grown crops, indicating an influence of the environmental conditions on the microbial composition, which was expected.

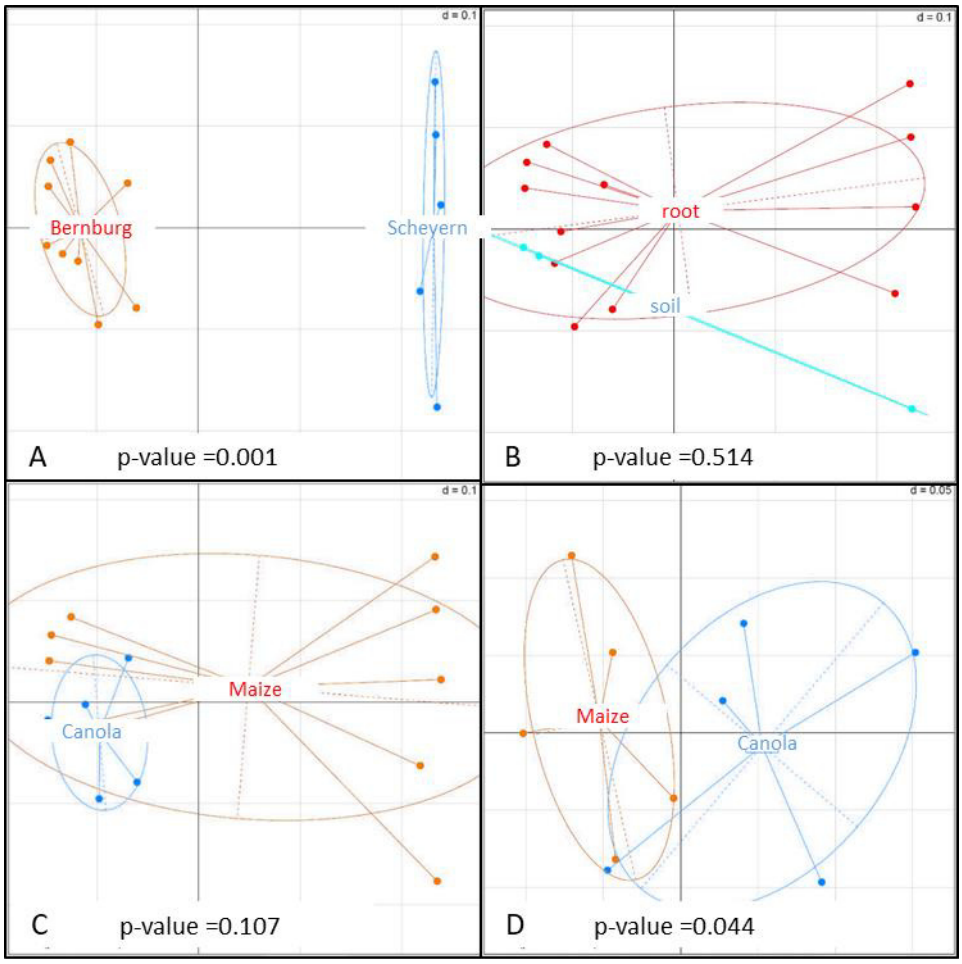

Figure 3: ß-diversity at the sampling sites. Root and rhizosphere microbiota from Bernburg and Scheyern are separated by the factor (A) location, (B) compartment, (C) pre-crop and (D) pre-crop Bernburg samples only. Data is presented in two-dimensional MDS plots. P-values < 0.05 indicate significant differences; d = 0.1 refers to 10% difference per grid.

2.2 Characterization of culture collection and phylogenetic classification of isolates

Bacteria were isolated from roots and rhizosphere of wheat to establish a large culture collection, as a pre-requisite for later characterization of potential PGPB. In total the culture collection contains 1751 bacterial isolates of which 1225 isolates were derived from roots and rhizosphere of Bernburg samples and 526 isolates were acquired from Scheyern samples. From Bernburg samples 543 isolates were derived from samples with the pre-crop maize, whereas 682 isolates were derived from samples with the pre-crop canola. The isolates per medium are listed in **Table 1**. The isolation process from plates was stopped as soon as bacterial and fungal colonies started overgrowing each other on the plate hampering isolation of pure cultures.

Table 1: Isolates per medium and sampling site

Medium	Number of isolates per sampling site		
	Scheyern	**Bernburg (pre-crop maize)**	**Bernburg (pre-crop canola)**
Cha	38	8	44
King's B	108	55	110
M9	91	29	63
Nutrient broth	38	92	114
R2A	133	115	158
Starch casein agar	27	134	117
2 x Tryptone yeast medium	91	110	76

Isolated bacteria were classified in phylogenetic groups based on their RFLP patterns to avoid excessive sequencing of all isolates. In the culture collection derived from the Scheyern samples 48 different RFLP patterns could be identified, whereas for Bernburg samples 50 different RFLP patterns were identified. Both locations shared 40 RFLP patterns. Scheyern samples had 8 unique RFLP patterns and Bernburg samples had 10 unique RFLP patterns (**Table 2**).

Table 2: Properties of culture collection.

RFLP	**Scheyern**	**Bernburg**
Bacterial isolates	526	1225
Total RFLP patterns	48	50
Shared patterns	40	
Unique patterns	8	10
Total identified taxa in culture collection	16	21
Shared taxa	6	

16S rRNA gene sequence of representative isolates from each pattern revealed the taxa mainly represented by the RFLP patterns. For some patterns more than one genus could be identified and some genera were represented by more than one pattern. For classification the highest common taxon for each pattern was chosen. RFLP patterns of the Scheyern isolates represent 16 taxa, whereas the patterns from Bernburg isolates represent 21 taxa of which 6 taxa are shared between the locations (**Table 2**). Scheyern culture collection was dominated by Proteobacteria (mainly *Pseudomonas*) and Bacteroidetes (mainly *Flavobacterium*), whereas Bernburg culture collection was dominated by Proteobacteria (mainly *Acinetobacter* and *Pseudomonas*) and Firmicutes (mainly *Bacillus*) (**Figure 4B**).

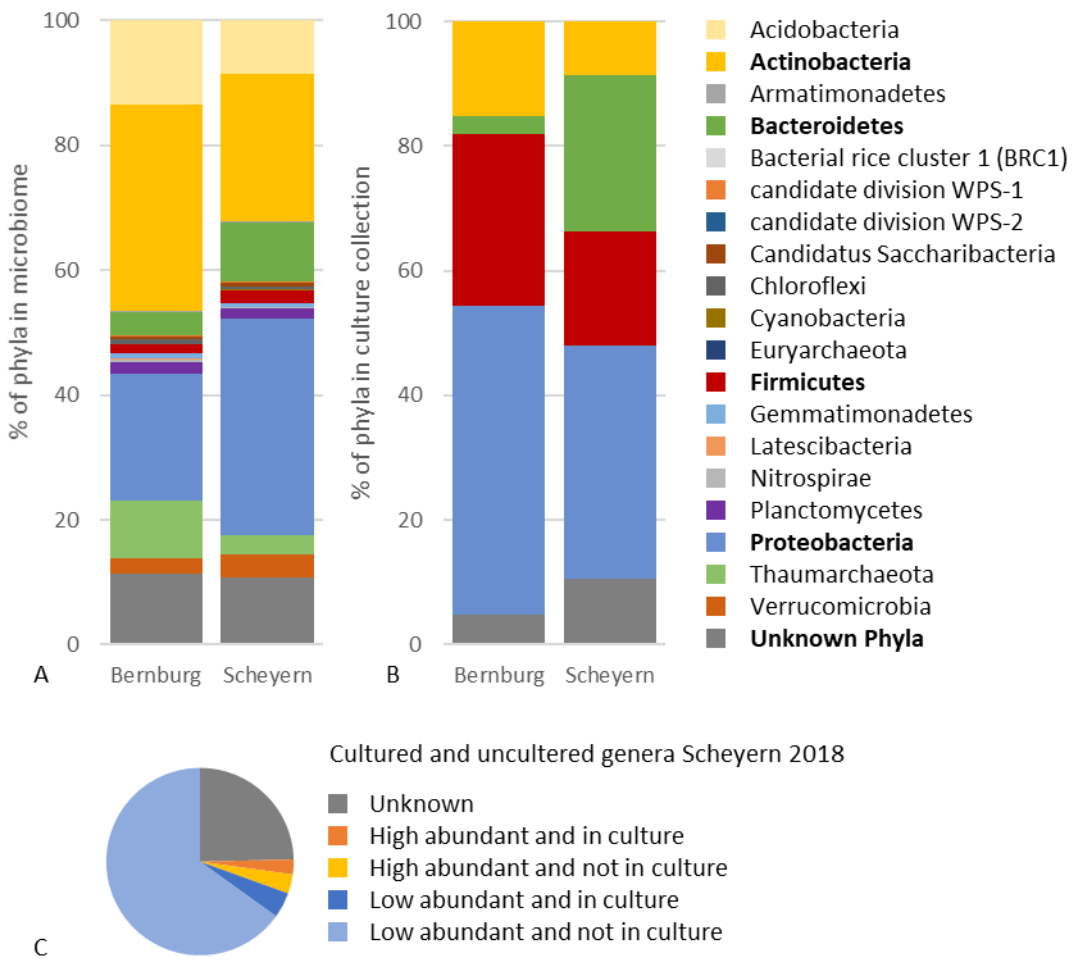

Figure 4: Bacterial phyla and genera at the sampling sites. (**A**) Phyla identified in the 16S rRNA gene amplicon analysis of root and rhizosphere samples from Bernburg and Scheyern. (**B**) Phyla isolated from the root and rhizosphere of wheat plants from Bernburg and Scheyern. Phyla in bold are shared between the microbiota and the culture collection. (**C**) High and low abundant genera in the Scheyern root and rhizosphere microbiota and their respective culturable fraction. High abundant genera were defined to have at least 1% average abundance in root and rhizosphere microbiota.

The culturing method was successful for both sampling sites, despite small differences between the number of isolates on each medium. Although the number of Bernburg isolates was surpassing the number of Scheyern isolates a similar number of taxa was identified for both sampling sites and Proteobacteria dominated both culture collections, indicating that the culture dependent isolation was selective for certain bacterial groups. If the culture collection could represent the natural microbiota was addressed in the following analysis for Scheyern samples.

2.3 Comparison of Scheyern microbial composition and Scheyern culture collection

The Scheyern culture collection was compared to the original Scheyern microbial composition to evaluate to which extend the former represents the latter. An additional sequencing run was performed for Scheyern samples to test the reproducibility of the sequencing results of the first run described in section 2.1. The 16S rRNA gene amplicon sequencing of three root and rhizosphere samples and three soil samples from Scheyern generated a total of 680,468 reads. Merging and filtering resulted in 441,221 high-quality sequences with a range 50,618 to 89,633 sequences per sample and a median of 76,620. Sequences could be assigned to 1927 species-level Operational Taxonomic Units (OTUs; ≥ 97% similarity) applying an abundance cutoff of 0.01%. The rarefaction curve was asymptotic indicating a sufficient sequencing depth for exploration of bacterial communities. In both runs the number of OTUs and identified genera (276 genera in first run, 271 genera in second run) for Scheyern samples were equal, indicating reproducible results. Analysis of the microbial composition revealed a clear separation of root (+ rhizosphere) samples from soil samples (**Supplementary Figure S1**). Therefore, the comparison between diversity in culture collection and rhizosphere samples was performed with the run described in this section (2.3).

In total 271 genera were identified in Scheyern root (+ rhizosphere) samples of which 204 belong to known genera, whereas 67 are unknown. Diversity in root microbiota of Scheyern samples and the Scheyern culture collection reveals a partial representation of the root microbiota on phylum level (**Figure 4A, B**), but not on genus level. Four phyla (Proteobacteria, Actinobacteria, Bacteriodetes and Firmicutes) of 17 Phyla in the Scheyern root microbiota were identified in the Scheyern culture collection. Bacteroidetes and Firmicutes are with 29.8% and 14.7%, respectively, overrepresented in the culture collection compared to the root and rhizosphere microbiota, where Bacteroidetes represent 9.3% and Firmicutes 2% of the identified phyla (**Figure 4A, B**). In total 18 genera of the Scheyern microbiota had culturable representatives in the culture collection representing an isolation rate of 8.8%. 7 genera of the 16 high abundant genera with an average abundance of >1% had culturable representatives in the culture collection, whereas a smaller proportion of 11 genera of 189 low abundant (<1% average abundance) genera had representatives in culture (**Figure 4C**). High abundant genera in culture were *Arthrobacter*, *Flavobacterium*, *Rhizobacter*, *Rhizobium*, *Polaromonas*, *Sphingomonas* and *Streptomyces*. Low abundant genera in culture were *Bacillus*, *Bosea*, *Dyadobacter*, *Kaistia*, *Luteibacter*, *Microbacterium*, *Paenibacillus*,

Pedobacter, *Pseudomonas*, *Rhodococcus* and *Variovorax*. Comparison of diversity and abundance in Bernburg microbiota and Bernburg culture collection was performed by master's student Furkan Tunc (thesis in preparation).

The Scheyern culture collection partially represents the Scheyern microbiota on phylum level and almost half of the high abundant genera have representatives in culture, which indicates that the culture collection represents a valuable source for future microbiota manipulation experiments. This link allows a selection of isolates based on their abundance in the natural wheat microbiota, which was used for the assembly of the consortium K2. For selection of further candidates for consortia the isolates had to be characterized for their plant beneficial traits performed in the next experiments.

2.4 *In vitro* assays of selected bacteria for PGP traits and stress tolerance

After phylogenetic classification a total of 30 bacterial isolates obtained from Scheyern sampling site and 27 bacterial isolates obtained from Bernburg sampling site were selected based on the criteria described in methods section 6.4 for further characterization of their plant beneficial traits, interaction with other microorganisms and stress tolerance against various stresses. Experiments were performed to select appropriate candidates for the assembly of a microbial consortium for application to wheat plants (section 2.5). Characterization of Bernburg isolates was performed by master's student Furkan Tunc (thesis in preparation) and are therefore not further mentioned in the results.

2.4.1 Characterized bacterial isolates show plant beneficial traits *in vitro*

The selected isolates were tested for common plant beneficial traits *in vitro*, which are relevant to assemble a consortium based on PGP functions for application in the plant experiments (section 2.5).

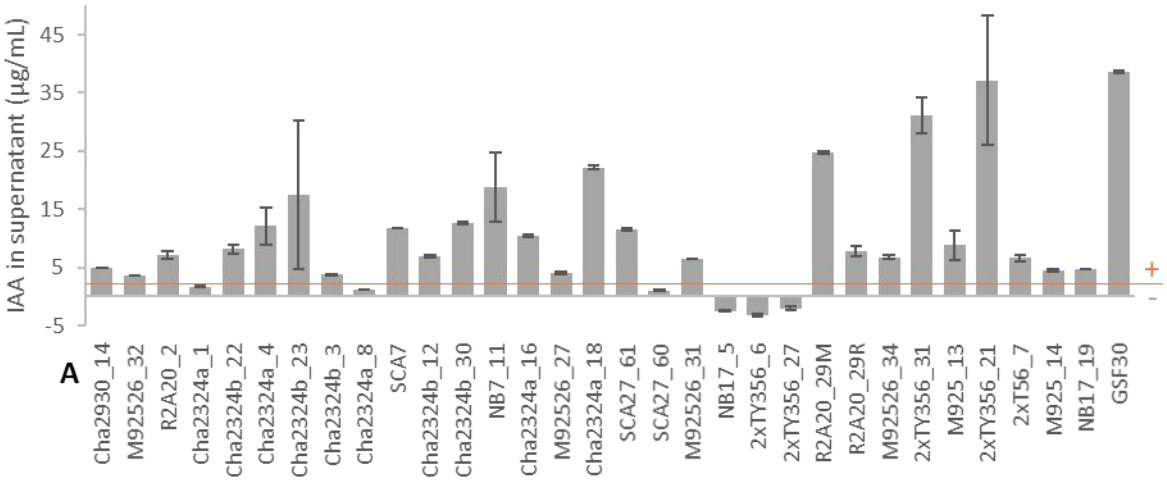
IAA in supernatant (µg/mL)
45
35
25
15
5
-5
+
-
Cha2930_14
M92526_32
R2A20_2
Cha2324a_1
Cha2324b_22
Cha2324a_4
Cha2324b_23
Cha2324b_3
Cha2324a_8
SCA7
Cha2324b_12
Cha2324b_30
NB7_11
Cha2324a_16
M92526_27
Cha2324a_18
SCA27_61
SCA27_60
M92526_31
NB17_5
2xTY356_6
2xTY356_27
R2A20_29M
R2A20_29R
M92526_34
2xTY356_31
M925_13
2xTY356_21
2xT56_7
M925_14
NB17_19
GSF30

A

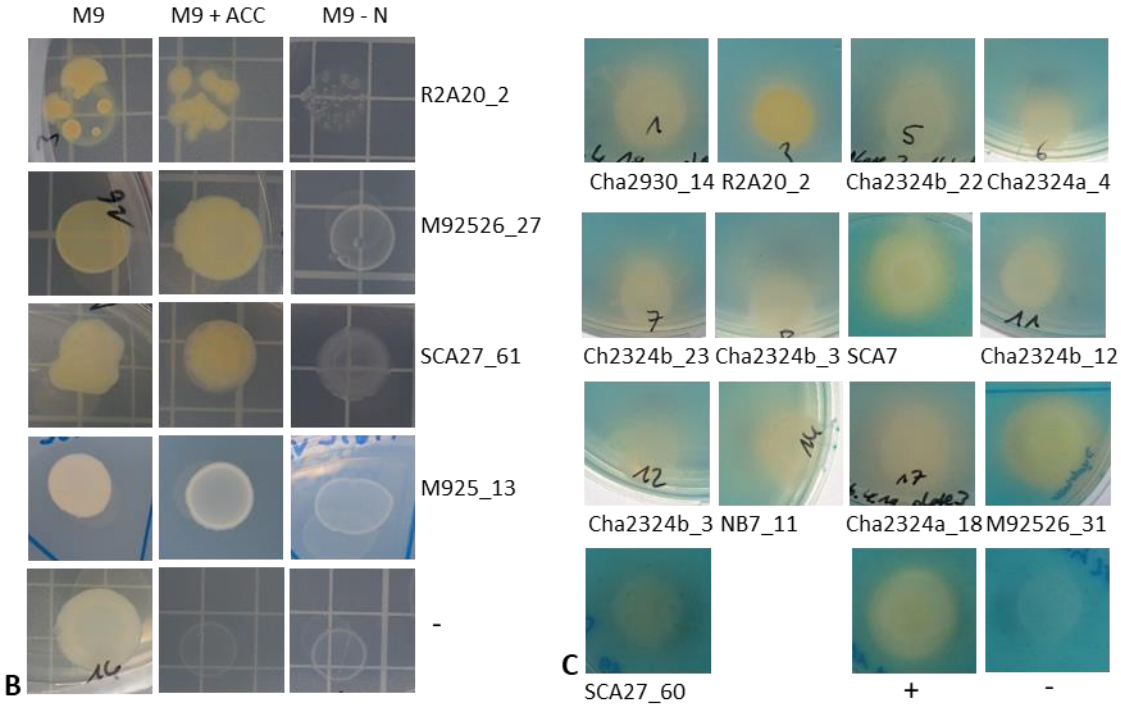
M9
M9 + ACC
M9 - N
R2A20_2
M92526_27
SCA27_61
M925_13
-
B
Cha2930_14 R2A20_2 Cha2324b_22 Cha2324a_4
Ch2324b_23 Cha2324b_3 SCA7 Cha2324b_12
Cha2324b_3 NB7_11 Cha2324a_18 M92526_31
C
SCA27_60
+
-

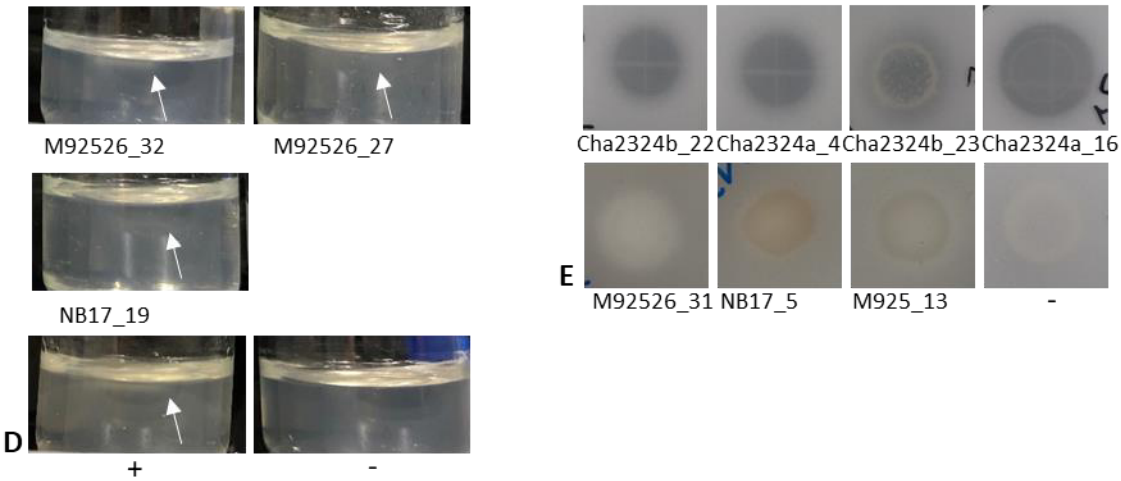
M92526_32
M92526_27
NB17_19
D
+
-
Cha2324b_22 Cha2324a_4 Cha2324b_23 Cha2324a_16
M92526_31 NB17_5 M925_13 -
E

Figure 5: Plant beneficial *in vitro* traits of selected Scheyern isolates. (**A**) Amount of IAA in culture supernatant (N = 3). GSF30 served as positive control. Orange line marks detection limit of 2 µg/mL. (**B**) ACC deaminase activity was tested in three media combinations: medium (M9), medium supplemented with ACC (M9 + ACC) and nitrogen-free medium (M9 – N). Growth on M9 and M9 + ACC indicates ACC deaminase activity. NB7_11 served as negative control. (**C**) Siderophore production is indicated by a color change of the medium from blue to orange. RL1 served as positive control and 2xTY356_6 served as negative control. (**D**) Nitrogen fixation is indicated by pellicle formation in semi-soli nfb-medium. Sp7 served as positive control and R2A20_2 served as negative control. White arrows point on pellicle. (**E**) Phosphate solubilization is indicated by a clearance of the NBRIP medium. Cha2324a_1 served as negative control.

2.4.1.1 IAA production

Scheyern isolates were tested for presence or absence of IAA production. 23 Scheyern isolates produced IAA amounts above 2 µg/mL after 48 h and were therefore identified as IAA producing isolates (**Table 3, Figure 5A**). Two isolates 2xTY356_31 and 2xTY356_21 belonging to *Arthrobacter* produced similar high amounts of IAA as the positive control GSF30 with 38 ± 0.21 µg/ml.

2.4.1.2 Siderophore production

A total of 13 Scheyern isolates produced siderophores indicated by the color change of the overlay agar from blue to orange similar to the positive control RL1 (**Table 3, Figure 5C**). Most of the positive isolates belong to the genus *Pseudomonas*, which was expected, because this genus is well-known for harboring strains with PGP or biocontrol activity.

2.4.1.3 Phosphate solubilization

7 isolates were able to solubilize phosphate indicated by clear halo formation and SI values above 2 indicating phosphate solubilization ability (**Table 3, Figure 5E**).

2.4.1.4 1-aminocyclopropane-1-carboxylate utilization

Growth on minimal medium and minimal medium with ACC and no growth on nitrogen-free minimal medium indicate ACC utilization. 4 isolates showed ACC deaminase activity indicated by growth on M9 and M9 with ACC, but not on M9 without nitrogen (**Table 3, Figure 5B**). As expected, M92526_27 and SCA27_61 belong to the genus *Variovorax*, which is well-known for ACC deaminase activity.

2.4.1.5 Nitrogen fixation

Scheyern isolates M92526_32, M92526_27, M92526_34 and NB17_19 associated with different genera could grow on nitrogen free Nfb-medium (**Table 3, Figure 5D**). Pellicle formation of all tested isolates in Nfb-medium was smaller compared to positive control *Azospirillum brasilense* Sp7.

86% of Scheyern isolates (= 26 of 30 characterized isolates) showed plant beneficial traits *in vitro* (**Table 3**), which was an unexpected high number. This suggests that roots and rhizosphere of wheat are a rich source for bacterial isolates with plant beneficial traits *in vitro*, despite a media-based selection for some taxa. For application as consortia the isolates need to be tested for their compatibility tested in experiments of the next chapter.

Table 3: Plant beneficial traits of characterized isolates. Isolate ID was composed of the abbreviation of the medium, plate number and colony number on the plate. (Cha = cha medium, M9 = M9 medium, R2A = R2A medium, NB = nutrient broth medium, SCA = starch casein agar, 2xTY = 2x tryptone yeast medium)

Isolate ID	Genus	Phosphate solubilization (SI values)	Siderophore production	ACC deaminase activity	IAA production (µg/mL)	Nitrogen fixation
Cha2930_14	*Bacillus*		+		4.9	
M92526_32	*Sphingomonas*				3.5	+
R2A20_2	*Flavobacterium*		+	+	7	
Cha2324a_1	*Bacillus*					
Cha2324b_22	*Pseudomonas*	2.2	+		8.1	
Cha2324a_4	*Pseudomonas*	2.2	+		12.1	
Cha2324b_23	*Pseudomonas*	2.2	+		17.4	
Cha2324b_3	*Pedobacter*		+		3.7	
Cha2324a_8	*Bacillus*					
SCA7	*Pseudomonas*		+		11.7	
Cha2324b_12	*Pseudomonas*		+		6.9	
Cha2324b_30	*Pseudomonas*		+		12.5	
NB7_11	*Pseudomonas*		+		18.8	
Cha2324a_16	*Luteibacter*	2.7			10.4	
M92526_27	*Variovorax*			+	3.9	+
Cha2324a_18	*Pseudomonas*		+		22.1	

Isolate ID	Genus	Phosphate solubilization (SI values)	Siderophore production	ACC deaminase activity	IAA production (µg/mL)	Nitrogen fixation
SCA27_61	*Variovorax*			+	11.4	
SCA27_60	*Streptomyces*		+			
M92526_31	*Dyadobacter*	2.3	+		6.4	
NB17_5	*Rhodococcus*	2.1				
2xTY356_6	*Rhodococcus*					
2xTY356_27	*Rhodococcus*					
R2A20_29M	*Rhizobacter*				24.7	
R2A20_29R	*Polaromonas*				7.7	
M92526_34	*Rhizobium*				6.7	+
2xTY356_31	*Arthrobacter*				31.1	
M925_13	*Arthrobacter*	2.2		+	8.8	
2xTY356_21	*Arthrobacter*				37.1	
2xT56_7	*Arthrobacter*				6.5	
M925_14	*Arthrobacter*				4.4	
NB17_19	*Arthrobacter*				4.7	+

2.4.2 Characterized bacterial isolates show interaction with other microbes *in vitro*

2.4.2.1 Confrontation assay against plant-pathogenic fungi

The genera *Pseudomonas* and *Bacillus* are well-known to harbor members with biocontrol ability. Therefore, bacterial isolates of these genera (**Table 4**) were tested for their antagonistic activity against plant-pathogenic fungi *in vitro*. Positive results were indicated by inhibition zones. *Pseudomonas* isolates Cha2324b_22, Cha2324b_23, Cha2324b_12, Cha2324b_30 and NB7_11 (**Figure 6C, D, F, G, H**) inhibited growth of the tested plant-pathogenic fungi *Rhizoctonia solani*, *Fusarium oxysporum* and *Fusarium culmorum*. *Bacillus* isolate Cha2324a_8 (**Figure 6E**) inhibited growth of the plant-pathogenic fungus *Rhizoctonia solani*. *Bacillus* isolate Cha2930_14 and Cha2324a_1 (**Figure 6A, B**) as well as negative control *Luteibacter* isolate Cha2324a_16 (**Figure 6I**) showed no growth inhibition of the tested plant-pathogenic fungi. The positive control for antifungal activity *B. velezensis* FZB42 inhibited the plant-pathogenic fungi *Rhizoctonia solani*, *Fusarium oxysporum* and *Fusarium culmorum* (**Figure 6K**). Clear evaluation of *Alternaria alternata* plates was not possible, because the fungus did not reach the interaction zone with bacteria due to overall low growth on the plates. PCR detection of genes encoding for antimicrobial

lipopeptides revealed amplification of surfactin (*srfC*), iturin A (*ituD*) and bacillomycin D (*bamC*) genes in the positive control strain FZB42, but no amplification in the other tested *Bacillus* isolates (**Table 4**). Most tested isolates, which inhibited growth of the tested plant-pathogenic fungi, belong to the genus *Pseudomonas*, which was expected and confirmed the assumption to find potent plant-pathogenic antagonists among members of this genus.

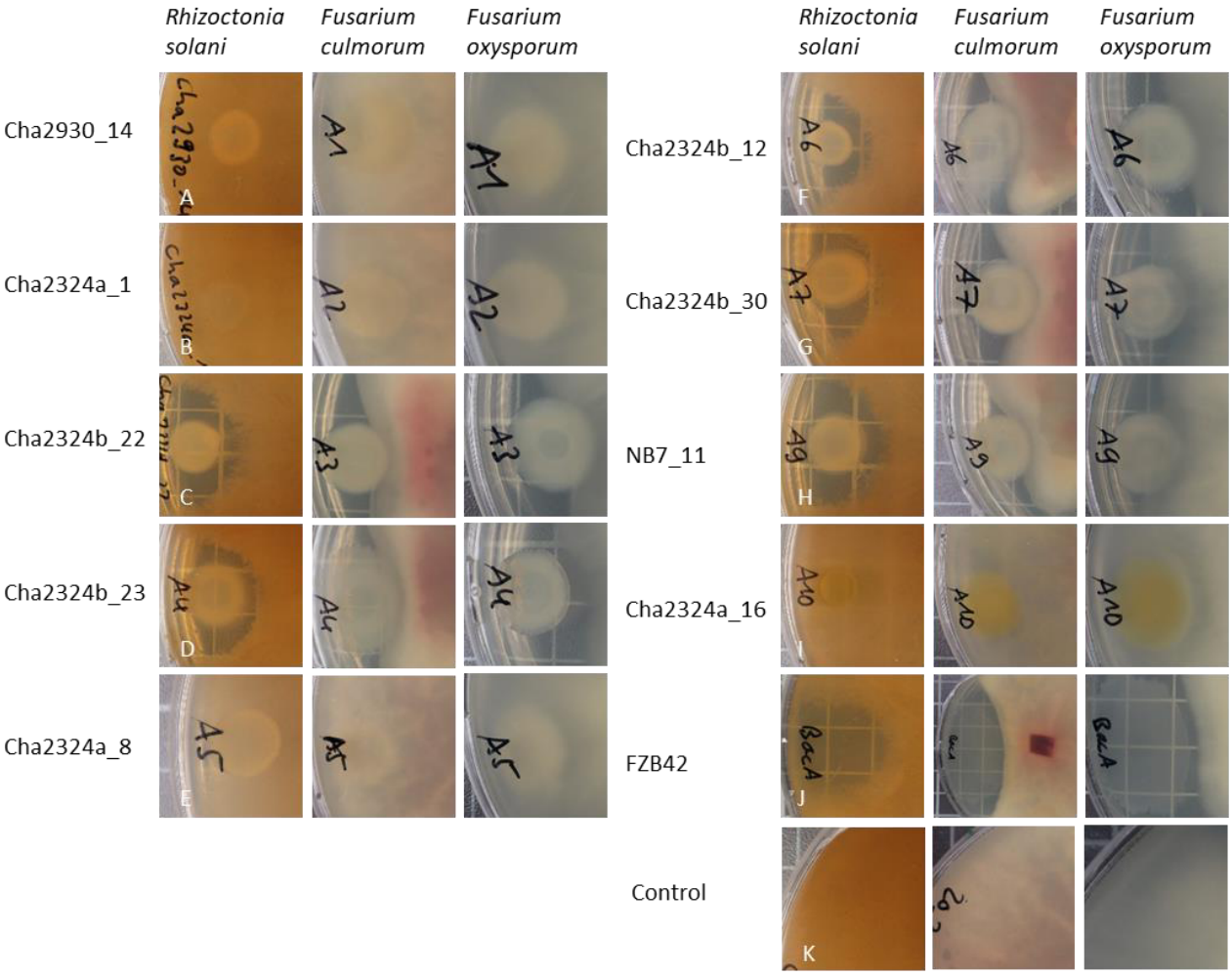

Figure 6: Antagonistic activities of selected Scheyern isolates. Confrontation assay of *Bacillus* isolates (**A, B, E**) and *Pseudomonas* isolates (**C, D, F, G, H**) against plant pathogenic fungi. *Luteibacter* Cha2324a_16 (**I**) served as negative control and FZB42 (**J**) served as positive control. Plates were evaluated after 14 days of cultivation. Antagonistic activity is indicated by inhibition zone around bacteria. Control plates (**K**) without bacteria.

Table 4: Biocontrol activity of selected isolates against plant pathogenic fungi.

Isolate ID	Genus	Biocontrol activity	Lipopeptide gene
Cha2930_14	*Bacillus*	no	No
Cha2324a_1	*Bacillus*	no	No
Cha2324b_22	*Pseudomonas*	yes	Not tested
Cha2324b_23	*Pseudomonas*	yes	Not tested
Cha2324a_8	*Bacillus*	Only *Rhizoctonia solani*	No
Cha2324b_12	*Pseudomonas*	yes	Not tested
Cha2324b_30	*Pseudomonas*	yes	Not tested
NB7_11	*Pseudomonas*	yes	Not tested
Cha2324a_16	*Luteibacter*	no	Not tested
FZB42	*Bacillus*	yes	*SrfC, BamC, ItuD*

2.4.2.2 Pairwise interaction of bacterial isolates reveals growth inhibition *in vitro*

To exclude limitations in the beneficial effect caused by competition the compatibility of the members in a microbial consortium is important. Therefore, Scheyern isolates were tested for reciprocal growth inhibition *in vitro* to exclude growth inhibiting isolates from the consortium. The growth inhibiting effect was stronger in short distance between the colonies (example: **Figure 7A, B**). Analysis of pairwise microbial interaction revealed a mild inhibition of one other isolate by R2A20_2, SCA27_60 and Cha2324b_30, belonging to different genera. All isolates, which inhibited more than one isolate were associated with the genus *Pseudomonas* (**Table 5**). The isolate SCA7 inhibited 11 other bacterial isolates in growth, which was the highest detected number (**Table 5**). The growth inhibition of SCA7 was only detectable in comparison to other plates without growth inhibition, as shown for e.g. R2A20_2 (**Figure 7 C, D**). The colonies on plates confronted with SCA7 were equally inhibited in growth independent from the distance to SCA7, which suggested that the reaction was equally strong on the whole plate (**Figure 7C, D**). This could indicate a mediation of the reaction by e.g. volatiles.

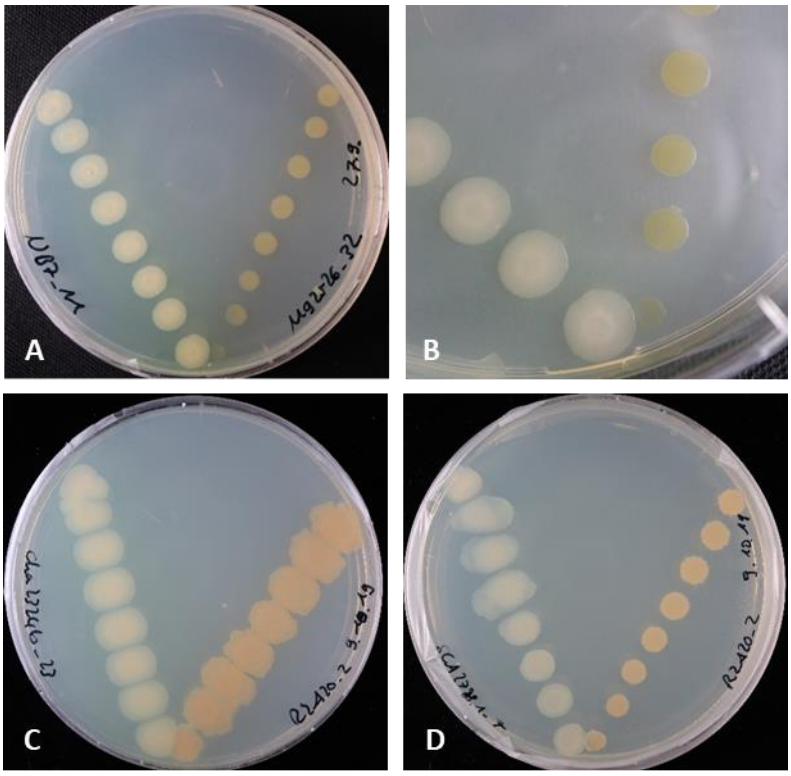

Figure 7: Examples of pairwise microbial interaction between (**A**) *Pseudomonas* sp. NB7_11 (white colonies) inhibiting *Sphingomonas* sp. M92526_32 (yellow colonies) after 4 days of growth. (**B**) shows a detailed picture of (**A**). (**C**) *Pseudomonas* sp. Cha2324b_23 (white colonies) and *Flavobacterium* sp. R2A20_2 (yellow colonies) without growth inhibition after 6 days of growth. In comparison (**D**) shows *Pseudomonas* sp. SCA7 (white colonies) and *Flavobacterium* sp. R2A20_2 (yellow colonies) with growth inhibition over the whole plate after 6 days of growth.

Most inhibiting isolates belong to the genus *Pseudomonas* as expected and SCA7 showed the strongest inhibiting effect, which could be related to the biocontrol traits (section 2.4.2.1) and the production of siderophores (**Table 3**) of the same isolates. The results led to the exclusion of SCA7, NB7_11 and Cha2324b_22 from the consortium experiments to avoid competition. SCA7 was further characterized in section 2.11.1. For application of the isolates in plant experiments including drought stress they need to be tolerant to abiotic stress condition, which was tested in the next chapter.

Table 5: Growth inhibiting isolates.

Bacterial growth inhibiting isolate	**Growth inhibited bacterial isolate**
Flavobacterium sp. R2A20_2	*Luteibacter* sp. Cha2324a_16
Streptomyces sp. SCA27_60	*Bacillus* sp. Cha2930_14
Pseudomonas sp. Cha2324b_30	*Dyadobacter* sp. M92526_31
Pseudomonas sp. Cha2324a_4	*Pseudomonas* sp. Cha2324b_12 *Dyadobacter* sp. M92526_31
Pseudomonas sp. Cha2324b_12	*Bacillus* sp. Cha2930_14 *Dyadobacter* sp. M92526_31
Pseudomonas sp. Cha2324a_18	*Bacillus* sp. Cha2324a_8 *Dyadobacter* sp. M92526_31 *Luteibacter* sp. Cha2324a_16
Pseudomonas sp. Cha2324b_22	*Bacillus* sp. Cha2324a_1 *Bacillus* sp. Cha2324a_8 *Dyadobacter* sp. M92526_31 *Luteibacter* sp. Cha2324a_16 *Sphingomonas* sp. M92526_32
Pseudomonas sp. NB7_11	*Bacillus* sp. Cha2324a_1 *Dyadobacter* sp. M92526_31 *Pseudomonas* sp. Cha2324a_4 *Luteibacter* sp. Cha2324a_16 *Sphingomonas* sp. M92526_32 *Variovorax* sp. M92526_27
Pseudomonas sp. SCA7	*Bacillus* sp. Cha2930_14 *Bacillus* sp. Cha2324a_1 *Dyadobacter* sp. M92526_31 *Flavobacterium* sp. R2A20_2 *Luteibacter* sp. Cha2324a_16 *Rhizobium* sp. M92526_34 *Pseudomonas* sp. Cha2324b_12 *Pseudomonas* sp. NB7_11 *Sphingomonas* sp. M92526_32 *Variovorax* sp. M92526_27 *Variovorax* sp. SCA27_61

2.4.3 Characterized bacterial isolates show stress tolerance traits *in vitro*

Bacteria were isolated from sampling sites during a hot and dry summer period. Therefore, I hypothesized to isolate many bacteria tolerant to heat, salt and osmotic stress, related to their potentially drought stressed habitat. The tested traits were also relevant for the upcoming experiments where plants were exposed to drought stress. In order to provide their potential plant beneficial effect, the applied isolates needed to survive under these harsh conditions.

2.4.3.1 Growth ability at different temperature ranges

Temperature tolerance of the tested isolates ranged from 28°C to 45°C (**Table 6**). Eight isolates were tolerant up to 28°C, ten isolates were tolerant up to 35°C, four isolates were tolerant up to 37°C, M92526_27 was tolerant up to 40°C and four isolates of the genera *Bacillus* as well as *Luteibacter* were tolerant up to 45°C. M92526_34 was not tested for temperature tolerance. High temperature tolerance of *Bacillus* sp. was expected, as these bacteria are able to withstand difficult environmental conditions e.g. via spore formation.

2.4.3.2 Osmotic stress tolerance

All isolates except of Cha2324a_8 were tolerant to osmotic stress up to -1.5 MPa, which was the tested maximum (**Table 6**). As the tested bacteria were isolated from rhizosphere after a hot and dry summer period osmotic stress tolerance as adaption to these abiotic conditions was expected.

2.4.3.3 Salt stress tolerance

Salt tolerance ranged from no salt tolerance to 7.5% NaCl in the medium (**Table 6**). Seven isolates were tolerant up to 1%, Cha2830_14 and Cha2324_1 were tolerant up to 2.5%, nine isolates were tolerant up to 3.5% (**Table 6**). The highest salt tolerance of 7.5% NaCl in the medium showed NB17_5 belonging to the genus *Rhodococcus*, followed by further *Rhodococcus* and *Arthrobacter* isolates tolerant to up to 5.5% NaCl in the medium (**Table 6**), which was expected for both of these well-known stress-tolerant genera and is consistent with the findings on high stress tolerance of *Rhodococcus* sp. also shown in section 2.10.2.

A total of 29 Scheyern isolates, were evaluated and a surprisingly high proportion showed stress tolerance against the tested abiotic stresses *in vitro* (**Table 6**), indicating their ability to survive under drought stress in the rhizosphere and showing that it is possible to isolate many drought stress tolerant bacteria from a drought stressed habitat.

Table 6: Stress tolerance traits of characterized isolates.

Isolate ID	Genus	Max. growth temperature (°C)	Max. salt conc. (%)	Osmotic Stress (-1.5 MPa)
Cha2930_14	*Bacillus*	45	2.5	+
M92526_32	*Sphingomonas*	35	1	+
R2A20_2	*Flavobacterium*	35	1	+
Cha2324a_1	*Bacillus*	45	2.5	+
Cha2324a_4	*Pseudomonas*	28	3.5	+
Cha2324b_23	*Pseudomonas*	28	3.5	+
Cha2324b_3	*Pedobacter*	35	1	+
Cha2324a_8	*Bacillus*	45	3.5	-
SCA7	*Pseudomonas*	not tested	not tested	+
Cha2324b_12	*Pseudomonas*	28	5.5	+
Cha2324b_30	*Pseudomonas*	28	3.5	+
Cha2324a_16	*Luteibacter*	45	3.5	+
M92526_27	*Variovorax*	40	1	+
Cha2324a_18	*Pseudomonas*	28	3.5	+
SCA27_61	*Variovorax*	37	1	+
SCA27_60	*Streptomyces*	37	1	+
M92526_31	*Dyadobacter*	37	1	+
NB17_5	*Rhodococcus*	37	7.5	+
2xTY356_6	*Rhodococcus*	35	3.5	+
2xTY356_27	*Rhodococcus*	35	5.5	+
R2A20_29M	*Rhizobacter*	35	0	+
R2A20_29R	*Polaromonas*	35	0	+
M92526_34	*Rhizobium*	not tested	0	+
2xTY356_31	*Arthrobacter*	28	3.5	+
M925_13	*Arthrobacter*	35	3.5	+
2xTY356_21	*Arthrobacter*	28	5.5	+
2xT56_7	*Arthrobacter*	35	5.5	+
M925_14	*Arthrobacter*	35	5.5	+
NB17_19	*Arthrobacter*	28	5.5	+

2.5 Effect of consortia on plant growth in wheat under drought and non-drought conditions

The characterized isolates were assembled as consortia and applied to wheat plants under drought and non-drought conditions in order to verify if the identified PGP traits *in vitro* have actually a beneficial effect *in planta* and identify the best assembling strategy. The consortia were assembled

from the characterized isolates based on present PGP traits (K1) for functional redundancy and complementation of functions, abundance in the natural wheat microbiota (K2) or absent PGP traits *in vitro* (K3) as negative control.

All plants treated with a bacterial consortium recovered from drought stress, whereas in the control treatment one plant did not recover. Most plants recovered after one night (ON). More plants treated with consortium K1 and K2 recovered after two nights (2 ON) compared to K3 and control (**Figure 8**). The recovery rate from drought stress was only evaluated in consortium experiment 3.

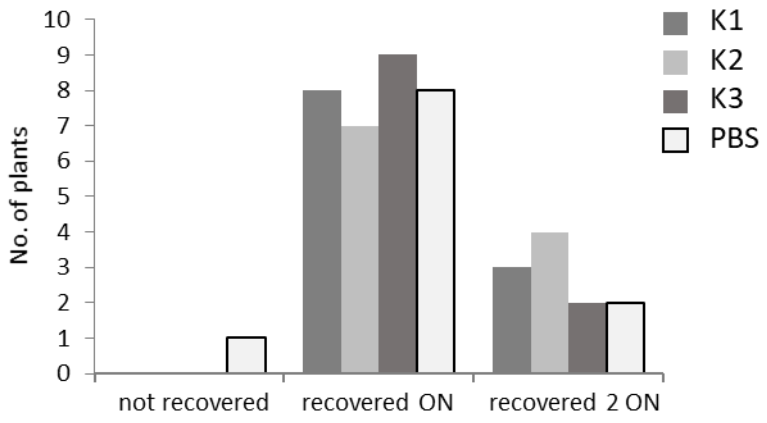

Figure 8: Recovery time of wheat plants inoculated with consortia. Recovery was evaluated of wheat plants inoculated with consortium K1, K2, K3 and control (PBS) grown under drought conditions in consortium experiment 3 after one night (ON) or two nights (2 ON). N = 10

For increase of sample size to receive a higher statistical power, the results of consortium experiments 1-3 were combined according to the requirements of the LM model. Under drought stress plants inoculated with K1 had a significant lower shoot dry weight ($p= 0.04892$) and shoot length ($p= 0.000137$) compared to the control PBS (**Figure 9H, I**). Differences of these parameters compared to consortia K2 and K3 were analyzed based on data of experiment 3 only and showed no significant difference (**Figure 9B, C**). Other tested plant parameters, such as root length, root dry weight, complete dry weight and number of leaves, were not significant different under drought stress (**Figure 9**). Fresh weight was excluded from analysis, because the data would have been biased due to the drought stress treatment.

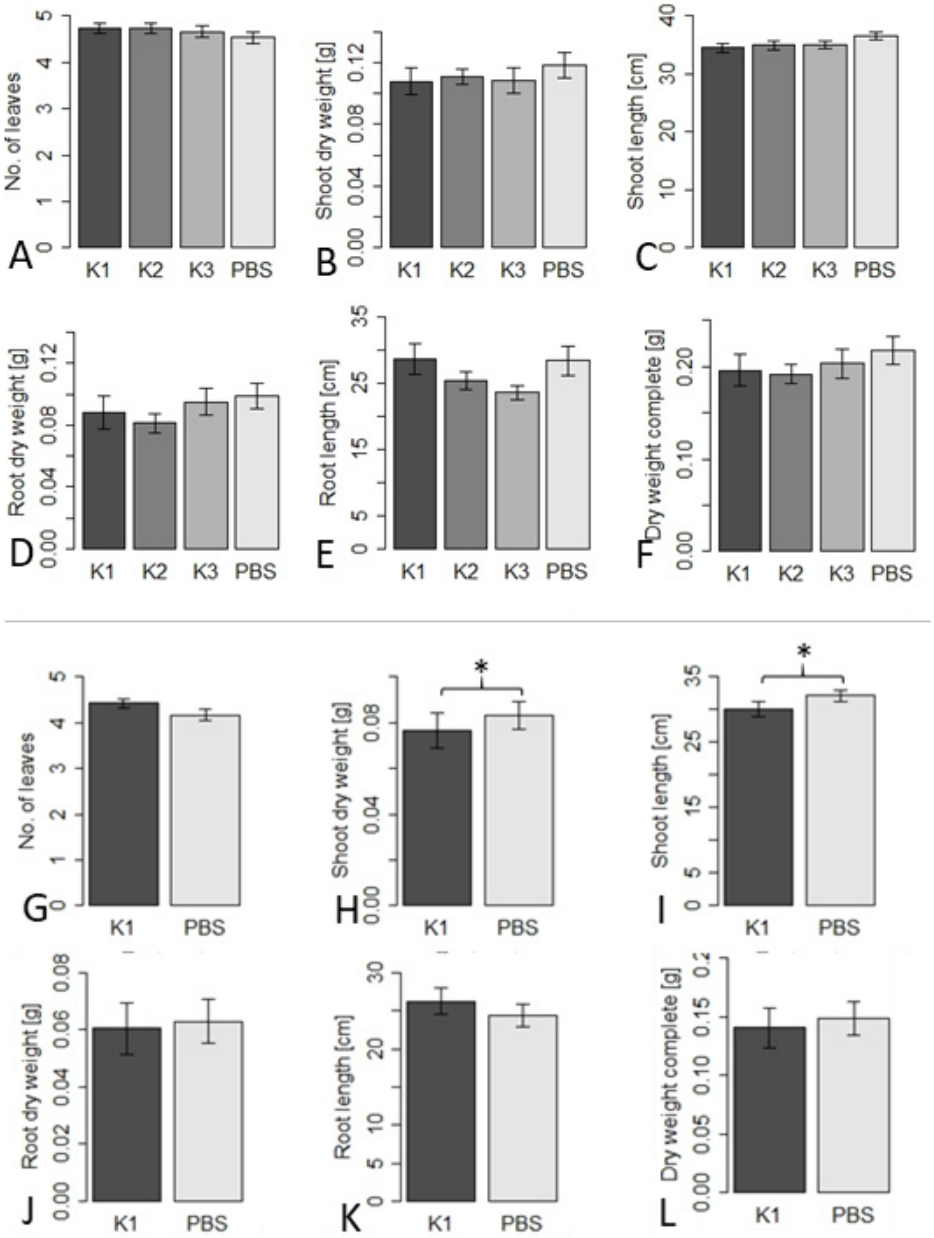

Figure 9: Effect of consortia on wheat plants grown under drought conditions. (**A-F**) shows plant parameter of wheat plants inoculated with consortia K1, K2, K3 and control (PBS) in experiment 3 (fresh weight N = 11, dry weight N = 8). (**G-L**) shows combined results of consortium experiment 1 and 3 of wheat plants inoculated with K1 and control (PBS) (N = 26). Evaluated plant parameters were the number of leaves (**A, G**), shoot dry weight (**B, H**), shoot length (**C, I**), root dry weight (**D, J**), root length (**E, K**) and complete dry weight (**F, L**). Fresh weight was excluded due to bias by drought treatment. Error bars indicate standard error. Significant difference is indicated by asterisks representing * = $P < 0.05$.

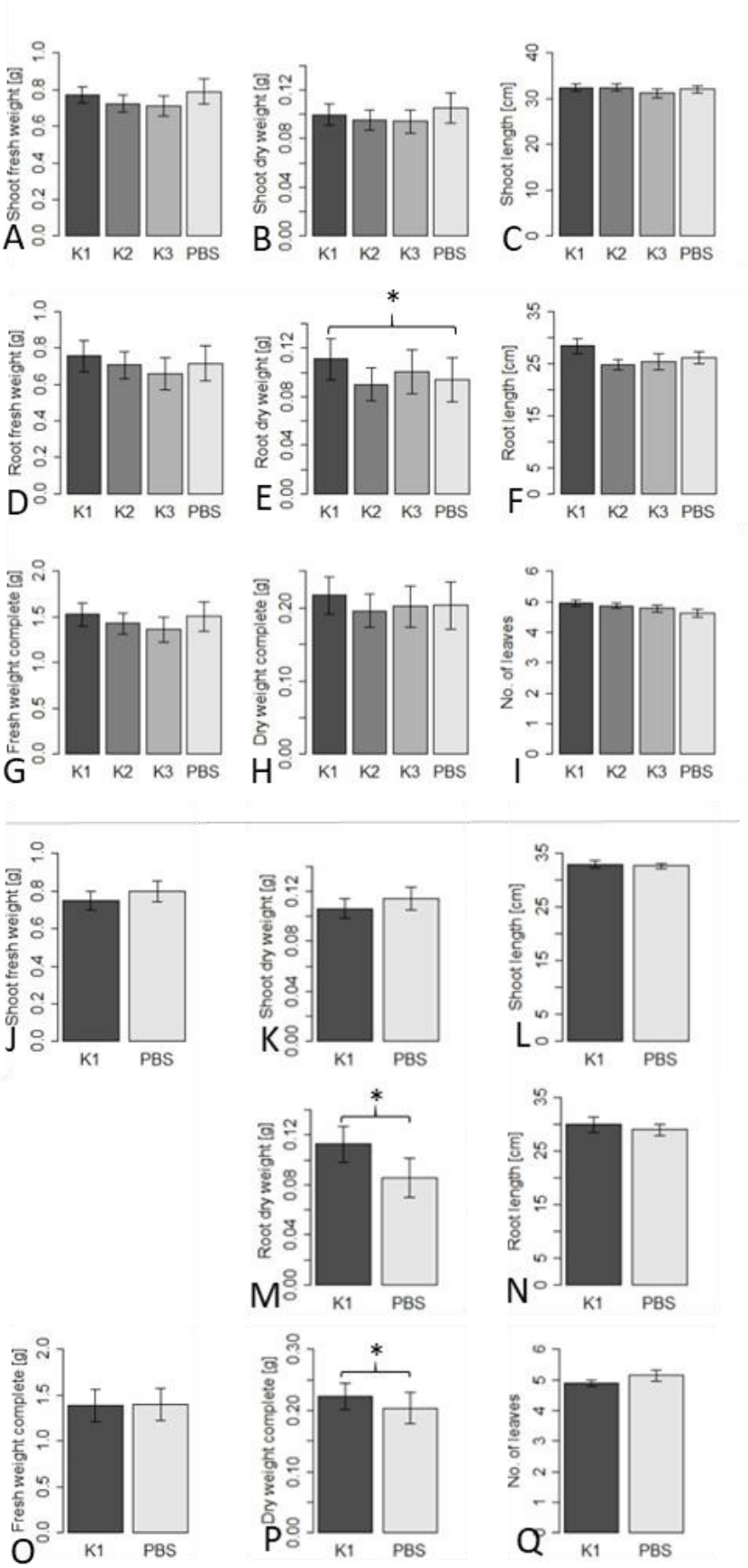
A
Shoot fresh weight [g]
0.0 0.2 0.4 0.6 0.8 1.0
K1 K2 K3 PBS
B
Shoot dry weight [g]
0.00 0.04 0.08 0.12
K1 K2 K3 PBS
C
Shoot length [cm]
0 10 20 30 40
K1 K2 K3 PBS
D
Root fresh weight [g]
0.0 0.2 0.4 0.6 0.8 1.0
K1 K2 K3 PBS
E
Root dry weight [g]
0.00 0.04 0.08 0.12
*
K1 K2 K3 PBS
F
Root length [cm]
0 5 15 25 35
K1 K2 K3 PBS
G
Fresh weight complete [g]
0.0 0.5 1.0 1.5 2.0
K1 K2 K3 PBS
H
Dry weight complete [g]
0.00 0.10 0.20
K1 K2 K3 PBS
I
No. of leaves
0 1 2 3 4 5 6
K1 K2 K3 PBS
J
Shoot fresh weight [g]
0.0 0.2 0.4 0.6 0.8 1.0
K1 PBS
K
Shoot dry weight [g]
0.00 0.04 0.08 0.12
K1 PBS
L
Shoot length [cm]
0 5 15 25 35
K1 PBS
M
Root dry weight [g]
0.00 0.04 0.08 0.12
*
K1 PBS
N
Root length [cm]
0 5 15 25 35
K1 PBS
O
Fresh weight complete [g]
0.0 0.5 1.0 1.5 2.0
K1 PBS
P
Dry weight complete [g]
0.00 0.10 0.20 0.30
*
K1 PBS
Q
No. of leaves
0 1 2 3 4 5 6
K1 PBS

Figure 10: Effect of consortia on wheat plants grown under non-drought conditions. (**A-I**) shows combined results of consortium experiment 2 and 3 of wheat plants inoculated with consortium K1, K2, K3 and control (PBS) (K1 N = 24, K2 N = 26, K3 N = 25, PBS N = 20). (**J-Q**) shows combined results of consortium experiment 1 and 3 of wheat plants inoculated with consortium K1 and control (PBS) (N = 25). Evaluated plant parameters were shoot fresh weight (**A, J**), shoot dry weight (**B, K**), shoot length (**C, L**), root fresh weight (**D**), root dry weight (**E, M**), root length (F, N), complete fresh weight (**G, O**), complete dry weight (**H, P**) and the number of leaves (**I, Q**). Root fresh weight was excluded for experiment 1 and 3 due to bias in experiment 1 (see results). Error bars indicate standard error. Significant difference is indicated by asterisks representing * = $P < 0.05$.

Under non-drought conditions plants inoculated with K1 had an increased root dry weight compared to the control (**Figure 10E** (p = 0.02123)**, Figure 10M** (p= 0.0000957)) as well as an increased complete dry weight (**Figure 10P,** p= 0.02986). Increase in root dry weight was almost significant different between K1 and K2 (p-value = 0.07551) (**Figure 10E**). Root dry weight results were reproducible throughout the experiments. Root fresh weight was excluded from one analysis, because plant roots of experiment 1 were exsiccated short after harvest before parameter could be taken. Other tested plant parameters showed no significant difference under non-drought conditions (**Figure 10**). The results indicate a reproducible beneficial effect of K1 on root growth under non-drought conditions, but not under drought stress, which was unexpected. The question emerged if the applied bacteria could have a beneficial effect on the molecular level, which was addressed in the next paragraph. Further experiments and analysis were performed to understand the dynamics of the interactions under drought stress as well as to further optimize the consortium composition.

2.6 Quantitative gene expression analysis of consortium experiments

The gene expression of drought stress related genes in wheat was evaluated to identify potential molecular effects of the bacterial inoculation under drought stress. The differential gene expression analysis revealed an upregulation of the genes TaMYB80, TaLOX, TaGSTU4 and TaRD29B, whereas genes TaSOD, TaCAT, TaMPK4, TaGSTZ and TaDREB2A are downregulated under drought conditions indicated by the fold change ratio (**Figure 11**). No differential gene expression was observed for the 10 other analyzed genes and no differential gene expression was observed between the consortium treatments. This indicates that the applied bacteria had no effect on the gene expression of the drought related genes in wheat tested in this study.

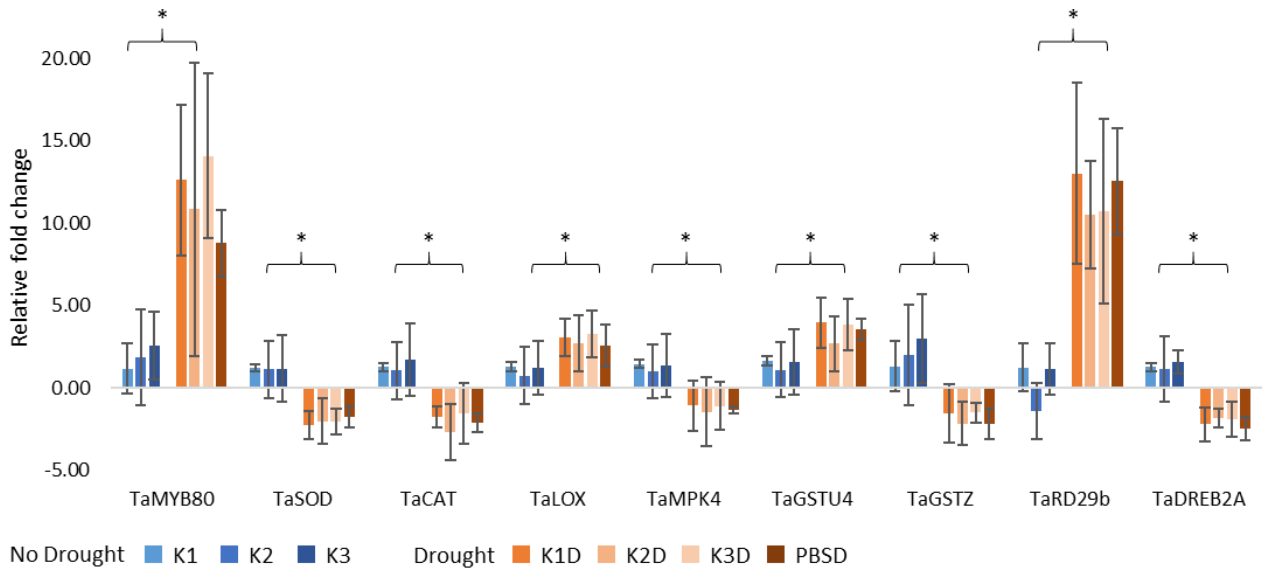

Figure 11: Differentially expressed drought-stress related genes in wheat. Relative fold change of the genes expressed in shoots of consortium experiment 3 were normalized to the non-drought control (PBS). Fold change ratio for non-drought conditions is depicted in blue. Fold change ratio for drought conditions is depicted in orange. Error bars indicate standard deviation. Significant difference is indicated by asterisks representing * = $P < 0.05$, N = 3.

2.7 Bacterial load consortium experiment 3

The bacterial load was analyzed in samples of consortium experiment 3 to identify the effect of drought stress as well as application of the consortia on absolute bacterial numbers in the rhizosphere. Bacterial numbers were not significantly different between the different consortia and the control. Under drought stress bacterial numbers were significant higher compared to non-drought conditions (**Figure 12, Supplementary Figure S2**), which was an unexpected result. Further analysis was performed to identify drought or application induced changes in the microbial composition.

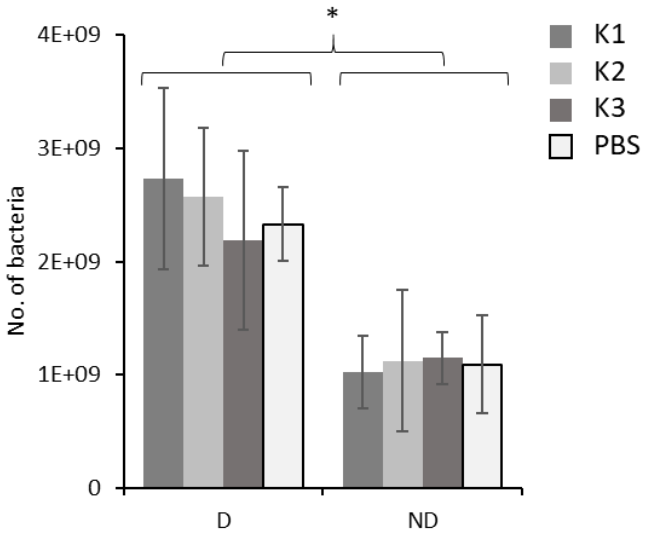

Figure 12: Bacterial load on wheat roots. Numbers of bacteria were evaluated per 1 g wheat root and rhizosphere of consortium experiment 3. Error bars indicate standard deviation. Significant difference is indicated by asterisks representing * = $P < 0.05$, N = 5.

2.8 Amplicon-based community profiling of consortium experiments 1 and 3

The microbial community was analyzed to estimate effects of drought stress and the application of the consortia on the microbial composition as well as to verify the establishment of the applied isolates. The 16S rRNA gene amplicon sequencing of 84 root and rhizosphere samples from consortium experiment 1 and 3 using Illumina MiSeq technology generated a total of 8,989,001 reads. Merging and filtering yielded in 7,784,592 high-quality sequences with a range of 9,947 to 186,627 sequences per sample and a median of 86,456. After removal of mitochondrial and chloroplast OTUs the sequences were clustered in 617 species-level Operational Taxonomic Units (OTUs; ≥ 97% similarity) applying an abundance cutoff of 0.01%. The rarefaction curve was asymptotic indicating a sufficient sequencing depth for exploration of bacterial communities. Effective richness was significantly higher in K2 compared to the control under drought stress conditions (**Supplementary Figure S3A**, p-value = 0.0289). Evenness was significantly higher in K1 and K2 compared to the control (**Supplementary Figure S3B**, p-value = 0.017). Under non-drought conditions both parameters were not significantly different between the treatments. Both parameters were not significantly different between drought and non-drought conditions. The microbial composition between the consortium treatments was significantly different (**Figure 13A**: p-value = 0.001). The microbial composition under drought and non-drought conditions as well as

between pre-drought, drought, non-drought, recovery from drought and end of experiment under non-drought condition (= end no drought) was significantly different (**Figure 13B, C**, p-value = 0.001; **Figure 14**).

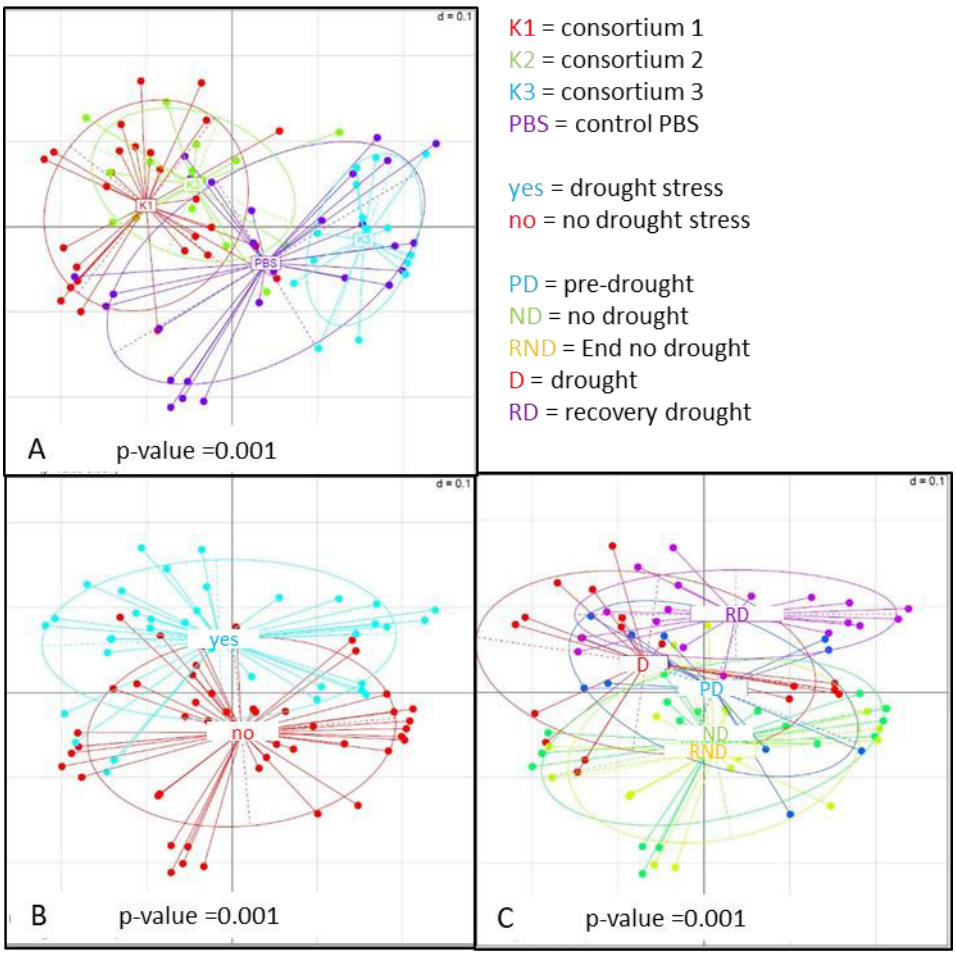

Figure 13: ß-diversity in consortium experiments. Root and rhizosphere microbiota of combined consortium experiments 1 and 3 separated by the factor (**A**) consortium, (**B**) drought stress and (**C**) drought stress at different sampling points (PD: pre-drought, D: drought, ND: no drought, RD: recovery drought, RND: end of experiment without drought). Data is presented in two-dimensional MDS plots. Significant differences are indicated by $P < 0.05$; d = 0.1 refers to 10% difference per grid.

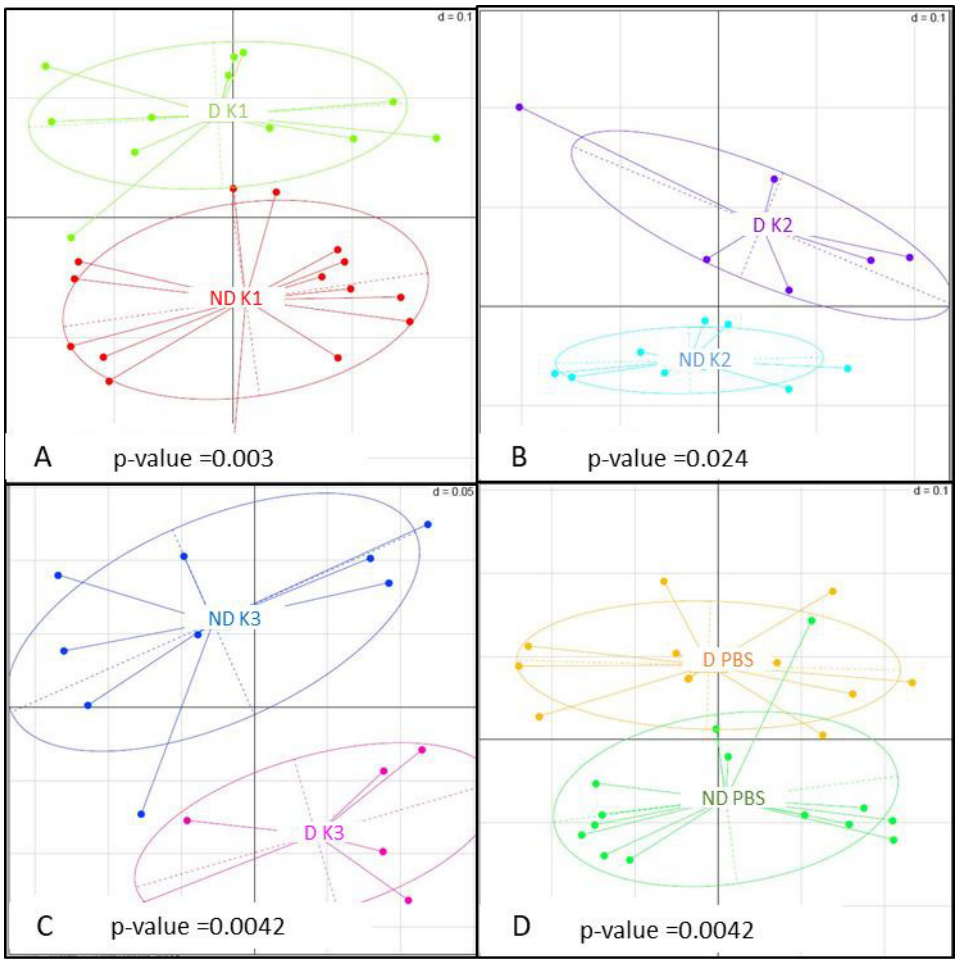

Figure 14: ß-diversity in consortium experiments (pairwise comparison). Root and rhizosphere microbiota of combined consortium experiments 1 and 3 presented with pairwise comparison of drought and non-drought stress samples in consortium K1 (**A**), K2 (**B**), K3(**C**) and PBS (**D**). Data is presented in two-dimensional MDS plots. Significant differences are indicated by $P < 0.05$; d = 0.1 refers to 10% difference per grid.

A total of 272 genera were identified in the taxonomic analysis of the analyzed dataset. Abundances of taxa differed under the different abiotic conditions and between the different consortia (**Supplementary Figure S4**). The genus *Rheinheimera* was high abundant under non-drought conditions. The genus *Massilia* was equally distributed in all samples. 12 of 13 genera with representatives in the consortium K1 were identified in the K1 samples at the end of the experiment after 29 days. The genus *Polaromonas* was not identified. The genera *Luteibacter* and *Variovorax* were exclusively found in K1. The genera *Sphingomonas*, *Flavobacterium*, *Variovorax*, *Dyadobacter* and an unknown genus belonging to *Rhizobiacea* are high abundant under non-drought conditions in K1 treatment, and *Flavobacterium* also in K2 treatment. The genus

Lysobacter was enriched in samples with treatment K1 in both conditions. Under drought stress the genera *Variovorax*, *Flavobacterium*, *Sphingomonas* and *Dyadobacter* were high abundant in samples with treatment K1. *Flavobacterium* and *Sphingomonas* were enriched in treatment K2 under drought stress. The genera *Paenibacillus*, *Limnohabitans* and *Rhodococcus* were enriched under drought stress conditions in samples with treatment K3 and control samples. Proteobacteria were enriched in K3 and the control treatment under drought and non-drought conditions.

For 22 consortium isolates 16S rRNA gene sequences showed similarities >97% with OTUs from the amplicon-based community profiling (**Supplementary Table S8**). For example, OTU 2, 11, 14 and 33 showed highest similarity with the inoculated isolates of the genera *Flavobacterium, Sphingomonas, Dyadobacter* and *Variovorax*. The results indicate a significant influence of drought stress and the application of microbial consortia on the microbial composition, which was expected, and a substantial fraction of the applied isolates was present in the microbial community. Thus, the establishment of most consortium members in the rhizosphere of treated wheat plants was verified. The question emerged if the identified genera are also correlate in their occurrence, which was analyzed in the next chapter.

2.9 Co-occurrence network analysis of consortium K1

The co-occurrence network was analyzed for consortium K1, because here the largest phylogenetic change was observed, to identify the position of OTUs representing members of the applied consortium in the network. This would help to develop new hypothesis on the role of the isolates in the consortium and the microbiome based on their position. The network analysis of drought and non-drought stressed samples of K1 obtained in consortium experiment 1 and 3 revealed a loss of correlations between the microbial OTUs under drought stress conditions (**Figure 15**). Edge density was higher under non drought conditions with 0.688 compared to drought stress conditions 0.206. However, these values were not significant due to the low sample size of six samples. Under non-drought conditions hub OTUs were OTU 22, 37, 123, 239 and 401 identified as the taxa *Emticicia*, *Pseudarthrobacter*, *Solimonadacea*, *Sphingobium* and *Rhodocyclaceae*, respectively, whereas under drought stress conditions hub OTUs 21, 60, 135, 259 and 993 were identified as the taxa *Rhodococcus*, *Rhizobiaceae*, *Legionella*, *Comamonadaceae* and *Rhizobium*, respectively (**Figure 15A**). OTUs 2, 11, 14 and 33 represent members of the consortium K1 of the genera *Flavobacterium*, *Dyadobacter*, *Sphingomonas* and *Variovorax*, respectively, and were identified to be connected in the network under non-drought stress conditions (**Figure 15B, Supplementary**

Figure S5). Under drought stress conditions the correlation between OTU 11 (*Sphingomonas*) and OTU 33 (*Variovorax*) was lost (**Figure 15B, Supplementary Figure S5**), which was unexpected. The results suggest a key role in the interaction with the plant of the isolates in K1 belonging to the genera *Flavobacterium*, *Dyadobacter*, *Sphingomonas* and *Variovorax*, which was tested in the following experiment. Additionally, if the microbial consortium could be optimized based on these results or if the observed effect was caused by a single high abundant member of K1 was also tested in the next experiment.

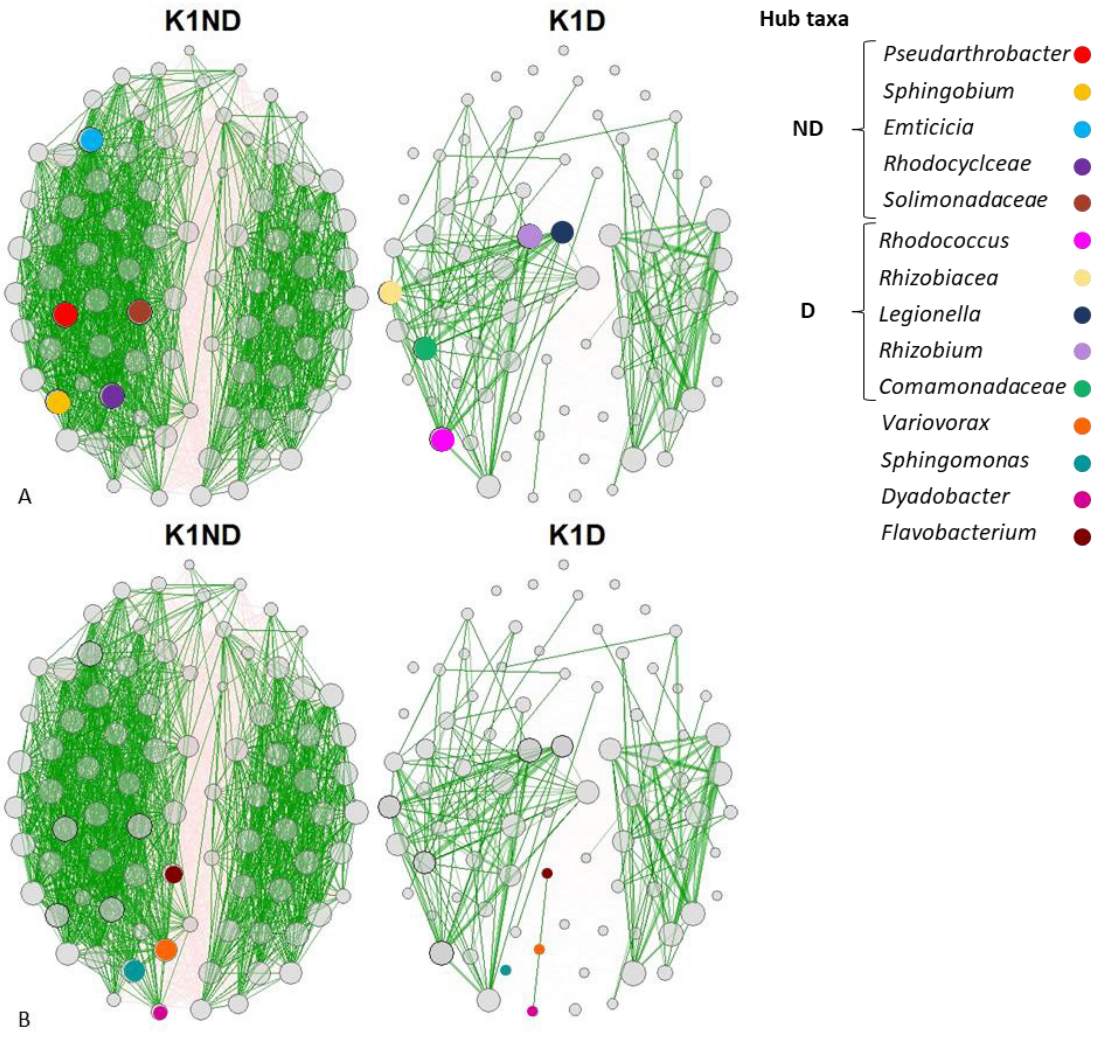

Figure 15: Co-occurrence networks of bacterial genera present in K1. Combined data of consortium experiment 1 and 3 under drought (D) and non-drought conditions (ND) represent hub species (**A**) and the genera *Variovorax*, *Sphingomonas*, *Flavobacterium* and *Dyadobacter*, which were high abundant in the K1 microbiota and selected for consortium K4 (**B**). The correlation coefficient was calculated for pairwise relative abundance of bacterial genera using Pearson correlation implemented in the used R-package NetCOMI (Peschel *et al*., 2020), N = 6.

2.10 Effect of optimized consortium K4 on plant growth

The five isolates *Variovorax* sp. SCA27_61, *Variovorax* sp. M92526_27, *Flavobacterium* R2A20_2, *Sphingomonas* sp. M92526_32 and *Dyadobacter* sp. M92526_31 were selected based on their high abundance in the microbial composition in samples of K1 (section 2.6) as well as their connectedness in the co-occurrence network under non-drought conditions (section 2.9) to analyze the relevance of their potential interaction, to optimize the applied consortium and to test if the observed effect was caused by only a single member of the consortium. The isolates were applied single as well as combined as consortium K4 to evaluate the relevance of their interaction. K1 served as positive control. The results showed a significant increase of 13-16% in root dry weight in plants inoculated with K4 or K1 compared to treatments D, F, S, VM and the control PBS (**Figure 16G,** p-value = 0.044). The complete dry weight of the plant increased significantly up to 10% under treatment with K1 and K4 compared to D, F, S, VM and the control PBS (**Figure 16I,** p-value = 0.0379). Shoot length increased significantly up to 6% in plants treated with K4 compared to K1, VM, VS and control PBS (**Figure 16H** p-value = 0.067), whereas treatment VS significantly decreased shoot length. The number of leaves was not significant different between the treatments. All plants had four leaves except for two plants in K1 and VS and one plant in D, F and VM with five leaves. Fresh weight of root and shoot, shoot dry weight and root length showed no significant difference between the plants under treatment (**Figure 16**). Plants treated with K4 had a changed root architecture compared to PBS (**Figure 16B**). Overall, K1 and K4 had a beneficial effect on plant biomass compared to the single strains and the control, with a stronger effect of K4. Thus, the results indicate that the interaction of the isolates in K4 play a key role in the observed effect and the application was more successful than the application as single strains.

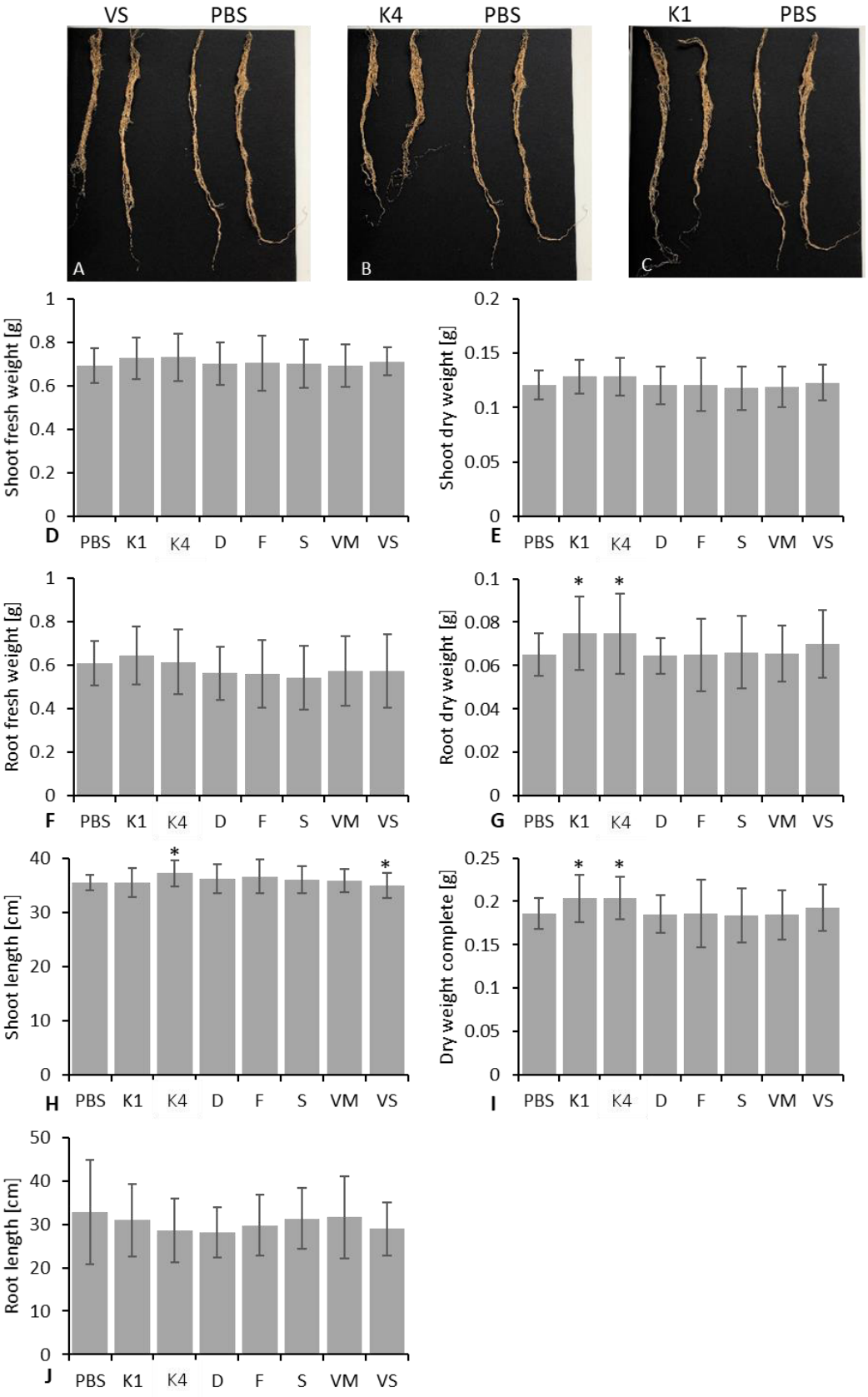
VS
PBS
K4
PBS
K1
PBS
A
B
C
Shoot fresh weight [g]
D
Shoot dry weight [g]
E
Root fresh weight [g]
F
Root dry weight [g]
G
Shoot length [cm]
H
Dry weight complete [g]
I
Root length [cm]
J
PBS K1 K4 D F S VM VS

Figure 16: Effect of consortia and single strains on wheat plants under non-drought conditions. Representative wheat plants inoculated with the single strain *Variovorax* sp. SCA27_61 (VS) (**A**), consortium K4 (K4) (**B**), consortium K1 (**C**) in direct comparison to control (PBS) grown under non-drought conditions. Evaluated plant parameters were shoot fresh weight (**A**), shoot dry weight (**B**), root fresh weight (**C**), root dry weight (**D**), shoot length (**E**), complete dry weight (**F**) and root length (**H**). PBS = control, K1 = consortium K1, K4 = consortium K4, D = *Dyadobacter* sp. M92526_31, F = *Flavobacterium* sp. R2A20_2, S = *Sphingomonas* sp. M92526_32, VM = *Variovorax* sp. M92526_27, VS = *Variovorax* sp. SCA27_61. Error bars indicate standard deviation. Significant difference is indicated by asterisks representing * = $P < 0.05$, N = 25.

2.11 Genomic analyses of *Pseudomonas* sp. SCA7 and *R. qingshengii* RL1

An additional approach to select and identify plant beneficial candidates in depth includes whole genome sequencing, which was used for the wheat isolate *Pseudomonas* sp. SCA7 and the rucola isolate *R. qingshengii* RL1.

2.11.1 *Pseudomonas* sp. SCA7

Pseudomonas sp. SCA7 showed PGP traits *in vitro* (**Table 3**) and strongly inhibited growth of 11 other bacterial strains (**Table 5**), which could be mediated by volatile production. This led to the exclusion from the microbial consortia, but raised interest for a genomic characterization for PGP and biological control traits in SCA7. In order to estimate the full genomic potential as well as to phylogenetically classify SCA7 the whole genome was sequenced. The sequence assembly of SCA7 produced one linear contig with 6,782,730 bp and 59.1% G+C content available at NCBI accession number NZ_CP073104 (**Table 7**) and was used for the phylogenetic classification of SCA7.

2.11.1.1 Phylogenetic analysis of SCA7

SCA7 was phylogenetically classified to identify its closest related species and to discriminate SCA7 from pathogens, which is a pre-requisite for a future application in agriculture. Based on 16S rRNA gene sequence SCA7 was closest related to the type strains of *Pseudomonas reinekei* (99.6%) followed by *Pseudomonas helmanticensis* (99.2%), *Pseudomonas baetica* (99.1%), *Pseudomonas koreensis* (99.2%) and *Pseudomonas jessenii* (99.4%). The closest related type strains based on TYGS results were *Pseudomonas atagonensis* PS14 followed by *Pseudomonas baetica* LMG 25716, *Pseudomonas koreensis* LMG 21318, *Pseudomonas granadensis* LMG 27940, *Pseudomonas atacamensis* M7D1, *Pseudomonas moraviensis* LMG 24280, *Pseudomonas glycinae* MS586, *Pseudomonas kribbensis* KCTC 32541T, *Pseudomonas reinekei* MT1,

Pseudomonas jessenii DSM 17150 and *Pseudomonas prosekii* LMG 26867. All digital DNA-DNA-Hybridization (dDDH) values were below the species delineation threshold of 70%.

The phylogenetic tree for 307 *Pseudomonas* genomes was built out of a core of 70 genes per genome from 21630 in total (**Supplementary Figure S6**). Based on this phylogenetic tree 11 genomes of closest related *Pseudomonas* type strains to SCA7 were chosen to calculate the full genome based phylogenetic subtree built out of a core of 1510 genes per genome from 19630 in total (**Figure 17**). The ANI matrix based on 11 closest related strains revealed an ANI value of 96.23% with *Pseudomonas koreensis* CFBP13504 (NZ_QFZV01000085) and 97.23% with *Pseudomonas koreensis* CI12 (NZ_MPLD01000016) (**Supplementary Figure S7**). The ANI matrix based on 11 closest related type strains revealed closest relation to *P. helmanticiensis* (92.04%) (**Supplementary Figure S8**). All ANI values to type strains were below species delineation threshold of 94%. These surprising results indicate that SCA7 could be assigned to a novel *Pseudomonas* species together with *Pseudomonas koreensis* CFBP13504 and *Pseudomonas koreensis* CI12. Moreover, SCA7 was not closely related to pathogenic *Pseudomonas* strains.

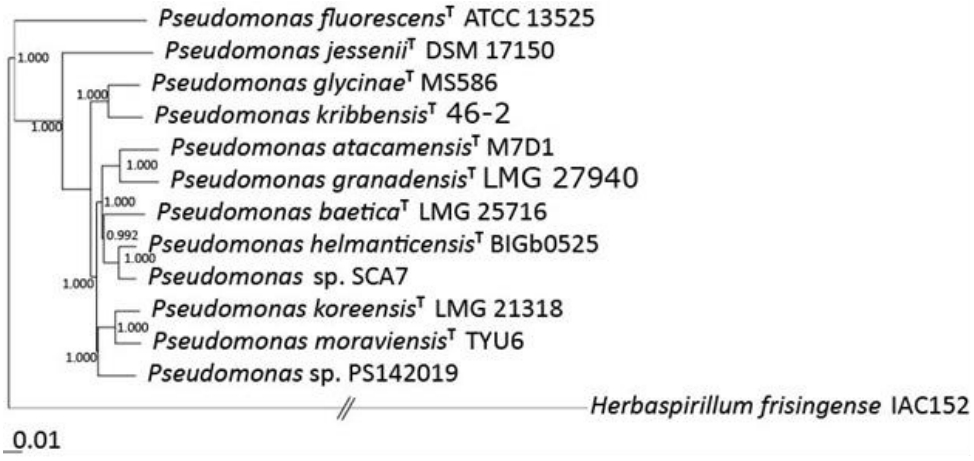

Figure 17: Maximum-likelihood phylogenetic tree of *Pseudomonas* sp. SCA7. The tree was generated from SCA7 and the 11 closest related type strains with FastTree 2.1 from a core of 1510 genes per genome. Values represent local support values based on Shimodaira-Hasegawa test (1 SH = 100% bootstrap). The scale bar represents nucleotide substitutions per site (0.01 scale = 1% nucleotide substitutions per site).

2.11.1.2 Functional annotation of SCA7

Functional annotation of the SCA7 genome was performed to identify the full genomic potential of SCA7 and develop hypotheses for upcoming experiments. For the genome of SCA7 a total of 5,981 (RAST) and 5,982 (PGAP) coding sequences were predicted and 52% of the coding sequences were sorted in 26 main RAST categories and 557 subsystems. The tool antiSMASH revealed 11 biosynthetic gene clusters (BGC) with the potential to produce antifungal compounds, arylpolyene, antibiotics, siderophores as well as BGCs, which could be involved in osmotic stress tolerance (**Supplementary Table S1**). The identified biosynthetic gene cluster for lokisin showed the highest similarity of 85% for the analyzed genome with known lokisin biosynthesis genes. The genome annotation with RAST identified genes potentially involved in (beneficial) plant-microbe interactions, microbe-microbe interactions as well as stress resistance and were partly verified by manual annotation with blastp alignment. In more details, SCA7 is equipped with several genes involved in volatile metabolism and biosynthesis, production of antifungal and antibacterial compounds, such as phenazine and bacteriocin (e.g. Colicin V) as well as auxin biosynthesis and siderophore production. Moreover, genes involved in stress resistance against osmotic stress, oxidative stress, cold shock, heat shock, detoxification, periplasmic stress and general stress response genes were identified (**Supplementary Table S2**). Based on these results the further *in vitro* and *in planta* analysis was focused on plant beneficial and biocontrol traits including volatile production performed by master's student Isabella Gantner (March 2021) under my supervision.

2.11.2 *Rhodococcus qingshengii* RL1

To my knowledge, RL1 is the first cultured member of the genus *Rhodococcus* isolated from rucola and represents a lesser known member of the rucola microbiome as well as plant microbiomes in general. Additionally, the genus is rather known for its stress resistance relevant for biotechnology applications instead of potential interactions with plants. Therefore, a broader genome analysis was performed to identify the full potential of RL1. Based on the sequencing results *in vitro* and *in planta* experiments were performed with a focus on interaction with plants as well as stress tolerance. The closely related strains djl6 and BG43 were included to compare RL1 to already known strains and understand its possible functions provided within the plant meta-organism.

2.11.2.1 Genome properties of RL1 (adapted from Kuhl *et al*. (2019, 2021))

The sequence assembly of the RL1 genome produced three contigs representing one chromosome and two plasmids (chromosome, 6,253,838 bp; plasmid 1, 144,038 bp; plasmid 2, 448,745 bp) with a G+C content of 62.4%. The chromosome and plasmid 1 were circular closed. The whole-genome sequencing project was deposited in NCBI GenBank under accession no. CP042915, CP042916, and CP042917 and in SRA (raw data) under accession no. SRR10070368 and SRR10070367 **(Table 7)**. The sequence was used to identify the phylogenetic position of RL1.

Table 7: General genome properties of RL1, djl6, BG43 and SCA7 (adapted from Kuhl *et al*. (2021)).

Genome properties	**RL1**	**Djl6**	**BG43**	**SCA7**
Chromosome size (Mbp)	6.25	6.52	6.33	6.78
No. plasmids (size in kbp)	2 (144, 448.7)	3 (84.6, 80.9, 15.8)	3 (240.1, 266.7, 30)	0
GC content (%)	62.40%	62.40%	62.30%	59.1
Total genes (PGAP)	6.328	6.332	6.394	5981
RNAs	72	77	71	6
NCBI Accession Numbers	NZ_CP042917, NZ_CP042916, NZ_CP042915	NZ_CP025959, NZ_CP025960, NZ_CP025961, NZ_CP025962	NZ_CP011295, NZ_CP011296, NZ_CP011297, NZ_CP011298	NZ_CP073104
Reference	Kuhl et al. (2019)	Xu et al. (2007), Wang et al. (2010), Tancsics et al. (2014)	Rückert et al. 2015	

2.11.2.2 Phylogenetic analysis of RL1 (adapted from Kuhl *et al*. (2019, 2021))

RL1 was phylogenetically classified to identify its position within the complicated *Rhodococcus* phylogeny and to contribute to the verification of the *R. erythropolis* clade. The RL1 genome harbors the 16S rRNA gene sequence in two versions differing at position 1074 (A or C) of the complete 16S rRNA gene. Based on the 16S rRNA sequence RL1 was placed within a cluster consisting of *Rhodococcus erythropolis*^{T}, *Rhodococcus qingshengii djl-6*^{T}, *Rhodococcus degradans* CCM 4446^{T} and *Rhodococcus baikonurensis*^{T}. The full genome based phylogenetic tree of *Rhodococcus* was constructed on a core genome of 633 genes from 39246 genes in total (**Supplementary Figure S9**). Based on this phylogenetic tree 15 genomes of the *R. erythropolis* clade were chosen to calculate the full genome based phylogenetic tree of the *R. erythropolis* clade.

It was built on a core genome of 1211 genes from 20587 genes in total and revealed that the clade can be separated into two groups (**Figure 18**). The first group includes *R. erythropolis* strains only. The second group harbors a mix of *R. erythropolis* and *R. qingshengii* strains. ANI values between all analyzed *R. erythropolis* or *R. qingshengii* genomes were higher than 94% (**Supplementary Figure S10**). The ANI value within the first group was 98.02% - 98.8% and within the second group 97.17% - 99.3%. The outgroups *Rhodococcus aethiovorans* and *Streptomyces albus* had ANI values of 72.13% - 72.57% and 66.79% - 67.9%, compared to the first group and the second group, respectively. AAI values between the first and the second group of the *R. erythropolis* clade were all above 98% (**Supplementary Figure S11**), and between both groups and the outgroups *R. aethiovorans* and *S. albus* AAI values were 56.45% - 57.33% and 76.71% - 76.81, respectively. *R. qingshengii* djl6 and RL1 grouped together in the second group. *R. erythropolis* BG43 was allocated to the first group.

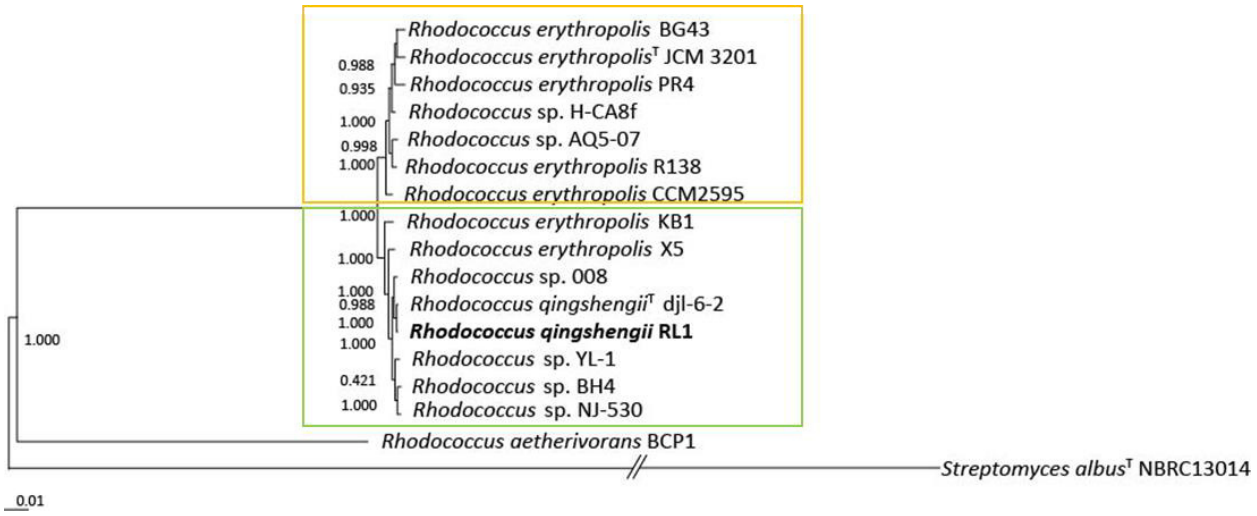

Figure 18: Maximum-likelihood phylogenetic tree of the *Rhodococcus erythropolis* clade. The tree was generated from 15 genomes with FastTree 2.1 from 1211 genes of the core genome adapted from Kuhl *et al*. (2021). Values represent local support values based on Shimodaira-Hasegawa test (1 SH = 100% bootstrap). The scale bar represents nucleotide substitutions per site (0.01 scale = 1% nucleotide substitutions per site). The *Rhodococcus erythropolis* subgroup is marked in orange and the *Rhodococcus qingshengii* subgroup in green.

Comparing the RL1 genome with the genomes of *R. qingshengii* djl6 and *R. erythropolis* BG43, 5293 genes could be identified that were shared between all three strains (**Figure 19**). RL1 and djl6 shared more genes (294) than each of them with BG43 (69; 70). For RL1 39 singleton genes could be identified of which 17 were annotated as hypothetical proteins (**Supplementary Table S7**). Concluding, RL1 could be classified as *Rhodococcus qingshengii* and based on the results the *R.*

erythropolis clade could be clearly separated into two groups, which was unexpected. For estimation of the functional potential of RL1 the genome was annotated with known functions presented in the next chapter.

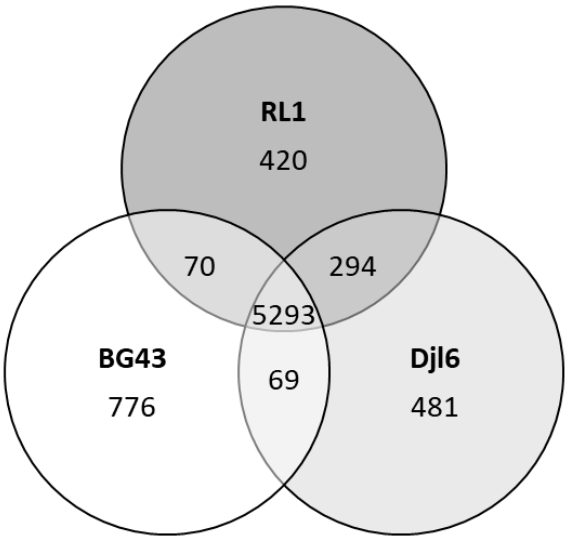

Figure 19: Shared genes between RL1, djl6 and BG43 adapted from Kuhl *et al*. (2021). Data represents comparative distribution and was obtained with EDGAR Software from the bacterial genomes. Unique genes or singletons are here genes without any hit (BLAST) against any other genome.

2.11.2.3 Functional annotation of RL1 (adapted from Kuhl *et al*. (2021))

Functional annotation of the RL1 genome was performed to identify the full genomic potential of RL1 and develop hypotheses for the upcoming experiments. 6,554 protein coding sequences were predicted from the genome of RL1 with (RAST) and 6,328 genes with PGAP (**Table 7**). 5918 of the predicted genes could be annotated to an assigned function and 92.4% of them were classified into 21 clusters of orthologous groups (COG) identified with eggNOG (**Figure 20**). Genes involved in metabolism represented the largest fraction (37.1%), followed by information and storage processing (19.2%), and cellular processes and signaling (12.7%) (**Figure 20**). In more details, the highest number of genes could be assigned to be involved in transcription (K, 11.5%), followed by amino acid transport and metabolism (E, 7.5%) and energy production and conversion (C, 6.9%). 3.6% of the genes could be assigned to the category of secondary metabolites biosynthesis, transport, and catabolism (Q). 9.4% of the genes were assigned to more than one category (> 1 cat.). 21.4% of the genes could not be assigned to a known function (S). 35% of the coding sequences in the RL1 genome were sorted in 23 main RAST categories and 424 subsystems

(subsystem coverage). With KEGG pathway analysis genes involved in 273 pathways were identified (**Supplementary Table S3**). The genome was further analyzed for presence of genes known to be involved in interactions with plants using the web-based tool PIFAR and 45 genes representing 14 categories could be identified (**Supplementary Table S4**). Using the tool antiSMASH 18 biosynthetic gene clusters (BGC) with the potential to produce secondary metabolites, such as ectoine, erythrochelin and heterobactin A/heterobactin S2, could be identified (**Supplementary Table S5**). Focus was on the clusters with highest similarity (> 50%) to known secondary metabolite biosynthesis pathways.

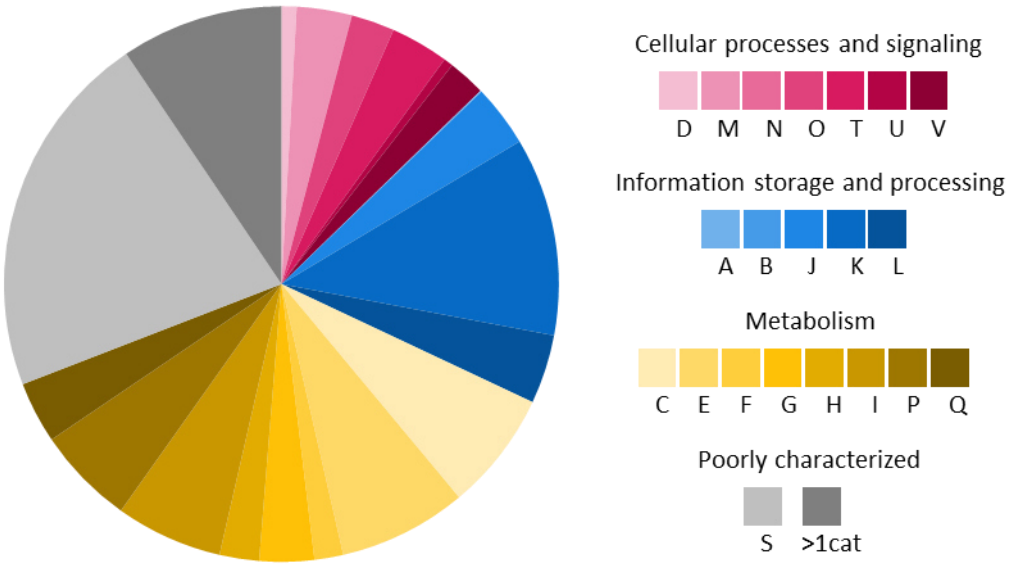

Figure 20: Functional classification of genes encoding proteins in RL1 based on cluster of orthologous groups (COG) (Tatusov *et al*., 2000) adapted from Kuhl *et al*. (2021). All characters represent different COG functional classes: **A**, RNA processing and modification; **B**, Chromatin structure and dynamics; **C**, energy production and conversion; **D**, cell cycle control, cell division, and chromosome partitioning; **E**, amino acid transport and metabolism; **F**, nucleotide transport and metabolism; **G**, carbohydrate transport and metabolism; **H**, coenzyme transport and metabolism; **I**, lipid transport and metabolism; **J**, translation, ribosomal structure, and biogenesis; **K**, transcription; **L**, replication, recombination, and repair; **M**, cell wall, cell membrane, and cell envelope biogenesis; **N**, cell motility; **O**, posttranslational modification, protein turnover, and chaperones; **P**, inorganic ion transport and metabolism; **Q**, secondary metabolites biosynthesis, transport, and catabolism; **S**, no functional prediction; **T**, signal transduction mechanisms; **U**, intracellular trafficking, secretion, and vesicular transport; and **V**, defense mechanisms; **>1cat**, classified in more than one category.

The genome annotation of RL1 revealed several genes which have been previously identified to be involved in stress tolerance under different abiotic stress conditions, bioremediation of toxic compounds, rhizosphere colonization and (beneficial) plant-microbe interactions and were partly

verified by manual annotation with blastp alignment (**Supplementary Table S6**). In more details, the RL1 genome harbors many genes, which can be expressed to withstand osmotic, salt, oxidative and acidic stress and are relevant for heavy metal tolerance (mercury, lead, cadmium, arsenic) and bioremediation of aromatic hydrocarbons (*alkB*, *catA*) and fossil fuels (*dszB*). Moreover, genes potentially involved in multiple drug resistance, DNA repair by phosphorothioation, antibiotic resistance and degradation of CO and hydrogen could be identified, for example the complete carbon monoxide dehydrogenase (CODH) and a [NiFe]-hydrogenase cluster. The RL1 genome annotation indicated that it is equipped with several genes which could enable it to interact with the plant and survive in the plant environment via plant hormone and siderophore production of the siderophores enterobactin, bacillibactin, arthrobactin, and heterobactin as well as nitrogen fixation, iron acquisition, phosphate solubilization, biofilm formation, and stress protection. Additionally, the RL1 genome harbors genes involved in quorum quenching, glucosinolate metabolism, aldoxime, isothiocyanate (ITC) and nitrile degradation, as well as genes important for the production of volatiles, exopolysaccharides (EPS), proteases and microbe-associated molecular patterns (MAMP). Based on these results the following functional analysis was focused on functional traits of stress tolerance and plant-microbe interactions.

2.11.2.4 Functional characterization of stress-related traits *in vitro* (adapted from Kuhl *et al*. (2021))

Based on the functional annotation of the RL1 genome, RL1 as well as the closely related strains djl6 and BG43 were analyzed for various stress tolerance traits to reveal if the identified genes were actually transferred into functional traits (**Table 8**).

2.11.2.4.1 Growth ability at different temperature ranges of *Rhodococcus* strains

RL1, djl6 and BG43 were able to grow in different temperatures ranging from 15°C to 37°C with their temperature optimum at 28°C.

2.11.2.4.2 Osmotic stress tolerance of *Rhodococcus* strains

The gene cluster for ectoine biosynthesis was identified in RL1 with 75% identity to the ectoine biosynthetic cluster of *Streptomyces anulatus*. Therefore, *Rhodococcus* strains were tested for osmotic stress tolerance and were able to withstand up to -1.5 MPa, which was the tested maximum.

2.11.2.4.3 Salt stress tolerance of *Rhodococcus* strains

The RL1 genome harbors genes for the complete Na+/H+ antiporter operon (**Supplementary Table 6**), which was the reason to test the strains for salt stress tolerance. RL1, djl6 and BG43 and the positive control strain FZB42 grew up to 7.5% NaCl in the medium (**Table 8**), whereas the negative control strain GSF30 grew up to 3.5% NaCl in the medium. All strains were additionally tested for recovery from higher salt concentrations. Although there was no visible growth, all tested *Rhodococcus* strains were able to recover from salt stress of up to 15% NaCl in the medium. The Gram-positive control strain *B. velezensis* FZB42 did not recover from medium with 15% NaCl. The Gram-negative control strain *H. frisingense* GSF30 could not recover from 7.5% NaCl in the medium or higher.

2.11.2.4.4 Mercury tolerance of *Rhodococcus* strains

The RL1 genome harbors genes possibly involved in mercury tolerance (**Supplementary Table S6**). Therefore, the *Rhodococcus* strains RL1, djl6 and BG43 were tested for mercury tolerance. Active growth determined by optical density was detectable in the medium with 0.001 mM mercury for djl6 and BG43. RL1 was able to grow in the medium with up to 0.01 mM mercury. RL1 and BG43 could recover from up to 1mM mercury in the medium, whereas djl6 recovered from up to 0.1 mM mercury. The Gram-positive control strain *B. velezensis* FZB42 could grow in the medium with up to 0.01 mM mercury and the Gram-negative control strain *H. frisingense* GSF30 only in medium with 0.001 mM mercury. Both control strains did not recover from medium containing 0.1 mM mercury.

2.11.2.4.5 Acidic pH tolerance of *Rhodococcus* strains

The RL1 genome harbors genes possibly involved in acidic pH tolerance (**Supplementary Table S6**), which was the reason to test the *Rhodococcus* strains for acidic pH tolerance. The *Rhodococcus* strains RL1, djl6 and BG43 were able grow up to pH 5 and recovered after 48h in pH 3 and 4h in pH 2. Control strains GSF30 and FZB42 were able to grow up to pH 5 and recovered from pH 4.

2.11.2.4.6 Antibiotic resistance of *Rhodococcus* strains

The RL1 genome harbors genes possibly involved in antibiotic resistance (**Supplementary Table S6**). Therefore, the *Rhodococcus* strains RL1, djl6 and BG43 were tested for antibiotic resistance. RL1 was tolerant to Kanamycin up to the concentration of 96 µg/ml, Ampicillin up to 6 µg/ml, Rifampicin up to 0.025 µg/ml, but not tolerant to Vancomycin. Djl6 was tolerant to Kanamycin up

to 12 µg/mL, Ampicillin up to 3 µg/mL, Rifampicin up to 0.047 µg/ml and Vancomycin up to 0.023 µg/ml. BG43 was tolerant to Kanamycin up to 48 µg/ml, Ampicillin up to 2 µg/ml, Rifampicin up to 0.023 µg/ml and Vancomycin up to 0.5 µg/ml. RL1 was able to grow on NB plates containing 100 µg/ml potassium tellurite trihydrate. The other strains were not tested for this trait.

All strains showed a remarkable stress tolerance against osmotic, salt, acidic pH and heavy metal stress as well as antibiotic resistance. Surprisingly, RL1 shared most stress tolerance traits with BG43, which belongs to a different, but closely related species, *R. erythropolis*.

Table 8: Stress tolerance traits of *Rhodococcus* strains RL1, djl6 and BG43.

StrainID	Species	Max. growth temperature (°C)	Max. salt conc. (%)	Osmotic Stress (-1.5 MPa)	Max. pH stress	Max. mercury conc. (mM)
RL1	*Rhodococcus qingshengii*	15-37 (28)	7.5	+	5	1
Djl6	*Rhodococcus qingshengii*	15-37 (28)	5.5	+	5	0.1
BG43	*Rhodococcus erythropolis*	15-37 (28)	7.5	+	5	1

2.11.2.5 Traits involved in plant-microbe-interactions *in vitro* (adapted from Kuhl *et al*. (2021))

Functional annotation of the RL1 genome revealed many traits involved in plant-microbe-interactions. Therefore, RL1 as well as the closely related strains djl6 and BG43 were analyzed for potential plant beneficial traits to reveal if the identified genes were actually transferred into functional traits (**Table 9**).

2.11.2.5.1 IAA production of *Rhodococcus* strains

The genes encoding for amidase *amiE* and amine oxidase *iaaM* as well as genes involved in tryptophan metabolism were identified in the RL1 genome (**Supplementary Table S6**). Therefore, IAA production of RL1, djl6 and BG43 was tested and compared to the positive control strain GSF30. RL1 produced after 48h 16 ± 2.6 µg/ml of IAA which is the highest amount compared to djl6 and BG43 with 10.7 ± 2.4 µg/ml and 10.9 ± 3.8 µg/ml, respectively (**Table 9**). The positive control GSF30 produced 41 ± 9.8 µg/ml IAA after 48 h.

2.11.2.5.2 Siderophore production of *Rhodococcus* strains

In the RL1 genome, biosynthesis cluster for erythrochelin was identified with 57% identity and heterobactinA/heterobactin S2 identified with 100% identity compared to the heterobactin BGC of *R. erythropolis* PR4 (**Figure 21A**). Genes encoding for relevant proteins of the heterobactin BGC are isochorismate synthase, isochorismatase, 2,3-dihydro-2,3-dihydroxybenzoate dehydrogenase, 2,3-dihydroxybenzoate-AMP ligase, amino acid adenylation domain-containing protein and related transporter were identified in the RL1 genome (**Supplementary Table S6**). Therefore, the *Rhodococcus* strains were tested for their ability to produce siderophores. RL1 produced siderophores indicated by the color change of the overlay agar from blue to orange (**Table 9, Figure 21B**), whereas BG43 and djl6 showed no siderophores.

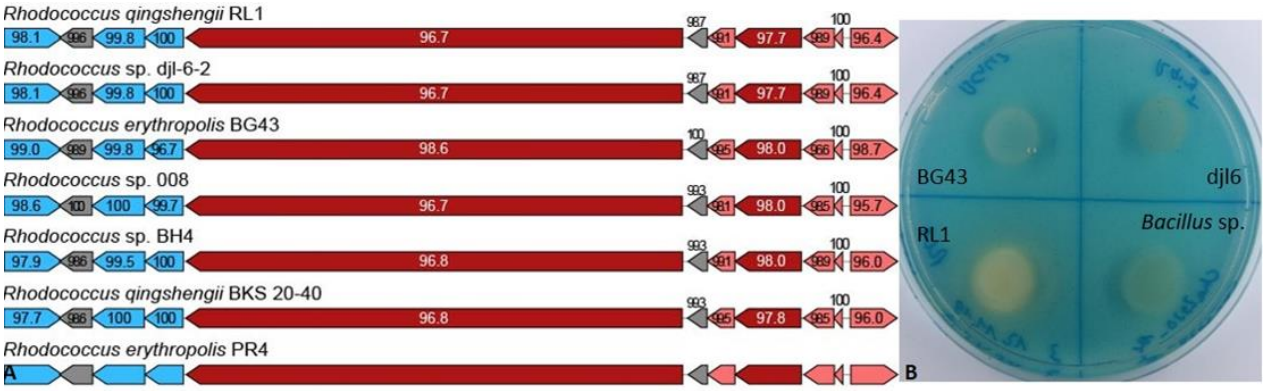

Figure 21: Siderophore biosynthetic gene clusters and *in vitro* assay adapted from Kuhl *et al*. (2021). (**A**) Heterobactin biosynthetic gene cluster based on antiSMASH results of *Rhodococcus qingshengii* RL1 compared to the reference genome of *R. erythropolis* PR4 and other *Rhodococcus* strains. Depicted as arrows are the core biosynthetic genes in dark red, additional biosynthetic genes in light red, transport-related genes in blue and additional genes in grey. The biosynthetic genes (dark and light red) are presented in order of their appearance from right to left encoding for isochorismate synthase, isochorismatase, 2,3-dihydro-2,3-dihydroxybenzoate dehydrogenase, 2,3-dihydroxybenzoate-AMP ligase, isochorismatase, and an amino acid adenylation domain-containing protein. Numbers indicate percentage of similarity to PR4. (**B**) *In vitro* assay for siderophore production of RL1, BG43, djl6 and *Bacillus* sp. detected with Chrome Azurol Blue overlay agar. Siderophore production is indicated by color change of the medium from blue to orange.

2.11.2.5.3 Phosphate solubilization ability of *Rhodococcus* strains

The RL1 genome harbors genes involved in organic acid production (**Supplementary Table S6**). Therefore, the Rhodococcus strains were tested for their ability to solubilize phosphate. *R. qingshengii* strains RL1 and djl6 were able to solubilize phosphate indicated by clear halo formation and SI values above 2 indicating phosphate solubilization ability (**Table 9**). BG43 showed no halo formation.

2.11.2.5.4 ACC deaminase activity of *Rhodococcus* strains

RL1, BG43 and djl6 were tested for ACC deaminase activity, because this is a common PGP trait frequently tested to characterize potential PGPB. The tested strains could grow on medium supplemented with ACC and on regular M9 medium. However, the strains could also grow on nitrogen-free M9 medium (**Figure 22A**). Therefore, the ACC deaminase activity of *Rhodococcus* strains remained unclear.

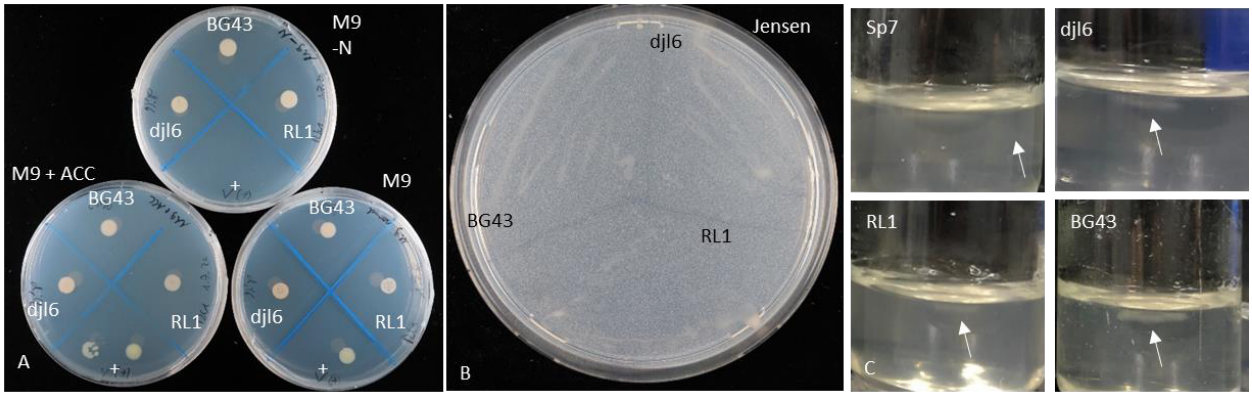

Figure 22: Growth characterization of RL1, djl6 and BG43 on nitrogen-free media adapted from Kuhl *et al*. (2021). Growth of bacterial strains on (**A**) M9-N, M9 (control) and M9+ACC (**B**) Jensen's medium (**C**) Nfb-semisolid medium (Döbereiner, 1995). Sp7 = *Azosprillum brasilense* Sp7 (positive control for nitrogen fixation), + = *Variovorax* sp. (positive control for ACC deaminase activity). White arrows mark pellicle formation.

2.11.2.5.5 Nitrogen fixation ability of *Rhodococcus* strains

The RL1 genome harbors an uncharacterized nifU-like protein (**Supplementary Table S6**). Therefore, the strains RL1, djl6 and BG43 were tested for their ability to grow on nitrogen-free media. All strains could grow on nitrogen-free M9 medium (**Figure 22A**), Ashby's medium, Jensen's medium (**Figure 22B**) and Nfb-medium (**Figure 22C**). Pellicle formation of all tested

isolates in Nfb-medium was smaller compared to positive control *Azospirillum brasilense* Sp7. Amplification of *nifH* gene was negative for the RL1, djl6 and BG43. Nevertheless, the results indicate that the *Rhodococcus* strains are able to fix nitrogen.

2.11.2.5.6 Glucosinolate (GSL) metabolism in *Rhodococcus* strains

RL1 was isolated from rucola, which produces GSLs as protection against herbivores and genes potentially involved in GSL metabolism were identified in the RL1 genome (**Supplementary Table S6**). Therefore, RL1, BG43, djl6 and the control GSF30 were analyzed for their potential to metabolize GSLs. Content of the GSL glucoerucin increased and decreased over varying times in medium with rucola leaf extract inoculated with RL1, BG43, djl6 and GSF30 **(Figure 23A, B, D)**.

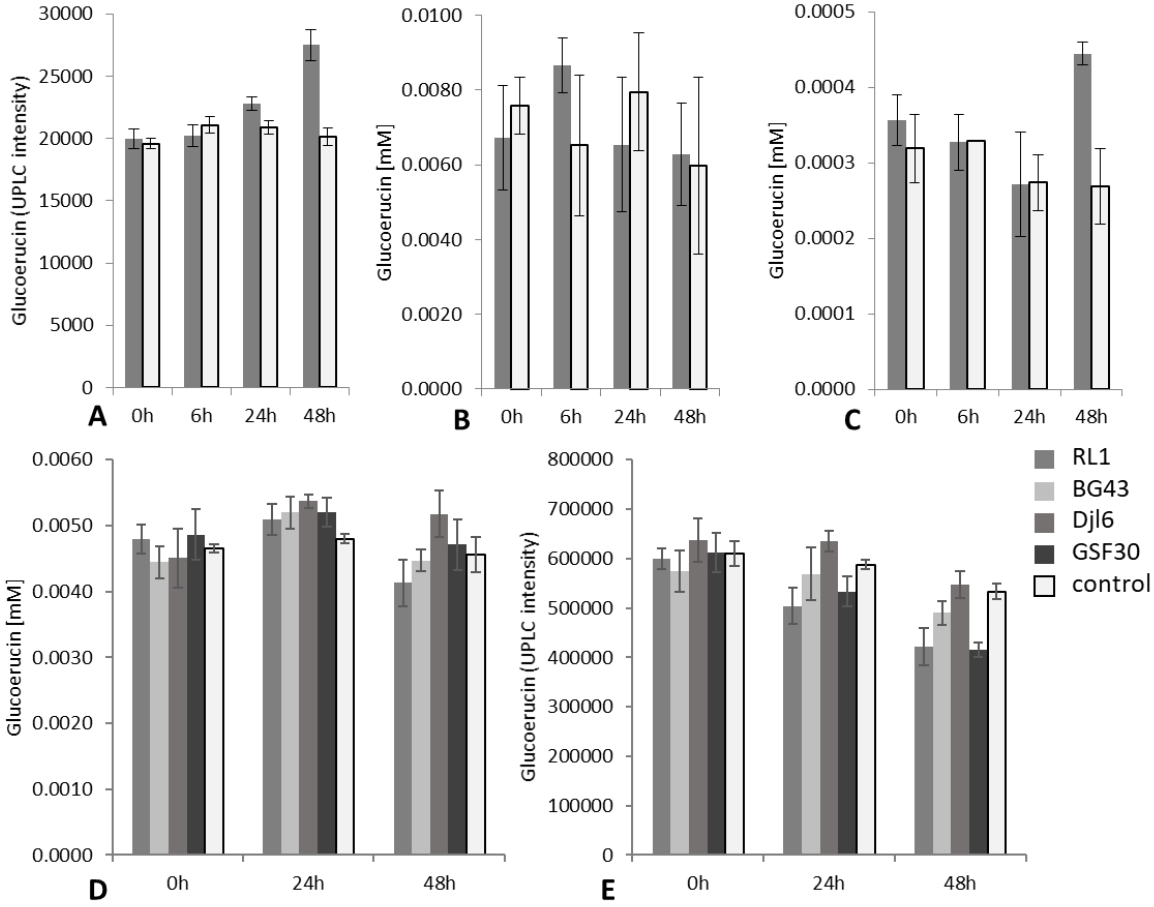

Figure 23: Glucoerucin content in medium inoculated with bacterial strains. Medium was supplemented with rucola leaf extract (**A, B, D**), *Arabidopsis* leaf extract (**C**) or the pure compound glucoerucin (**E**) and inoculated with the bacterial strains RL1, djl6, BG43 or GSF30. Measurements took place at the time points 0h, 6h, 24h and 48h. Error bars indicate standard deviation. (**A, B, D, E**) N = 6, (**C**) N = 3 (except 6h: N = 2). In (**A**) and (**E**) Glucoerucin content is given in UPLC intensities, because no glucoerucin standard was included in this experiment.

RL1 showed the largest changes. A similar but milder pattern was observed in the control. In medium with Arabidopsis leaf extract inoculated with RL1 glucoerucin content decreased after 24h and increased after 48h **(Figure 23C).** The control shows an unstable pattern. No GSLs could be detected in medium with wheat leaf extract. In medium supplemented with the pure compound glucoerucin, the glucoerucin content decreased over time in all treatments including control. Largest changes were observed in RL1 and GSF30 and overall glucoerucin decrease was stronger in bacterial treatments. No GSL degradation products like nitriles or isothiocyanates (ITCs) could be detected in the supernatant under the tested conditions measured with GC-MS. Results on GSL metabolism were not consistently reproducible. Therefore, the ability of RL1, djl6, BG43 and GSF30 to metabolize GSLs remains unclear.

The results revealed that the three tested strains shared many functional traits involved in plant-microbe-interaction. However, RL1 showed overall the best performance.

Table 9: Plant-microbe-interaction traits of *Rhodococcus* strains RL1, djl6 and BG43.

Strain	**Species**	**Phosphate solubilization** (SI values)	**Siderophore production**	**IAA production (µg/mL) Normalized (OD=1)**	**Nitrogen fixation**
RL1	*Rhodococcus qingshengii*	2.2	+	16 ± 2.6 (48h)	+
djl6	*Rhodococcus qingshengii*	2.4		10.7 ± 2.4 (48h)	+
BG43	*Rhodococcus erythropolis*			10.9 ± 3.8 (48h)	+

2.11.2.6 Interaction of *Rhodococcus* strains with other microorganisms

RL1 was tested for various interactions with other microorganisms, which could become relevant to successfully survive in the plant meta-organism.

2.11.2.6.1 Confrontation assay against plant-pathogenic fungi

RL1 was tested for a potential antagonistic activity against plant-pathogenic fungi interesting for biocontrol applications. RL1 inhibited the plant-pathogenic fungus *Fusarium oxysporum*. The

positive control for antifungal activity *B. velezensis* FZB42 inhibited the plant-pathogenic fungi *Rhizoctonia solani*, *Fusarium oxysporum* and *Fusarium culmorum* (**Figure 24**). The effect on *Alternaria alternata* could not be evaluated, because the fungus showed overall low growth also on the control plates.

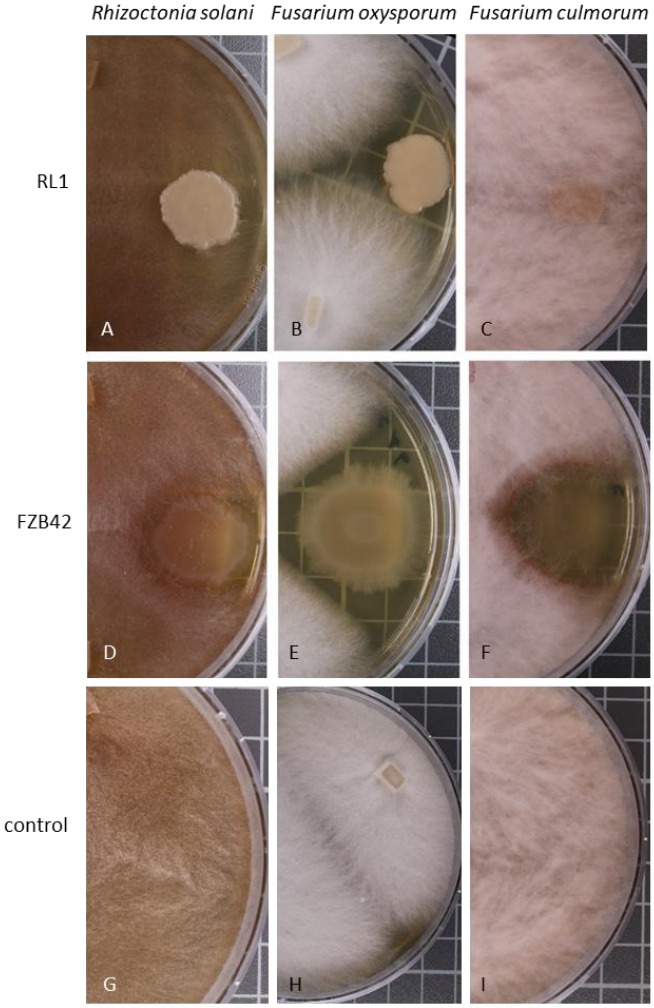

Figure 24: Confrontation assay of RL1 (**A-C**) and FZB42 (**D-F**) against plant-pathogenic fungi adapted from Kuhl *et al*. (2021). Plates were evaluated after 9 days of cultivation. Antagonistic activity is indicated by inhibition zone around bacteria. Control plates (**G-I**) without bacteria.

2.11.2.6.2 Degradation of N-Acyl-Homoserinelactones (AHLs) by *Rhodococcus* strains

A *qsdA* gene (QEM30276) could be identified in the RL1 genome, which belongs to a class of large-spectrum quorum-quenching lactonases also present in other *Rhodococcus* spp. (**Figure 25A**). Therefore, AHL degradation ability was tested in RL1, djl6 and BG43 using the sensor strain A136. In this set-up it could be clearly shown that RL1, djl6 and BG43 were able to degrade

synthetic C12-HSL (**Figure 25B-D**). Additionally, co-culturing of *A. radicis* N35e with RL1 resulted in no visible blue color formation by the sensor strain, indicating degradation of the bacterially produced AHL (**Figure 25B**). Finally, v-shaped spotting of *A. radicis* N35e and RL1, djl6 and BG43 showed an inhibition of blue color formation where strains were in direct contact (**Figure 25E-H**). In order to test if the observed effect was related to growth inhibition, *B. velezensis* FZB42, *A. radicis* N35e and *A. tumefaciens* A136 were confronted with RL1. The tested bacteria were not inhibited in growth by RL1.

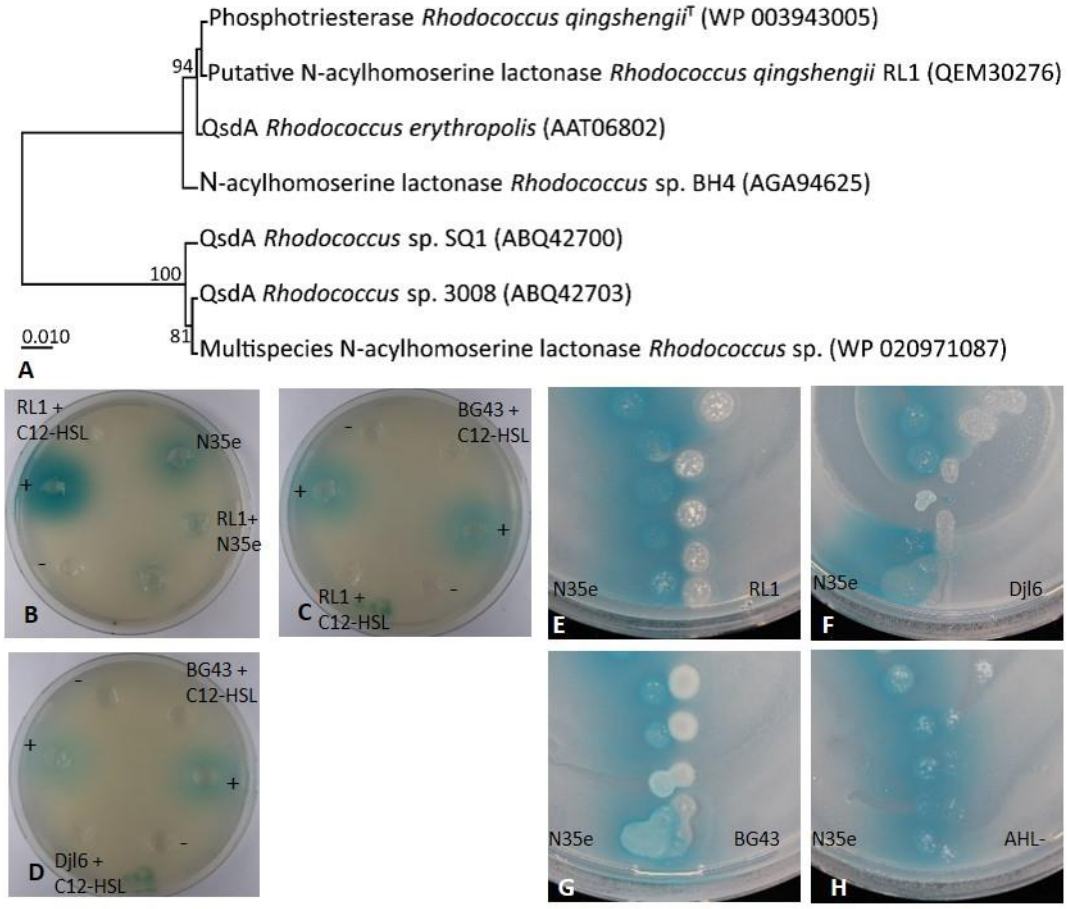

Figure 25: AHL degradation and quorum quenching by RL1, djl6 and BG43 adapted from Kuhl *et al*. (2021). (**A**) UPGMA phylogenetic tree of translated *qsdA* (quorum-sensing signal degradation) gene of RL1 and related sequences from *Rhodococcus* strains generated by Dr. Soumitra Paul Chowdhury. The percentage of replicate trees in which the associated taxa clustered together in the bootstrap test (1000 replicates) are shown next to the branches. The evolutionary distances were computed using the Poisson correction method. All ambiguous positions were removed for each sequence pair (pairwise deletion option). There were a total of 323 positions in the final dataset. Evolutionary analyses were conducted in MEGA X (Kumar *et al*., 2018). (**B-D**) Well-diffusion plate assays on NB plates all supplemented with the sensor strain A136 and X-Gal. Except for the cultures containing AHL producing strain *A. radicis* N35e, C12-HSL was

added during cultivation of all bacteria. Supernatants of these cultures were added to the wells and blue color formation by the sensor strain indicated remaining AHL in the tested supernatant. NB with C12-HSL (+) served as positive control, and NB without C12-HSL (-) as negative control. (**E-H**) V-shaped assays on NB after 30 h supplemented with the sensor strain A136 and X-Gal. AHL negative mutant *A. radicis* N35e AHL- served as control. Presence of AHLs is detected by the sensor strain *Agrobacterium tumefaciens* A136 indicated by blue color change of X-Gal.

Overall, RL1 showed mild antagonistic activity against one plant-pathogenic fungus and was able to interfere with quorum sensing molecules of other bacteria, without inhibiting their growth. These traits could be interesting for biocontrol applications.

2.12 Interactions of *Rhodococcus* strains with plants

In order to test if the functional traits identified *in vitro* effect plants in a natural system, RL1 was applied to rucola and wheat plants and the interactions were evaluated.

2.12.1 Rhizosphere competence of *Rhodococcus* strains

Rhizosphere competence is a pre-requisite for successful plant-microbe-interaction on roots and includes traits, such as biofilm formation.

2.12.1.1 Biofilm formation of *Rhodococcus* strains (adapted from Kuhl *et al*. (2021))

Genes encoding for a phosphoglucomutase and a signal peptidase I were identified in the RL1 genome (**Supplementary Table S6**). Therefore, the strains RL1, djl6 and BG43 were tested for their ability to produce biofilms, also relevant for successful root colonization. All *Rhodococcus* strains were able to produce biofilms in varying intensities (**Figure 26B**), but stronger than the negative control *Escherichia coli* DH5α. Djl6 showed the strongest biofilm formation. The normalized biofilm formation of the positive control *Pseudomonas simiae* WCS417 was lower compared to djl6, but stronger compared to RL1 and BG43.

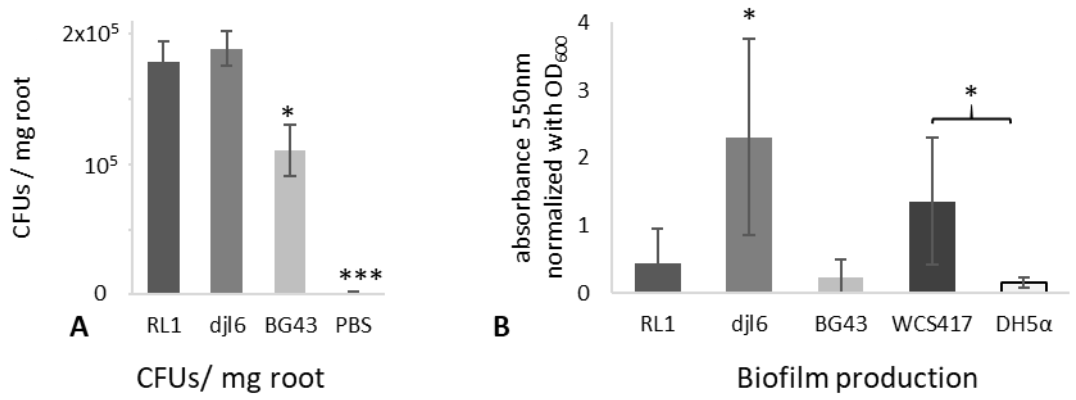

Figure 26: Interaction of RL1, BG43 and djl6 with rucola roots adapted from Kuhl *et al*. (2021). (**A**) Quantification of root colonization one week after inoculation (**B**) Ability to produce Biofilms with averaged results from 3 experiments normalized to OD600 = 1. Significant difference is indicated by asterisks representing * = $P < 0.05$ and *** = $P < 0.001$

2.12.1.2 Root colonization in axenic system (adapted from Kuhl *et al*. (2021))

Root colonization was analyzed with fluorescence *in situ* hybridization using the probes EUB Mix Fluos and HGC69A Atto550 or HGC69A Cy3. Single cells of RL1 could be found on the root surface of its host plant rucola when grown in the axenic system (**Figure 27B-D**), while dense cell patches were identified on roots from MS agar plates (**Figure 27A**). Similar colonization patterns were found for strains djl6 and BG43. All strains were localized rather in the basal mature part of the root in areas of emergence of root hairs. No endophytic colonization was observed. Quantitative estimation based on CFU/mg root mass (**Figure 26A**) showed significantly higher colonization numbers for RL1 and djl6 (p-value = 0.012) than BG43. Djl6 showed a trend towards higher root colonization compared to RL1. CFU numbers of all strains were significantly higher compared to the uninoculated control.

The results indicate that RL1 as well as djl6 and BG43 were able to successfully colonize rucola roots. In the following experiments the influence of RL1 on different plant developmental stages was analyzed.

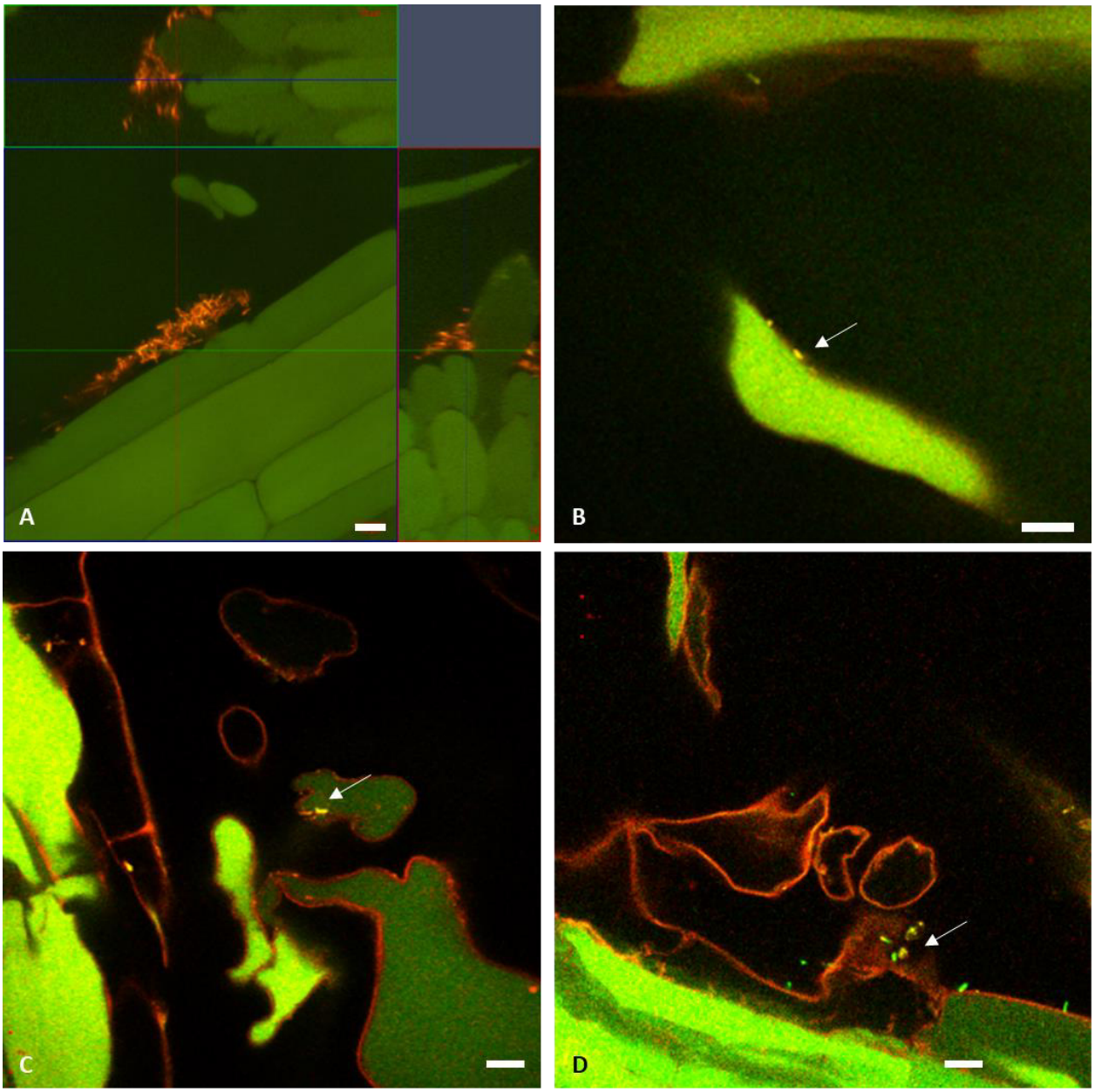

Figure 27: *In situ* detection of root colonization on rucola roots adapted from Kuhl *et al*. (2021) (**A**) RL1 on 2 weeks old *Eruca sativa* roots grown on MS agar without additional sucrose visualized by fluorescence *in situ* hybridization (FISH). (**B**) RL1, (**C**) djl6 and (**D**) BG43 on one week old *Eruca sativa* roots grown in axenic quartz-sand system and visualized by fluorescence *in situ* hybridization (FISH). Arrows indicate bacterial cells identified by yellow color from overlaying channels of probes EUB (green) and HGC (red). Root autofluorescence is assigned in green and red. Scale bar represents 10µm.

2.12.2 Seed germination upon inoculation with *Rhodococcus* strains

Genes encoding for parts of the gibberellin-producing operon were identified in the RL1 genome (**Supplementary Table S6**). Therefore, the *Rhodococcus* strains were tested for their ability to increase plant germination. Rucola seeds treated with GA 100 µm germinated most followed by 1x PBS and heat-killed RL1 (**Table 10; Figure 28**). Lowest germination was identified for BG43 with 52.5% germinated seeds after 6 days. *Arabidopsis thaliana* germinated best treated with GA 100 µm followed by djl6, heat-killed RL1, PBS, BG43 and RL1 after 4 days (**Table 10**). Plates with wheat seeds had fungal contamination and were not evaluated. Rucola seeds, tested on water agar with medium, germinated best with BG43 supernatant, followed by GA 100 µM, RL1 supernatant, RL1, djl6 supernatant, djl6, BG43 and the control TSB (**Table 10**).

Germination of rucola seeds in the sand-clay system was slightly increased by the application of RL1 to 47.3% compared to the control 42.5% (**Table 10**). This result was not reproducible in a follow-up experiment where the control showed the highest germination rate of 42% followed by BG43, GA 100µM, RL1, djl6 and heat-killed RL1 (**Table 10**). Overall, results show inconsistent effects of treatment with bacteria or bacterial supernatant on germination of rucola seeds in different systems.

Table 10: Seed germination of plants inoculated with *Rhodococcus* strains. "x" indicates not tested treatments.

% seed germination					
Set-up	sand-clay 1	sand-clay 2	water agar	water agar with medium	water agar
days	12	13	6	2	4
plant	Rucola	Rucola	Rucola	Rucola	Arabidopsis
Treatment					
RL1	47.3	36	56.0	83.3	87.5
RL1 HK	42.5	31.3	66.0	x	90
djl6	x	33.3	54.0	70.8	93.6
BG43	x	40.6	52.5	62.5	89.4
GA 100µm	x	40	89.0	87.5	99.1
1xPBS	x	42	60.0	x	89.7
S RL1	x	x	x	87.5	x
S djl6	x	x	x	79.2	x
S BG43	x	x	x	91.7	x
TSB	x	x	x	62.5	x

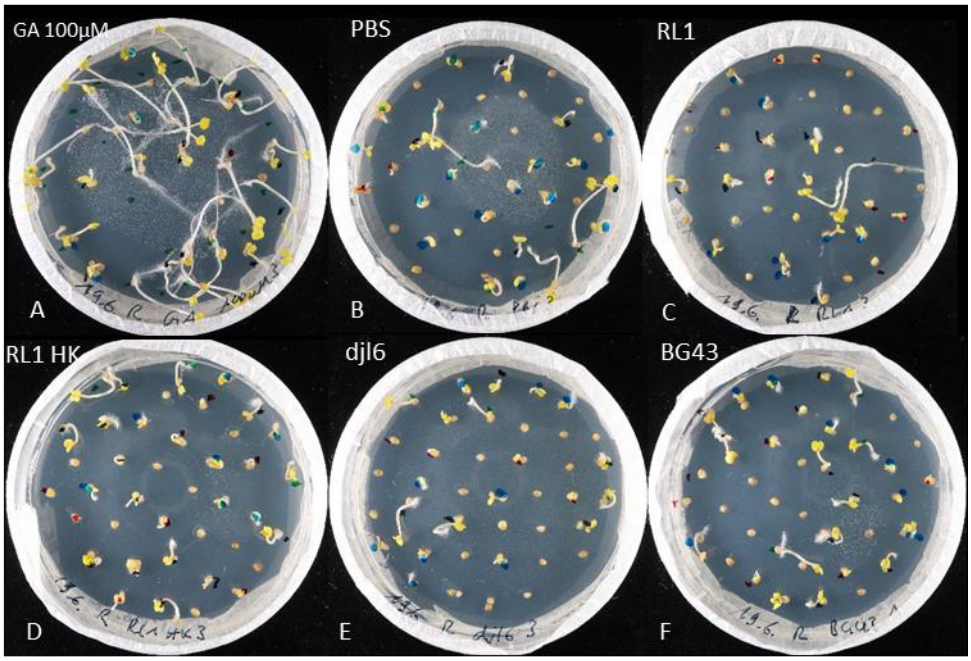

Figure 28: Germination of rucola seeds on water agar. Seeds were inoculated with gibberellic acid 100 µm (GA 100µM) (**A**), control (PBS) (**B**), *Rhodococcus qingshengii* RL1 (**C**), heat-killed *Rhodococcus qingshengii* RL1 (**D**), *Rhodococcus qingshengii* djl6 (**E**) and *Rhodococcus erythropolis* BG43 (**F**).

2.12.3 Flowering of rucola upon inoculation with *Rhodococcus* strains

Genes encoding for parts of the gibberellin-producing operon were identified in the RL1 genome (**Supplementary Table S6**), which could also influence flowering in plants. Therefore, RL1 and BG43 were tested for their ability to alter the development of flowers in rucola. Development of buds, flowers and fruits on rucola plants was evaluated after 12 weeks. Rucola treated with RL1, heat-killed RL1 and the control (1xPBS) showed an equal development of buds and fruits (**Table 11**). Rucola plants treated with RL1 and heat-killed RL1 developed more flowers (3, 4) compared to PBS (1) and BG43 (1). Rucola plants treated with BG43 developed less buds and no fruits. RL1 and heat-killed RL1 increased flowering rate.

Table 11: Flowers and fruits of plants inoculated with *Rhodococcus* strains.

Treatment	Buds	Flowers	Fruits	total plants
RL1	9	3	1	23
RL1 HK	8	4	1	19
BG43	5	1	0	24
1xPBS	9	1	1	24

2.12.4 Plant experiments with *Rhodococcus* strains

2.12.4.1 Effect of RL1, djl6 and BG43 on plant growth of rucola

The *Rhodococcus* strains were tested for their ability for plant growth promotion in their host plant rucola, based on the results of the *in vitro* assays. The treatment with RL1 showed an altered root architecture of rucola roots with an increased lateral root formation (**Figure 29V**) compared to the control treatment with 1 x PBS (**Figure 29W**). Bacterial colonies are visible attached to the root surface of RL1 treated plants (**Figure 29V**).

Plants inoculated with RL1 showed in two experiments a significantly increased root length (**Figure 29A,** p-value = 0.05, **Figure 29F**, p-value = 0.047) and shoot fresh weight (**Figure 29D**, p-value = 0.0016, **Figure 29I**, p-value = 0.02453), which was not reproducible in two additional experiments. In one experiment plants inoculated with RL1 showed an increased root fresh weight (**Figure 29B,** p-value = 0.0005), which was not reproducible in other experiments. Plants treated with djl6 showed an increase in root length (**Figure 29K,** p-value = 0.0121), shoot fresh weight (**Figure 29N,** p-value = 0.000013) and shoot dry weight (**Figure 29O**, p-value = 0.00605), which was not reproducible in a second experiment. No difference between bacterial treatments and the control was observed for the other plant parameter (**Figure 29**). In soil substrate no difference was observed in the tested plant parameter upon inoculation with RL1 (**Supplementary Figure S12**). Under drought stress no significant difference in the tested plant parameters was observed between plants inoculated with RL1 and control (**Supplementary Figure S13**). Plants were evaluated for their recovery status recovered or not recovered from drought (**Supplementary Figure S13G-H**). An equal number of approximately 70% of plants recovered from drought under RL1 and control treatment (**Supplementary Figure S13F**). Further analyzed parameters were the survival rate of plants and the plant developmental stage, indicated by the number of leaves. Results showed a higher survival rate of RL1 (9 plants) compared to the control (5 plants), which was not reproducible in a large scale experiment (RL1 58 plants and control 60 plants). Treatment with RL1, djl6 or BG43 increased survival of plants compared to the control (**Figure 29U**), which was not reproducible. A shift in the number of leaves, representing the developmental stage of the plant, was observed towards more leaves in plants treated with RL1 compared to PBS under drought and non-drought conditions (**Supplementary Figure S13I**).

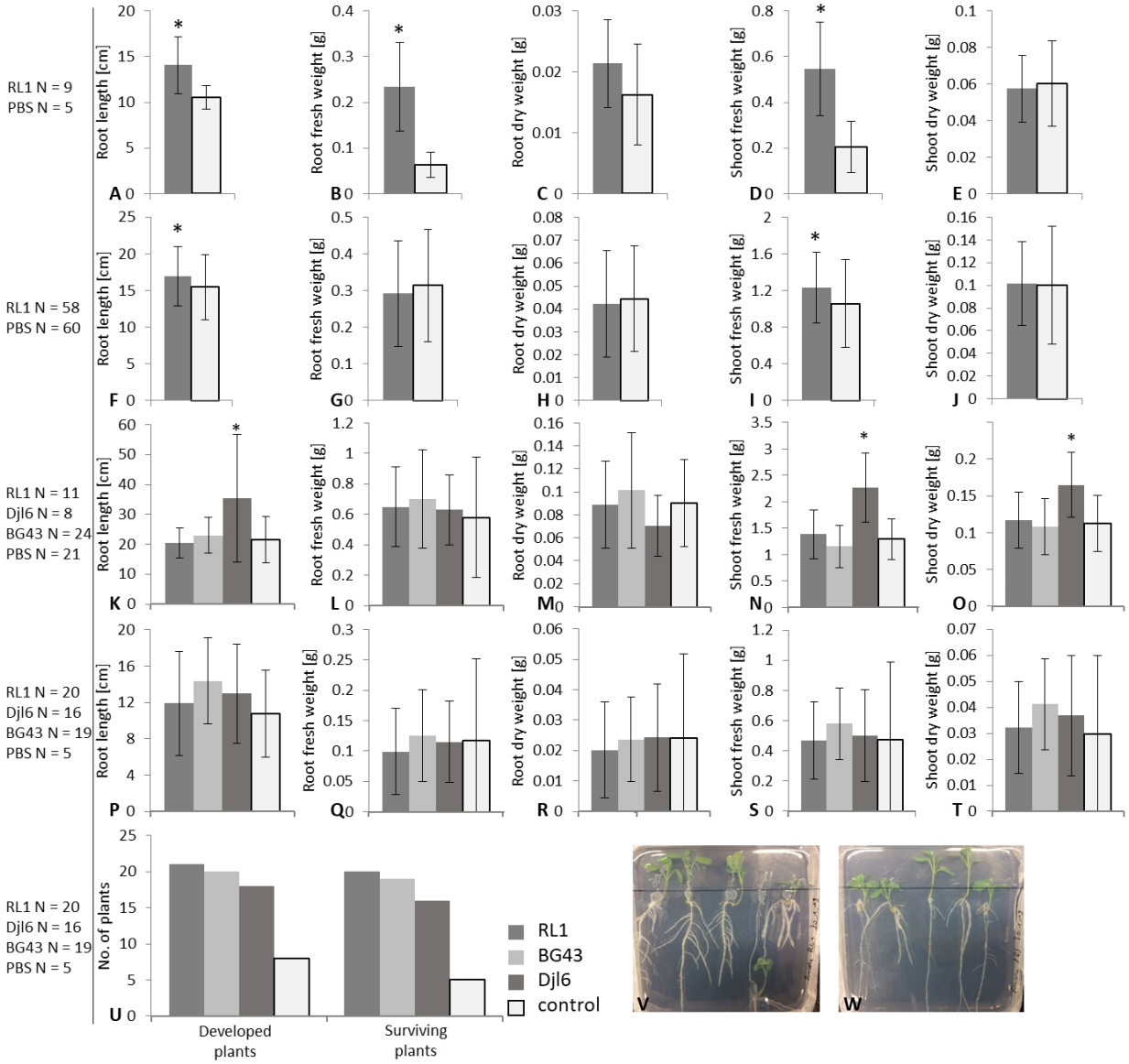

Figure 29: Effect of RL1, djl6 and BG43 on rucola plants. Results of four consecutive experiments of plants grown in sand-clay pot system under non-drought conditions. Evaluated plant parameters were root length (**A, F, K, P**) root fresh weight (**B, G, L, Q**), root dry weight (**C, H, M, R**), shoot fresh weight (**D, I, N, S**) and shoot dry weight (**E, J, O, T**) and plant survival (**U**). Rucola plants inoculated with RL1 (**V**) and control (PBS) (**W**) grown in axenic system on MS agar. Error bars indicate standard deviation. Significant difference is indicated by asterisks representing * = $P < 0.05$.

Results indicating a PGP effect of RL1 and djl6 on root and shoot growth of rucola as well as an increased survival rate upon treatment with bacteria, but were not consistently reproducible in follow-up experiments with same (sand-clay system) or varying set-ups (soil substrate or drought stress). Therefore, a final conclusion on the PGP ability of the tested *Rhodococcus* strains on rucola could not be drawn, which was unexpected due to the presence of many PGP traits *in vitro*.

2.12.4.2 Effect of RL1 on non-host plant wheat under drought stress

In order to test the effect of RL1 on non-host plants under drought stress, RL1 was applied to wheat plants. Under drought stress conditions plants treated with RL1 showed a significant increase in shoot dry weight (**Figure 30B**, p-value = 0.000004). Plants treated with NB17_5 showed a significant increase in root fresh weight under non-drought conditions (**Figure 30D**, p-value = 0.001) and a significant decrease under drought conditions in root dry weight (**Figure 30E**, p-value = 0.0003), shoot dry weight (**Figure 30B**, p-value = 0.000004) and shoot length (**Figure 30C**, p-value = 0.004). No significant difference between the treatments was observed under non-drought conditions for fresh weight shoot (**Figure 30A**), dry weight shoot (**Figure 30B**), shoot length (**Figure 30C**), dry weight root (**Figure 30E**) and root length (**Figure 30F**) and under drought conditions for root length (**Figure 30F**). No significant difference in the evaluated plant parameters was observed for plants treated with FZB42. The results indicate a positive effect on plant growth in wheat plants of RL1 under drought stress, whereas the NB17_5 had a negative effect on plant growth under drought stress, which was unexpected. NB17_5 had a positive effect on plant growth in wheat under non-drought stress.

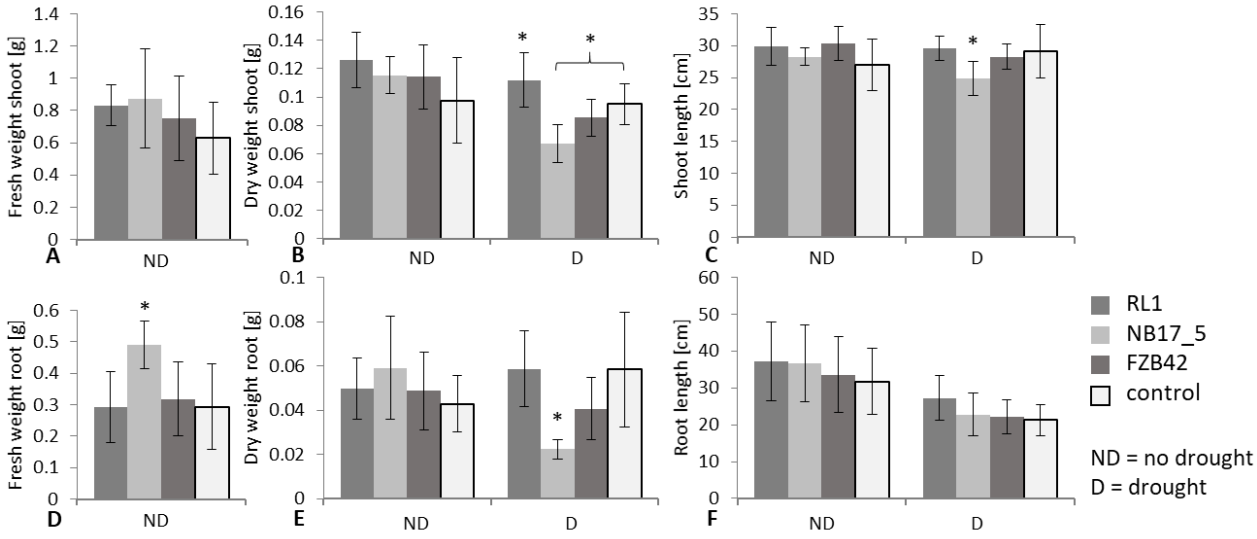

Figure 30: Effect of RL1, NB17_5 and FZB42 on wheat plants. Wheat plants grew in sand-clay pot system under drought (D) and non-drought (ND) conditions. Evaluated plant parameters were shoot fresh weight (**A**), shoot dry weight (**B**), shoot length (**C**), root fresh weight (**D**), root dry weight (**E**) and root length (**F**). Fresh of root and shoot under drought conditions were excluded due to treatment bias. Error bars indicate standard deviation. Significant difference is indicated by asterisks representing * = $P < 0.05$, N = 10.

3 Discussion

Abiotic and biotic stresses such as intensive use of mineral fertilizer and chemical pesticides as well as climate change induced drought and heat waves (Hutchins *et al*., 2019), threaten agroecosystems and generate a need for sustainable alternatives in agricultural practices. Plants live in association with a plethora of microorganisms including many, which can support plant growth and health especially under biotic and abiotic stress. Therefore, PGPB could be a sustainable solution for modern agriculture. Many studies have shown successful application of PGPB as single strains and consortia to improve plant growth and health (Hu *et al*., 2016; Molina-Romero *et al*., 2017; Berendsen *et al*., 2018; Berg and Koskella, 2018; De Vrieze *et al*., 2018; Finkel *et al*., 2020), but the demand for new PGPB is high to meet the needs of the different plant species and cultivars growing under varying environmental conditions. For this reason, the goal of this thesis was to find and characterize PGPB in order to apply them as single strain or consortia with a beneficial effect on the plant. Additionally, also under abiotic stress conditions PGPB have previously been shown to successfully improve plant growth and health, such as drought stress (Kumar *et al*., 2019; Hone *et al*., 2021; Rashid *et al*., 2021). Therefore, a second goal of this thesis was to find beneficial bacteria, which also support plants under drought stress and to understand plant-microbe- and microbe-microbe-interaction dynamics under this condition. The hypothesis was that drought stressed habitats would harbor a high proportion of drought resistant isolates and that those isolates would be well suited for supporting plants under drought stress. The second hypothesis was that consortia would be more successful in supporting plants compared to single strain application. To address the goal, bacterial isolates were characterized using two different approaches. First the isolates were selected based on information derived from the microbiota analysis (chapter 3.1) and experimentally screened for common PGP traits (chapter 3.2). The consortia were assembled based on the functional performance as well as the microbial composition and applied to plants under non-drought or drought conditions (chapter 3.2). Drought related changes in the plant and associated microbiota were analyzed to elucidate potential beneficial effects (chapter 3.3). In parallel, the strategies to apply bacterial single strains or consortia to plants under non-drought conditions were evaluated (chapter 3.4). In the second approach the genomes of two bacterial isolates were sequenced to identify their full PGP potential in depth with subsequent *in vitro* and *in planta* experiments to see if the genetic potential was actually transferred into functional traits (chapter 3.5). Both approaches, i.e. large scale

standardized screening of an unknown culture collection as well as targeted functional tests on promising isolates based on comprehensive genome analysis, could be used complementary in a consecutive process. First, isolates with high plant beneficial potential are identified and second, these isolates are characterized in depth for a safe as well as plant and site specific application.

3.1 Characterization and isolation of natural wheat microbiota

Although wheat is one of the most important crops worldwide the number of PGPB used to improve wheat cultivation is rather scarce. In order to find new PGPB, which could be used to improve plant growth and health in wheat, bacteria were isolated from wheat roots and rhizosphere derived from two different sampling sites. First, the microbial composition of the different sampling sites was compared (chapter 3.1.1). Afterwards the bacterial isolates of the vast culture collection were phylogenetically grouped (chapter 3.1.2) and compared to the original microbiota (chapter 3.1.3) in order to see if the culture collection can represent the natural microbial composition.

3.1.1 The two sampling sites have a different microbial composition

Two different sampling sites were chosen to ensure robustness of the findings and to identify potential PGPB from varying environmental conditions. As a first step the microbial composition of the different sampling sites was compared to identify influencing factors and major phyla. The 16S rRNA gene amplicon sequencing revealed that differences in the microbial composition between Scheyern and Bernburg were strongly correlated with the different locations and the different previously grown crops. These findings confirmed previous studies on the wheat microbiome composition, which was shown to be influenced by geographic and local edaphic factors (Kavamura *et al*., 2021), such as soil properties (e.g. pH or nitrate levels) (Bender *et al*., 2016; Rascovan *et al*., 2016) or previously grown crops (Bender *et al*., 2016; Peralta *et al*., 2018). Furthermore, anthropogenic, environmental or host related factors (Lebeis *et al*., 2015; Castrillo *et al*., 2017; Zhang *et al*., 2020; Kavamura *et al*., 2021; Wippel *et al*., 2021), such as cultivar (Philippot *et al*., 2013; Winston *et al*., 2014; Agnolucci *et al*., 2019; Hone *et al*., 2021; Kavamura *et al*., 2021) play a role. Unlike other studies (Hartman *et al*., 2017; Santos-Medellín *et al*., 2017) the compartments root (and rhizosphere) and (bulk) soil were not found to be significantly different from each other (**Figure 3B,** p=0.514), which was probably due to the fact, that the sampled bulk soil was also heavily rooted, so it was not possible to clearly separate bulk from rhizosphere soil. Additionally, soil particles were difficult to remove from the root surface as a result of the dry weather conditions at sampling time and soil texture. Sampling bulk soil from a position with less

vegetation or removing soil from root samples by a more rigid cleansing procedure could improve the separation. However, the former method bears the risk of sampling at a site with different or no management (e.g. at the edge of the field), and the latter of losing also part of the rhizosphere microbiota. In both sampling sites the phyla Proteobacteria and Actinobacteria were enriched, confirming previous studies on the dominant phyla in wheat rhizosphere (Rascovan *et al*., 2016; Kavamura *et al*., 2021). Overall, the results were as expected and allow to use the data for upcoming comparative analysis.

3.1.2 A vast culture collection was obtained from wheat root and rhizosphere

Large culture collections provide an important base for microbial research (Turkovskaya and Golubev, 2020) and culturing of root-associated microbes is a necessary first step to retrieve culturable microbial strains required for application to improve crop productivity by e.g. microbiome modulation (Berg, 2009; Schlaeppi and Bulgarelli, 2015; Bender *et al*., 2016; Compant *et al*., 2019). Roots and rhizosphere of plants are a valuable source for PGPB and many bacterial groups have been shown to contain culturable members in the plant microbiota (Bai *et al*., 2015; Rascovan *et al*., 2016). About 10% (Kavamura *et al*., 2021) to sometimes up to 65% (in *A. thaliana*) (Bai *et al*., 2015) of root-associated microbes are amendable to culture making the "1% culturability paradigm" obsolete (Martiny, 2019). However, successful application of microbial inoculants is facing obstacles, such as rhizosphere competence and survival rate under field conditions (Herrmann and Lesueur, 2013; Compant *et al*., 2019; French *et al*., 2021). Therefore, some authors suggested that members of the naturally occurring microbiota of a plant could be better adapted to the respective environmental conditions (Saad *et al*., 2020; Wippel *et al*., 2021), such as drought stress, and that tailored microbial inoculants could help to overcome these obstacles (Compant *et al*., 2019; Bakker *et al*., 2020; Berg *et al*., 2021; French *et al*., 2021). In line with these suggestions, a vast culture collection of 1751 isolates was derived from roots and rhizosphere of the two different sampling sites Scheyern and Bernburg using seven different culture media. The isolates represent members of the four phyla Proteobacteria, Actinobacteria, Firmicutes and Bacteroidetes, which dominate the root microbiome (Bulgarelli *et al*., 2012; Lundberg *et al*., 2012; Knights *et al*., 2021) and are common in the wheat rhizosphere (Rascovan *et al*., 2016; Kavamura *et al*., 2021). Interestingly, although the number of Bernburg isolates was surpassing the number of Scheyern isolates a similar number of taxa was identified for both sampling sites, which could indicate that the culture dependent isolation was selective for certain bacterial groups

(Armanhi *et al*., 2016; Rascovan *et al*., 2016) and/or that the rhizosphere is dominated by specific bacteria (Bulgarelli *et al*., 2012; Lundberg *et al*., 2012; Knights *et al*., 2021). However, on strain level the individual composition of the culture collection of the two sampling sites differed considerably. *Pseudomonas* was one of the most abundant genera in the culture collection from both sites, which was already reported to be high abundant in a previously described wheat culture collection (Rascovan *et al*., 2016). The microbial composition in the culture collection was expected and includes taxa, which are common in the wheat rhizosphere (Rascovan *et al*., 2016; Kavamura *et al*., 2021).

For an initial grouping of the isolates and in order to avoid excessive sequencing of all isolates (of which many might be the same species or even strain) the RFLP method was used. As this method has obvious limitations determining the isolates on genus or species level (Oger *et al*., 1998; Hashim and Al-Shuhaib, 2019), representatives of each RFLP pattern had to be phylogenetically allocated via 16S rRNA gene sequencing. For deeper taxonomic analysis without sequencing the use of a combination of multiple restriction enzymes would be necessary (Oger *et al*., 1998). Nevertheless, the RFLP method as used in this work was appropriate, fast and cost-efficient to meet the purpose of systematic reduction of the number of isolates into a manageable amount for further characterization and conduction of upcoming plant experiments.

3.1.3 The culture collection partly represents the natural microbiota on phylum level

In order to estimate if the established culture collection can represent the natural wheat microbiota, which can be relevant e.g. for experiments mimicking the natural microbial community or abundance based selection of isolates, the microbial composition of the culture collection was compared to the microbiota of the root and rhizosphere. The comparison revealed a partial representation of the microbiota by the culture collection on phylum level with representatives of the four phyla Proteobacteria, Actinobacteria, Firmicutes and Bacteroidetes in culture. Proteobacteria and Actinobacteria harbor many culturable members (Rascovan *et al*., 2016, Hone *et al*. 2021) and were high abundant in the natural community. Therefore, it is not surprising that many isolated bacteria in the culture collection belong to these phyla. In the Bernburg culture collection Firmicutes were overrepresented whereas in the Scheyern culture collection Firmicutes and Bacteroidetes were overrepresented compared to the natural community (**Figure 4A, B**). Members of the phylum Bacteroidetes have been reported to be crucial degraders of complex organic matter and are versatile in the use of compounds as carbon and energy source, which could

be advantageous during the isolation process (Thomas *et al*., 2011). The phylum Firmicutes includes for example the spore-forming genus *Bacillus* (Tan and Ramamurthi, 2014), which enables members of this genus to survive harsh abiotic conditions or starvation periods. Spores, which were in the dormant state in the rhizosphere, could awake on nutrient rich cultivation media. This could be one reason why Firmicutes are frequently found in cultivation based isolation approaches (Rascovan *et al*., 2016; Armanhi *et al*., 2016).

The taxonomic composition based on the microbiota amplicon sequencing of the Scheyern root and rhizosphere was analyzed in depth, because the information was relevant to assemble the consortium K2 (chapter 3.2.2). The results revealed 271 identified genera of which 108 were frequently found in the wheat core microbiome (Agnolucci *et al*., 2019; Kavamura *et al*., 2021), such as *Massilia, Bradyrhizobium* and *Sphingomonas* associated with plant protection against plant-pathogenic fungi (Araujo et al., 2019) or plant growth promotion (Luo *et al*., 2019; Kavamura *et al*., 2021). Most of the 18 culturable genera in the Scheyern culture collection were reported to be commonly associated with plants and found in at least two previous wheat microbiome studies (Kavamura *et al*., 2021). The genera *Bosea*, *Microbacterium*, *Kaistia* and *Polaromonas* are less common members of the wheat microbiome (Schmalenberger *et al*., 2008; Kavamura *et al*., 2021; Yin *et al*., 2021). Many identified genera harbor strains with PGP activities, for example *Pseudomonas* (Pieterse *et al*., 2020) or *Variovorax* (Chen *et al*., 2013), which increases the chance to find new PGPB species or strains in the culture collection. Linking the information of the rhizosphere microbial community to the bacterial isolates showed that the culture collection represents a valuable resource for future microbiota manipulation experiments and the knowledge on microbial abundances was used in this thesis to assemble consortium K2.

3.2 Assembly and application of microbial consortia under different abiotic conditions

Finding the one beneficial bacterial strain with all desired characteristics colonizing all plants and soil types is unlikely (Kavamura *et al*., 2013). This is one reason that the application of microbial consortia is an emerging approach to enhance PGP and biocontrol effects, which can be achieved by using synergies between the microbial partners leading to a more pronounced and resilient PGP effect (Compant *et al*., 2019). Therefore, one aim of this thesis was to find a consortium with a plant beneficial effect. Besides, consortia add more complexity to the studied system and help to understand microbe-microbe-plant-interactions, especially relevant under abiotic stress conditions

(Marín *et al*., 2021). Plants developed many adaptions to survive under drought stress, such as stomatal closure to avoid water loss by transpiration (Harb *et al*., 2010), altering the root architecture with increased root hair formation and proliferated lateral roots for an increased root surface area with improved water uptake (Siddiqui *et al*., 2021) as well as long primary roots to reach deeper moisture layers in soil under drought stress. Despite these adaptions plants are still susceptible to drought. As single strains or consortia have been previously shown to also successfully support plants under drought stress conditions (Kumar *et al*., 2019; Hone *et al*., 2021; Rashid *et al*., 2021), one important aim of this thesis was to identify a consortium that supports plants under this abiotic stress. The underlying hypothesis was, that isolates from a drought stressed habitat will more likely bear the desired stress tolerance traits and will therefore be better suited for assembling such a plant beneficial consortium. For this reasons, *in vitro* characterization of the isolates for their stress resistance, plant beneficial traits and competitive behavior was the necessary next step to select appropriate candidates for the application as plant beneficial consortium (chapter 3.2.1). 30 isolates of the Scheyern culture collection representing 13 genera, which met the criteria described in methods section 6.4, were further characterized, assembled to consortia (chapter 3.2.2) and applied to wheat plants under different abiotic conditions (chapter 3.2.3). The establishment of the consortia in the rhizosphere (3.2.4) and their influence on the microbial composition (chapter 3.2.5) were analyzed to link observed effects to the applied bacteria. Selected isolates from Bernburg were further characterized by master's student Furkan Tunc (thesis in preparation) under my supervision.

3.2.1 Selected isolates show many plant beneficial and stress tolerance traits *in vitro*

Beneficial plant-microbe interactions are mediated by functions including plant hormone production, nitrogen fixation, siderophore production for iron acquisition, phosphate solubilization and stress protection e.g. via ACC deaminase activity (Glick, 2012; Glick *et al*., 2014; Gu *et al*., 2020). Therefore, selected isolates were screened for these plant-beneficial traits using *in vitro* assays to identify their plant beneficial potential and to allow a targeted selection of bacteria for application as consortium. A surprisingly high proportion of the characterized isolates (86%) showed plant beneficial traits *in vitro* spanning across groups with different physiological properties and metabolisms (Brenner *et al*., 2005). A similar high amount (92%) of isolates with plant beneficial traits *in vitro* were identified for the Bernburg isolates, indicating that the used isolation and selection strategy was successful. Additionally, these observations could be related

to an interplay of successful recruitment of beneficial bacteria by the plant (Lebeis *et al*., 2015) as well as the adaption of the bacteria to root and rhizosphere conditions (Saad *et al*., 2020), which could lead to enrichment of plant beneficial bacteria in the rhizosphere. Most of the characterized isolates belong to genera, which have been previously reported to show one or more of these PGP traits *in vitro* or *in planta* in wheat, such as *Arthrobacter*, *Bacillus*, *Dyadobacter, Flavobacterium, Rhizobium, Pedobacter, Pseudomonas, Sphingomonas, Streptomyces*, *Variovorax, Rhizobacter* (Kavamura *et al*., 2021) or other cereal crops, such as *Luteibacter* (Guglielmetti *et al*., 2013). However, the genus *Polaromonas* was not yet described as PGPB in wheat, although members of this genus were involved in desulfurization in wheat rhizosphere providing carbon-bound sulfur to plants (Schmalenberger *et al*., 2008). To my knowledge, the *Polaromonas* strain of this thesis is the first one reported to produce IAA. Other *Polaromonas* spp. were previously described as PGPB in sugar beet without characterization of PGP traits (Okazaki *et al*., 2021), indicating a PGP potential for members of this genus. However, the *Polaromonas* isolate investigated in this thesis did not establish in the rhizosphere, which is a pre-requisite for successful PGPB candidates (Romano *et al*., 2020; French *et al*., 2021). The isolates, which tested positive for siderophore production, belong mainly to the genus *Pseudomonas*, which confirms previous studies (Pieterse *et al*., 2020). The genus is well-known for this trait, which provides iron and is often related to successful competition against other microbes in the rhizosphere (Ahmed and Holmström, 2014; Gu *et al*., 2020). Two isolates showed ACC deaminase activity and are associated with the genus *Variovorax*, which has been shown before to protect plants under stress by degradation of the ethylene precursor (Chen *et al*., 2013). The results showed that, despite the selection by media and growth conditions for some taxa, common for culture-dependent approaches, roots and rhizosphere of wheat are a rich source of new bacterial isolates with plant beneficial traits, which confirms previous studies (Rascovan *et al*., 2016; Hone *et al*., 2021).

One aspect of the underlying hypothesis was that the sampling sites, which were exposed to a hot and dry summer period, would harbor a high proportion of bacteria resistant to drought and heat stress. Moreover, due to regular root exudation the rhizosphere can be an environment with higher salt concentrations compared to bulk soil resulting in increased osmotic pressure for bacteria even under non-drought conditions (Hartmann *et al*., 2019). For successful plant-growth promotion under these harsh conditions bacteria need to be able to survive several abiotic stresses. *In vitro* experiments revealed that many of the characterized isolates were able to grow under osmotic

pressure, survive salt stress and grow at elevated temperatures. Isolates withstanding the highest temperature of 45 °C belonged to the genus *Bacillus*. In literature, other mesophilic members of this genus are reported to show a broad temperature range between 7°C to 46°C (Von Stetten *et al*., 1999) or actively grow at even higher temperatures up to 53°C (Munna *et al*. 2015), which could be related to the expression of molecular chaperones or other compounds and indicates that many *Bacillus* spp. are well adapted to elevated temperatures, such as 45°C. Moreover, members of the genus *Bacillus* are able to form spores at critical high temperatures, although spore formation is rather induced above 45°C (Tan and Ramamurthi, 2014). In this thesis, the highest salt tolerance against 7.5% NaCl in the medium was found in isolates belonging to the genus *Rhodococcus*. This genus is well-known for its high tolerance to various stresses (Pátek *et al*., 2021) which could also be confirmed by characterization of RL1 in this thesis (chapter 3.5.2). Despite the lack of comparison to isolates from non-stressed soil, the results showed that a high amount of heat, salt and osmotic stress tolerant bacteria could be isolated from the sampling sites after a hot and dry summer period. These findings also confirm previous studies on isolation of abiotic stress resistant bacteria from stressed environments (Jochum *et al*., 2019a).

The rhizosphere is a resource-rich environment, which attracts a plethora of different organisms including plant pathogens. Therefore, bacteria need to evolve competitive mechanisms in order to establish themselves successfully in the rhizosphere, which can also be employed to protect plants against pathogens (Berg, 2009; Gu *et al*., 2020). For this reason, a selection of Scheyern isolates, belonging to the genera *Bacillus* and *Pseudomonas*, were confronted *in vitro* with the plant-pathogenic fungi *F. oxysporum*, *F. culmorum* and *R. solani.* They showed growth inhibiting effects against these fungi, which could indicate their biocontrol potential. The genera *Bacillus* and *Pseudomonas* harbor many strains well known for their antifungal activity, such as *Bacillus velezensis* FZB42 (Chowdhury *et al*., 2015a) or *Pseudomonas chlororaphis* MA 342 (Johnsson *et al*., 1998). The antagonistic activity of *Pseudomonas* isolates could be related to their ability to produce siderophores described earlier, known to be involved in microbial competition (Gu *et al*., 2020). The production of the antifungal lipopeptides surfactin, iturin A and bacillomycin D was shown to be involved in the antifungal activity of *Bacillus velezensis* FZB42 (Chowdhury *et al*., 2015b). However, genes encoding for these lipopeptides could not be identified in the investigated *Bacillus* isolates. Nevertheless, in depth analysis of released substances in the confrontation assay

could lead to identification of new antifungal compounds and further studies with application to plants would reveal the full antifungal potential of the investigated isolates.

Incompatibility of the members in a microbial inoculant, such as growth inhibiting interactions, can impede the beneficial effect (De Vrieze *et al*., 2018; Thomloudi *et al*., 2019; Marín *et al*., 2021). Therefore, some authors criticized that the interactions between the individual members of a microbial consortium have not been tested before application to the plant (Schlaeppi and Bulgarelli, 2015; Thomloudi *et al*., 2019; Marín *et al*., 2021). Antagonistic interactions have been considered to be responsible for the sometimes observed limited performance of microbial consortia compared to single strain applications (Pertot *et al*., 2017; De Vrieze *et al*., 2018; Bradáčová *et al*., 2019). The isolation of the individual strains from the same habitat does not necessarily imply their neutral coexistence, especially because concentrations of individual strains are much higher in a microbial inoculant (Marín *et al*., 2021). For these reasons, the isolates selected for the consortium were tested in a plate assay for growth-inhibiting interactions. Three *Pseudomonas* isolates strongly inhibited growth of other bacteria and were therefore excluded from the consortium to develop a well-compatible plant beneficial inoculum. However, it should be kept in mind that inhibiting strains are natural members of the rhizosphere. Therefore, they should be considered when the aim of an experiment is to understand multifaceted microbe-microbe-interactions in the plant habitat. Moreover, the growth inhibiting effect of *Pseudomonas* sp. SCA7 toward other microbes indicating potent biocontrol activity led to its further characterization (see chapter 3.5.1).

The culture collection was successfully established and revealed an unexpected high number of bacteria showing plant beneficial traits as well as stress tolerance against heat, salt and osmotic stress *in vitro*. This indicates that the selection criteria in combination with the *in vitro* characterization were a successful and efficient strategy to identify PGPB candidates. However, bacterial PGP traits evolved in the first place to ensure growth and survival of the bacteria in the plant habitat, whereas the beneficial effect for the plant is secondary (Glick, 2012). Therefore, the identified PGPB candidates need to be tested for their beneficial effect *in planta*. 28 isolates were selected to be applied to plants in different combinations as discussed in the next chapter.

3.2.2 Assembly of the microbial consortia

Four different combinations of microbes were used as consortia in order to compare different assembly strategies for consortia. Isolates for consortium K1 were selected based on their PGP traits *in vitro* combining multiple isolates with similar traits, with IAA and siderophore production as the most common ones, to increase diversity and functional redundancy. These aspects have been suggested to improve ecosystem functioning (Bender *et al*., 2016; Duran *et al*., 2018; Wagg *et al*., 2019) and might also lead to improved performance of microbial inoculants. Moreover, traits of the different isolates can complement each other for an improved PGP effect (Compant *et al*., 2019; Santoyo *et al*., 2021).

Selection of bacteria based on their PGP traits *in vitro* has recently been on the rise for selecting consortium members (Chakraborty *et al*., 2013; Hu *et al*., 2016; De Vrieze *et al*., 2018; Herrera Paredes *et al*., 2018; Santhanam *et al*., 2019) and is also frequently used to select single strains for application to plants (e.g. Majeed *et al*., 2015; Masmoudi *et al*., 2021; Wang *et al*., 2021b). Thus, the approach represents the state of the art. Consortium K2 contained only those isolates of K1, which were highly abundant in the Scheyern root and rhizosphere microbiota hypothesizing that this indicates an important role of these isolates in the microbiome (Wippel *et al*., 2021). Using only high abundant isolates is a common approach in SynCom studies to mimic the natural community (Bodenhausen *et al*., 2014; Hartman *et al*., 2017; Niu *et al*., 2017), but was also used successfully to select microbial inoculants with enhanced plant growth or biocontrol effects (Armanhi *et al*., 2018; Niu *et al*., 2017). Consortium K3 was assembled as negative control combining four isolates without PGP traits *in vitro*, although it has to be considered that a PGP effect after application to the plant cannot be strictly excluded, because some PGP traits are only observed among interaction with other organisms (De Vrieze *et al*., 2018). Consortium K4 was an optimized consortium based on five isolates representing four OTUs, which were highly abundant in the microbiota of plants treated with K1 and connected in the co-occurrence network under non-drought conditions (chapter 3.3.3). Therefore, I hypothesized that these bacteria applied as single strains as well as their interaction in the consortium K4 play a special role for the observed effect on root growth. Successful application of the consortia to the plant can be dose-dependent, which was reported for single strains as well as consortia (Berg and Koskella, 2018). For this reason, two different concentrations of CFUs measured by optical density were evaluated and based on the outcome the experiments were performed with the higher dose. The assembled consortia were

applied to wheat plants under drought and non-drought conditions to evaluate the most successful assembly as discussed in the following chapter.

3.2.3 Applied microbial consortia increased root growth under non-drought conditions

In order to analyze a potential beneficial effect of the applied consortia, growth chamber experiments with inoculated wheat plants grown in pots with a sand-clay mix were conducted under drought and non-drought conditions. The beneficial effect differed between drought stressed and unstressed plants. The application of K1 and K4 significantly improved root growth under non-drought conditions in wheat (**Figure 10, 16**), whereas K3 had no significant effect, which was expected according to the selection of the isolates (chapter 3.2.2). Surprisingly, K2 had no significant effect on root growth, although selected strains showed PGP traits and were high abundant in the natural microbial community. This indicates that K2 is missing important isolates, such as *Variovorax* and *Dyadobacter* (chapter 3.4), which could be relevant for the observed beneficial effect under the tested conditions. Roots are the first point of contact for the applied bacteria and the region where interaction was expected. Therefore, root growth was a good proxy to indicate plant-microbe-interaction. The results were in line with previous studies on plant growth promotion effects of consortia (Ansari and Ahmad, 2019; Belimov *et al*., 2020; Hone *et al*., 2021) and could be related to the ability of the isolates to produce IAA, which is involved in root growth and development (Zhao, 2010; Spaepen and Vanderleyden, 2011). Biomass increase such as root growth is at first always an energy investment for the plant, that needs to pay off. On the one hand, an increased root system has several advantages for the plant, such as an increased surface area for water and nutrient uptake as well as stronger anchorage in the soil (Bardgett and van der Putten, 2014; Siddiqui *et al*., 2021). On the other hand, beside the energy investment for growth, an increased root system also bears the danger of providing a larger area for plant pathogens to attack. Therefore, root development is carefully controlled by hormones such as auxin, cytokinin and ethylene (Cary *et al*., 1995; Brumos *et al*., 2018; Siddiqui *et al*., 2021). Consequently, it is also coupled to the interaction with beneficial microbes, which can influence this hormone balance e.g. towards a stronger root branching and subsequently colonize the newly formed surface area (Finkel *et al*., 2020). Through this interaction-driven development pathogens can be outcompeted by the beneficial microbes (Niu *et al*., 2017). *Vice versa*, also the plant via its roots can influence the microbial composition e.g. via physical formation of niches or excretion of certain rhizodeposits,

and thus actively recruits beneficial microbes from the soil (Philippot *et al*., 2013; Lebeis *et al*., 2015; Rascovan *et al*., 2016; Castrillo *et al*., 2017; Kavamura *et al*., 2020). Therefore, the observed increase in root growth could be beneficial for the plant and the plant-microbe-interaction. In terms of agronomy, increased root growth could be of special interest for yield gain in root vegetable, such as carrots (Junia *et al*., 2016) or sugar beet (Sacristán-Pérez-Minayo *et al*., 2020). Further analyses of plant physiological parameters, such as chlorophyll, nitrogen and phosphate content and evaluation of grain yield as well as comparison to conventional fertilization could reveal additional beneficial effects on the plant with biological and agronomic relevance, but were out of scope for this thesis.

The results of the drought stress experiments in wheat showed a trend towards longer primary roots and reduced root biomass in plants inoculated with K1, which could indicate an adaption to drought stress (Siddiqui *et al*., 2021) or a loss of the beneficial effect observed under non-drought conditions. Moreover, a modest increase in survival rate was observed for all plants inoculated with bacterial consortia. The hypothesis of an adaption to drought stress is strengthened by a study on the comparison of two wheat cultivars with large and small root systems, which revealed that the cultivar with larger roots depleted water faster from soil and the cultivar with smaller roots was better adapted to drought with improved water use efficiency especially during grain development (Figueroa-Bustos *et al*., 2020). However, overall plant biomass was reduced in plants treated with K1 compared to the control and inoculation of plants with stress-protecting bacteria normally leads to larger roots and shoots in inoculated plants compared to the control under drought stress (Jochum *et al*., 2019a; Mahmoudi *et al*., 2019; Jayakumar *et al*., 2020; Yang *et al*., 2020; Hone *et al*., 2021; Rashid *et al*., 2021). This clearly indicates a loss of the plant beneficial effect of K1 under non-drought conditions and that the plant-microbe-interaction is sensitive to drought stress. The loss of the beneficial effect was confirmed by a collaborative experiment together with the environmental Simulation Research Unit (EUS) at Helmholtz Center Munich (HMGU), where the effect on plant biomass of a natural microbiome derived from agriculturally used soil in Jülich was directly compared to a microbial consortium consisting of 14 strains of K1 in a potting soil substrate. The experiment was performed to evaluate the performance of the microbial inoculant in potting soil as part of the transition from application in the lab to the field (Compant *et al*., 2019; Berg *et al*., 2021). The natural microbial community from Jülich significantly increased plant biomass compared to non-inoculated potting soil, whereas the applied microbial consortium showed no PGP

effect. The results indicate that the small consortium could not fully mimic the complexity of the microbial community of a natural soil. Lack of establishment in the rhizosphere, due to competition of the consortium members and the indigenous microbiome in the soil substrate or an inappropriate number of applied bacteria in the soil (Compant *et al*., 2019; Berg *et al*., 2021) could be possible reasons for the observed effect. Further experiments with higher cell numbers in the microbial inoculant or an application of the consortium together with the natural community could improve the outcome. However, the results of the performed experiments clearly point towards a loss of the beneficial effect under drought stress.

Taken together, in this thesis the strategy to assemble a plant beneficial consortium based on the selection via *in vitro* plant beneficial traits was found to be successful. With this root growth under non-drought conditions could be increased, but not under drought stress. If the observed effect can be linked to the applied consortia and whether this is dependent on successful establishment of the isolates in the rhizosphere and their influence on the microbial composition will be discussed in the next chapters.

3.2.4 Microbial consortia established in the rhizosphere in the sand-clay system

Verification of consortium establishment in the rhizosphere is a crucial step in the evaluation of consortium experiments in order to link the beneficial effect to the applied bacteria (Romano *et al*., 2020; Marín *et al*. 2021) and was performed based on 16S rRNA gene amplicon sequencing data. The sand-clay substrate, which was selected as trade-off between axenic systems and natural soil, had a reduced intrinsic microbiota compared to soil. This allowed to track the members of the applied consortia until the end of the experiment. A substantial portion of the selected isolates identified at the end of the experiment was phylogenetically very close or identical with the detected OTUs. However, the amplified 16S rRNA gene fragment of the V4 region was not long enough to identify the bacteria unambiguously on strain level. Nevertheless, the findings provide clear indications that the consortium isolates established in the rhizosphere under drought and non-drought conditions in the sand-clay system.

3.2.5 Application of consortia caused shift in microbial composition

Short- and long-term shifts in the microbial composition are part of a whole set of microbiome modulations upon inoculation with consortia, which is considered as a novel and efficient mode of action of microbial inoculants (Berg *et al*., 2021). Therefore, the effect of the applied consortia on

the microbial community was analyzed using a 16S rRNA gene amplicon sequencing approach. The application of the three tested consortia K1, K2, K3 caused a significant shift in the microbial composition different from the control treatment. Two-dimensional MDS plots of ß-diversity in root and rhizosphere microbiota showed that control samples were more spread apart (**Figure 13A**) indicating a more random assembly of the microbiota. Samples with consortium treatments are more similar to each other, indicating a targeted structuring of the microbial composition. In samples inoculated with K1 the largest phenotypic change of the plants was observed. Therefore, these samples were analyzed in depth. The difference between K1 and control samples was significant (**Figure 13A**), which was the desired effect, because the applied consortia should push the original microbial community towards a beneficial composition. Enriched genera in this treatment include *Flavobacterium*, *Sphingomonas*, *Dyadobacter, Variovorax* and unknown *Rhizobiacea*. The genera *Flavobacterium* and *Sphingomonas* were also highly abundant in the original Scheyern microbiota and members of the mentioned genera are well known as PGPB (e.g. Rathi *et al*., 2013; Kumar *et al*., 2018; Luo *et al*., 2019). Therefore, they could be involved in the root growth promotion under non-drought conditions. The genus *Lysobacter* was not a member of the applied consortium, but was nevertheless shown to be more abundant in all K1 samples compared to the other inoculations and the non-inoculated control. This could indicate a favorable interaction of this strain with the K1 consortium leading to its enrichment in the rhizosphere from the growth substrate.

Proteobacteria were enriched in treatments inoculated with K3 and the control and could indicate a dysbiotic state of the plant root microbiome. Dysbiotic microbiome shifts can cause negative effects on the host and are often associated with enriched Proteobacteria also in humans (Chen *et al*., 2020; Xu *et al*., 2021). However, plants did not show severe disease symptoms as was shown for *Arabidopsis thaliana* with dysbiotic microbiomes (Chen *et al*., 2020). Besides, Proteobacteria are frequently found in healthy wheat plants as well (Rascovan *et al*., 2016), so their presence is not necessarily indicative for a detrimental microbiome shift.

Overall, the development and application of a beneficial consortium based on *in vitro* plant beneficial traits, which increased root growth under non-drought conditions was successful. However, the beneficial effect on root growth was lost under drought stress. Therefore, the hypothesis that a bacterial consortium with isolates derived from a drought stressed rhizosphere would have a beneficial effect via biomass increase under similar drought stress conditions, could

not be confirmed. Further analyses were conducted to elucidate other effects of the plant inoculation with consortia during drought stress independent from biomass increase and are discussed in the following chapter.

3.3 Drought stress related changes in plant gene expression and the microbiota

Understanding the mechanisms, underlying alterations and adaptions of the plant microbiome in crop plants to drought stress can help in the development of more resilient crops (De Vries *et al*., 2020). Therefore, drought stress-related changes in the plant and the associated microbiota were investigated in order to identify potential beneficial effects for the plant independent from biomass increase. The effects were analyzed based on gene expression analysis of drought stress related genes (chapter 3.3.1), analysis of the microbial composition and the bacterial load (chapter 3.3.2) as well as the correlations in a microbial co-occurrence network (chapter 3.3.3).

3.3.1 Gene expression differed under drought stress, but not upon microbial inoculation

Plant root and shoot biomass is a good proxy to estimate the beneficial effect of bacteria on plants. However, analysis of altered expression patterns of drought stress related genes in plants upon inoculation with microbial consortia could also reveal beneficial effects not yet translated into biomass changes. For example, inoculation of wheat with the *Flavobacterium* sp. IG15 attenuated the expression of *TaDREB2A* leading to drought stress adaptions in plants and larger plant biomass compared to the control (Gontia-Mishra *et al*., 2016). Therefore, the differential gene expression of the drought stress related genes *TaMY80*, *TaRD29b*, *TaDREB2A* and *TaHSF6b* potentially mediated by abscisic acid signaling (Gontia-Mishra *et al*., 2016; Zhang *et al*., 2017; Zhao *et al*., 2017; Begcy *et al*., 2018) were analyzed using qPCR. Results revealed differential expression patterns of the genes between drought and non-drought conditions, but not between consortium treatments. These findings indicate that the plants were drought stressed, but the applied consortia had no beneficial effect on the analyzed genes, which is consistent with the lacking beneficial effect on root growth observed in the growth chamber experiments. It needs to be considered that the bacteria were applied to the root, whereas the gene expression was analyzed in the shoot. Therefore, the expected effect might have been reduced or delayed. Performing a similar analysis with root material would have been an option to overcome this problem, but the development and validation of a suitable primer set was out of the scope of this study and the focus was on the microbial composition.

3.3.2 Drought caused shift in microbial composition and bacterial load on the roots

Despite the careful selection considering stress related traits *in vitro* the effect on improved root growth of the consortium K1 was lost under drought stress. Therefore, the potential influence of drought on the microbial composition was analyzed using 16S rRNA gene sequencing and qPCR for bacterial load to elucidate if important genera were lost and use this information to adapt future strategies for consortium assemblies.

The microbial community of the consortium experiments changed significantly under drought stress. However, alpha-diversity remained higher in plants inoculated with K1 and K2 compared to K3 and the control, indicating a stabilization of diversity which is normally reduced under drought stress (Jochum *et al*., 2019b; Hone *et al*., 2021). The ability of plants to modify the rhizosphere microbial community via rhizodeposits including root exudates is altered by drought stress, which triggers changes in amount and composition of excreted compounds, such as osmolytes (Song *et al*., 2012; Philippot *et al*., 2013; Lebeis *et al*., 2015; Singh *et al*., 2015; Sasse *et al*., 2018). Moreover, under drought stress the rhizosphere keeps moisture longer than bulk soil (Carminati *et al*., 2010). Both aspects could be in favor of growth of specific bacteria (Santos-Medellín *et al*., 2017) and nutrient fluctuations could cause changes in bacterial compositions and correlations (de Vries *et al*., 2018; Kaul *et al*., 2021). Thus, drought is a major driver of the microbial community structure (de Vries *et al*., 2018; Kavamura *et al*., 2021). Moreover, under drought stress the bacterial load on the roots was strongly increased, which seems contradictory, because drought conditions imply not to be in favor of increased bacterial population density. However, a similar observation without detrimental effects was reported for rice roots under drought stress (Santos-Medellín *et al*., 2017; Guo *et al*., 2020) indicating that increased bacterial load is a key feature of the root microbiome under drought stress (Guo *et al*., 2020). The underlying mechanisms of this reaction are not fully understood yet. A possible explanation could be related to the formation of biofilms, which protect bacteria, among other stresses, against osmotic stress (Knights *et al*., 2021). It is thinkable that the protective effects of biofilms produced by the bacteria could be also beneficial for the plant root as protection against desiccation. However, further experiments need to be conducted to confirm this hypothesis. It should also be taken into account, that the used analysis did not provide any data about the viability status of the colonizing microbes.

Interestingly most of the applied bacteria of inoculum K1, including the mentioned genera, could still be detected under drought stress and some members of the applied consortia have been reported

to support plants under drought stress, such as *Flavobacterium* sp. IG15 (Gontia-Mishra *et al*., 2016) and *Sphingomonas* sp. Cra20 (Luo *et al*., 2019). This was surprising and indicates that the loss of the beneficial effect was not caused by the loss of certain taxa. The effect could be rather related to changes in the expression of PGP traits of bacteria, which might be down-regulated to conserve energy and resources (Haskett *et al*., 2021) or changes in the microbial interactions with effects on the plant. Surviving bacteria could still provide their beneficial functions again and enhance plant growth after a longer recovery phase, which could be a follow-up experiment to this work.

3.3.3 Bacterial co-occurrence networks reveal loss of correlations under drought stress

Microorganisms form complex communities with crucial ecological interactions relevant for ecosystem functioning (Bardgett and van der Putten, 2014; de Vries and Wallenstein, 2017). Co-occurrence networks allow analysis of these complex communities in terms of microbial correlations based on microbial abundance (de Vries *et al*., 2018; Duran *et al*., 2018), which can be used to interpret bacteria-habitat-interactions with implications of vulnerability to disturbances (Wagg *et al*., 2019; Hernandez *et al*., 2021), such as drought stress (de Vries *et al*., 2018), agricultural intensification (Banerjee *et al*., 2019) or pathogen invasion (Trivedi *et al*., 2017). Therefore, the co-occurrence network was used in this thesis to analyze if correlations differed between drought and non-drought conditions and if this information could help to identify specific OTUs potentially relevant for the observed effect on root growth. However, it should be considered that correlations are predictive relationships, which allow to develop hypotheses on potential interactions between microbes, but for reliable information on direct biotic interactions experimental validation is required (Carr *et al*., 2019).

The co-occurrence network was analyzed for K1 samples for drought and non-drought conditions using the bioinformatics tool NetCOMI (Peschel *et al*., 2021), because this treatment revealed the strongest phenotypic change in the plants in terms of root growth. The analysis revealed a loss of correlations between bacterial OTUs under drought stress, which could be related to a changed ratio between the bacteria, which was also observed in drought stressed grassland mesocosms (de Vries *et al*., 2018). The authors found that bacterial communities were more vulnerable with a prolonged effect of drought induced changes compared to fungal communities and the changes in the bacterial community led to altered soil moisture as well as vegetation composition in the

mesocosms (De Vries *et al*., 2018). This indicates that drought destabilizes microbial networks and the changes could lead to a loss of interactions between the bacteria with phenotypic effects, also observed during this thesis. However, the small sample size in this thesis does not allow final conclusions. Additionally, bacterial co-occurrence networks should be interpreted with care, because they can either represent a range of bacterial interactions or just indicate that the bacteria respond in the same way to a changed environment (de Vries *et al*., 2018; Barberan *et al*., 2012; Freilich *et al*., 2018). Thus, bacteria can still interact despite the loss of correlations and the changes in bacterial co-occurrence networks not necessarily affect the plant. The observations of the co-occurrence network could be related to interactions analyzed by metagenome or transcriptome analysis to identify interrupted functions and their biological relevance.

Identification of hub or keystone taxa was used previously to identify potential beneficial candidates for plant application (Poudel et al., 2016; Toju et al., 2018, 2020; Trivedi et al., 2020). Therefore, the co-occurrence network was also used to identify potential hub genera and the positions of the consortium isolates in the network. The genus *Rhodococcus* was identified as one of the hub genera in the drought stress network, which could be related to the remarkable tolerance of this genus against various stresses (Pátek *et al*., 2021) and could indicate a special relevance of the genus *Rhodococcus* for a functional microbiome. Four genera of consortium K1, namely *Variovorax*, *Flavobacterium*, *Sphingomonas* and *Dyadobacter*, were found to be highly enriched in K1 inoculated wheat plant rhizosphere after cultivation in both drought and non-drought conditions. Additionally, these genera were connected in the co-occurrence network from non-drought samples, whereas in the drought stress network, the correlation between *Variovorax* and *Sphingomonas* was lost. This led to the hypothesis that these genera might positively influence each other and play a specific role in the plant growth promotion effect of the root that was lost under drought stress, which was analyzed in the next chapter.

3.4 Consortia more effective than single strain application

The increase in root biomass upon treatment of wheat plants with K1 under non-drought conditions could be an effect caused by the whole consortium or by single members of the consortium. Following recent suggestions to use synergies between the microbial partners leading to a more pronounced and resilient PGP effect (Compant et al., 2019), the hypothesis was that the consortium application would be more successful in plant growth promotion than single strains. Therefore, a growth chamber experiment was performed with five selected consortium strains to compare their

performance as single strains and as consortium, to elucidate their possible interactions hypothesized from their correlations in the co-occurrence network and to fine-tune the microbial composition of the beneficial microbial inoculant K1. The five consortium isolates *Variovorax sp.* SCA27_61, *Variovorax sp.* M92526_27, *Flavobacterium* R2A20_2, *Sphingomonas sp.* M92526_32 and *Dyadobacter sp.* M92526_31 were selected based on their high abundance in the amplicon sequencing analysis of roots treated with K1 and their connection in the co-occurrence network under non-drought conditions.

Inoculation with *Variovorax* strain SCA27_61 showed a trend to increased root dry weight, whereas the other single isolates showed no difference to the control regarding the observed plant parameter. The joint inoculation of the isolates as consortium K4 resulted in an increased root and shoot dry weight, exceeding the effect of the consortium K1 used as positive control. The results indicate that the beneficial effect was dependent on the interaction between the five selected isolates. Similar results have been observed in previous studies where the plant beneficial effect was only observed by interaction of isolates in a consortium, but not by the individual strains (Hartman *et al*. 2017; deVrieze *et al*. 2018). Thus, the hypothesis that consortia would be more successful in plant growth promotion than single strains under the tested conditions could be confirmed. Overall the application of K4 improved plant growth most efficiently, indicating that the five selected isolates are key taxa and of special importance in plant growth promotion in this set-up. Underlying mechanisms for the successful plant growth promotion, also observed in this study, could be synergistic effects between the consortium isolates leading to production of e.g. secondary metabolites upon interaction. Moreover, the consortium members could benefit from pathway side products of the co-inoculated strains or balance the metabolite levels (Finkel *et al*., 2020; Salas-Gonzalez *et al*., 2021; Carlström *et al*., 2019).

Plants inoculated with K4 and SCA27_ 61 showed a trend to shorter, but heavier roots, which is a typical plant beneficial effect of bacteria related to auxin and ethylene balancing (Spaepen and Vanderleyden, 2011; Finkel *et al*., 2020). In line with this observation, the experimental evidence was positive for IAA production of the five isolates as well as ACC deaminase activity in the *Variovorax* isolates included in K4. The five isolates belong to genera, which include PGPB, but are less well-known for plant growth promotion compared to *Pseudomonas* (Pieterse *et al*., 2020) or *Bacillus* (Chowdhury *et al*., 2015). The genus *Flavobacterium* belongs to the phylum Bacteroidetes, which is often enriched in disease-suppressive soils supporting the plant under

fungal pathogen attack (Carrión *et al*., 2019). Additionally, members of the genus *Flavobacterium* have been shown to support plant growth (Rathi *et al*., 2013; Kumar *et al*., 2018) also under abiotic stress, such as salt or drought stress (Mayak *et al*., 2004; Soltani *et al*., 2010; Gontia-Mishra *et al*., 2016). The genus *Dyadobacter* is known to support plant growth under nitrogen limited conditions (Kumar *et al*. 2018) or shows bioremediation potential (Yadav *et al*., 2021). *Sphingomonas* strains have been reported to enhance plant growth (Luo *et al*., 2019; Wang *et al*., 2020). Members of the genus *Variovorax* have been shown to be involved in desulfurization processes (Schmalenberger et al., 2008) and are important for chemical homeostasis of plant hormones (Sun *et al*., 2018; Finkel *et al*., 2020). For example, they have been reported to support plant growth under drought stress by ACC deaminase activity (Chen *et al*., 2013) or balance IAA level in *Arabidopsis* roots (Finkel *et al*., 2020). Therefore, the *Variovorax* isolates of K4 could play a key role in plant hormone balancing also in the conducted experiment. Presence of *Variovorax* and *Dyadobacter* in K4 was also a major difference between the consortia K4 and K2 and could be responsible for the improved performance of K4 on root growth compared to K2. Both taxa were also present in K1 indicating an important role for the observed effect. Metagenome or transcriptome analyses could reveal insights into metabolic interactions and dependencies between the identified key isolates, but were out of scope for this thesis due to time restrictions. However, such analyses are already planned as follow-up to this thesis in order to complete the presented data for publication. Further insights into specific traits and the genomic potential of single strains could clarify their roles in the plant microbiome.

Overall, the most successful strategy to assemble a beneficial consortium was based on a trait-based selection with focus in functional redundancy (K1) followed by a subsequent fine-tuning based on abundance in combination with correlation (consortium K4). High-abundance and correlation of the five selected isolates in the plant microbiota of the experiments could either indicate their better adaption to changing conditions or a plant-mediated selection for them as most relevant strains for the analyzed conditions from the previously applied selection of beneficial strains (Berg, 2009; Lebeis *et al*., 2015; Bai *et al*., 2015; Niu *et al*., 2017). The latter could demonstrate a new approach to develop plant beneficial microbial inoculants by combining *in vitro* pre-screens of isolated bacteria for relevant PGP traits with plant-mediated selection (French *et al*., 2021). In terms of application, narrowing down the number of consortium members to the most relevant strains would improve feasibility for the production of microbial inoculants and could fuel

the trend to employ consortia instead of currently dominating single strain products in the market (Vishwakarma *et al*., 2020).

3.5 Genome-based characterization of *Pseudomonas* sp. SCA7 and *R. qingshengii* RL1

Besides the screening for common PGP traits in the culture collection, whole genome sequencing allows a rather targeted selection of PGPB based on the genetic identification of plant beneficial traits. The analysis of the genome sequence can also help to uncover additional traits, such as heavy metal resistance or volatile production. Those traits are often not included in screens for common plant beneficial traits, used e.g. in the first approach of this thesis, because their functional analyses are more complex. Therefore, whole genome sequencing represents a powerful complementary approach for in depth characterization of potential PGPB. Whole genome sequencing of single strains is also important to improve functional annotation of sequences generated in meta-omics studies (Schlaeppi and Bulgarelli, 2015). The genome-based characterization allows to identify the genetic potential of the analyzed strain, predict its potential role in the plant microbiome and can be used to define selection criteria (Levy *et al*., 2018). Moreover, whole genome sequencing allows reliable phylogenetic classification to discriminate beneficial bacteria from pathogens. In this thesis, the approach was used to address the goal of analyzing the genomic and functional potential of the two bacterial strains *Pseudomonas* sp. SCA7, isolated from wheat rhizosphere (3.5.1), and *R. qingshengii* RL1, isolated from rucola leaves (3.5.2). However, the efficiency of PGPB and their abundant molecular PGP traits are not necessarily correlated (Vishwakarma *et al*., 2020). Therefore, *in vitro* and *in planta* experiments were performed with both isolates after identification of relevant PGP genes to elucidate if the genetic potential was actually transferred into functional traits.

3.5.1 Genome-based characterization of SCA7

The isolate SCA7 belongs to the genus *Pseudomonas*, which is a highly diverse genus and one of the most abundant taxa in soil encompassing more than 220 described and validated species (Bakker *et al*., 2013; Gomila *et al*., 2015; Meena *et al*, 2017; Lalucat *et al*., 2020; Parte *et al*., 2020). SCA7, isolated from wheat rhizosphere during this thesis, inhibited growth of eleven bacterial isolates in the pairwise microbial interaction assay. This led to the exclusion from the microbial consortia, but raised interest for an in depth characterization of its potential PGP and biological control traits. Therefore, the whole genome of SCA7 was sequenced, which helped to

assign a phylogenetic position in the complex bacterial phylogeny of the genus *Pseudomonas* (chapter 3.5.1.1). This is also relevant for a potential registration as biocontrol agent. Moreover, the genomic potential for plant beneficial traits could be identified (chapter 3.5.1.2). Further *in vitro* and in *planta* characterization of the identified genes was performed by master's student Isabella Gantner (March 2021) under my supervision.

3.5.1.1 Phylogeny reveals indications for discovery of a new *Pseudomonas* species

In order to identify the phylogenetic position of SCA7 the whole genome sequence was compared to other *Pseudomonas* strains. SCA7 was closely related to the type strain of *Pseudomonas helmanticiensis* (Ramírez-Bahena *et al*., 2014), *Pseudomonas koreensis* CFBP13504 (Torres-Cortés *et al*., 2019) and *Pseudomonas koreensis* CI12 (Lozano *et al*., 2017). However, the average nucleotide identity between SCA7 and *P. helmanticiensis* was 92% and thus below the threshold for species delineation of 94% (Goris *et al*., 2007; Sangal *et al*., 2016). This indicates that SCA7 could form a new *Pseudomonas* species together with *P. koreensis* CFBP13504 and *P. koreensis* CI12. Moreover, the whole genome sequencing revealed that SCA7 is not closely related to plant or human pathogens, which is a requirement for the application in agriculture.

3.5.1.2 SCA7 genome harbors genes potentially involved in plant growth promotion and pathogen suppression

As SCA7 showed growth inhibition of other bacteria *in vitro* and was isolated from the rhizosphere, it was hypothesized that SCA7 would harbor genes relevant for competitive traits against other microorganisms as well as genes encoding for plant beneficial traits. The targeted screening of the SCA7 genome for PGP and biocontrol traits revealed many genes and clusters potentially involved in plant growth promotion and biocontrol. Genes involved in the production of tryptophan relevant for IAA biosynthesis are present in the genome and SCA7 produced IAA *in vitro*, indicating a plant growth promoting potential. Presence of genes encoding for siderophores in the SCA7 genome and siderophore production *in vitro* indicate the capability of SCA7 to support the plant in growth under iron-limiting conditions and under pathogen attack (Ahmed and Holmström, 2014; Gu *et al*., 2020; Pollak and Cordero, 2020).

Members of the genus *Pseudomonas* are known for the production of secondary metabolites involved in biocontrol mechanisms against plant-pathogenic fungi and oomycetes (de Vrieze *et al*., 2018; Johnsson *et al*., 1998; Tagele *et al*., 2019) as well as bacterial pathogens (Hu *et al*., 2016).

Therefore, SCA7 was analyzed for genes related to antagonistic activities against plant pathogens. Secondary metabolites are often encoded by biosynthetic gene clusters (BGCs) (Dutta *et al*., 2020). A total of 11 BGCs were identified in SCA7, which is a common number of BGCs found in *Pseudomonas* species (Zhao *et al*., 2019; Dutta *et al*., 2020) indicating the potential of SCA7 to produce antimicrobial substances. For example, arylpolyene (APE), which is the most common BGC of Gram-negative bacteria and among other functions involved in biocontrol, was identified in SCA7 (Dutta *et al*., 2020). Moreover, a common antifungal compound produced by *Pseudomonas* species, is phenazine (Yu *et al*., 2018; Tagele *et al*., 2019). For example, a phenazine-producing *Pseudomonas chlororaphis* was reported to suppress the fungal pathogen *Rhizoctonia solani* protecting maize plants from infection with banded leaf and sheath blight (Tagele *et al*., 2019). Another antifungal compound is the cyclic lipopeptide lokisin, which was shown to protect rice plants against the rice blast fungus *Magnaporthe oryzae* (Omoboye *et al*., 2019). The antibiotic compound Colicin V is a peptide antibiotic originally produced by *Enterobacteriacea*, which disrupts the membrane potential of sensitive cells (Gérard *et al*., 2005; Cascales *et al*., 2007). Structurally similar antibiotics in the genus *Pseudomonas* are called pyocins (Cascales *et al*., 2007; Ghequire and De Mot, 2014). Lankacidin C, which is originally produced by *Streptomyces rochei* and active against Gram-positive bacteria (Harada *et al*., 1971), was also identified in the strain *Pseudomonas kilonensis* F113 (Rieusset *et al*., 2020). Genes involved in the biosynthesis of the antifungal and antibiotic compounds lokisin, lankacidin C, bacteriocin and phenazine were identified in the SCA7 genome indicating the antagonistic potential of SCA7 against plant pathogens.

In vitro and *in planta* characterization of SCA7 performed by master's student Isabella Gantner (March 2021) showed enhanced plant growth in *Arabidopsis thaliana* and wheat as well as biocontrol activity against plant-pathogenic fungi and bacteria accompanied by volatile production. Her results confirmed that the identified genes and functions of the genome annotation are actually transferred into functional traits and that SCA7 is a good candidate for single strain application with antagonistic potential against pathogens.

3.5.2 Genome-based characterization of RL1 (adapted from Kuhl *et al*. (2019, 2021))

In contrast to SCA7, which belongs to a well-known genus found in plant microbiomes, *R. qingshengii* RL1 represents a lesser known member of the plant microbiome and is the first

Rhodococcus isolated from rucola. Although, the genus *Rhodococcus* is frequently found in the plant microbiome (Francis and Vereecke, 2019; Vereecke *et al*., 2020) descriptions of plant-associated traits in this genus are scarce. Indeed, the genus is rather known to harbor many stress tolerant strains often used in biotechnological applications (Busch et al., 2019; Pátek *et al*., 2021). Therefore, a broader genome analysis was performed to identify the potential of the plant-associated RL1 with a special focus on stress tolerance (chapter 3.5.2.1) as well as interaction with plants (chapter 3.5.2.2) or other microorganisms (chapter 3.5.2.3), also in comparison to the closely related strains djl6 and BG43. Functional analyses of identified traits were performed *in vitro* and *in planta* (chapter 3.5.2.4) to evaluate their functionality and the phylogenetic analysis allowed a clear taxonomic assignment (chapter 3.5.2.5). The results allowed to identify additional specific traits beyond commonly analyzed PGP traits, such as heavy metal resistance, which could help to understand the possible functions RL1 could provide within the plant meta-organism.

3.5.2.1 RL1 genome harbors several genes involved in survival and tolerance to different stress conditions

Genome and functional analyses were used to address the question on how RL1 is equipped to overcome several stress conditions often found in the plant or soil habitat and if the results can confirm previous reports on high stress tolerance of *Rhodococcus* strains (Pátek et al., 2021).

Conventional agricultural practices and soil exploitation can lead to increased soil acidity (Goswami *et al*., 2017). Therefore, acidic pH tolerance is an important trait of plant-associated and soil bacteria to maintain a functional plant microbiome also under acidic soil conditions. Genes involved in acidic pH tolerance were identified in RL1, which are either involved in the production of the compound squalene, a precursor of hopanoid (Schmerk *et al*., 2011) or in the expression of the arginine deiminase (ADI) cluster. The latter is a mechanism to overcome acidic stress often found in Gram-positive bacteria, but dependent on the presence of arginine (Cotter and Hill, 2003). Acidic pH tolerance was reported for *R. qingshengii* BBG1 (Benedek *et al*., 2012) and for the mammalian pathogen *Rhodococcus equi*, which can withstand a pH of 4 (Benoit *et al*., 2000). The experimental evidence in this thesis proved the ability of RL1 to survive and recover from acidic pH conditions. This trait was also shared by the closely related strains djl6 and BG43, indicating that this trait may be widespread amongst the genus *Rhodococcus*.

Regular root exudation by plants or drought stress due to lack of water can increase the osmotic pressure on plant-associated bacteria (Hartmann *et al*., 2019). Therefore, bacteria evolved mechanisms based on e.g. biosynthesis or uptake of osmolytes, such as ectoine (Bremer and Krämer, 2019). The gene cluster for ectoine biosynthesis and transporters was identified in RL1, indicating the ability of RL1 to synthesize ectoine under osmotic stress. Alternative to biosynthesis, bacteria can take up compatible solutes, such as proline or betaine from their environment (Bremer and Krämer, 2019). Genes encoding the respective transporters were found in the RL1 genome. Additionally, the full operon of Na+/H+ antiporter was identified in the RL1 genome, which could play a role in salt stress tolerance (Liu *et al*., 2016; Bhat *et al*., 2020). Results of the *in vitro* experiments of the tested *Rhodococcus* strains growing under high salt and osmotic stress confirmed previous reports of osmotic and salt stress tolerant members of the genus *Rhodococcus*. For example, an upregulation of genes involved in ectoine biosynthesis was observed in *Rhodococcus jostii* RHA1 under desiccation (LeBlanc *et al*., 2008) and rapid adaption to salt stress was described for *R. erythropolis* DSM 1069 (De Carvalho *et al*., 2014). Moreover, plant-associated bacteria tolerant to osmotic and salt stress could also be beneficial for the plant via support of ion homeostasis (Bhat, *et al*. 2020; Salas-Gonzalez *et al*., 2021) and upregulation of osmoprotective compound uptake as well as biosynthesis in the plant (Hartmann *et al*., 2019). For example, *Bacillus* sp. can directly influence proline biosynthesis in plants to improve osmotolerance (Kaushal and Wani, 2016; Bhat *et al*., 2020).

The bacterially produced polyamine spermidine increases biofilm formation and overall bacterial fitness (Xie *et al*., 2014; Liu *et al*., 2016). Additionally, it is an important PGP compound in strains such as *B. subtilis* OKB105 or *Klebsiella* sp. D5A (Xie *et al*., 2014; Liu *et al*., 2016). The upregulation of spermidine export proteins in *Stenotrophomonas rhizophila* DSM14405 upon salt stress in combination with exposure to root exudates emphasizes the role of spermidine as key substance in stress protection in roots (Alavi *et al*., 2013). Presence of genes encoding for the enzymes involved in the biosynthesis of spermidine in the RL1 genome indicate the ability of RL1 to function as stress-protecting agent and support plants under abiotic stress.

Heavy metals, such as mercury, are highly persistent environmental pollutants and a threat to all living organisms (Boyd and Barkay, 2012). Organomercury compounds were used in several agricultural applications, for example as common pest control agent in the 1900's. Although its use has been banned in several countries, it is still used in Australia to treat the plant pathogenic fungus

Ceratocystis paradoxa (Schneider, 2021). Mercury resistant bacteria can convert organomercury compounds or Hg(II) to gaseous Hg(0) to reduce the mercury concentration in their environment (Boyd and Barkay, 2012). Mercury resistance was described in *R. erythropolis* BD2 and *Pseudomonas fluorescens* SBW25 to be located and transferred on a plasmid (Dabrock et al., 1994; Hall *et al*., 2020) containing the *mer*-operon (Boyd and Barkay, 2012). Loss of this plasmid caused a loss of mercury resistance (Dabrock *et al*., 1994; Hall *et al*., 2020). However, in RL1 the identified mercury resistance genes, such as a transcriptional regulator *MerR* and a unique alkylmercury lyase involved in the degradation of toxic organomercury compounds (e.g. MeHg) (Schaefer *et al*., 2004), are located in the chromosome. For the first time it can be reported that mercury tolerance is also present in an isolate of *R. qingshengii* based on the results of the *in vitro* experiment. BG43 and RL1 were both able to survive up to 1 mM of mercury in the growth medium. Survival and detoxification of heavy metals have been reported for other members of the genus *Rhodococcus* (Trivedi *et al*., 2007; Irawati *et al*., 2012), emphasizing the exceptional stress tolerance of this genus. Heavy metal resistance in bacteria in combination with a close association with plants could indicate the adaptation to toxic heavy metal residues of such compounds previously used as pesticides.

Apart from tolerance to heavy metals, several operons in the genome of RL1 were identified, which show that this bacterium has the ability to survive under selective environmental conditions by metabolizing trace gases like CO and H_2. Comparison of deduced amino acid sequences revealed that the identified CODH belongs to the functional type1-CODH enzymes, which catalyze the unidirectional conversion of CO to CO_2 (King and Weber, 2007). This type of enzyme has been extensively studied in aerobic CO-oxidizers, or carboxydotrophic Actinobacteria (Quiza *et al*., 2014). Sequence similarity revealed that the identified [NiFe]-hydrogenase cluster belongs to the high-affinity group 1h/5 Actinobacteria type of hydrogenases which have been shown to scavenge electrons from atmospheric H_2 to sustain aerobic respiration during starvation (Constant *et al*., 2011; Greening *et al*., 2016). Interestingly, less is known about plant-associated atmospheric H_2-oxidizing bacteria. Atmospheric H_2 may serve as the maintenance energy during starvation and sporulation of high-affinity H_2-oxidizing Actinobacteria, providing them the advantage of survival in plant tissues, as was shown for endophytic *Streptomyces* spp. (Greening *et al*., 2016; Kanno *et al*., 2016). The simultaneous presence of the carbon monoxide dehydrogenase (CODH) genes and the [NiFe]-hydrogenase cluster indicate that RL1 can use CO and H_2 as energy source.

The functional annotation of the RL1 genome also revealed that it harbors genes involved in multidrug resistance, tellurite resistance and antibiotic resistance. Tellurite is a metalloid often used as antibiotic compound in *in vitro* experiments and is toxic to eukaryotic and prokaryotic cells (Chien and Han, 2009). Resistance against tellurite can be mediated by a reduction of tellurite (TeO_3^{2-}) to elemental tellurium, indicated by the color change of the colonies, which was also observed in RL1. Moreover, the RL1 genome harbors genes potentially involved in protection against oxidative stress. These genes could be involved in detoxification of tellurite, because the toxicity of tellurite is eventually caused through its strong oxidizing ability or intracellular generation of reactive oxygen species (ROS) (Pérez *et al*., 2007). *In vitro* experiments with antibiotics revealed resistance of RL1 against kanamycin and ampicillin, whereas djl6 and BG43 are more resistant to rifampicin and vancomycin respectively. Antibiotic resistance was mainly investigated and is widespread in the horse pathogen *Rhodococcus equi* (Giguère *et al*., 2017), because of its relevance in livestock animal infections. Antibiotic resistance in plant-associated *Rhodococcus* species was not intensively studied yet. It could confer them a competitive advantage in surviving against other antibiotic-producing microbes in specialized niches like the rhizosphere (Raaijmakers *et al*., 2009; Mendes *et al*., 2013).

The results showed that the RL1 genome harbors many genes, which can be expressed to withstand various stress conditions, confirming the high stress tolerance attributed to several members of the genus *Rhodococcus* (Pátek et al., 2021).

3.5.2.2 RL1 genome reveals successful interaction and survival strategies in association with plants

Several (beneficial) plant-microbe and microbe-microbe associations are involved to maintain a functional plant meta-organism. Such interactions are mediated by functions including plant hormone production, nitrogen fixation, siderophore production and iron acquisition, phosphate solubilization, biofilm formation, stress protection, production of volatiles, exopolysaccharides (EPS), proteases and microbe-associated molecular patterns (MAMP). Genome and functional analyses were used to identify traits relevant for the interaction of RL1 with plants.

An important trait of plant-associated bacteria is the ability to colonize plant roots to facilitate e.g. the exchange of metabolites (Kloepper and Beauchamp, 1992; Pandit *et al*., 2020). For successful root colonization it can be beneficial for the bacteria to be able to produce biofilms (Pandit *et al*.,

2020), which was demonstrated for RL1, djl6 and BG43. Accordingly, the RL1 genome harbors genes encoding for enzymes involved in biofilm formation. Qualitative evaluation of rhizosphere competence via FISH revealed that all three strains were able to colonize the roots of rucola epiphytically. However, quantitative evaluation via CFU counting showed that RL1 and djl6 had significantly more CFUs per mg rucola root than BG43, which indicates a better root colonization ability of *R. qingshengii* species. Verification of endo- or epiphytic leaf colonization of RL1 analyzed with FISH did not deliver clear results due to high auto-fluorescence of the leaves and transformation of fluorescent markers into RL1 was not successful. Therefore, final conclusions upon leaf colonization of RL1 cannot be drawn.

The leaves of *Brassicacea*, such as rucola, contain glucosinolates (GSLs), which are sulfur-containing secondary metabolites involved in the protection of plants against herbivores (Textor and Gershenzon, 2009; Bell *et al*., 2015). Since RL1 was isolated from the leaves of rucola, the question was if the genome reveals information about its ability to metabolize glucosinolates. The results showed that the genome harbors genes potentially involved in the metabolic pathways of GSLs, such as myrosinase, methionine sulfoxide reductase (*msrA*, *msrB*) or aldoxime dehydratase *oxd*. Degradation of GSLs was investigated for gut microbes regarding beneficial effects of ITC production as a chemoprotective function against cancer (Mullaney *et al*., 2013a, 2013b; Mokhtari *et al*., 2018; Bessler and Djaldetti, 2018). However, *in vitro* experiments with rucola leaf extract and pure GSLs did not reveal clear and consistent results on GSL synthesis, bioconversion or degradation by RL1, djl6 and BG43.

The RL1 genome harbors genes related to the production of volatiles, exopolysaccharides and proteases, which are important in microbial communication, plant colonization and microbial detection by the host (Flemming *et al*., 2016; Netzker *et al*., 2020). The chemotaxis protein CheY relevant for the transmission of sensory signals from the chemoreceptors to the flagella motors, which is additionally a microbe-associated molecular pattern (MAMP) (Paul *et al*., 2010) was identified in the RL1 genome. As *Rhodococcus* is a non-motile genus CheY has a rather different function e.g. in sensory signal transduction in another pathway or interaction with the plant. Additionally, in the RL1 genome genes encoding for a LacI transcription regulator and an aldo-keto reductase were identified, which were found to be enriched in genomes of plant beneficial microbes (Levy *et al*., 2018).

RL1 produced a higher amount of IAA in comparison to the strains djl6 and BG43 *in vitro*. Plant hormone balancing or production, such as gibberellin or IAA, by plant-associated bacteria in general can influence root growth, germination, flowering and developmental stages (Kang *et al*., 2014; Panke-Buisse *et al*., 2017; Salazar-Cerezo *et al*., 2018; Finkel *et al*., 2020). The best-known pathway for IAA production includes the enzyme indolepyruvate decarboxylase (*ipdC*), which is not present in the RL1 genome. Instead genes of the alternative indole-3-acetamide pathway for IAA production (Spaepen *et al*., 2007) were identified in the RL1 genome. The ability to produce IAA *in vitro* was not only shown for RL1 but also in another *R. qingshengii* strain (Hasuty *et al*., 2018) and other members of the genus *Rhodococcus* (Francis and Vereecke, 2019). Bacterial production of IAA can be beneficial for the plant by increasing the root system (Spaepen and Vanderleyden, 2011) and balancing IAA production is an important function of the root microbiome (Finkel *et al*., 2020). Gibberellin production is encoded by a conserved operon, which was characterized in α- and ß-Proteobacteria (Nagel *et al*., 2018). Essential parts of the gibberellin operon were identified in the RL1 genome. To my knowledge, this is the first report about the presence of genes of the gibberellin operon in any Actinobacteria. Some plant-pathogenic bacteria produce bioactive GA4, which can have a detrimental effect on seedling development. Beneficial bacteria only produce the precursor GA9 as they lack the cytochrome P450 (CYP115) for the final step in the production of the bioactive GA4 (Nagel and Peters, 2017). As RL1 also lacks the cytochrome P450 (CYP115) this indicates its allocation to the plant beneficial bacteria. An *in vivo* experiment inoculating rucola and *Arabidopsis thaliana* seeds with RL1, djl6 or BG43 did not show clear and consistent results. Preliminary results of an experiment with inoculated plants showed an effect on early flowering by RL1 and heat-killed bacteria. This indicates that simply the presence of the bacterial cells or cell compounds were enough to induce earlier flowering, which needs to be confirmed in further experiments. Verification of the production of IAA and gibberellin by RL1 with gas chromatography and high performance liquid chromatography was beyond the scope of this work.

In an *in vitro* plate assay RL1, djl6 and BG43 were able to grow on nitrogen-free M9 plates with ACC in the medium, indicating ACC deaminase activity, which can protect the plant from detrimental effects of long exposure to ethylene (Glick, 2014; Dubois *et al*., 2018). However, the essential gene *acdS* encoding for ACC deaminase is missing in the RL1 genome. Additionally, all three tested *Rhodococcus* strains were able to grow on all tested nitrogen free media. The results

indicate that the isolates grow on N-free media through utilization of atmospheric nitrogen rather than using ACC as a nitrogen source. Biological nitrogen fixation describes the bacterial conversion of dinitrogen to ammonia mainly through the expression of canonical *nif* gene products (Dos Santos *et al*., 2012; Higdon *et al*., 2020). In the RL1 genome the SUF system FeS assembly protein of the *nifU* family was identified (MSMEG_2718 **Table S6**), which stabilizes the nitrogenase complex and is relevant for diazotrophy especially under low temperature conditions (Suyal *et al*., 2014). The *nifH* gene was previously identified in a diazotrophic *R. qingshengii* strain (Suyal *et al*., 2014; Joshi *et al*., 2019) and used as molecular marker to directly link to a diazotrophic lifestyle. However, no *nifH* gene was identified in the RL1 genome. In a large scale genome analysis Higdon *et al.* (2020) identified three distinct groups of diazotrophic bacteria defined by *nif* gene content and structural variation, indicating that the trait is much more common in nature than previously thought. The genus *Rhodococcus* was classified as DS-negative (= no Dos Santos model *nif* gene homolog present in genome). This implies the presence of alternative *nif* genes and metabolic pathways relevant for nitrogen fixation in *Rhodococcus* genomes beyond the currently known models. Transcriptome analysis and mutant construction would reveal insights to alternative nitrogen fixation mechanisms in RL1 as representative of the genus *Rhodococcus*. In general, nitrogen-fixing bacteria are important, because they allow to reduce the intensive use of artificial fertilizers and with this reduce nitrogen pollution (Imran *et al*., 2021).

Genes involved in iron acquisition and siderophore production were identified in the RL1 genome, for example for the siderophore heterobactin, which is unique to the *Rhodococcus* genus (Carrano *et al*., 2001; Bosello *et al*., 2013; Khilyas *et al*., 2020). The *in vitro* assay for siderophore production was positive for RL1, corroborating that the identified genes were actually expressed and indicating that RL1 could have a plant beneficial effect. Moreover, RL1 could have an advantage under iron-limiting conditions in competition with other microbes for iron (Ahmed and Holmström, 2014; Gu *et al*., 2020; Pollak and Cordero, 2020). These results were in contrast to djl6 and BG43, showing a negative result for the functional analysis. Iron acquisition and ferrous iron transport can occur via two systems, the FeoABC and EfeUOB transporters (Lau *et al*., 2016). The EfeUOB was reported to be low-pH-induced (Cao *et al*., 2007) and was predicted in the genome of a *Leptospirillum* sp. tolerant to acidic pH (Osorio *et al*., 2008). RL1 harbors the genes encoding for the EfeUOB operon, which could contribute to the low pH tolerance of RL1, because it allows iron acquisition under these conditions.

The RL1 genome harbors genes relevant for organic acid production, which are involved in phosphate solubilization and genes potentially relevant for phosphate metabolism and transport. However, genes involved in gluconic acid production, which is the main driver in phosphate solubilization could not be identified (Rodríguez *et al*., 2006). Despite of that, the *in vitro* assay for this trait was positive for RL1 which suggests the presence of alternative organic acids involved in phosphate solubilization. Phosphate solubilization capacity was previously reported for *Rhodococcus globerulus* isolated from *Plectranthus amboinicus* (Murugappan *et al*., 2017).

3.5.2.3 RL1 genome reveals competitive potential against other microorganisms

Members of the genus *Rhodococcus* have been reported to show antifungal activity *in vitro* against plant-pathogenic fungi (Chiba *et al*., 1999; Iwatsuki *et al*., 2007; Santos *et al*., 2020) and RL1 reduced growth of *F. oxysporum in vitro,* but showed no inhibition against *R. solani* and *F. culmorum*. Further studies using model plants will reveal the full potential of RL1 as biocontrol agent against plant pathogenic fungi.

The *qsdA* gene, encoding for a *N*-acyl-HSL lactonase was first described by Uroz *et al*., (2003) for the strain *R. erythropolis* W2 and could also be identified in the RL1 genome. Moreover, the RL1 genome harbors a two-component transcriptional AHL responsive regulator from the *luxR*-family. However, as RL1 is not producing AHLs this regulator is likely a so-called *luxR*-solo, which allows bacteria to respond to quorum sensing signals from neighboring cells without itself contributing to signal synthesis (Hartmann *et al*., 2021). This was also previously described for the genus *Rhodococcus* and other Gram-positive bacteria (Subramoni and Venturi, 2009; Santos *et al*., 2012). *In vitro* experiments showed the ability of RL1 to degrade AHLs. To my knowledge, this is the first report of an AHL-degrading *R. qingshengii*. Also it is the first description of functional AHL degradation by BG43, which was previously reported only to interfere with the quinolone signal of *Pseudomonas aeruginosa* (Müller *et al*., 2014). Quorum quenching ability was intensively studied in *R. erythropolis* R138 (Cirou *et al*., 2007; Barbey *et al*., 2013; Latour *et al*., 2013; Kwasiborski *et al*., 2015), which was able to reduce the soft-rot pathogen *Pectobacterium* in potatoes and most likely uses the degraded AHLs as carbon source. Quorum quenching can also be a beneficial trait in other crop-pathogen systems as reported for example in *Pseudomonas segetis* (Rodríguez *et al*., 2020) or *Bacillus thuringiensis* (Dong *et al*., 2004). Further analysis of RL1 quorum quenching abilities, e.g. against plant pathogens such as *Pectobacterium carotovorum* or *Pseudomonas syringae*, would reveal its full potential as plant biocontrol agent. In a pairwise

microbial interaction assay RL1 was not inhibited in growth and showed no antagonistic activities against the tested strains, indicating a rather mutualistic or neutral position in the plant microbiome, qualifying RL1 as a suitable candidate for employment also in microbial consortia (Thomloudi *et al*., 2019). The identified traits indicate a PGP potential of RL1, which was tested *in planta* and is discussed in the following chapter.

3.5.2.4 Application of RL1 to plants allows no final conclusion on plant growth promotion

Traits identified *in vitro* indicated a potential of RL1 for plant growth promotion also under different stress conditions. Moreover, the genus *Rhodococcus* is frequently found in the rhizosphere (Francis and Vereecke, 2019), such as the wheat rhizosphere used in this thesis. Therefore, RL1 was tested for application under specific soil habitat conditions, which were analysed in a newly developed set-up for rucola plants using the sand-clay system in growth chamber experiments. The focus of this work was to find plant beneficial strains applicable in the rhizosphere. Results of the initial experiment indicating a PGP effect of RL1 on roots could not be consistently confirmed in larger scale experiments under drought and non-drought conditions as well as in comparison to BG43 and djl6. These results were unexpected, but confirms that PGP traits evolved in bacteria to survive in the plant habitat in the first place and that a beneficial effect for the plant is secondary. This means that varying PGP effects can be related to undesirable genetic regulations, which repress PGP traits when their expression is no longer beneficial for the bacteria (Haskett *et al*., 2021). Moreover, despite all the identified traits the competition between RL1 and the initial microbiome (even in a reduced system) could lead to suboptimal rhizosphere colonization and persistence (Thomloudi *et al*., 2019; Marin *et al*., 2021; Haskett *et al*., 2021). Additionally, RL1 was originally isolated from leaves, which could also influence its performance in the rhizosphere. Another obstacle could be related to the rucola cultivar, because different plant cultivars interact in varying intensities with beneficial microbes and an appropriate cultivar is needed for successful application of PGPB (Compant *et al*., 2019; Rodriguez *et al*., 2019). Nevertheless, the genus *Rhodococcus* was reported to be increased in the wheat microbiome after inoculation of plants with beneficial microbes (Agnolucci *et al*., 2019), which could indicate that a beneficial effect can be exploited in association with other microbes. This could indicate that similar to the findings described in the previous chapters also in this case consortia are more successful in plant growth promotion than single strains. But this needs to be explored in further experiments.

Interestingly, RL1 showed a beneficial effect on non-host plants by increasing plant biomass under drought stress in wheat in preliminary experimental data. RL1 belongs to Actinobacteria which are known to be high abundant under drought conditions (Santos-Medellín *et al*., 2017; Hone *et al*., 2021) and was also high abundant in plants inoculated with K3 under drought stress. RL1 was compared to the Scheyern strain *Rhodococcus* sp. NB17_5, which is closely related to *R. qingshengii* based on its 16S rRNA gene sequence and showed phosphate solubilization *in vitro*. NB17_5 enhanced root growth under non-drought conditions, whereas plant growth was decreased under drought stress, indicating that RL1 is better adapted to drought stress in the rhizosphere compared to NB17_5. These findings could also explain the observation in the consortium experiments, where the beneficial effect under drought stress was missing although *Rhodococcus* was identified as a hub species and high abundant in treatment K3 in the wheat microbiome under drought stress. A lower adaption of NB17_5 to drought and the lack of PGP traits in the two other applied *Rhodococcus* strains could explain the missing beneficial effect and shows that not all plant-associated *Rhodococcus* strains have PGP traits. Further experiments need to be conducted to confirm these hypotheses.

3.5.2.5 Genome comparison of related *R. erythropolis* and *R. qingshengii* isolates show potential for re-classification of clade members

Rhodococcus is a genus well-known for its high potential to produce versatile secondary metabolites and the RL1 genome annotation confirms previous studies (Ceniceros *et al*., 2017; Thompson *et al*., 2020). The number of genes from the genome of RL1, which were assigned to the COG group for secondary metabolites, were higher compared to other bacteria, for example *Stenotrophomonas* or *Enterobacter* (Alavi *et al*., 2014; Andrés-Barrao *et al*., 2017). Additionally, 17 biosynthetic gene cluster (BGC) for secondary metabolites were identified in RL1. The average number of BGCs in the *R. erythropolis* clade are 13-24 BGCs and are mostly shared by *R. erythropolis* and *R. qingshengii* strains (Thompson *et al*., 2020). Four BGC cluster were highly conserved among the *R. erythropolis* clade and three of them were also identified in RL1. The remaining unknown BGCs in the RL1 genome are potentially capable of producing novel compounds which could be analyzed in future studies.

Rhodococcus is a heterogeneous genus with eight identified phylogenetic clades (Alvarez, 2019). Phylogenetic analysis based on complete genome sequences of the *R. erythropolis* clade reveals a clear separation into two subgroups at an ANI value of 97%. The first one includes sequences

belonging to only *R. erythropolis*, the second includes *R. qingshengii* and *R. erythropolis* strains. Based on the clear separation previous recommendations can be confirmed and verified to separate the *R. erythropolis* clade into the two groups consisting of the species *R. qingshengii* and *R. erythropolis* respectively (Sangal *et al*., 2016; Khilyas *et al*., 2020; Thompson *et al*., 2020). Additionally, the *R. erythropolis* strains assigned to the *R. qingshengii* group should be re-named as previously recommended (Sangal *et al*., 2016; Thompson *et al*., 2020). The genomes of RL1 and djl6 were clearly identified as belonging to the *R. qingshengii* cluster (Xu *et al*., 2007) and had more genes in common with each other than with BG43, whereas the BG43 genome was classified as *R. erythropolis* (Müller *et al*., 2014; Rückert *et al*., 2015). Despite the clear separation the strains RL1 and BG43 had many functional traits in common, indicating a close functional overlap between the species. At the same time, djl6 and RL1 showed different results in the *in vitro* experiment for siderophore production and mercury tolerance, indicating differences on the genetic and functional level also within the species *R. qingshengii*. RL1 showed overall the best performance in the tested traits. This emphasizes the importance of RL1 and the necessity to analyze the genetic and functional potential of individual strains to understand the role also of lesser known members of the plant microbiome.

3.6 Strengths and challenges of applied approaches

Applications of PGPB as promising solution for sustainable agriculture in form of single strains or consortia are both eligible and depend on the situation. This work has shown examples for the successful use of single strains (chapter 3.5.1) and consortia (chapter 3.2, 3.4). Crucial for the successful application in both cases are the specific traits of the applied isolates and their interactions. Therefore, the rational selection of candidates requires a thorough characterization of the isolates. Common approaches are the large scale standardized screening of an unknown culture collection or the targeted functional tests on promising isolates based on comprehensive genome analysis. Both approaches were used in a complementary manner in this thesis and are discussed here.

A promising and frequently used approach to select plant beneficial bacteria from a culture collection is based on tested functions derived from *in vitro* experiments (Santhanam *et al*., 2019; Herrera Paredes *et al*., 2018; Hu *et al*., 2016) often combined with information derived from the microbial composition, such as abundance (Hartman *et al*., 2017; Niu *et al*., 2017), which was also successfully used in this thesis. For *in vitro* screening often technically easy methods, such as

selective media (Niu *et al*., 2017; Bai *et al*., 2015) are used and can be also performed in mediocratic laboratories with budget limitations. However, the screen can only uncover a selection of PGP traits and might miss a lot of the microbial potential. Additionally, some traits are only expressed under specific conditions, which are only present in the natural habitat, e.g. interaction with other microbes and/or the plant (de Vrieze *et al*., 2018). In that case, genome sequencing can complement information on the genetic potential of strains as far as the involved genes are known. Nevertheless, the trait-based selection is well-suitable for a rather fast screening of large culture collections to identify interesting candidates e.g. for subsequent application to plants or for whole genome sequencing.

Whole genome sequencing reveals the genomic potential of a specific bacterial strain not limited to PGP traits and can elucidate phylogenetic positions, as demonstrated for RL1 and SCA7. The full genome sequence allows more reliable taxonomic assignments compared to 16S rRNA gene based approaches (Hartmann *et al*., 2019). A clear phylogenetic identification is important to discriminate beneficial bacteria from pathogens, because all plant-associated phyla harbor beneficial as well as pathogenic species (Rodriguez *et al*., 2019). Therefore, a clear species discrimination is a pre-requisite for the application of PGPB in agriculture and consequently important for successful market entries of products (Berg *et al*., 2009; Hartmann *et al*., 2019). The identification of genes in the genome sequence related to plant-microbe-interactions can help to select PGP candidates (Levy *et al*., 2018) or plant colonizer (de Souza *et al*., 2020) tailored for specific plant needs or environmental conditions. Considering dropping costs for whole genome sequencing it will become feasible to sequence and analyze full culture collections (Bai *et al*., 2015; Levy *et al*., 2018). Nevertheless, not all plant-beneficial traits can be linked to genes yet and the genomes still harbor a large proportion of hypothetical proteins with unknown functions. For example, Higdon *et al.* (2020) showed that the ability for biological nitrogen fixation could involve new, recently unknown pathways not limited to the expression of canonical *nif*-genes. In these cases, sequencing of representative strains combined with development of mutant lines could link unknown genes to actual functions and is important to improve functional annotation of sequences derived from meta-omics studies (Schlaeppi and Bulgarelli, 2015). Apart from the lack of information from unknown genes, presence of specific genes cannot warrant that genes are actually expressed and transferred into functional traits, as observed e.g. for siderophore production in RL1,

djl6 and BG43. Thus, whole genome sequencing is a helpful tool to select candidates, but the isolates need to be further investigated *in vitro* and *in planta*.

Overall, both approaches were successfully used in this thesis to identify PGPB candidates and complement each other for a targeted selection. The choice of the approach depends on the purpose, budget and time. Nevertheless, identified traits neither genomic nor *in vitro* can guarantee functionality of the strains on the plant. Therefore, in terms of application all strains need to be tested *in planta* and subsequently in the field under varying conditions and should generate reproducible outcomes to be considered as new agriculturally used biological product (Breakfield *et al*., 2021).

4 Concluding remarks

In this thesis it was shown that wheat rhizosphere is a rich source of potential plant beneficial bacteria. In order to identify novel PGPB a vast culture collection was established. The first approach using large scale standardized screening of a large culture collection revealed a surprisingly high number of selected isolates showing plant beneficial traits and tolerance against drought-related stresses. These data confirmed the hypothesis that drought stressed habitats would harbor a high proportion of drought resistant isolates and showed that the applied methods were successful to identify potential PGP candidates. The trait-based assembly and application of the isolates as consortia effectively generated a plant beneficial consortium, which altered the microbial composition and increased root growth in wheat plants under non-drought conditions. The hypothesis that isolates from drought stressed environments would be well suited for supporting plants under drought stress conditions could not be confirmed, because the beneficial effect of the consortium was lost under drought stress. Regarding the beneficial effect under non-drought conditions the interactions between the microbes and in particular between five isolates was decisive. These isolates were high abundant and correlated under non-drought conditions. Furthermore, the five isolates were significantly more successful in supporting plants when applied as consortium compared to their application as single strains. In a second approach the relevance of in depth genome-based characterizations to identify the genomic repertoire of *R. qingshengii* RL1 and *Pseudomonas* sp. SCA7 was demonstrated. Many identified stress resistance, PGP and biocontrol traits could be confirmed *in vitro* and partly *in planta*. Beyond that, their phylogenetic analysis revealed the potential for re-classifications in the *Rhodococcus* clade as well as a potentially new *Pseudomonas* species. The functional analysis showed many shared traits between the two species *R. qingshengii* and *R. erythropolis*, some of them described for the first time in the strains djl6 and BG43. However, RL1 showed overall the best performance. By the thorough characterization of bacterial isolates this thesis contributes to a better understanding of relevant attributes of bacteria for their interactions with plants. Both approaches were successful and can be used complementary to identify potential plant beneficial isolates. However, the evaluation of the actual beneficial effect for the plant requires the application of consortia and single strains *in planta*. Overall, this work pursues the vision of tailored microbial inoculants for sustainable agriculture by establishing a large culture collection and characterizing new PGPB as single strains or consortia *in vitro* and *in planta* including their effect on the microbial composition.

5 Outlook

The characterization of the single strains RL1 and SCA7 opened up further questions on central microbial traits. Transcriptome analysis of RL1 could reveal intriguing aspects such as an alternative nitrogen fixation pathway. Further investigation of the quorum quenching ability against various plant-pathogenic bacteria could advance the understanding of the role of RL1 in biological control. Application of SCA7 as protecting agent against infection of crop plants under field conditions could reveal its full potential as biocontrol agent. For reliable outcomes consortia and single strains still need to be tested under varying conditions on different plants. Despite the involved effort, this still represents the state of the art, also used in industry (Breakfield *et al*., 2021; Manker, 2020). Therefore, future research should focus on upscaling screens for PGP candidates and of microbial inoculants in large scale plant experiments. Moreover, current knowledge on existing strains and formulations should be systematically ordered and easier to use. Therefore, the development of predictive algorithms and databases listing and selecting tailored consortia is required. The current trend of vertical, indoor farming and soilless agriculture, such as hydroponic or aquaponic systems could be an emerging application area for PGPM (Azizoglu *et al*., 2021; French *et al*., 2021). Revolutionizing agriculture is a multidisciplinary approach and most likely there is not one solution fitting all needs (French *et al*., 2021). Nevertheless, healthy plants in a sustainable agricultural system finally also benefits human health and this is worth major efforts.

6 Material and Methods

6.1 Sampling of wheat roots and rhizosphere from Scheyern and Bernburg

Roots and rhizosphere were sampled from an organically managed agricultural field from a long term field trial (since 1990) with flat tillage from the research farm of the Helmholtz Center Munich in Scheyern, Bavaria on 16.07.2018. Sampling took place after a hot and dry summer period (**Supplementary Figure S14A and S14B**; data derived from wetterkontor.de accessed on 02.08.2021). The soil is composed of luvisol with a sandy and loamy texture (43% sand, 33% silt and 24% clay) (Yang *et al*., 2020). Summer wheat was grown on the field with the pre-crop maize. Ten randomly selected root and rhizosphere samples and three bulk soil samples were taken from the field in plastic bags. Separation of roots was performed with sterilized forceps. Bacterial isolation was performed from pooled roots and rhizosphere of randomly selected sample 6 and 9.

Roots and rhizosphere were sampled from soil in Bernburg, Saxony-Anhalt, Germany in collaboration with the university of applied science Saxony-Anhalt on 2.7.2019. Sampling took place after a hot and dry summer period (**Supplementary Figure S14C and S14D**; data derived from wetterkontor.de accessed on 02.08.2021). Samples were taken from two long-term (since 1992) agriculturally used fields growing winter wheat with cultivator tillage (CT) and extensive fertilization (50% less fertilizer, no fungicides, no growth regulator). The fields had either the pre-crop canola or the pre-crop maize. The soil is composed of loess chernozem over limestone (22% clay, 70% silt and 8% sand) (Sommermann *et al*., 2018). Four root samples and one sample of bulk soil were taken per field in plastic bags. Separation of roots was performed with sterilized forceps. Isolation of bacteria from four pooled roots and rhizosphere samples was done separately according to the pre-crop.

6.2 Isolation of root and rhizosphere-associated microbes

Approximately 1 g of wheat root and rhizosphere pooled from 3 plants was washed in 1 x PBS to remove attached bulk soil, ground with 1 mL 1 x PBS and diluted three times (10^1, 10^2, 10^3). 100 µL of each dilution was plated on seven different media (NB, 2 x TY, R2A, King's B, M9, SCA, Cha (composition **Supplementary Table S9**)) and incubated at room temperature for a maximum of 10 days. Emerging colonies were picked every day with sterilized tooth picks, streaked out on a fresh plate with the respective medium and grown overnight for 18 h at 28 °C for colony purification. Purified colonies were transferred to the respective liquid medium and incubated

overnight for 18 h at 28 °C at 180 rpm. Afterwards 1 mL of the overnight grown bacterial culture was transferred in a 2 mL cryotube. 1 mL of 50% glycerol with 50% 1 x PBS mix was added (resulting in 50% bacterial liquid culture 25% 1 x PBS and 25% glycerol) and stored at -80 °C.

For root and rhizosphere samples from Bernburg a high throughput approach was applied where purified colonies were transferred to 700 µL medium in 1.5 mL deep-well plates and shaken at 28 °C at 230 rpm for 18 h overnight. Afterwards 700 µL of 50% 1 x PBS/glycerol were added to each well and glycerolstocks were stored at -80 °C.

6.3 Phylogenetic classification

For initial phylogenetic classification the 16S rRNA gene of the bacterial isolates from Scheyern and Bernburg was amplified with a colony PCR and afterwards analyzed with restriction fragment length polymorphism (RFLP). The 16S rRNA gene sequence was used for phylogenetic identification of bacteria and amplified via colony PCR using the DreamTaq Polymerase (Life Technologies, ThermoScientific®, Germany) and a PCR cycler (LifeEco Thermal Cycler, Biozym). Each PCR reaction contained 3 µL of 10 X DreamTaq buffer (Life Technologies, ThermoScientific®, Germany), 0.25 mM desoxy-nucleoside-tri-phosphate (dNTPs) (Life Technologies, ThermoScientific, Germany), 0.2 µL DreamTaq Polymerase (5 U/µL) (Life Technologies, ThermoScientific®, Germany), 0.2 µM of the primers 27F (5'-AGAGTTTGATCCTGGCTCAG-3') and 1492R (5'-ACGGYTACCTTGTTACGACTT-3') (Metabion International AG, Germany) and 2 µL bacterial solution as DNA template per 30 µL reaction.

For Scheyern samples bacterial colonies were picked from plate, diluted in 10 µL sterile H_2O and 2 µL of the diluted colonies were added to the PCR reaction for Scheyern samples. For the high throughput approach of the Bernburg samples glycerol stock plates were thawed; 5 µL were transferred to a microtiter plate with a ViaFlo Multipipette (Integra®, Switzerland) containing 150 µL NB medium and incubated at 28 °C on a cell shaker (VibraTranslator®, Union Scientific, USA) with speed 4.5 for 24 h. Afterwards the bacteria that grew were transferred to fresh medium using the hitpicking function of a liquid handling robot of the series Freedom EVO (Tecan®, Switzerland) and incubated at 28 °C on a cell shaker (VibraTranslator®, Union Scientific, USA) with speed 4.5 for 24 h. 2 µL were used as DNA template for the colony PCR reaction. The rest was frozen as glycerol stock as described above. The PCR conditions consisted of denaturation at 94 °C for 10

min, followed by 35 cycles at 94 °C for 30 s, 50 °C for 30 s, 72 °C for 2 min and one final elongation step at 72 °C for 5 min. The amplified gene product was visualized and correct size of about 1500 bp was confirmed on a 1% agarose gel.

In the RFLP method the 16S rRNA amplicon is digested with a restriction enzyme, which cuts the amplicon in specific fragments (Botstein *et al*., 1980; Oger *et al*., 1998). Visualization of these fragments on an agarose gel allows the phylogenetic grouping of bacteria according to their specific pattern. A total of 5 µL containing approximately 1 µg of DNA with the 16S rRNA gene amplified as described above was cut with 5 units of the restriction enzyme MspI (New England Biolabs, Frankfurt, Germany). The mix was incubated in a final volume of 50 µL with sterile H_2O and the 10 x CutSmart-Enzyme Buffer (New England Biolabs, Frankfurt, Germany) for 1 h at 37 °C without denaturation step required. Afterwards the cut product was visualized on 2.5% agarose gel running at 200 V for 2 h for clear separation of bands. The RFLP patterns were analyzed manually.

Representatives for each RFLP pattern and candidates with interesting colony formation on plate were sent for sequencing (Eurofins Genomics, Germany). Plates were filled with 2 µL of 10 µM primer 27F or 1492R and 15 µL of PCR product. Results were blasted using NCBI basic local alignment search tool (BLAST, Madden et al., 2002) and closest species identity was evaluated based on highest sequence similarity and highest query overlap. Phylogenetic identity of bacterial isolates, which were chosen for further characterization (see below), was confirmed by sequencing of 16S rRNA gene derived from genomic DNA. A single colony of each strain was picked from a fresh NB plate and grown overnight for 18 h at 28 °C in NB medium. DNA was isolated with DNeasy®UltraClean®Microbial Kit (Qiagen, Germany) following the manufacturer's protocol. 16S rRNA gene was amplified, sent for sequencing and blasted as described above.

6.4 Bacterial strains and growth conditions

Bacterial isolates from wheat root and rhizosphere were selected for further characterization based on their closest BLAST hit, including isolates that were described as closely associated to plants but not yet described as PGPB, which are therefore candidates for new PGPB. Additionally, also isolates were included, which belong to genera known to be drought resistant, such as *Arthrobacter* sp. (Hone *et al*., 2021), were high abundant genera of the Scheyern microbiome or additional genera to increase diversity of the consortium. A total of 30 isolates from Scheyern soil, named hereafter Scheyern isolates, and a total of 27 isolates from Bernburg soil, named hereafter Bernburg isolates,

met these criteria (**Table 3**) and were cultivated in NB or solid NB agar (1.7% agar) with pH 6.8. Strain names were composed of the abbreviation of the respective medium, the number of the plate and the colony number per plate. The strain *Pseudomonas* sp. SCA2728.1_7 was later renamed to SCA7.

Rhodococcus strains were used according to Kuhl *et al*. (2021): *Rhodococcus qingshengii* RL1, named hereafter RL1, is a Gram-positive Actinobacterium and was isolated from rucola leaves. Colonies appear in off-white, beige colors. The 18 h overnight grown culture corresponds with OD_{600} = 0.42 representing approximately 4 x 10^7 CFU (colony forming units). *Rhodococcus qingshengii* djl6 DSM 45222 (type strain), named hereafter djl6, (Xu *et al*., 2007) and *Rhodococcus erythropolis* BG43 DSM 46869, named hereafter BG43, (Müller *et al*., 2014) were obtained from German Collection of Microorganisms and Cell Cultures (DSMZ, Braunschweig). The 18 h overnight grown cultures correspond with OD_{600} = 0.5 representing approximately 5 x 10^7 CFU and OD_{600} = 0.92 representing approximately 5 x 10^8 CFU, respectively. *Rhodococcus* strains were cultivated in TSB or solid TSB agar (1.7% agar) with pH 7.3.

For the conducted experiments the strains in **Table 12** were used as control organisms as described in Kuhl *et al*. (2021): The strains were cultivated in NB or solid NB agar (1.7% agar) with pH 6.8. Unless further specified all strains were cultivated at 28 °C and 180 rpm.

Table 12: Control strains for the conducted experiments.

Bacterial strain	Relevant traits for this study	Reference
Bacillus velezensis FZB42 DSM 23117	produces fungal antagonistic compounds like surfactin, fengycin and iturin	Chowdhury *et al*., 2015b
Agrobacterium tumefaciens A136 ATCC 51350	AHL biosensor strain	Stickler *et al*., 1998; Han *et al*., 2016
Acidovorax radicis N35 DSM 23535	AHL producer strain	Li *et al*., 2011
Acidovorax radicis N35 AHL-*araI::tet*	non-AHL-producing mutant strain	Han *et al*., 2016
Rhizobium radiobacter F4 AHL-	AHL-degrading mutant strain expressing an AHL lactonase (AiiA) and able to grow on potassium tellurite trihydrate ($K2TeO_3*3H_2O$) 100 µg/ml	Alabid *et al*., 2020
Luteibacter sp. Cha2324a_16	phosphate solubilizing strain isolated from wheat roots	This study
Variovorax sp. M92526_27	ACC utilizing strain isolated from wheat roots	This study
Herbaspirillum frisingense GSF30 DSM 1328	nitrogen-fixing and IAA producing strain	Kirchhof *et al*., 2001
Azospirillum brasilense Sp7 DSM 1690	nitrogen-fixing strain	Hartmann and Hurek, 1988
Pseudomonas simiae WCS417r	biofilm-producing strain	Pieterse *et al*., 2020
Escherichia coli DH5α	non-biofilm-producing strain	Anton and Raleigh, 2016

6.5 Whole genome sequencing of *R. qingshengii* RL1 and *Pseudomonas* sp. SCA7

A single colony of SCA7 was picked from a fresh NB agar plate and grown overnight for 18 h at 28 °C in NB medium. DNA was isolated with DNeasy®UltraClean®Microbial Kit (Qiagen, Germany) following the manufacturer's protocol. A microbial library was prepared for PacBio® Sequel system using SMRTbell Express Template Prep Kit® 2.0 and Barcoded Overhang Adapter Kit® 8A. PacBio sequencing was performed with the Sequel sequencing kit® 3.0 (4 reactions) and single-molecule realtime (SMRT) cell® 1 M v3 tray.

The DNA for RL1 was extracted and prepared for sequencing as described in Kuhl *et al*. (2019): A single colony of RL1 was picked from a fresh TSB agar plate and grown overnight for 18 h in TSB at 28 °C. DNA was isolated via standard phenol-chloroform extraction with previous lysis

with 600 µg/ml ampicillin for 3 h before extraction. For the PacBio Sequel system, the library was prepared with the SMRTbell template prep kit 1.0 SPv3 and SMRTbell barcoded adapter complete prep kit-96. PacBio sequencing was performed with the Sequel sequencing kit 2.0 (8 reactions) and single-molecule realtime (SMRT) cell 1 M v2 tray. For Illumina MiSeq sequencing, the library was prepared using the TruSeq DNA PCR-free library preparation kit (Illumina, San Diego, CA, USA). Genomic DNA was fragmented by applying the Covaris E220 system according to the manufacturer's protocol for a 550-bp average insert size and sequenced using MiSeq reagent kit v3 (600 cycles) (Illumina). The genomes were sequenced in the Core Facility of the Institute of Comparative Microbiome Analysis.

6.5.1 Genome assembly RL1 and SCA7

The genome of RL1 was assembled as described in Kuhl *et al*. (2019): The RL1 genome was assembled from 376,794 PacBio long reads (average read lengths of 15,245 bp, 16,813 bp, and 34,341 bp [3 SMRT cells]; 209 X coverage) and a total of 1,068,580 Illumina short reads (read length, 300 bp; 49 X coverage), quality checked with FastQC 0.11.8 (Andrew, 2010) using the hybrid assembler MaSuRCA 3.2.1_01032017 (Zimin *et al*., 2013) and circularity was checked with circlator version 1.5.5 (Hunt *et al*., 2015). All bioinformatics tools were used with default parameters.

The genome of SCA7 was assembled from a total of 579,331 PacBio long reads (average read length 13,249 bp, 284 X coverage) with the microbial assembly pipeline of the single molecule real-time (SMRT) portal interface (v9.0 PacBio SMRTLink®, Pacific Biosciences, Menlo Park, CA, USA) with default parameters and internal quality check.

6.5.2 Functional genome annotation of RL1 and SCA7

The RL1 and SCA7 genomes were annotated as described in Kuhl *et al*. (2021) upon submission to NCBI with the NCBI Prokaryotic Genome Annotation Pipeline (PGAP) with the annotation using the method best-placed reference protein set with GeneMarkS-2+ and the Rapid Annotation using Subsystem Technology 2.0 (RAST) with default parameter of the classicRAST annotation scheme plus frameshift fixing and backfilling of gaps allowed (Aziz *et al*., 2008). Afterwards the annotated genomes were browsed in the SEED environment (Aziz *et al*., 2008; Overbeek *et al*., 2014). Identification of gene clusters for biosynthesis of secondary metabolites was performed with

the antibiotics and secondary metabolite analysis shell antiSMASH (Blin *et al*., 2017) using default parameters.

Further functional annotation of the RL1 genome was performed by grouping genes in clusters of orthologous groups (COG) of proteins according to Tatusov *et al*. (2000) with eggNOG v5.0 (Jensen *et al*., 2008). Genes were annotated with the KEGG (Kyoto Encyclopedia of Genes and Genomes) orthology (KO) identifiers, or the K numbers, and directly linked to the KEGG pathways with the KEGG automatic annotation server (KAAS) (Moriya *et al*., 2007) and KEGG Mapper. Identification of plant microbe interaction factors and gene clusters for biosynthesis of secondary metabolites was performed with Plant-bacteria Interaction Factors Resource (PIFAR) (Martínez-García *et al*., 2016).

6.5.3 Phylogenetic Analysis RL1 and SCA7

The Software ARB (5.3) was used to identify closest related species to RL1 based on the 16S rRNA gene. 61 complete genomes of the genus *Rhodococcus* and the genome of the out-group *Streptomyces albus* NBRC 13014 (type strain) were downloaded from NCBI GenBank (accessed on 15.07.2020) and used for the full-genome approximately-maximum-likelihood phylogenetic tree build in the efficient database framework for comparative Genome Analyses using BLAST score Ratios – EDGAR (Blom *et al*., 2016). 15 genomes identified in the phylogenetic tree as members of the *R. erythropolis* clade and two out-group genomes were used for the approximately-maximum-likelihood phylogenetic tree calculated in EDGAR using FastTree Software with the Shimodaira-Hasegawa test for bootstrap values. Average nucleotide identity (ANI) and Average amino acid identity (AAI) was calculated in EDGAR (Blom *et al*., 2016) as described in Goris *et al*. (2007) and Konstantinidis and Tiedje (2005).

The Software ARB (5.3) was used to identify closest related species to SCA7 based on the 16S rRNA gene. In Type Strain Genome Server (TYGS) (Meier-Kolthoff and Göker, 2019) the closest related type strains based on the full genome sequence of SCA7 were identified. The full-genome maximum-likelihood phylogenetic tree build in EDGAR was based on 307 genomes of the genus *Pseudomonas* and two genomes *Herbaspirillum frisingense IAC152* and *Streptomyces albus* NBRC 13014 (type strain) as outgroup, downloaded from NCBI GenBank (accessed on 25.04.2021), using FastTree Software with the Shimodaira-Hasegawa test for bootstrap values. A subtree including the 11 closest related type strains and *Herbaspirillum frisingense IAC152* as

outgroup was calculated with EDGAR (Blom *et al*., 2016). Two average nucleotide identity (ANI) matrices were calculated in EDGAR (Blom *et al*., 2016) as described in Goris *et al*. (2007) and Konstantinidis and Tiedje (2005). The first was based on the 11 *Pseudomonas* strains closest related to SCA7; the second was based on the 11 closest related *Pseudomonas* species type strains.

6.5.4 Genome comparison *Rhodococcus* strains RL1, djl6 and BG43

The genome of RL1 (Kuhl *et al*., 2019) was compared to the genomes of the type strain djl6 (Xu *et al*., 2007; Wang *et al*., 2010; Táncsics *et al*., 2014), as well as the closely related soil isolate BG43 (Rückert *et al*., 2015) as described in Kuhl *et al*. (2021). The genome djl6 is based on the species *R. jialingiae* (Wang *et al*., 2010), which was later identified as a synonym of the type strain *R. qingshengii* (Táncsics *et al*., 2014). For the genome comparison and the identification of orthologous and unique genes in the three different genomes the tool EDGAR (Blom *et al*., 2016) was used.

6.6 *In vitro* characterization of microbe-plant interaction traits

Unless further specified, *Rhodococcus* strains were pre-cultured in liquid TSB and Scheyern isolates (**Table 3**) were pre-cultured in liquid NB. All isolates were incubated at 28 °C for 18 h overnight. Bernburg isolates were further characterized by Master's student Furkan Tunc (thesis in preparation). Description of the following methods in this chapter is according to Kuhl *et al*. (2021).

6.6.1 IAA production

IAA production was determined by the colorimetric method of Gordon and Weber (1951) with modifications. For Scheyern isolates IAA production was analyzed in a high throughout approach using deep-well plates according to Caneschi *et al*. (2018). 18 h overnight grown cultures were transferred to fresh NB medium for Scheyern isolates and TSB medium for *Rhodococcus* strains with the IAA precursor 5 mM tryptophan (1 mg/mL, Sigma) and grown for 48 h. Tryptophan powder was diluted in medium and the mix was sterile filtered with a 0.22 µm filter. Liquid cultures were centrifuged for 2 min at 5000 x g. 100 µL of supernatant was mixed with 100 µL of Salkowski reagent (**supplementary table S9**) (Loper and Schroth, 1986) and 1 µL of orthophosphoric acid (Sigma, USA). After incubation in the dark for 30 min for the small batch and 2h for the high throughput approach in deep-well plates amounts of IAA in the supernatant were analyzed in a plate reader (Spectra Max iD3, Molecular Devices) at 530 nm wavelength. A standard curve was prepared from commercial indole-3-acetic acid (Fluka Biochemika, Germany) in TSB or NB,

respectively, with concentrations ranging from 0-100 µg/mL. *H. frisingense* GSF30 was used as positive control. Supernatant measurements were performed in triplicates and results were averaged. Due to detection limits of the used method (Glickmann and Dessaux, 1995) the threshold for positive IAA production was 2 µg/mL according to Caneschi *et al*. (2018). Quantification of IAA production was performed for RL1, djl6 and BG43 based on the amount of produced IAA normalized to OD_{600} = 1.

6.6.2 Siderophore production

Siderophore production was performed according to Pérez-Miranda *et al*. (2007) and Lynne *et al*. (2011) with modifications. 25 µL of overnight grown cultures were spotted on TSB agar plate and grown for 48 h. Dye solutions (chrome azurol blue S (Sigma, USA), $FeCl_3$ (Fluka Biochemika, Germany), HDTMA (Hexadecyltrimethylammonium bromide, Sigma, USA)) were prepared and mixed according to Lynne et al. (2011). Piperazin-N,N'-bis-(2-ethanesulfonic acid) (Pipes, Roth, Germany) was added to H_2O with 0.9% agar and pH was adjusted to 6.8. After autoclaving separately, the dye solution was slowly mixed with the Pipes-Agar mix. Cooled but still liquid overlay agar (10 mL) was poured on plates with bacteria. After 2 h siderophore production was analyzed by detection of color change from blue to orange. The experiment was prepared with three technical replicates and repeated twice.

6.6.3 Phosphate solubilization

Phosphate solubilization ability was analyzed according to Nautiyal (1999). 18 h overnight grown cultures were washed twice in 1 x PBS and 25 µL were spotted on National Botanical Research Institute's phosphate growth medium (NBRIP) according to Nautiyal (1999) and incubated at 28 °C. After 6 days, phosphate solubilization activity was determined according to the formation of a clear halo surrounding the spotted colony using the Phosphate Solubilization Index (SI): (Colony diameter + Halo zone diameter)/colony diameter). The phosphate-solubilizing *Luteibacter sp.* Cha2324a_16 served as positive control. The experiment was performed with three technical replicates and repeated twice.

6.6.4 ACC deaminase activity

1-aminocyclopropane-1-carboxylate (ACC, Biozol Diagnostica GmbH, Germany) utilization as nitrogen source was analyzed according to Brown and Dilworth (1975) and Rothballer *et al*. (2008) with modifications. 18 h overnight grown cultures were washed twice in 1 x PBS and 25 µL were

spotted on M9 minimal medium (Na_2HPO_4 33.1 mM, KH_2PO_4 22 mM, NaCl 8.55 mM, (NH_4Cl 9.35 mM), glucose 0.4%, $MgSO_4$ 1 mM, $CaCl_2$ 0.3 mM) containing NH_4Cl 9.35 mM (Roth, Germany) or ACC 3 mM as nitrogen source or no nitrogen source. After 10 days, ACC utilization as nitrogen source was analyzed by comparing bacterial growth on M9, M9 with ACC and nitrogen-free M9 plates. ACC utilizing *Variovorax* sp. M92526_27 served as positive control. The experiment was prepared with three technical replicates.

6.6.5 Biological nitrogen fixation

Nitrogen fixation was performed using nitrogen-free semi-solid Nfb-medium according to Döbereiner (1995), Jensen's medium and only for RL1, djl6 and BG43 Ashby's mannitol medium (composition in **Supplementary Table S9**). 18 h overnight grown cultures were washed twice in 1 x PBS and 10 µL were spotted on nitrogen-free semi-solid Nfb-medium and incubated at 28 °C. Pellicle formation was evaluated after 48 h. Bacterial strains were streaked on a fresh TSB or NB plate from glycerol stocks and grown overnight for 18 h at 28° C. A single colony of each strain was picked and streaked on Jensen's agar. 10 µL of washed overnight cultures of *Rhodococcus* strains were streaked on Ashby's mannitol agar. Bacteria on Ashby's medium and Jensen's medium were incubated at 28 °C and growth was evaluated after 3 days. The experiments were repeated twice with two replicates. Nitrogen-fixing *Azospirillum brasilense* Sp7 (and Sp245) served as positive control. *Escherichia coli* DH5α served as negative control.

6.6.6 PCR for *nifH* gene in RL1, djl6 and BG43

The *nifH* gene which encodes the iron protein of the nitrogenase relevant for nitrogen fixation in diazotrophic bacteria was amplified using PCR according to Poly *et al*. (2001). PCR was performed using genomic DNA of RL1, djl6 and BG43 extracted as described above and the following primers, forward PolF (TGC GAY CCS AAR GCB GAC TC) and reverse PolR (ATS GCC ATC ATY TCR CCG GA) (Metabion International AG, Germany). The PCR conditions consisted of denaturation at 94 °C for 3 min, followed by 30 cycles at 94 °C for 1 min, 55 °C for 1 min, and 72 °C for 2 min. The amplified gene product was visualized on 1% agarose gel. Genomic DNA of *A. brasilense* Sp7 served as positive control.

6.6.7 Glucosinolate metabolism

6.6.7.1 Preparation of leaf extract

Leaves of rucola and wheat of three weeks old plants and leaves of *Arabidopsis thaliana* of six weeks old plants were immediately frozen in liquid nitrogen and lyophilized for 2-4 days in the Institute of Biochemical Plant Pathology (BIOP) (Alpha 2-4LDplus, Martin Christ Gefriertrocknungsanlagen, Germany). Dry leaves were ground manually and 150 mg of the leaf powder were mixed with 4 mL Methanol 70%. The mix was shaken at 70 °C at 1000 rpm for 20 minutes and vortexed every 5 minutes. Afterwards, the mix was centrifuged at maximum speed of 4000 rpm for 15 minutes in an ultracentrifuge at the Institute of Analytical Biogeochemistry at 4 °C and supernatant was sterile filtered with 0.2 µm PTFE filter. The remaining methanol was evaporated in a SpeedVac® Vacuum concentrator (ThermoScientific) at the Institute of Analytical Biogeochemistry at 40 °C for 24 h. Leaf extracts were stored at -20 °C until further use.

6.6.7.2 Glucosinolate Experiment

The ability of RL1 to metabolize glucosinolates was evaluated in experiments with leaf extract infused medium and with pure glucosinolate compounds. 100 µL from 18 h overnight grown *Rhodococcus* strains RL1, djl6 and BG43 and *H. frisingense* GSF30 as negative control were transferred in glass culture tubes filled with 2.5 mL fresh TSB medium supplemented with 0.5% rucola, wheat and *A. thaliana* leaf extract or with 0.1 mM glucoerucin ROTICHROM® HPLC (Roth, Germany) with six technical replicates per treatment. TSB inoculated with bacteria without supplements served as no compound control. In each treatment three tubes without bacteria served as no bacteria control. Tubes were incubated at 28 °C 180 rpm for 48 h. Samples were taken at 0 h, 24 h and 48 h. All replicates were processed directly after sampling. Bacterial growth was monitored at each time point by optical density measurement at 600 nm (OD_{600}). Afterwards each sample was centrifuged for 2 minutes at 5000 x g. Supernatant was transferred in a 5 mL syringe and sterile-filtered with 0.2 µm PTFE filter in sterile Eppendorf tubes. All samples were stored at -20 °C until further processed.

6.6.7.3 Ultra Performance Liquid Chromatography (UPLC) and Gas Chromatography Mass Spectrometry (GC-MS) Analysis

For UPLC analysis samples were thawed, vortexed and 50 µL transferred to UPLC glass vials. Standard curve was prepared from glucoerucin pure compound ranging from 0.0025 mM – 0.1 mM

concentrations. Afterwards samples were processed in a ACQUITY UPLC system (Waters GmbH, Germany) at the Institute of Analytical Biogeochemistry by Jenny Uhl with settings adapted from Mullaney *et al*. (2013a) and analyzed with the Software Genedata®.

Samples for detection of glucosinolate degradation products ITC and nitriles with gas chromatography mass spectrometry (GC-MS) analysis were prepared according to Mullaney *et al*. (2013a) with modifications. Sterile filtered samples were mixed in 1:2 ratio with dichloromethane (500 µL sample + 1mL dichloromethane). Tubes were inverted for 15 minutes and afterwards centrifuged for 5 minutes at 2000 x g. The organic phase (bottom layer) was taken with Pasteur pipette and transferred to a new tube and stored at -20 °C until further use. Commercially available sulforaphane (Sigma, USA) was used as standard ranging from 0-40 mg/L concentrations. GC analysis was performed at the Research Unit Environmental Simulation (EUS) by Andrea Ghirardo using GC-MS (GC type: 7890A; MS type: 5975C; both from Agilent Technologies, Palo Alto, CA, USA) with settings adapted from Mullaney *et al*. (2013a).

6.6.8 Biofilm formation

Biofilm formation was analyzed according to O'Toole (2011) with modifications. 18 h overnight grown cultures were washed in 1 x PBS and OD_{600} was adjusted to 0.1. Bacterial strains were cultivated in a microtiter plate in 100 µL modified M9 minimal medium with 0.5% casamino acids (Biozol Diagnostica Vertrieb GmbH, Germany) without shaking at 28 °C. After incubation OD_{600} was measured in the plate reader (SpectraMax iD3, Molecular Devices). After 24 h OD_{600} was measured and unattached cells were dumped out of the plate. The plate was washed twice by submerging it in MilliQ water to further remove unattached cells. 125 µL of 0.1% crystal violet (Roth, Germany) solution was added to each well. After 15 minutes the plate was rinsed three times in MilliQ water and dried for 1.5 h before visual inspection of biofilm production. For quantification of the biofilm 125 µL of 30% acetic acid (Roth, Germany) was added to each well and incubated for 15 minutes at room temperature. The solution was transferred to a new microtiter plate and color intensity was quantified at the plate reader (SpectraMax iD3, Molecular Devices) with absorbance at 550 nm and 30% acetic acid as blank. Biofilm-forming *Pseudomonas simiae* WCS417 served as positive control and non-biofilm-producing *Escherichia coli* DH5α served as negative control. The experiment was repeated 3 times with 6-12 technical replicates per strain.

6.7 Interactions with other organisms

6.7.1 Biocontrol activity against plant pathogenic fungi

The interaction of bacterial isolates Cha2930_14, Ch2324a_1, Cha2324b_22, Cha2324b_23, Cha2324a_8, Cha2324b_12, Cha2324b_30, NB7_11 and RL1 with well-known plant pathogenic fungi was investigated with an *in vitro* confrontation assay as described in Kuhl *et al*. (2021): Plant pathogenic fungi used in this experiment were *Rhizoctonia solani*, causing potato stem cancer and black scurf (Yang and Li, 2012), wheat pathogenic fungus *Fusarium culmorum* G2191 causing seedling blight, foot rot and head blight (Wagacha and Muthomi, 2007), the wilt-causing *Fusarium oxysporum* DSM62297 (Gerlach *et al*., 1958) and the leaf spot disease causing *Alternaria alternata* DSM62006 (Troncoso-Rojas and Tiznado-Hernández, 2014) with varying host plants. Fungi were cultivated on potato dextrose agar (PDA) at room temperature in the dark and stored at 4 °C until further use. 18 h overnight grown bacterial cultures were diluted to OD_{600} = 0.1 with fresh NB or TSB medium and 10 µL were dripped on the plate. Approximately 1 mm^3 PDA pieces grown with fungi were aseptically transferred to NB or TSB plates at a distance of approximately 3 cm. After 9-14 days of growth the zone of inhibition formation was visually analyzed and documented photographically. *Luteibacter* sp. Cha3424a_16 served as negative control and *B. velezensis* FZB42, a known fungal antagonistic strain (Chowdhury *et al*. 2015a) served as positive control. Confrontation assays were performed in triplicates.

6.7.2 PCR for Lipopeptide genes

The genes encoding for the antibiotic lipopeptides surfactin (*sfp* and *srfC*), iturin A (*ituD*), fengycin (*fenD*) and bacillomycin D (*bamC*) were amplified according to Gond et al. (2015). PCR was performed as described in 6.3 with the primers for lipopeptide genes *sfp*, *srfC*, *ituD*, *fenD*, *bamC* according to Gond *et al*. (2015) (**Table 13**) and genomic DNA of bacterial isolates (**Table 4**) extracted using the DNeasy®UltraClean®Microbial Kit (Qiagen, Germany) following the manufacturer's protocol. The PCR conditions consisted of denaturation at 94 °C for 3 min, followed by 35 cycles at 94 °C for 30 s, 55 °C for 30 s, 72 °C for 2 min and one final elongation step at 72 °C for 5 min.

Table 13: Primer list for lipopeptide genes.

Antibiotic	Target gene	Primer	Sequences (5'-3')	Reference
Surfactin	*sfp*	*sfp*-f *sfp*-r	ATGAAGATTTACGGAATTTA TTATAAAAGCTCTTCGTACG	Gond *et al*., 2015
Iturin A	*ItuD*	*ItuD1f* *ItuD1r*	GATGCGATCTCCTTGGATGT ATCGTCATGTGCTGCTTGAG	Gond *et al*., 2015
Surfactin	*SrfC*	*Sur3f* *Sur3r*	ACAGTATGGAGGCATGGTC TTCCGCCACTTTTTCAGTTT	Gond *et al*., 2015
Fengycin	*FenD*	*FenD1f* *FenD1r*	TTTGGCAGCAGGAGAAGTTT GCTGTCCGTTCTGCTTTTTC	Gond *et al*., 2015
Bacillomycin D	*BamC*	*Bacc1f* *Bacc1r*	GAAGGACACGGAGAGAGTC CGCTGATGACTGTTCATGCT	Gond *et al*., 2015

6.7.3 Degradation of synthetic and bacterial N-Acyl-Homoserine lactones (AHLs) of RL1, djl6 and BG43

The identified *qsdA* gene sequence of the RL1 genome encoding the AHL lactonase was used to construct a phylogenetic tree with nearest relatives with MEGA X (Kumar *et al*., 2018) by Dr. Soumitra Paul Chowdhury. Degradation of synthetic and bacterial N-Acyl-Homoserine lactones (AHLs) of RL1, djl6 and BG43 was analyzed as described in Kuhl *et al*. (2021) with a well diffusion agar-plate assay (Rodríguez *et al*., 2020) and a V-shaped assay (Berendsen *et al*., 2018) with modifications:

6.7.3.1 Well diffusion plate assay

18 h overnight grown cultures were transferred to fresh TSB liquid medium supplemented with synthetic AHL 10 µM C12-HSL (Biomol GmbH, Germany). Cell-free TSB medium supplemented with 10 µM C12-HSL served as negative control. For the co-cultivation experiment RL1 and *A. radicis* N35e 18 h overnight cultures were adjusted to OD_{600} = 0.2 and co-cultured in fresh liquid NB medium. Pure culture of *A. radicis* N35e served as AHL positive control. For the supernatant experiment *Rhodococcus* strains were transferred to the supernatant of an 18 h overnight grown culture of *A. radicis* N35e. Cell-free supernatant of the *A. radicis* N35e culture served as AHL positive control. All experiments were incubated at 28 °C at 180 rpm.

The well diffusion plates were prepared as follows: The AHL biosensor strain *A. tumefaciens* A136 was pre-grown in NB. NB plates were overlaid with soft NB agar (0.5 % agar) supplemented with the biosensor strain A136 and 80 µg/mL 5-bromo-4-chloro-3-indolyl-ß-D-galactopyranoside (X-

gal, Life Technologies GmbH, Germany). 20 µL of each supernatant from the co-cultivation, synthetic AHL or supernatant experiment were filled in wells prepared in the soft agar and incubated at 28 °C for 30 h. Remaining AHLs were detected by color change. Pure NB was used as negative control for presence of AHLs.

6.7.3.2 V-shaped plate assay

The AHL biosensor strain *A. tumefaciens* A136 was pre-grown in NB. *A. tumefaciens* A136 and 80 µg/mL 5-bromo-4-chloro-3-indolyl-ß-D-galactopyranoside (X-gal, Life Technologies GmbH, Germany) were spread on NB plates. *Rhodococcus* strains were pre-grown in TSB. The AHL producing strains *A. radicis* N35e was pre-grown in NB, non-AHL-producing mutant strain *A. radicis* N35 AHL- *araI::tet* was pre-grown in NB with tetracycline 20 µg/mL and kanamycin 50 µg/mL. 18 h overnight grown cultures were washed in 1 x PBS and optical density was adjusted to OD_{600} = 0.1. Eight times 1 µL of each culture was dripped in a first parallel than diagonal row on the prepared NB plates in V-shape with increasingly distant inoculation sites. Plates were incubated for 30 h at 28 °C. AHL degradation was detected by color change.

6.7.4 Colony attraction experiment

Bacterial isolates were pre-grown in NB. 18 h overnight grown cultures were transferred to fresh NB medium and diluted to OD_{600} = 0.1. Eight times 1 µL of each culture was dripped in a diagonal row on the prepared NB plates in V-shape with increasingly closer inoculation sites. Plates were incubated for 4-6 days at 28 °C. Interaction in terms of increased or decreased colony formation was observed every day.

6.8 Evaluation of growth and tolerance to different stress factors

6.8.1 Growth ability at different range of temperature

18 h overnight grown cultures of Scheyern isolates and *Rhodococcus* strains were streaked on fresh NB or TSB medium plates and incubated at temperatures of 4 °C, 15 °C, 20 °C, 28 °C, 35 °C, 37 °C, 40 °C, 45 °C. Colony formation was evaluated after 24 h and 48 h.

Description of the following methods in this chapter is according to Kuhl *et al*. (2021):

6.8.2 Salt stress

18 h overnight grown cultures were transferred to fresh NB or TSB medium with increasing sodium chloride (NaCl, Merck, Germany) levels 0%, 1%, 2.5%, 3.5%, 5.5%, 7.5%, 12%, 15% according

to De Carvalho *et al*. (2014) and incubated at 28 °C. Growth rates were evaluated by spectrophotometric measurement of OD_{600} after 24 h and 48 h. For treatments without detectable growth (12% and 15% NaCl), the recovery of cells was evaluated by the ability to form colonies on NB or TSB agar plates without NaCl. 100 µL of cultures from the treatments 12% and 15% were plated on NB or TSB agar without NaCl and incubated at 28 °C for 24 h and 48 h. Experiment was repeated three times. Less salt tolerant *H. frisingense* GSF30 and *B. velezensis* FZB42 served as negative controls.

6.8.3 Osmotic stress

18 h overnight grown cultures were transferred to fresh NB or TSB medium with increasing osmotic stress levels 0 MPa, - 0.25 MPa, -0.5 MPa, -0.75 MPa, -1 MPa, -1.25 MPa and -1.5 MPa and incubated at 28 °C. Increasing osmotic stress was adjusted with polyethylene glycol 6000 (PEG6000, Serva Electrophoresis GmbH, Heidelberg, Germany) based on decreasing water potential with the formula of Kaufmann and Michel (1973), according to Kumar *et al*. (2014) and Jayakumar *et al*. (2020) with modifications. -1.5 MPa is the water potential plants in regular soil start to wilt irreversibly. Growth rates were evaluated by spectrophotometric measurement of OD_{600} after 24 h and 48 h. Experiment was repeated three times. Gram-negative *H. frisingense* GSF30 and Gram-positive *B. velezensis* FZB42 served as controls.

6.8.4 Mercury tolerance of RL1, djl6 and BG43

18 h overnight grown cultures were transferred to fresh TSB medium with increasing mercury levels 0.001 mM, 0.01 mM, 0.1 mM, 1 mM adjusted with mercury-II-chloride ($HgCl_2$, Roth, Germany) according to Dziewit *et al*. (2013) and incubated at 28 °C. Growth rates were evaluated by spectrophotometric measurement of OD_{600} after 24 h and 48 h. For treatments without detectable growth (=0.1 mM and 1 mM mercury), the recovery of cells was evaluated by the ability to form colonies on TSB agar plates without mercury. 100 µL of cultures from the treatments with 0.1 mM and 1 mM mercury were plated on TSB without mercury and incubated at 28 °C for 24 h and 48 h. Experiment was repeated three times. Non-mercury-tolerant strains *H. frisingense* GSF30 and *B. velezensis* FZB42 served as negative controls.

6.8.5 pH tolerance of RL1, djl6 and BG43

18 h overnight grown cultures were transferred to fresh TSB medium with pH values 8, 7, 6, 5, 4, 3, 2 adjusted with hydrochloric acid (HCl, Merck, Germany) or sodium hydroxide (NaOH, Sigma,

USA) and incubated at 28 °C. Growth rates were evaluated by spectrophotometric measurement of OD_{600} after 24 h and 48 h. Recovery was evaluated by the ability to form colonies on TSB agar plates at pH 7.3 after 48 h in treatments without detectable growth (pH 4, 3 and 2). 100 µL of medium from the treatments pH 4, 3 and 2 were plated on TSB and incubated at 28 °C for 24 h and 48 h. The experiment was repeated three times. *H. frisingense* GSF30 and *B. velezensis* FZB42 which did not grow in low pH (below 5) served as negative controls.

6.8.6 Antibiotic resistance of RL1, djl6 and BG43

18 h overnight grown cultures were diluted 1:10 with fresh TSB medium. 200 µL of the diluted overnight cultures were spread on TSB agar plates and antimicrobial susceptibility test stripes (Himedia Laboratories, India) for kanamycin (0.016-256 µg/mL), ampicillin (0.016-256 µg/mL), rifampicin (0.002-32 µg/mL) and vancomycin (0.016-256 µg/mL) were placed according to manufacturer's protocol. The inhibition zone was evaluated after 24 h and 48 h.

RL1 was streaked on a fresh TSB plate from glycerol stock and grown overnight for 18 h. A single colony of RL1 was picked and streaked on nutrient broth (NB) agar plates with 100 µg/mL potassium tellurite trihydrate (K_2TeO_3 * $3H_2O$, Sigma, USA) for 48 h. Dark grey colony growth was evaluated as positive growth. The strain *R. radiobacter* F4 AHL- aiiA- genetically modified to tolerate a tellurite concentration of 100 µg/mL served as positive control.

6.9 Application of bacterial isolates to plants

6.9.1 Substrate verification for plant experiments

Different substrates including glass beads, plant substrate (Pikiererde CL P, Profisubstrat, Einheitserde classic), coarse and fine quartz sand, a mix of plant substrate (Pikiererde CL P, Profisubstrat, Einheitserde classic) and quartz sand (50% and 75%) as well as a mix of fine quartz sand (90%) with clay (10%) supplemented with Hoagland's solution were tested for growth ability and cleaning of roots for rucola and wheat. In the sand-clay-system with 10% clay (30 mL) and 90% (270 mL) fine quartz sand supplemented with 20 mL Hoagland's solution rucola and wheat grew well and roots could be cleaned easily (**Figure 31A**). Therefore, the sand-clay system was used for the following plant experiments.

6.9.2 Seed sterilization

6.9.2.1 Rucola

Rucola seeds were sterilized as described in Kuhl *et al*. (2021). Seeds were washed in Tween 80 (Sigma, USA) 1% for 2 min, surface sterilized with sodium hypochlorite 12% (NaOCl, Roth, Germany) for 8 min and washed three times in sterile deionized water for 2 min each. Sterilized seeds were placed on Hoagland's solution (Sigma, USA) with 0.8% agar to germinate 4 days. Stratification of 2, 4 and 10 days had no effect on equalizing germination and was therefore omitted. For experiments equally germinated seeds were picked.

6.9.2.2 Wheat

Seeds were stratified at 4 °C for 10 hours on water soaked filter paper. Stratified seeds were washed in 1% Tween 80 (Sigma, USA) for 2 min, sterilized in 12% NaOCl (Roth, Germany) for 7 min and afterwards washed three times in sterile water for 5 min each. Washed seeds were placed in antibiotic solution (0.6 mg/mL Penicillin-G, 0.25 mg/mL Streptomycin) for 10 min under continuous shaking 180 rpm. Sterile seeds were placed on Hoagland's solution agar (0.8%) and 1 drop of sterile water was applied on each seed to increase humidity. Seeds were left to germinate in unclosed Anaerocult®A boxes (Merck, Germany) covered with wet tissue (to keep the humidity high) for 96 h in the dark.

6.9.2.3 Arabidopsis

Seeds were placed on a filter tube (from e.g. DNeasy®UltraClean®Microbial Kit (Qiagen, Germany)). 700 µL 75% EtOH were added to the filter tube and the seeds were incubated for 4 min while shaking at 300 rpm. Tubes were centrifuged for 1 min at 11000 x g to remove EtOH. 700 µL 100% EtOH were added to the filter tube and the seeds were incubated for 4 min while shaking at 300 rpm. Tubes were centrifuged for 1 min at 11000 x g to remove EtOH. Seeds were centrifuged for 5 min at 11000 x g to dry the seeds. Sterilized seeds were placed in Eppendorf tube with 200 µL sterile water and stratified for 48 h at 4 °C.

6.9.3 Evaluation of rhizosphere competence of RL1, djl6 and BG43

Description of the following methods in this chapter is according to Kuhl *et al*. (2021):

6.9.3.1 Root inoculation in axenic system

Rucola seeds were sterilized as described in 6.9.2.1. 18 h overnight grown cultures were washed two times in 1 x PBS (AppliChem, Germany) and diluted to a concentration of 10^7 CFUs. Sterilized seedlings were inoculated in the prepared bacterial solution of RL1, BG43 and djl6 for 1 h under shaking at 180 rpm at 28 °C. Seedlings inoculated in 1 x PBS served as negative control. Inoculated seedlings were transferred to an axenic system with 80 mL sterile quartz sand and 20 mL Hoagland's solution in a sterile Phytatray II (Sigma, USA). Seedlings inoculated with RL1 were also transferred to plates with 0.5 x Murashige & Skoog Medium (0.5 x MS) including vitamins (Duchefa Biochemie, Netherlands) with pH adjusted to 5.7 with 2N KOH. No additional sucrose was added to 0.5 x MS. The axenic system was placed in a Phytochamber (Weiss Technik, Modell SGC120PG2, Germany) with 23 °C, 55% humidity, day-night-cycle 12 h : 12 h. After 7 and 14 days freshly harvested roots were washed in 1 x PBS, fixed in 55% EtOH and 1 x PBS mix and stored at -20 °C until further use.

6.9.3.2 Fluorescence *in situ* hybridization (FISH)

Fluorescence *in situ* hybridization was performed following the protocol of (Alquéres *et al*., 2013). Chemicals were obtained from AppliChem, Germany. After an increasing ethanol series (50%, 80% and 96% [vol/vol] for 3 min each) for fixation and desiccation, roots were incubated in 50 µL hybridization buffer (0.9 M NaCl, 0.01% sodium dodecyl sulfate (SDS), 10 mM Tris-HCl (pH 8.0), 35% deionized formamide) with 15 pmol of the fluorescently labeled probes EUB338, specific for eubacteria (Amann *et al*. 1990, Daims *et al*. 1999) and labelled with fluorescein (FITC, Metabion International AG, Germany), and HGC69a (Roller et al., 1994), specific for bacteria with high G+C content in their 16S rRNA and labelled with Cy3 (Thermo Scientific, Germany) or ATTO550 (Metabion International AG, Germany). Hybridization was performed for 1.5 h at 46 °C.

6.9.3.3 Confocal Laser Scanning Microscopy (CLSM)

FISH stained roots and bacterial cells were investigated at the Zeiss confocal laser scanning microscope LSM880 (Zeiss, Oberkochen, Germany) with argon ion laser and helium neon laser for excitation of FITC (488 nm), Cy3 (561 nm) and an unlabeled control channel (633 nm). Cells

were observed with a 64 x C-Apochromat water immersion objective. Micrographs were recorded using the software Zen Black Edition (Zeiss, Oberkochen, Germany).

6.9.3.4 Quantitative evaluation

Rhizosphere competence of the investigated bacterial strains was estimated via counting of colony forming units (CFU). Sterilized rucola seedlings were inoculated in bacterial solution and planted in the axenic system as described 6.9.3.1. After seven days three roots were harvested, weighed and ground in a sterilized mortar with 1 mL 1 x PBS. Ground roots were diluted 3 times (10^{-3}), 100 µL of each dilution was plated in triplicates on TSB plates and incubated at 28 °C. After 48 h CFUs of dilution 10^{-3} were counted and mean values were compared between treatments. Plating of dilutions 10^{-1} and 10^{-2} resulted in too many CFUs for counting.

6.9.4 Plant experiments RL1

Unless further specified the following instructions apply to all plant experiments with RL1. Rucola seeds were sterilized as described in section 6.9.2.1. 18 h overnight grown bacterial cultures were washed two times in 1 x PBS (AppliChem, Germany) and diluted to a concentration of 10^7 CFUs. Sterilized seedlings were inoculated in the prepared bacterial solution for 1 h under shaking at 160 rpm at 28 °C. Seedlings inoculated in 1 x PBS served as negative control. Inoculated seedlings were transferred to the respective experimental system. The experiments were conducted in a phytochamber (Weiss Technik, Modell SGC120PG2, Germany) with 23 °C, 55% humidity, day-night-cycle 12 h : 12 h with light intensity of 76 µmol/(m^2s). Unless stated differently measured plant parameter upon harvest were root length, root and shoot fresh weight and dry weight. For dry weight, plants were dried for 48-96 h at room temperature until plant tissue breaks upon folding.

6.9.4.1 Effect of RL1 on germination of plants on water agar

Rucola, wheat and *Arabidopsis thaliana* seeds were sterilized according to the protocols described in section 6.9.2 without germination step. Seeds were inoculated with RL1, BG43, djl6, 100 µM gibberellic acid (GA3, Duchefa Biochemie, Netherlands) or 1 x PBS. 18 h overnight grown bacterial cultures were washed two times in 1 x PBS (AppliChem, Germany) and diluted to a concentration of 10^7 CFUs. Sterilized seeds were inoculated as described in 6.9.4. Inoculated seeds were transferred to plates with water agar (0.8%) to evaluate the influence of RL1 on germination in a reduced system. Gibberellic acid (GA3, Duchefa Biochemie, Netherlands) was dissolved in water, sterile filtered and adjusted to 100 µM final concentration in the medium, which was used

as positive control adapted from Yin *et al*. (2017) and Li *et al*. (2017). GA3 remains active for 4 days at room temperature. Heat-killed RL1 and 1 x PBS served as negative control. Germination was evaluated every day for 4 (*A. thaliana*), 6 (rucola) and 10 days (wheat) and percentage of germinated seeds was calculated.

6.9.4.2 Effect of RL1 on germination of rucola on water agar with medium

Rucola seeds were sterilized as described in section 6.9.2.1 without germination step and transferred on water agar (0.8%) in 96-well microtiter plates with one seed per well. 18 h overnight grown cultures of RL1, BG43 and djl6 were adjusted to 10^7 CFUs or centrifuges at 500 g for 2 min to receive culture supernatant. Afterwards 20 µL of bacterial solution, bacterial supernatant, 100 µM gibberellic acid (GA3) or TSB medium was added to each seed. Germination was evaluated for 3 days and percentage of germinated seeds was calculated.

6.9.4.3 Effect of RL1 on germination of rucola in sand-clay system

Per treatment 150 rucola seeds were sterilized as described in 6.9.2.1 without germination step. Seeds were immediately inoculated with RL1, heat killed RL1 (= boiled RL1 culture at 95 °C for 20 min), BG43, djl6, 100 µM gibberellic acid (GA3) or 1 x PBS as described in 6.9.4. Afterwards five seeds were planted per pot filled with sand-clay mix as described in 6.9.1 with approximately 3 cm distance to each other and allowed to germinate for 96 h in the dark. Every pot was placed on a petridish to guarantee similar water conditions for each of the plants. Plants were watered every 2-3 days. After 12 days, the total number of emerged and living seedlings per treatment was counted and calculated in percent of total seeds. The experiment was repeated twice. The first experiment included only the treatments RL1 and 1 x PBS. The second experiment included all above described treatments.

6.9.4.4 Effect of RL1 on flowering of rucola in sand-clay system

Twelve days old seedlings inoculated with RL1, heat killed RL1 (= boiled RL1 culture at 95 °C for 20 min), BG43 or 1 x PBS of the experiment described in section 6.9.4.7 were used to analyze the effect of bacterial strains on flowering time in rucola. Only the largest seedling of the five seedlings per pot was retained. Plants were grown for additional 12 weeks and watered every 2-3 days. After 18 days, plants were re-inoculated with 1 mL bacterial solution prepared as described in section 6.9.4. Development of flowers was evaluated every 2-3 days.

6.9.4.5 Effect of RL1 on root growth of rucola in agar system

A total of 5 sterilized seedlings inoculated with RL1 or 1 x PBS as described in section 6.9.4 were transferred on plates with 0.5 x Murashige & Skoog Medium (0.5 x MS) including vitamins (Duchefa Biochemie, Netherlands). pH was adjusted to 5.7 with 2N KOH. No additional sucrose was added to 0.5 x MS. Plates were incubated in a phytochamber as described in 6.9.4. After 14 days, changes in root system were evaluated and documented by photography.

6.9.4.6 Effect of RL1 on plant growth in rucola in sand-clay system

In a first experiment 10 seedlings per treatment were inoculated with either RL1 or 1 x PBS as described in section 6.9.4. In a second experiment 100 seedlings per treatment were inoculated with either RL1 or 1 x PBS as described above. Afterwards inoculated seedlings of each experiment were transferred to pots filled with sand-clay mix as described in section 6.9.1. Plants were watered every 2-3 days. After two weeks additional 20 mL Hoagland's solution were added to each pot. After 4 weeks of growth in the phytochamber as described in 6.9.4 plants were harvested and plant parameters were evaluated as described in section 6.9.4.

6.9.4.7 Effect of RL1, djl6 and BG43 on plant growth of rucola in sand-clay system

A total of 40 seedlings were inoculated with either RL1, djl6, BG43 or 1 x PBS as described in section 6.9.4. Afterwards inoculated seedlings of each experiment were transferred to pots filled with sand-clay mix as described in section 6.9.1. Plants were watered every 2-3 days. After two weeks additional 20 mL Hoagland's solution were added to each pot. After 4 weeks of growth in the phytochamber as described in section 6.9.4 plants were harvested and plant parameters were evaluated as described in section 6.9.4. The experiment was repeated twice.

6.9.4.8 Effect of RL1 on root growth of rucola tested in soil substrate

A total of 10 sterilized rucola seedlings per treatment were inoculated with either RL1 or 1 x PBS as described in section 6.9.4 and transferred to pots filled with soil substrate (Pikiererde CL P, Profisubstrat, Einheitserde classic) without Hoagland's solution. Plants were watered every 2-3 days. After 4 weeks of growth in the phytochamber as described in section 6.9.4 plants were harvested. Evaluated plant parameter were root length and fresh and dry weight of leaves. Attachment of soil on roots prevented evaluation of the plant parameters root fresh and dry weight.

6.9.4.9 Effect of RL1 on rucola in sand-clay system under drought stress

A total of 60 seedlings per treatment were inoculated with either RL1 or 1x PBS as described in section 6.9.4 and transferred to pots filled with sand-clay mix as described in section 6.9.1. Every pot was placed on a petridish to guarantee similar water conditions for each of the plants and pots were distributed randomly over the trays (**Figure 31E**). After two weeks additional 20 mL Hoagland's solution were added to each pot. Plants were watered every 2-3 days with equal amount of water. Once a week all pots were weighed and filled up to 100% water capacity (90 g water in total). After 19 days of growth in the phytochamber as described in section 6.9.4 drought stress was applied individually by stopping of watering for 30 plants in each treatment for 5 to 7 days depending on the plants' drought status (none, mild, severe, **Figure 31B-D**). Detection of drought stress symptoms was evaluated every day during drought stress treatment. Plants were allowed to recover for 2 days after re-watering. State of recovery was evaluated after 1 h, 1.5 h, 2 h, 24 h and 48 h.

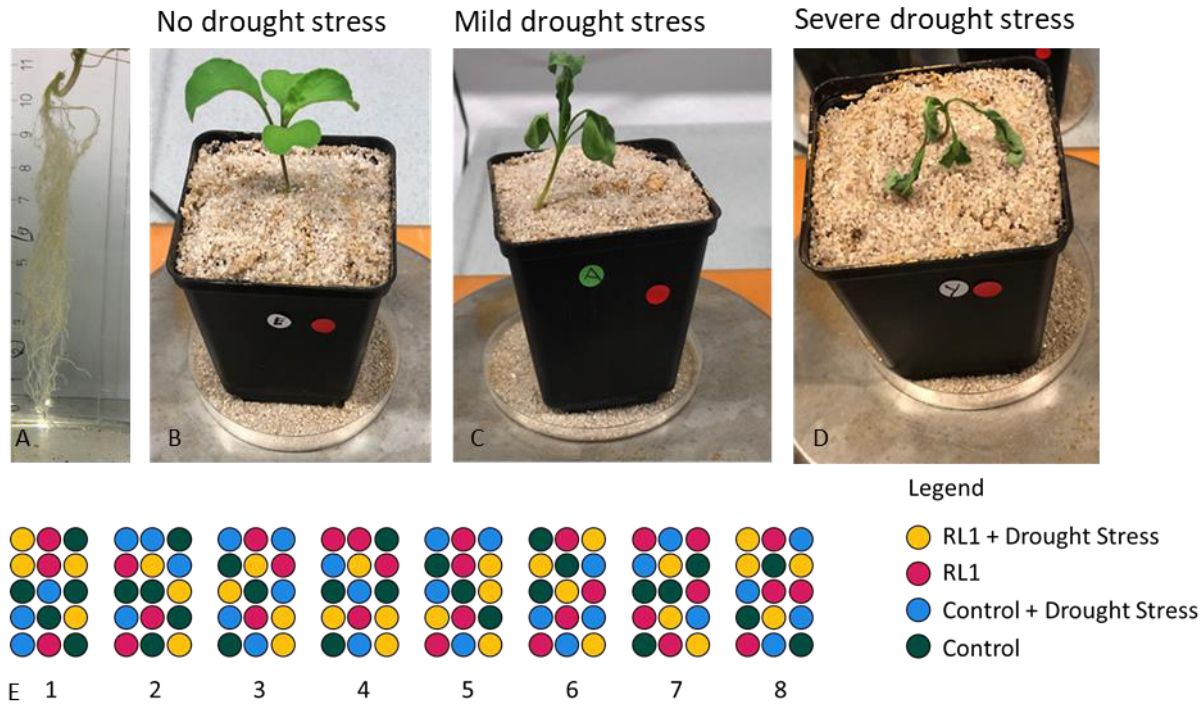

Figure 31: Overview experiments with Rucola plants. (**A**) Example of three weeks old rucola root after washing in water. (**B**) Representative rucola plants for no drought stress, (**C**) mild drought stress with hanging leaves or (**D**) severe drought stress with dry leaves and a collapsed stem. (**E**) Experimental set-up of the effect of RL1 on rucola with randomized pots with and without drought stress. Pots are depicted by colored circles. Each number represents a tray with 15 pots.

Plants were harvested after 4 weeks in the phytochamber as described in section 6.9.4 and plant parameter were taken as described in section 6.9.4. Fresh weight of root and shoot under drought stress was not evaluated, because of bias due to drought stress treatment.

6.9.4.10 Effect of RL1 on non-host plant wheat under drought stress

Wheat seeds were sterilized according to the protocol described in section 6.9.2.2. Twenty seedlings for each treatment were inoculated with RL1, *Rhodococcus* sp. NB17_5 isolated from wheat rhizosphere, *B. velezensis* FZB42 and 1 x PBS as described in section 6.9.4. Afterwards inoculated seedlings were transferred to pots filled with sand-clay mix as described in section 6.9.1. After 2 weeks, drought stress was applied traywise to 10 plants of each treatment for 4 days. Recovery phase lasted for 2 days. After 3 weeks of growth in the phytochamber as described in section 6.9.4 plants were harvested and plant parameters were evaluated as described in section 6.9.4. For wheat plants additionally shoot length in cm was measured and surviving plants under drought stress were counted.

6.9.5 Consortium experiments

In the consortium experiments the characterized bacterial isolates were applied as consortia or single strains under drought and non-drought conditions to the host plant wheat (*Triticum aestivum* (cultivar "Lemmy")) to analyze their effect on plant growth under different conditions. Bacterial isolates were pre-grown in NB. 18 h overnight grown cultures were washed twice in 1 x PBS, optical density (OD_{600}) was adjusted to $OD_{600} = 1$ (based on the results of consortium experiment 2) unless further specified and mixed in equal amounts to the microbial consortium solution. Wheat seeds were sterilized and germinated according to the protocol described in section 6.9.2.2. Sterilized wheat seedlings were inoculated for 1 h in the respective microbial consortium or 1 x PBS as negative control at 28 °C 180 rpm. Afterwards inoculated seedlings were transferred to pots filled with sand-clay-mix as described in section 6.9.1 and grown in a phytochamber (Weiss Technik, Modell SGC120PG2, Germany) at 55% humidity, 23 °C and 12 h : 12 h day and night cycle. Non-drought stressed plants were watered every 2-3 days unless further specified. Once per week pots were watered to 100% (90 g water in total) water content. After 14 days additional 20 mL of Hoagland's solution were added to each pot. Upon harvest the measured plant parameters were the number of leaves, root and shoot length, root and shoot fresh and dry weight. For

determination of dry weight plants were dried at room temperature for up 96 h or at 65° C for 12 h until plant tissue was breaking when folded. For RNA extraction plant leaves were cut from the plant, immediately frozen in liquid nitrogen and stored at -80 °C until further use. For DNA extraction roots were washed in 1 x PBS, frozen in liquid nitrogen and afterwards stored at -80 °C until further use.

6.9.5.1 Selection of microbial consortia

Based on the characterized PGPB traits, pairwise microbial interaction assay and stress assays (chapter 2.4) 28 isolates were chosen for microbial consortia applied to the plants in the consortium experiments 1-4. Cha2324b_22, NB7_11 and SCA7 were excluded from the assembled microbial consortia based on the results of pairwise microbial interaction assay. SCA7 was further characterized for its biocontrol activity by master's student Isabella Gantner (March 2021).

6.9.5.2 Consortium experiment 1

The consortium experiment 1 the consortium K1 consisting of all 28 consortium isolates (**Table 14**) on wheat was analyzed for its effect on plant growth under drought and non-drought conditions. The treatments K1 and 1 x PBS were each represented by 60 plants placed in 4 trays. Seedlings were inoculated with K1 or 1 x PBS as described in section 6.9.5 and transferred to pots filled with sand-clay mix as described in section 6.9.1. After 10 days two trays (=30 plants) experienced drought stress applied for 1 week without watering. Recovery phase lasted for 4 days after watering. Plants were harvested after growing three weeks in the phytochamber as described in 6.9.5 and plant parameters were evaluated as described in section 6.9.5. Shoot fresh weight of drought stress samples was excluded, because of the bias due to drought stress treatment. During the experiment samples for DNA and RNA extraction were taken after 10 days before the application of drought stress, after one week of drought stress before re-watering and from non-drought stressed controls and on the last day of the experiment. For RNA the flag leave from nine different plants was collected in each treatment and the flag leaves of three plants were pooled.

6.9.5.3 Consortium experiment 2

In the consortium experiment 2 three different consortia consisting of all 28 consortium isolates (K1), only genera which were high abundant in original Scheyern soil (K2) and only isolates without PGP traits *in vitro* (K3) (**Table 14**) were tested for their effect on plant growth in wheat plants under non-drought stress in two different concentrations. Bacterial cultures were prepared

and washed as described in section 6.9.5. Optical density (OD_{600}) of washed bacterial cultures was adjusted to OD_{600} = 1 or OD_{600} = 0.5 and cultures were mixed in equal amounts to the respective consortium solution. Wheat seeds were sterilized according to the protocol described in 6.9.2.2 and germinated on NB medium to identify bacterial contaminations. NB lowered germination rate in wheat seeds and was therefore replaced by Hoagland's solution agar for the follow-up experiments as described in 6.9.2.2. Each treatment (consortium K1, K2, K3 in two concentrations and 1 x PBS) was represented by 15 plants. Every pot was placed on a petridish to guarantee similar water conditions for each of the plants and pots were distributed randomly over the trays. Plants were harvested after growing three weeks in the phytochamber as described in 6.9.5 and plant parameters were evaluated as described in 6.9.5. No DNA and RNA samples were taken in this experiment.

6.9.5.4 Consortium experiment 3

In the consortium experiment 3 the three tested consortia K1, K2 and K3 (**Table 14**) were tested on wheat plants for their effect on plant growth under drought and non-drought conditions. Each treatment (consortium K1, K2, K3 and 1 x PBS) was represented by 30 plants. Seedlings were inoculated with K1, K2, K3 or 1 x PBS as described in section 6.9.5 and transferred to pots filled with sand-clay mix as described in section 6.9.1. Every pot was placed on a petridish to guarantee similar water conditions for each of the plants and pots were distributed randomly over the trays. After three weeks 15 plants of each treatment experienced drought stress applied for 6-8 days without watering. Re-watering was based on drought status of plant. Plant drought status was evaluated individually and every day based on mild (hanging leaves, flag leaf upright) or severe (all leaves hanging, dry tips, curled leaves) drought stress symptoms (**Figure 32**). Recovery phase lasted for 3-6 days after watering depending on time point of re-watering. State of recovery was evaluated after 1 h, 1.5 h, 2 h, 24 h and 48 h. Plants were harvested after growing four weeks in the phytochamber as described in 6.9.5 and plant parameters were evaluated as described in 6.9.5. During the experiment samples for DNA and RNA extraction were taken after three weeks before the application of drought stress, after one week of drought stress before re-watering and from non-drought control and on the last day of the experiment after recovery from drought and non-drought stressed plants. For RNA two leaves were harvested from three plants of each treatment at the same sampling points as DNA samples.

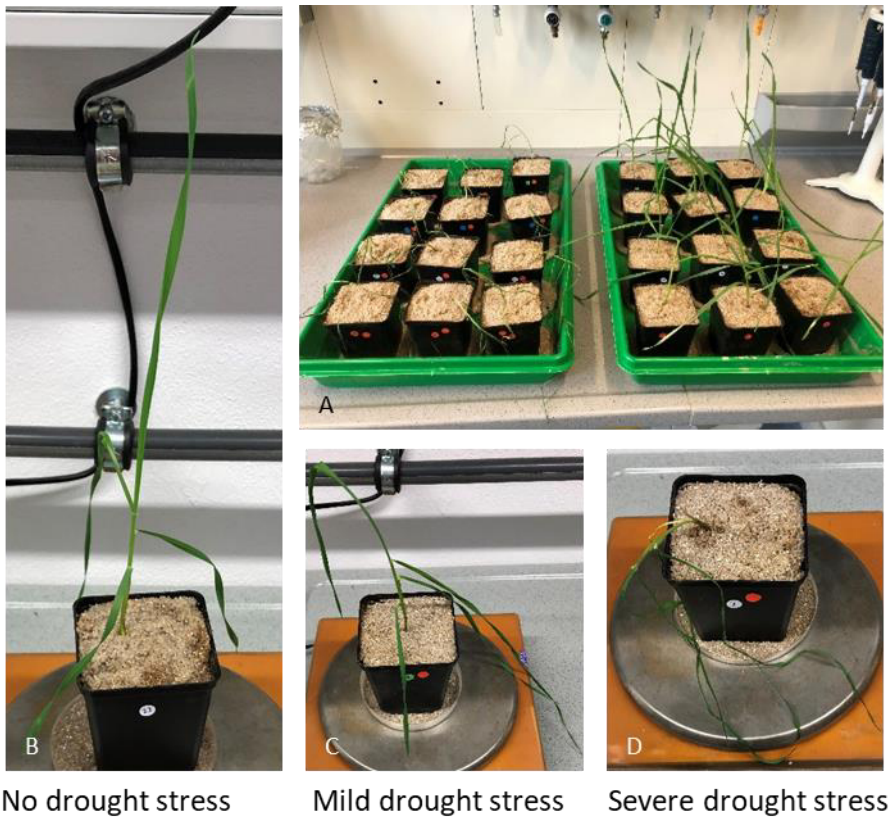

Figure 32: Representative wheat plants for drought stress. The drought stress status is (A) severe drought stress (left tray) or no drought stress (right tray). Individual wheat plants are depicted in (B) showing no drought stress symptoms, (C) mild drought stress symptoms with hanging leaves and (D) severe drought stress symptoms with dry leaves and a collapsed stem.

6.9.5.5 Consortium experiment 4

Five single isolates (**Table 14**) *Variovorax* sp. SCA27_61, *Variovorax* sp. M92526_27, *Flavobacterium* R2A20_2, *Sphingomonas* sp. M92526_32 and *Dyadobacter* sp. M92526_31 were selected based on their high abundance in the microbiota analysis of consortium experiments 1 and 3 as well as their connectedness in the co-occurrence network of the same samples. Additional treatments were the consortium K1 and the five isolates combined as consortium K4. All treatments were tested on wheat plants for their effect on plant growth under non-drought stress conditions. Each treatment (single strains, consortium K1, K4 and 1 x PBS) was represented by 25 plants. Every pot was placed on a petridish to guarantee similar water conditions for each of the plants and pots were distributed randomly over the trays. Seedlings were inoculated with K1, K4, SCA27_61, M92526_27, R2A20_2, M92526_32, M92526_31 or 1 x PBS as described in section 6.9.5 and transferred to pots filled with sand-clay mix as described in section 6.9.1. Plants were harvested

after growing three weeks in the phytochamber as described in 6.9.5 and plant parameters were evaluated as described in 6.9.5. No DNA or RNA samples were taken.

Table 14: Bacterial isolates used in the conducted experiments with wheat plants.

Strain	**Genus**	**K1**	**K2**	**K3**	**K4**	**Single strain**
Cha2930_14	*Bacillus*	X				
M92526_32	*Sphingomonas*	X	X		X	X
R2A20_2	*Flavobacterium*	X	X		X	X
Cha2324a_1	*Bacillus*	X		X		
Cha2324a_4	*Pseudomonas*	X				
Cha2324b_23	*Pseudomonas*	X				
Cha2324b_3	*Pedobacter*	X				
Cha2324a_8	*Bacillus*	X		X		
Cha2324b_12	*Pseudomonas*	X				
Cha2324b_30	*Pseudomonas*	X				
Cha2324a_16	*Luteibacter*	X				
M92526_27	*Variovorax*	X			X	X
Cha2324a_18	*Pseudomonas*	X				
SCA27_61	*Variovorax*	X			X	X
SCA27_60	*Streptomyces*	X	X			
M92526_31	*Dyadobacter*	X			X	X
NB17_5	*Rhodococcus*	X				
2xTY356_6	*Rhodococcus*	X		X		
2xTY356_27	*Rhodococcus*	X		X		
R2A20_29M	*Rhizobacter*	X	X			
R2A20_29R	*Polaromonas*	X	X			
M92526_34	*Rhizobium*	X	X			
2xTY356_31	*Arthrobacter*	X	X			
M925_13	*Arthrobacter*	X	X			
2xTY356_21	*Arthrobacter*	X	X			
2xT56_7	*Arthrobacter*	X	X			
M925_14	*Arthrobacter*	X	X			
NB17_19	*Arthrobacter*	X	X			

6.10 Quantitative gene expression analysis of consortium experiments

Expression of 19 selected genes (**Table 15**) in wheat plants from consortium experiment 3 was determined by quantitative PCR (qPCR) with Power SYBR Green Master Mix (Applied Biosystems, Darmstadt, Germany) using a peqSTAR® 96Q thermal cycler (PEQLAB Biotechnologie) following the protocol of Chowdhury *et al*. (2015b, 2019) and Alquéres *et al*. (2013). Chosen genes are associated with abiotic stress conditions, such as heat, drought and elevated salt stress or with nitrogen metabolism and iron transport in wheat. The gene coding for elongation factor 1α (*EF1α*) was used as reference gene. They were selected and validated for 100% (± 10%) primer efficiencies from my colleague Dr. Soumitra Paul Chowdhury (INET).

2 leaves from 3 plants (consortium experiment 3) were pooled and ground manually, while cooled with liquid nitrogen. Total RNA was extracted from 100 mg pulverized wheat leaves with RNeasy Plant Mini Kit (QIAGEN GmbH, Hilden, Germany) following the manufacturer's protocol. RNA was quantified with a NanoDrop® One spectrophotometer (Thermo Fisher Scientific, Waltham, MA, USA). Afterwards, cDNA was synthesized from 2 µg of RNA with the High Capacity cDNA Reverse Transcription Kit® with RNase Inhibitor (Applied Biosystems, Foster City, CA, USA). The following qPCR was performed in three technical replicates. Each qPCR reaction contained 10 µL of 2 X Power SYBR Green Master Mix® (LifeTechnologies, Darmstadt, Germany), 0.5 µM primers (Metabion International AG, Germany) and 25 ng of cDNA in 20 µL reaction volume. The qPCR conditions consisted of a pre-step at 50 °C for 2 min and denaturation at 95 °C for 10 min, followed by 40 cycles at 95 °C for 15 s, 60 °C for 1 min with data sampling. Generation of specific PCR products was confirmed by a melting curve with 95 °C for 15 s, 60 °C for 30 s and 95 °C for 15 s with data sampling. The relative quantification was determined with the comparative CT method (the ΔΔCT method) (Livak and Schmittgen, 2001). First the data was normalized to the endogenous control (reference gene) and afterwards logarithmically transformed to fold change difference. The standard error of the mean was calculated based on the average of the biological replicates.

Table 15: Genes and primers analyzed in quantitative gene expression analysis with qPCR.

Gene	**Forward P (5′ to 3′)** **Reverse P (5′ to 3′)**	**Reference**	**Related Function**
TaEF1α (Elongation factor 1α)	ATGATTCCCACCAAGCCCAT ACACCAACAGCCACAGTTTGC	Cruz *et al*., 2015	housekeepeing
TaLOX (Lipoxygenase)	CGACCCGCAGCTGTTGA CCCTTGTGATCGGAGGTGTT	Cruz *et al*., 2015	Signalling upon pathogen attack (Leaf blast)
TaAOS (Allene Oxide Synthase)	ACCGTGTTCAACAGCTACGG AGCGCCTCTATCGTCACCTT	Wang *et al*., 2017	Jasmonic acid signalling
TaSOD (JQ613154.1 Superoxide Dismutase)	CATTGTCGATAGCCAGATTCCTTT AGTCTTCCACCAGCATTTCCAGTA	Zhang *et al*., 2016	Antioxidant, increased in salt
TaCAT (GU984379.1 Catalase)	TTTGATGGGAGTCTTGTGCTTGTG ACGGTGAGGGAGTTGTCGTTGTT	Zhang *et al*., 2016	Antioxidant, increased in salt
*TaGSTU*4 (Glutathione-S-transferase 4)	TTCAAGCATCCAACCTCTCC GCTGTCACATCCATCCAAAA	Chowdhury *et al*., (in preparation)	Abiotic stress
TaGSTZ (Glutathione-S-transferase)	CCAAGCCCATTTGTTACCAG GTGGATGAGCACGGGTATCT	Chowdhury *et al*., (in preparation)	Abiotic stress
TaMYB80 (MYB Transcription Factor 80)	CAGATGCTCCTCCCTTGG GTGATCCTGGTGTAGTTGC	Zhao *et al*., 2017	Heat and drought tolerance
TaODORANT1 (MYB Transcription Factor)	CCGAAGCCCATGTACCTCC CGGATCTATGATCGGTCTATGTG	Wei *et al*., 2017	Drought and salt stress
TaWRKY49 (WRKY transcription factor)	CTTCCCTGCCGCATTCT ACGCTCTCGCCCTAGTG	Wang *et al*., 2017	Heat induced
TaWRKY62 (WRKY transcription factor)	TCGTTGACCACCACCAG AGCCGTCCCCAAATCCA	Wang *et al*., 2017	Heat induced
TaMPK4 (Mitogen activated Protein Kinase)	TCGAGCCTGGGATTTCTTCG GTCAACAGTGATGCGTCTGC	Goyal *et al*., 2018	Cold and salt stress
TaNR1 (Nitrate Reductase)	GGCCAATTCYTTCATCTCCTTCTG TACRTSCACAGATTGATGCGTCSA	Buchner and Hawkesford, 2014	Nitrogen related
TaNIR (Nitrite reductase)	ACGAGGAGTAGGCCGGCTASGAG ATCAGCCGCAGCCCATCTCTRC	Buchner and Hawkesford, 2014	Nitrate related
TaGDH2 (Glutamate dehydrogenase 2)	AGGATGGGAGCATTCACCTTGG GGATATAAGAACTKTCATCCACCA CG	Buchner and Hawkesford, 2014	Nitrogen related
TaVIT2 (Iron transporter)	CTCCCCCTACATGTTCGT CCCTTGACGTAGCCGAA	Connorton *et al*., 2017	Iron related
TaRD29b (low-temperature-induced protein)	CAAGTCGACGTGAGCAAAGA GCCGTATTCTTGAGCCTGTC	Zhang *et al*., 2017	Abscisic acid signaling, cold stress

TaDREB2A (dehydration-responsive element-binding protein 2A)	TGGCTTGGTTCATTCCCTAC CCCCATTAGACGTCAGCAAT	Zhang *et al*., 2017	Abscisic acid signaling, drought stress
TaHSFA6b (Heat stress transcription factor A-6b)	ACGACTTCTGGGAGGAGCTG CCTCCTCTCCAGCTCTAGCATC	Begcy *et al*., 2018	Abscisic acid signaling, heat stress
TaTIP1 (gamma-type tonoplast intrinsic protein)	GGAGATCGTGATGACCTTCG CTGCTCAGTAGTCGGTGGTG	Cevher-Keskin *et al*., 2015	Drought stress (ABA independent)

6.11 Quantification of bacterial load on wheat roots of consortium experiments

Estimation of bacterial load based on the number of 16S rRNA gene copies per sample was analyzed using qPCR. Genomic DNA was extracted from roots and rhizosphere as described in 6.10 using FastDNA SPIN Kit® for soil (MPbio GmbH, Germany). Extracted DNA was diluted 100 x according to Dineen *et al*. (2010) to remove polymerase-inhibiting compounds. Quantitative PCR was performed using Power SYBRGreen PCR Master Mix® 2 X (LifeTechnologies, Darmstadt, Germany) with a total of 3.75 ng DNA per well and bacterial 16S rRNA primers 926-F (5′-AAACTYAAAKGAATTGACGG-3′, *Escherichia coli* position 907–926 (Lane, 1991)) and 630-R (5′-CAKAAAGGAGGTGATCC-3′, *E. coli* position 1528–1544 (Juretschko *et al*., 1998)) in 0.5 µM concentration per well amplifying a fragment of approximately 602 bp. The standard curve was based on a dilution series of 10^3 to 10^7 genomes per µL derived from genomic DNA extracted from *Flavobacterium* sp. R2A20_2 pure culture, which was high abundant in Scheyern samples. The number of copies was calculated with the DNA copy Number calculator Thermofisher Scientific based on the formula:

$$\text{No of copies} = \frac{\text{ng DNA} * 6.0221 * 10^{23} \text{ molecules/mole}}{(\text{length of dsDNA amplicon} * 660\text{g/mole}) * 10^9 \text{ ng/g}}$$

The qPCR conditions were used as described in section 6.10. Total bacterial load per gram root and rhizosphere was calculated from the standard curve using Microsoft® Excel.

6.12 Amplicon-based community profiling

6.12.1 Samples for the amplicon-based community profiling

Amplicon-based community profiling was performed from four rhizosphere samples and one bulk soil sample each from Scheyern, Bernburg with pre-crop maize and Bernburg with pre-crop canola

described in section 6.1 as well as roots and rhizosphere samples from consortium experiments 1 and 3.

6.12.2 DNA extraction and library preparation

Genomic DNA was extracted from a maximum of 500 mg roots and rhizosphere or soil with the FastDNA SPIN Kit® for soil (MP Biomedicals GmbH, Germany) according to the manufacturer's protocol with modifications. Removal of precipitated proteins was performed in 2 mL microcentrifuge tubes (instead of 15 mL Falcons) and DNA was eluted in 50 µL DES. DNA amount was quantified with NanoDrop® One spectrophotometer (Thermo Fisher Scientific, Waltham, MA, USA). Library preparation was performed according to the protocol of the earth microbiome project (Thompson *et al*., 2017). Amplification of the V4-V5 region of 16S rRNA gene (approximately 250 bp) was performed with the NEBNext High Fidelity PCR Kit® (New England Biolabs, Frankfurt, Germany) with the primers 515F- GTGYCAGCMGCCGCGGTAA (Parada *et al*., 2016) and 806R- GGACTACNVGGGTWTCTAAT (Apprill *et al*., 2015) (Metabion International AG, Germany) tagged with the flowcell adaptor sequence. PCR conditions consisted of denaturation at 98 °C for 5 min, followed by 20 cycles at 98 °C for 10 s, 55 °C for 30 s, 72 °C for 30 s and one final elongation step at 72 °C for 5 min. The amplified gene products were visualized on 1% agarose gel.

Afterwards small fragments and primer dimers were removed from PCR products using MagSi-NGSPrep Plus kit® (Magtivio, The Netherlands) following the manufacturer's protocol for left side size selection. PCR products and magnetic beads were mixed in a ratio of 1 : 0.8. DNA was eluted in 20 µL of elution buffer. Purification of DNA was analyzed by Cornelia Galonska at the Institute of Comparative Microbiome Analysis, HMGU, with the bioanalyzer DNA 7500 Chip (Agilent Technologies, USA) using kit 374. Amplicon concentration was quantified using the Quant-iT™ PicoGreen™ dsDNA Assay Kit (Thermo Scientific, Germany) and a plate reader (SpectraMax iD3, Molecular Devices) with excitation at 480 nm and emission at 520 nm. A total of 10 ng DNA was transferred to the Index-PCR for barcoding (NEBNext Multiplex Oligos for Illumina® (Dual Index Primer Set1 (#E7600S), New England Biolabs, Frankfurt, Germany) and were amplified with NEBNext High Fidelity PCR Kit (New England Biolabs, Frankfurt, Germany). PCR conditions consisted of denaturation at 98 °C for 30 s, followed by 8 cycles at 98 °C for 10 s, 55 °C for 30 s, 72 °C for 30 s and one final elongation step at 72 °C for 5 min. Afterwards small fragments and primer dimers were removed from PCR products using MagSi-NGSPrep Plus kit® (Magtivio, The

Netherlands) following the protocol for left side size selection. PCR products and magnetic beads were mixed in a ratio of 1 : 0.8. DNA was eluted in 10 µL of elution buffer. Amplicon concentration was quantified using the Quant-iT™ PicoGreen™ dsDNA Assay Kit (Thermo Scientific, Germany). In a final step PCR products of the Index-PCR were diluted to a concentration of 4 nM DNA and 5 µL were transferred to the final pool.

6.12.3 Sequencing

Prepared sequencing libraries were sequenced at the sequencing facility of the Institute of Comparative Microbiome Analysis (COMI) at HMGU by Susanne Kublik using MiSeq® reagent kit v3 for Illumina sequencing (Illumina, San Diego, CA, USA). Demultiplexed data were provided from the sequencing facility as .fastq files for further analysis.

6.12.4 Amplicon-based microbial community analysis

16S rRNA gene amplicon data were analyzed using the pipeline provided on the IMNGS platform (Lagkouvardos *et al*., 2016) created for analysis of data retrieved from Illumina sequencing technology. The demultiplexed data were remultiplexed to be compatible with the pipeline running the provided Perl script "remultiplexor". The three generated files contain the separated forward and reverse reads and a file containing the indexes added to the reads from a pool of standard barcodes. These files are uploaded together with a mapping file containing the barcode information for each sample at https://www.imngs.org/, which has the UPARSE (Edgar, 2013) algorithm from the USEARCH11 (32-bit) package (Edgar, 2010) implemented. Parameter were adjusted to minimum read length 200 bp and maximum read length 400 bp, primers were trimmed with 19 bp at 5-end and 20 bp at 3-end. The abundance cutoff was set to 0.0001 (=0.01%) and was evaluated with identified bacterial genera in culture. The generated files including the operational taxonomic unit (OTU) table were analyzed using the Rhea pipeline (Lagkouvardos *et al*., 2016), which is a set of R scripts that encode different steps for downstream analysis of OTUs, such as normalization, alpha-diversity and beta-diversity analysis, taxonomic binning, statistical comparisons and calculation of correlations, using default parameters. Operational taxonomic units (OTUs) with a similarity of more than 97% are commonly considered as belonging to the same or a very closely related species, implying similar biological properties and potentially similar functions in a microbiome (Schloss & Handelsman 2005). Before analysis with Rhea mitochondrial and chloroplast reads were removed from the OTU table. Similarities between treatments were calculated with generalized UniFrac method, which is implemented in the Rhea pipeline

(Lagkouvardos *et al*., 2016) and a balanced version between unweighted and weighted UniFrac less sensitive to differing OTU abundances (Chen *et al*., 2012). Results of the multidimensional distance matrix were presented in two dimensions using Multi-Dimensional Scaling (MDS) plots implemented in the Rhea pipeline (Lagkouvardos *et al*., 2016). A permutational multivariate analysis of variance using distance matrices (vegan::adonis) is performed in each case to determine if the separation of groups is significant, as a whole and in pairs (Anderson, 2001) also implemented in the Rhea pipeline (Lagkouvardos *et al*., 2016). Similarities (threshold <97%) between consortium isolates and OTUs derived from Scheyern samples and from consortium experiment 1 and 3 were determined using BLAST to evaluate if consortium isolates belong to high abundant members of the microbiota.

6.12.5 Co-occurrence network consortium experiments

The co-occurrence network shows the pairwise occurrence of OTUs in the analyzed samples based on absolute OTU abundances. A co-occurrence network for the 16S rRNA gene data from 6 samples of consortium experiment 1 and 3 of the treatment K1. because treatment K1 showed the highest phenotypic difference. The network was calculated based on OTU abundances using the R based bioinformatics tool NetCOMI (Peschel *et al*., 2021) with default parameter, filtered by the 100 highest varying OTUs and calculated Pearson correlation. The OTU table derived from Rhea, as described above, was used without OTUs identified as mitochondria or chloroplasts. A co-occurrence shown by a green edge (connection between nodes) indicates the positive correlation between two OTUs, whereas a red edge indicates a negative correlation.

6.13 Statistical analysis

Sample size was not predetermined using statistical methods. Statistical analysis was performed with RStudio 3.6.1, Microsoft® Excel or Past 4.06b. Data were tested for normal distribution with Shapiro-Wilk-Test. Depending on the data distribution data were analyzed with Student's t-test, the non-parametric Fligner-Killeen-Test or with analysis of variances (ANOVA) followed by a post-hoc analysis with Tukey’s test. Significance level was 5% marked in the graphs by asterisks. Combined data of consortium experiments 1, 2 and 3 were statistically analyzed using linear models (lm) with normal distribution (best model fit) considering treatment as explanatory variable and the varying experimental conditions (duration, concentration) as covariates. The percentage of germinated seeds was calculated by dividing number of germinated seeds by total number of seeds.

7 Bibliography

Abbamondi, G. R., Tommonaro, G., Weyens, N., Thijs, S., Sillen, W., Gkorezis, P., Iodice, C., de Melo Rangel, W., Nicolaus, B., Vangronsfeld, J. (2016). Plant growth-promoting effects of rhizospheric and endophytic bacteria associated with different tomato cultivars and new tomato hybrids. *Chem. Biol. Technol. Agric.* 3, 1–10. doi:10.1186/s40538-015-0051-3.

Afanador-Barajas, L. N., Navarro-Noya, Y. E., Luna-Guido, M. L., and Dendooven, L. (2021). Impact of a bacterial consortium on the soil bacterial community structure and maize (*Zea mays* L.) cultivation. *Sci. Rep.* 11, 1–13. doi:10.1038/s41598-021-92517-0.

Agnolucci, M., Palla, M., Cristani, C., Cavallo, N., Giovannetti, M., De Angelis, M., Gobbetti, M., Minervini, F. (2019). Beneficial plant microorganisms affect the endophytic bacterial communities of durum wheat roots as detected by different molecular approaches. *Front. Microbiol.* 10, 1–14. doi:10.3389/fmicb.2019.02500.

Ahkami, A. H., White, R. A., Handakumbura, P. P., and Jansson, C. (2017). Rhizosphere engineering: Enhancing sustainable plant ecosystem productivity. *Rhizosphere* 3, 233–243. doi:10.1016/j.rhisph.2017.04.012.

Ahmed, E., and Holmström, S. J. M. (2014). Siderophores in environmental research: Roles and applications. *Microb. Biotechnol.* 7, 196–208. doi:10.1111/1751-7915.12117.

Alabid, I., Hardt, M., Imani, J., Hartmann, A., Rothballer, M., Li, D., Uhl, J., Schmitt-Koplin, P., Glaeser, S., Kogel, K.-H. (2020). The N-acyl homoserine-lactone depleted *Rhizobium radiobacter* mutant RrF4NM13 shows reduced growth-promoting and resistance-inducing activities in mono- and dicotyledonous plants. *J. Plant Dis. Prot.* 127, 769–781. doi:10.1007/s41348-020-00360-8.

Alavi, P., Starcher, M. R., Thallinger, G. G., Zachow, C., Müller, H., Berg, G. (2014). *Stenotrophomonas* comparative genomics reveals genes and functions that differentiate beneficial and pathogenic bacteria. *BMC Genomics* 15, 1–15. doi:10.1186/1471-2164-15-482.

Alavi, P., Starcher, M. R., Zachow, C., Müller, H., and Berg, G. (2013). Root-microbe systems: the effect and mode of interaction of Stress Protecting Agent (SPA) *Stenotrophomonas rhizophila* DSM14405T. *Front. Plant Sci.* 4, 1–10. doi:10.3389/fpls.2013.00141.

Aleklett, K., Kiers, E. T., Ohlsson, P., Shimizu, T. S., Caldas, V. E., Hammer, E. C. (2018). Build your own soil: Exploring microfluidics to create microbial habitat structures. *ISME J.* 12, 312–319. doi:10.1038/ismej.2017.184.

Alquéres, S., Meneses, C., Rouws, L., Rothballer, M., Baldani, I., Schmid, M., Hartmann, A. (2013). The bacterial superoxide dismutase and glutathione reductase are crucial for endophytic colonization of rice roots by *Gluconacetobacter diazotrophicus* PAL5. *Mol. Plant-Microbe Interact.* 26, 937–945. doi:10.1094/MPMI-12-12-0286-R.

Alvarez, H. M. (Ed. . (2019). *Biology of Rhodococcus* Switzerland: Springer. Available at: http://www.springer.com/gp/book/9783642129360.

Amann, R. I., Krumholz, L., Stahl, D. A. (1990). Fluorescent-oligonucleotide probing of whole cells for determinative and environmental studies in microbiology. *J. Bacteriol.* 172, 762–770. doi: 10.1128/jb.172.2.762-770.

Ampomah, O. Y., Huss-Danell, K. (2011). Genetic diversity of root nodule bacteria nodulating *Lotus corniculatus* and *Anthyllis vulneraria* in Sweden. *Syst. Appl. Microbiol.* 34, 267–275. doi:10.1016/j.syapm.2011.01.006.

Anderson, M.J. (2001). A new method for non-parametric multivariate analysis of variance. *Austral Ecology*, 26: 32–46. doi.org/10.1111/j.1442-9993.2001.01070.pp.x

Andrés-Barrao, C., Lafi, F. F., Alam, I., de Zélicourt, A., Eida, A. A., Bokhari, A., Alzubaidy, H., Bajic, V. B., Hirt, H., Saad, M. M. (2017). Complete genome sequence analysis of *Enterobacter* sp. SA187, a plant multi-stress tolerance promoting endophytic bacterium. *Front. Microbiol.* 8, 1–21. doi:10.3389/fmicb.2017.02023.

Andrew, S. (2010). FastQC: a quality control tool for high throughput sequence data. Available at: http://www.bioinformatics.babraham.ac.uk/projects/fastqc.

Angulo, J., Martínez-Salgado, M. M., Ortega-Blu, R., Fincheira, P. (2020). Combined effects of chemical fertilization and microbial inoculant on nutrient use efficiency and soil quality indicators. *Sci. Agropecu.* 11, 375–380. doi:10.17268/sci.agropecu.2020.03.09.

Ansari, F. A., Ahmad, I. (2019). Fluorescent *Pseudomonas* -FAP2 and *Bacillus licheniformis* interact positively in biofilm mode enhancing plant growth and photosynthetic attributes. *Sci. Rep.* 9, 1–12. doi:10.1038/s41598-019-40864-4.

Anton, B. P., Raleigh, E. A. (2016). Complete Genome Sequence of NEB 5-alpha, a Derivative of *Escherichia coli* K-12 DH5a. *Genome Announc*. 4, 6–7. doi: 10.1128/genomeA.01245-16.

Apprill, A., McNally, S., Parsons, R., Weber, L. (2015). Minor revision to V4 region SSU rRNA 806R gene primer greatly increases detection of SAR11 bacterioplankton. *Aquatic Microbial Ecology*, 75(2), 129–137. http://doi.org/10.3354/ame01753

Araujo, R., Dunlap, C., Barnett, S., Franco, C. M. M. (2019). Decoding Wheat Endosphere – Rhizosphere Microbiomes in *Rhizoctonia solani* – Infested Soils Challenged by *Streptomyces* Biocontrol Agents. *Front. Plant Sci*. 10:1038. doi: 10.3389/fpls.2019.01038

Araus, J. L., Cairns, J. E. (2014). Field high-throughput phenotyping: the new crop breeding frontier. *Trends Plant Sci*. 19, 52–61. doi: 10.1016/j.tplants.2013.09.008.

Armanhi, J. S. L., de Souza, R. S. C., Damasceno, N. de B., de Araújo, L. M., Imperial, J., Arruda, P. (2018). A community-based culture collection for targeting novel plant growth-promoting bacteria from the sugarcane microbiome. *Front. Plant Sci.* 8, 1–17. doi:10.3389/fpls.2017.02191.

Armanhi, J. S. L., De Souza, R. S. C., De Araújo, L. M., Okura, V. K., Mieczkowski, P., Imperial, J., Arruda, P. (2016). Multiplex amplicon sequencing for microbe identification in community-based culture collections. *Sci. Rep.* 6, 1–9. doi:10.1038/srep29543.

Aziz, R. K., Bartels, D., Best, A., DeJongh, M., Disz, T., Edwards, R. A., et al. (2008). The RAST Server: Rapid annotations using subsystems technology. *BMC Genomics* 9, 1–15. doi:10.1186/1471-2164-9-75.

Azizoglu, U., Yilmaz, N., Simsek, O., Ibal, J. C., Tagele, S. B., Shin, J. H. (2021). The fate of plant growth-promoting rhizobacteria in soilless agriculture: future perspectives. *3 Biotech* 11, 1–13. doi:10.1007/s13205-021-02941-2.

Barberan, A., Bates, S. T., Casamayor, E. O. Fierer, N. (2012) Using network analysis to explore co-occurrence patterns in soil microbial communities. *ISME J.* 6, 343–351 doi.org/10.1038/ismej.2011.119

Babin, D., Sommermann, L., Paul Chowdhury, S., Behr, J. H., Sandmann, M., Neumann, G., Nesme, J., Sørensen, S. J., Schellenberg, I., Rothballer, M., Geistlinger, J., Small, K., Grosch, R. (2021). Distinct rhizomicrobiota assemblages and plant performance in lettuce grown in soils with different agricultural management histories. *FEMS Microbiol. Ecol.* 97(4). fiab027. https://doi.org/10.1093/femsec/fiab027

Bai, Y., Müller, D. B., Srinivas, G., Garrido-oter, R., Potthoff, E., Rott, M., Dombrowski, N., Münch, P. C., Spaepen, S., Remus-Emsermann, M., Hüttel, B., McHardy, A.C., Vorholt, J. A., Schulze-Lefert, P. (2015). Functional overlap of the Arabidopsis leaf and root microbiota. *Nature* 528, 364–369. doi:10.1038/nature16192.

Bakker, P. A. H. M., Berendsen, R. L., Doornbos, R. F., Wintermans, P. C. A., Pieterse, C. M. J. (2013). The rhizosphere revisited: Root microbiomics. *Front. Plant Sci.* 4, 1–7. doi:10.3389/fpls.2013.00165.

Bakker, P. A. H. M., Berendsen, R. L., Van Pelt, J. A., Vismans, G., Yu, K., Li, E., Van Bentum, S., Poppeliers, S. W. M., Sanchez Gil, J. J., Zhang, H., Goossens, P., Stringlis, I. A., Song, Y., de Jonge, R., Pieterse, C. M. J. (2020). The Soil-Borne Identity and Microbiome-Assisted Agriculture: Looking Back to the Future. *Mol. Plant* 13, 1394–1401. doi:10.1016/j.molp.2020.09.017.

Bala, M., Kumar, S., Raghava, G. P. S., Mayilraja, S. (2013). Draft Genome Sequence of *Rhodococcus qingshengii* Strain BKS 20-40 *Genome Announc*. 1(2):e00128-13. doi:10.1128/genomeA.00128-13.

Banerjee, S., Walder, F., Büchi, L., Meyer, M., Held, A. Y., Gattinger, A., Keller, T., Charles, R., van der Heijden, M. G. A. (2019). Agricultural intensification reduces microbial network complexity and the abundance of keystone taxa in roots. *ISME J.* 13, 1722–1736. doi:10.1038/s41396-019-0383-2.

Barbey, C., Crépin, A., Bergeau, D., Ouchiha, A., Mijouin, L., Taupin, L., Orange, N., Feuilloley, M., Dufour, A., Burini, J.-F., Latour, X. (2013). *In planta* biocontrol of *Pectobacterium atrosepticum* by *Rhodococcus erythropolis* involves silencing of pathogen communication by the rhodococcal Gamma-lactone catabolic pathway. *PLoS One* 8, 1–9. doi:10.1371/journal.pone.0066642.

Bardgett, R. D., van der Putten, W. H. (2014). Belowground biodiversity and ecosystem functioning. *Nature* 515, 505–11. doi:10.1038/nature13855.

Bebber, D. P., Holmes, T., Gurr, S. J. (2014a). The global spread of crop pests and pathogens. *Glob. Ecol. Biogeogr.* 23, 1398–1407. doi:10.1111/geb.12214.

Bebber, D. P., Holmes, T., Smith, D., Gurr, S. J. (2014b). Economic and physical determinants of the global distributions of crop pests and pathogens. *New Phytol.* 202, 901–910. doi:10.1111/nph.12722.

Begcy, K., Weigert, A., Egesa, A. O., Dresselhaus, T. (2018). Compared to australian cultivars, european summer wheat (*Triticum aestivum*) overreacts when moderate heat stress is applied at the pollen development stage. *Agronomy* 8. doi:10.3390/agronomy8070099.

Belimov, A. A., Hontzeas, N., Safronova, V. I., Demchinskaya, S. V., Piluzza, G., Bullitta, S., Glick, B. R. (2005). Cadmium-tolerant plant growth-promoting bacteria associated with the roots of Indian mustard (*Brassica juncea* L. Czern.). *Soil Biol. Biochem.* 37, 241–250. doi:10.1016/j.soilbio.2004.07.033.

Belimov, A. A., Safronova, V. I., Sergeyeva, T. A., Egorova, T. N., Matveyeva, V. A., Tsyganov, V. E., Borisov, A. Y., Tikhonovich, I. A., Kluge, C., Preisfeld, A., Dietz, K. J., Stepanok, V. V. (2001). Characterization of plant growth promoting rhizobacteria isolated from polluted soils and containing 1-aminocyclopropane-1-carboxylate deaminase. *Can. J. Microbiol*. 47, 642–652. doi: 10.1139/w01-062

Belimov, A. A., Shaposhnikov, A. I., Azarova, T. S., Makarova, N. M., Safronova, V. I., Litvinskiy, V. A., Nosikov, V. V., Zavalin, A. A., Tikhonovich, I. A. (2020). Microbial consortium of PGPR, rhizobia and arbuscular mycorrhizal fungus makes pea mutant SGECdt comparable with indian mustard in cadmium tolerance and accumulation. *Plants* 9, 1–21. doi:10.3390/plants9080975.

Bell, L., Oruna-Concha, M. J., Wagstaff, C. (2015). Identification and quantification of glucosinolate and flavonol compounds in rocket salad (*Eruca sativa*, *Eruca vesicaria* and *Diplotaxis tenuifolia*) by LC-MS: Highlighting the potential for improving nutritional value of rocket crops. *Food Chem.* 172, 852–861. doi:10.1016/j.foodchem.2014.09.116.

Bell, L., Yahya, H. N., Oloyede, O. O., Methven, L., Wagstaff, C. (2017). Changes in rocket salad phytochemicals within the commercial supply chain: Glucosinolates, isothiocyanates, amino acids and bacterial load increase significantly after processing. *Food Chem.* 221, 521–534. doi:10.1016/j.foodchem.2016.11.154.

Bender, S. F., Wagg, C., van der Heijden, M. G. A. (2016). An Underground Revolution: Biodiversity and Soil Ecological Engineering for Agricultural Sustainability. *Trends Ecol. Evol.* 31, 440–452. doi:10.1016/j.tree.2016.02.016.

Benedek, T., Máthé, I., Salamon, R., Rákos, S., Pásztohy, Z., Márialigeti, K., Lány, S. (2012). Potential bacterial soil inoculant made up by *Rhodococcus* sp. and *Pseudomonas* sp. for remediation *in situ* of hydrocarbon - and heavy metal polluted soils. *Stud. Univ. Babes-Bolyai Chem.* 2012, 199–211.

Benoit, S., Taouji, S., Benachour, A., Hartke, A. (2000). Resistance of *Rhodococcus equi* to acid pH. *Int. J. Food Microbiol.* 55, 295–298. doi:10.1016/S0168-1605(00)00172-0.

Berendsen, R. L., Vismans, G., Yu, K., Song, Y., de Jonge, R., Burgman, W. P., Burmølle, M., Herschend, J., Bakker, P. A. H. M., Pieterse, C. M. J. (2018). Disease-induced assemblage of a plant-beneficial bacterial consortium. *ISME J.*, 1–12. doi:10.1038/s41396-018-0093-1.

Berg, G. (2009). Plant-microbe interactions promoting plant growth and health: Perspectives for controlled use of microorganisms in agriculture. *Appl. Microbiol. Biotechnol.* 84, 11–18. doi:10.1007/s00253-009-2092-7.

Berg, G., Alavi, M., Schmidt, C. S., Zachow, C., Egamberdieva, D., Kamilova, F., Lugtenberg, B. J. J. (2013). Biocontrol and osmoprotection for plants under salinated conditions. in *Molecular Microbial Ecology of the Rhizosphere*, New Jersey: Hoboken, John Wiley and Sons 2, 587–592.

Berg, G., Erlacher, A., Smalla, K., Krause, R. (2014). Vegetable microbiomes: Is there a connection among opportunistic infections, human health and our "gut feeling"? *Microb. Biotechnol.* 7, 487–495. doi:10.1111/1751-7915.12159.

Berg, G., Kusstatscher, P., Abdelfattah, A., Cernava, T., Smalla, K. (2021). Microbiome modulation—toward a better understanding of plant microbiome response to microbial inoculants. *Front. Microbiol.* 12, 1–12. doi:10.3389/fmicb.2021.650610.

Berg, G., Martinez, J. L. (2015). Friends or foes: Can we make a distinction between beneficial and harmful strains of the *Stenotrophomonas maltophilia* complex? *Front. Microbiol.* 6, 1–6. doi:10.3389/fmicb.2015.00241.

Berg, G., Rybakova, D., Fischer, D., Cernava, T., Vergès, M. C. C., Charles, T., et al. (2020). Microbiome definition re-visited: old concepts and new challenges. *Microbiome* 8, 1–22. doi:10.1186/s40168-020-00875-0.

Berg, G., Rybakova, D., Grube, M., Köberl, M., Price, A. (2017). The plant microbiome explored : implications for experimental botany. *Europe PMC Funders Group* 67, 995–1002. doi:10.1093/jxb/erv466.The.

Berg, M., Koskella, B. (2018). Nutrient- and dose-dependent microbiome-mediated protection against a plant pathogen. *Curr. Biol.* 28, 2487-2492.e3. doi:10.1016/j.cub.2018.05.085.

Bessler, H., Djaldetti, M. (2018). Broccoli and human health: immunomodulatory effect of sulforaphane in a model of colon cancer. *Int. J. Food Sci. Nutr.* 69, 946–953. doi:10.1080/09637486.2018.1439901.

Bhat, M. A., Kumar, V., Bhat, M. A., Wani, I. A., Dar, F. L., Farooq, I., Bhatti, F., Koser, R., Rahman, S., Jan, A. T. (2020). Mechanistic insights of the interaction of plant growth-promoting rhizobacteria (PGPR) with plant roots toward enhancing plant productivity by alleviating salinity stress. *Front. Microbiol.* 11, 1–20. doi:10.3389/fmicb.2020.01952.

Blin, K., Wolf, T., Chevrette, M. G., Lu, X., Schwalen, C. J., Kautsar, S. A., et al. (2017). AntiSMASH 4.0 - improvements in chemistry prediction and gene cluster boundary identification. *Nucleic Acids Res.* 45, W36–W41. doi:10.1093/nar/gkx319.

Blom, J., Kreis, J., Spänig, S., Juhre, T., Bertelli, C., Ernst, C., Goesmann, A. (2016). EDGAR 2.0: an enhanced software platform for comparative gene content analyses. *Nucleic Acids Res.* 44, W22–W28. doi:10.1093/nar/gkw255.

Blum, W. E. H., Zechmeister-Boltenstern, S., Keiblinger, K. M. (2019). Does soil contribute to the human gut microbiome? *Microorganisms* 7. doi:10.3390/microorganisms7090287.

Bodenhausen, N., Bortfeld-Miller, M., Ackermann, M., Vorholt, J. A. (2014). A synthetic community approach reveals plant genotypes affecting the phyllosphere microbiota. *PLoS Genet.* 10. doi:10.1371/journal.pgen.1004283.

Bosello, M., Zeyadi, M., Kraas, F. I., Linne, U., Xie, X., Marahiel, M. A. (2013). Structural characterization of the heterobactin siderophores from *Rhodococcus erythropolis* PR4 and elucidation of their biosynthetic machinery. *J. Nat. Prod.* 76, 2282–2290. doi:10.1021/np4006579.

Botstein, D., White, R. L., Skolnick, M., & Davis, R. W. (1980). Construction of a genetic linkage map in man using restriction fragment length polymorphism. *Am J Hum Gen*, 32, 314–331. PMCID: PMC1686077

Bottini, R., Cassán, F., Piccoli, P., (2004). Gibberellin production by bacteria and its involvement in plant growth promotion and yield increase. *Appl Microbial Biotechnol* 65: 497-503. https://doi.org/10.1007/s00253-004-1696-1

Boyd, E. S., and Barkay, T. (2012). The mercury resistance operon: From an origin in a geothermal environment to an efficient detoxification machine. *Front. Microbiol.* 3, 1–13. doi:10.3389/fmicb.2012.00349.

Bradáčová, K., Florea, A. S., Bar-Tal, A., Minz, D., Yermiyahu, U., Shawahna, R., Kraut-Cohen, J., Zolti, A., Erel, R., Dietel, K., Weinmann, M., Zimmermann, B., Berger, N., Ludewig, U., Neumann, G., Poşta, g. (2019). Microbial Consortia versus Single-Strain Inoculants: An advantage in PGPM-assisted tomato production? *Agronomy* 9. doi:10.3390/agronomy9020105.

Breakfield, N. W., Collett, D., Frodyma, M. E. (2021) Plant growth-promoting microbes — an industry view. *Emerg Top Life Sci*; 5 (2): 317–324. doi: https://doi.org/10.1042/ETLS20200313

Bremer, E., Krämer, R. (2019). Responses of microorganisms to osmotic stress. *Annu. Rev. Microbiol.* 73, 313–334. doi:10.1146/annurev-micro-020518-115504.

Brenner, D. J., Krieg, N. R., Garrity, G. M., Staley, J. T. (2005). *Bergey's manual of systematic bacteriology*, 2nd Edition, Vol. 2. *New York: Springer*.

Brown, C. M., Dilworth, M. J. (1975) Ammonia assimilation by *Rhizobium* cultures and bacteroids. *J Gen Microbiol* 86: 39–48. doi: 10.1099/00221287-86-1-39

Brumos, J., Robles, L. M., Yun, J., Vu, T. C., Jackson, S., Alonso, J. M., Stepanova, A. N. (2018). Local auxin biosynthesis is a key regulator of plant development. *Dev. Cell* 47, 306-318.e5. doi:10.1016/j.devcel.2018.09.022.

Buchner, P., Hawkesford, M.J., (2014). Complex phylogeny and gene expression patterns of members of the NITRATE TRANSPORTER 1/PEPTIDE TRANSPORTER family (NPF) in wheat. *Journal of experimental botany*, 65(19), pp.5697-5710. https://doi.org/10.1093/jxb/eru231

Bulgarelli, D., Rott, M., Schlaeppi, K., Ver Loren van Themaat, E., Ahmadinejad, N., Assenza, F., et al. (2012). Revealing structure and assembly cues for Arabidopsis root-inhabiting bacterial microbiota. *Nature* 488, 91–95. doi:10.1038/nature11336.

Bulgarelli, D., Schlaeppi, K., Spaepen, S., Van Themaat, E. V. L., Schulze-Lefert, P. (2013). Structure and functions of the bacterial microbiota of plants. *Annu. Rev. Plant Biol.* 64, 807–838. doi:10.1146/annurev-arplant-050312-120106.

Busby, P. E., Soman, C., Wagner, M. R., Friesen, M. L., Kremer, J., Bennett, A., Morsy, M., Eisen, J. A., Leach, J. E., Dangl, J. L. (2017). Research priorities for harnessing plant microbiomes in sustainable agriculture. *PLoS Biol.* 15, 1–14. doi:10.1371/journal.pbio.2001793.

Busch, H., Hagedoorn, P.-L., Hanefeld, U. (2019). *Rhodococcus* as a versatile biocatalyst in organic synthesis. *Int. J. Mol. Sci.* 20, 4787. doi:10.3390/ijms20194787.

Busson, M., Chetty, J., Robin, M.-H., Aubertot, J.-N. (2019). Definition Biocontrol. *Dictionnaire d'Agroecologie*, https://dicoagroecologie.fr/en/encyclopedia/biocontrol/ (accessed September 7, 2021)

Caneschi, W. L. Felestrino, E. B., Fonseca, N. P., Villa, M. M., de C. Lemes, C. G., Cordeiro, I. F., de A. B. Assis, R., Sanchez, A. B., Vieira, I. T., Kamino, L. H. Y., do Carmo, F. F., Garcia, C. C. M., Moreira, L. M. (2018). Brazilian ironstone plant communities as reservoirs of culturable bacteria with diverse biotechnological potential. *Front. Microbiol.* 9:1638. doi: 10.3389/fmicb.2018.01638

Cao, J., Woodhall, M. R., Alvarez, J., Cartron, M. L., Andrews, S. C. (2007). EfeUOB (YcdNOB) is a tripartite, acid-induced and CpxAR-regulated, low-pH Fe2+ transporter that is cryptic in *Escherichia coli* K-12 but functional in *E. coli* O157:H7. *Mol. Microbiol.* 65, 857–875. doi:10.1111/j.1365-2958.2007.05802.x.

Carlström, C. I., Field, C. M., Bortfeld-Miller, M., Müller, B., Sunagawa, S., Vorholt, J. A. (2019). Synthetic microbiota reveal priority effects and keystone strains in the Arabidopsis phyllosphere. *Nat. Ecol. Evol.* 3(10), 1445–1454 doi: 10.1038/s41559-019-0994-z.

Carminati, A., Moradi, A. B., Vetterlein, D., Vontobel, P., Lehmann, E., Weller, U., Vogel, H.-J., Oswald, S. E. (2010). Dynamics of soil water content in the rhizosphere. *Plant Soil* 332, 163–176. doi:10.1007/s11104-010-0283-8.

Carr, A., Diener, C., Baliga, N. S., Gibbons, S. M. (2019). Use and abuse of correlation analyses in microbial ecology. *ISME J.* 13, 2647–2655. doi:10.1038/s41396-019-0459-z.

Carrano, C. J., Jordan, M., Drechsel, H., Schmid, D. G., Winkelmann, G. (2001). Heterobactins: A new class of siderophores from *Rhodococcus erythropolis* IGTS8 containing both hydroxamate and catecholate donor groups. *BioMetals* 14, 119–125. doi:10.1023/A:1016633529461.

Carrión, V. J., Perez-Jaramillo, J., Cordovez, V., Tracanna, V., De Hollander, M., Ruiz-Buck, D., et al. (2019). Pathogen-induced activation of disease-suppressive functions in the endophytic root microbiome. *Science* 366, 606–612. doi:10.1126/science.aaw9285.

Cary, A. J., Liu Wennuan, Howell, S. H. (1995). Cytokinin action is coupled to ethylene in its effects on the inhibition of root and hypocotyl elongation in *Arabidopsis thaliana* seedlings. *Plant Physiol.* 107, 1075–1082. doi:10.1104/pp.107.4.1075.

Cascales, E., Buchanan, S. K., Duché, D., Kleanthous, C., Lloubès, R., Postle, K., Riley, M., Slatin, S., Cavard, D. (2007). Colicin Biology. *Microbiol. Mol. Biol. Rev.* 71, 158–229. doi:10.1128/mmbr.00036-06.

Cassán, F., Coniglio, A., López, G., Molina, R., Nievas, S., de Carlan, C. L. N., Donadio, F., Torres, D., Rosas, S., Pedrosa, F. O., de Souza, E., Díaz Zorita, M., de Bashan, L., Mora, V. (2020). Everything you must know about *Azospirillum* and its impact on agriculture and beyond. *Biol. Fertil. Soils* 56, 461–479. doi:10.1007/s00374-020-01463-y.

Castrillo, G., Teixeira, P. J., Paredes, S. H., Law, T. F., de Lorenzo, L., Feltcher, M. E., Finkel, O. M., Breakfield, N. W., Mieczkowski, P., Jones, C. D., Paz-Ares, J., Dangl, J. L. (2017). Root microbiota drive direct integration of phosphate stress and immunity. *Nature* 543, 513–518. doi: 10.1038/nature21417

Ceniceros, A., Dijkhuizen, L., Petrusma, M. (2017). Molecular characterization of a *Rhodococcus jostii* RHA1 γ-butyrolactone(-like) signalling molecule and its main biosynthesis gene gblA. *Sci. Rep.* 7, 1–13. doi:10.1038/s41598-017-17853-6.

Cevher-Keskin, B., Yildizhan, Y., Kulen, O., Onarici, S. (2015). Quantitative expression analysis of TaMPK4 and TaTIP1 genes in drought tolerant and non-tolerant wheat (*Triticum aestivum* L.) cultivars. *Plant Omics* 8, 270–277.

Chakraborty, U., Chakraborty, B. N., Chakraborty, A. P., Dey, P. L. (2013). Water stress amelioration and plant growth promotion in wheat plants by osmotic stress tolerant bacteria. *World J. Microbiol. Biotechnol.* 29, 789–803. doi:10.1007/s11274-012-1234-8.

Chane, A., Barbey, C., Robert, M., Merieau, A., Konto-Ghiorghi, Y., Beury-Cirou, A., Feuilloley, M., Pátek, M., Gobert, V., Latour, X. (2019). Biocontrol of soft rot: Confocal microscopy highlights virulent pectobacterial communication and its jamming by rhodococcal quorum-quenching. *Mol. Plant-Microbe Interact.* 31, 802–812. doi:10.1094/MPMI-11-18-0314-R.

Chen, J., Bittinger, K., Charlson, E. S., Hoffmann, C., Lewis, J., Wu, G. D., Collman, R.G, Bushman, F. D., Li, H. (2012). Associating microbiome composition with environmental covariates using generalized UniFrac distances. *Bioinformatics*, 28(16), 2106-2113 doi: 10.1093/bioinformatics/bts342

Chen, L., Dodd, I. C., Theobald, J. C., Belimov, A. A., Davies, W. J. (2013). The rhizobacterium *Variovorax paradoxus* 5C-2, containing ACC deaminase, promotes growth and development of *Arabidopsis thaliana* via an ethylene-dependent pathway. *J. Exp. Bot.* 64, 1565–1573. doi:10.1093/jxb/ert031.

Chen, T., Nomura, K., Wang, X., Sohrabi, R., Xu, J., Yao, L., et al. (2020). A plant genetic network for preventing dysbiosis in the phyllosphere. *Nature* 580, 653–657. doi:10.1038/s41586-020-2185-0.

Chiba, H., Agematu, H., Sakai, K., Dobashi, K., Yoshioka, T. (1999). Rhodopeptins, novel cyclic tetrapeptides with antifungal activities from *Rhodococcus* sp.. III. Synthetic study of rhodopeptins. *J. Antibiot. (Tokyo).* 52, 710–720. doi:10.7164/antibiotics.52.710.

Chien, C. C., Han, C. T. (2009). Tellurite resistance and reduction by a *Paenibacillus* sp. isolated from heavy metal-contaminated sediment. *Environ. Toxicol. Chem.* 28, 1627–1632. doi:10.1897/08-521.1.

Chowdhury, S.P., Babin, D., Sandmann, M., Jacquiod, S., Sommermann, L., Sørensen, S. J., Fliessbach, A., Mäder, P., Geistlinger, J., Smalla, K., Rothballer, M., Grosch, R. (2019). Effect of long-term organic and mineral fertilization strategies on rhizosphere microbiota assemblage and performance of lettuce. *Environ. Microbiol.* 21, 2426–2439. doi:10.1111/1462-2920.14631.

Chowdhury, S. P., Hartmann, A., Gao, X. W., Borriss, R. (2015a). Biocontrol mechanism by root-associated *Bacillus amyloliquefaciens* FZB42 - A review. *Front. Microbiol.* 6, 1–11. doi:10.3389/fmicb.2015.00780.

Chowdhury, S. P., Uhl, J., Grosch, R., Alquéres, S., Pittroff, S., Dietel, K., Schmitt-Kopplin, P., Borriss, R., Hartmann, A. (2015b). Cyclic lipopeptides of *Bacillus amyloliquefaciens* subsp. *plantarum* colonizing the lettuce rhizosphere enhance plant defense responses toward the bottom rot pathogen *Rhizoctonia solani*. *Mol. Plant-Microbe Interact.* 28, 984–995. doi:10.1094/MPMI-03-15-0066-R.

Cirou, A., Diallo, S., Kurt, C., Latour, X., Faure, D. (2007). Growth promotion of quorum-quenching bacteria in the rhizosphere of *Solanum tuberosum*. *Environ. Microbiol.* 9, 1511–1522. doi:10.1111/j.1462-2920.2007.01270.x.

Compant, S., Samad, A., Faist, H., Sessitsch, A. (2019). A review on the plant microbiome: Ecology, functions, and emerging trends in microbial application. *J. Adv. Res.* 19, 29–37. doi:10.1016/j.jare.2019.03.004.

Connorton, J.M., Jones, E.R., Rodríguez-Ramiro, I., Fairweather-Tait, S., Uauy, C. Balk, J., (2017). Wheat vacuolar iron transporter TaVIT2 transports Fe and Mn and is effective for biofortification. *Plant Physiology*, 174(4), pp.2434-2444. doi: 10.1104/pp.17.00672.

Constant, P., Chowdhury, S. P., Hesse, L., Pratscher, J., Conrad, R. (2011). Genome data mining and soil survey for the novel group 5 [NiFe]-hydrogenase to explore the diversity and ecological importance of presumptive high-affinity H 2-oxidizing bacteria. *Appl. Environ. Microbiol.* 77, 6027–6035. doi:10.1128/AEM.00673-11.

Cotter, P. D., Hill, C. (2003). Surviving the Acid Test: Responses of Gram-Positive Bacteria to Low pH. *Microbiol. Mol. Biol. Rev.* 67, 429–453. doi:10.1128/mmbr.67.3.429-453.2003.

Cruz, M.F., Debona, D., Rios, J.A., Barros, E.G., Rodrigues, F.A., 2015. Potentiation of defense-related gene expression by silicon increases wheat resistance to leaf blast. *Tropical Plant Pathology*, 40(6), pp.394-400. doi:10.1007/s40858-015-0051-7

Dabrock, B., Kesseler, M., Averhoff, B., Gottschalk, G. (1994). Identification and characterization of a transmissible linear plasmid from *Rhodococcus erythropolis* BD2 that encodes isopropylbenzene and trichloroethene catabolism. *Appl. Environ. Microbiol.* 60, 853–860. doi:10.1128/aem.60.3.853-860.1994.

Daims, H., Bruhl, A., Amann, R. I., Schleifer, K.-H., Wagner, M. (1999). The domainspecific probe EUB-338 is insufficient for the detection of all bacteria: development and evaluation of a more comprehensive probe set. *Syst. Appl. Microbiol.* 22, 434–444. doi: 10.1016/s0723-2020(99)80053-8

Das, S., Tyagi, A., Kaur, H. (2000). Cancer modulation by glucosinolates: a review. *Current Science*, 79, 1665-1671.

De Carvalho, C. C. C. R., Marques, M. P. C., Hachicho, N., Heipieper, H. J. (2014). Rapid adaptation of *Rhodococcus erythropolis* cells to salt stress by synthesizing polyunsaturated fatty acids. *Appl. Microbiol. Biotechnol.* 98, 5599–5606. doi:10.1007/s00253-014-5549-2.

de Souza, R. S. C., Armanhi, J. S. L., Arruda, P. (2020). From microbiome to traits: Designing synthetic microbial communities for improved crop resiliency. *Front. Plant Sci.* 11, 1–7. doi:10.3389/fpls.2020.01179.

de Vries, F. T., Griffiths, R. I., Bailey, M., Craig, H., Girlanda, M., Gweon, H. S., et al. (2018). Soil bacterial networks are less stable under drought than fungal networks. *Nat. Commun.* 9, 3033. doi:10.1038/s41467-018-05516-7.

de Vries, F. T., Wallenstein, M. D. (2017). Below-ground connections underlying above-ground food production: a framework for optimising ecological connections in the rhizosphere. *J. Ecol.* 105, 913–920. doi:10.1111/1365-2745.12783.

De Vrieze, M., Germanier, F., Vuille, N., Weisskopf, L. (2018). Combining different potato-associated *Pseudomonas* strains for improved biocontrol of *Phytophthora infestans*. *Front. Microbiol.* 9, 1–13. doi:10.3389/fmicb.2018.02573.

de Vries FT, Griffiths RI, Knight CG, Nicolitch O, Williams A. (2020). Harnessing rhizosphere microbiomes for drought-resilient crop production. *Science*. 368(6488):270-274. doi:10.1126/science.aaz5192.

Dineen, S. M., Aranda, R., Anders, D. L., Robertson, J. M. (2010). An evaluation of commercial DNA extraction kits for the isolation of bacterial spore DNA from soil. *J. Appl. Microbiol.* 109, 1886–1896. doi:10.1111/j.1365-2672.2010.04816.x.

Driscoll, J. A., Brody, S. L., Kollef, M. H. (2007). The epidemiology, pathogenesis and treatment of *Pseudomonas aeruginosa* infections. *Drugs* 67(3):351-68. doi: 10.2165/00003495-200767030-00003.

Döbereiner, J. (1995). *Isolation and identification of aerobic nitrogen-fixing bacteria from soil and plants* in Methods in Applied Soil Microbiology and Biochemistry. eds K. Alef and P. Nannipieri (London: Academic Press), 134–141.

Dong, Y.-H., Wang, L.-H., Xu, J.-L., Zhang, H.-B., Zhang, X.-F., Zhang, L.-H. (2001). Quenching quorum-sensing-dependent bacterial infection by an *N*-acyl homoserine lactonase. *Nature* 411, 813–817. doi:10.1038/35081101

Dong, Y. H., Zhang, X. F., Xu, J. L., Zhang, L. H. (2004). Insecticidal *Bacillus thuringiensis* silences *Erwinia carotovora* virulence by a new form of microbial antagonism, signal interference. *Appl. Environ. Microbiol.* 70, 954–960. doi:10.1128/AEM.70.2.954-960.2004.

Dos Santos, P. C., Fang, Z., Mason, S. W., Setubal, J. C.,Dixon, R. (2012). Distribution of nitrogen fixation and nitrogenase-like sequences amongst microbial genomes. *BMC Genomics* 13, 1–12. doi:10.1186/1471-2164-13-162.

Dubois, M., Van den Broeck, L., Inzé, D. (2018). The pivotal role of ethylene in plant growth. *Trends Plant Sci.* 23, 311–323. doi:10.1016/j.tplants.2018.01.003.

Duran, P., Thiergart, T., Garrido-Oter, R., Agler, M., Kemen, E., Schulze-Lefert, P., Hacquard, S. (2018). Microbial interkingdom interactions in roots promote Arabidopsis survival. *Cell* 175, 354167. doi:10.1101/354167.

Durán, P., Tortella, G., Viscardi, S., Barra, P. J., Carrión, V. J., de la Luz Mora, M., Pozo, M. J. (2018). Microbial community composition in take-All suppressive soils. *Front. Microbiol.* 9, 1–15. doi:10.3389/fmicb.2018.02198.

Dutta, S., Yu, S. M., Lee, Y. H. (2020). Assessment of the contribution of antagonistic secondary metabolites to the antifungal and biocontrol activities of *Pseudomonas fluorescens* NBC275. *Plant Pathol. J.* 36, 491–496. doi:10.5423/PPJ.FT.08.2020.0149.

Dziewit, L., Pyzik, A., Matlakowska, R., Baj, J., Szuplewska, M., Bartosik, D. (2013). Characterization of *Halomonas* sp. ZM3 isolated from the Zelazny most post-flotation waste reservoir, with a special focus on its mobile DNA. *BMC Microbiol.* 13, 1. doi:10.1186/1471-2180-13-59.

Edgar, R. C. (2010). Search and clustering orders of magnitude faster than BLAST. *Bioinformatics* 26, 2460–2461. doi:10.1093/bioinformatics/btq461.

Edgar, R. C. (2013). UPARSE: Highly accurate OTU sequences from microbial amplicon reads. *Nat. Methods* 10, 996–998. doi:10.1038/nmeth.2604.

Egamberdieva, D., Wirth, S., Bellingrath-Kimura, S. D., Mishra, J., Arora, N. K. (2019). Salt-tolerant plant growth promoting rhizobacteria for enhancing crop productivity of saline soils. *Front. Microbiol.* 10, 1–18. doi:10.3389/fmicb.2019.02791.

Fahad, S., Hussain, S., Bano, A., Saud, S., Hassan, S., Shan, D., et al. (2015). Potential role of phytohormones and plant growth-promoting rhizobacteria in abiotic stresses: consequences for changing environment. *Environ. Sci. Pollut. Res.* 22, 4907–4921. doi:10.1007/s11356-014-3754-2.

Fernández, M., Porcel, M., de la Torre, J., Molina-Henares, M. A., Daddaoua, A., Llamas, M. A., et al. (2015). Analysis of the pathogenic potential of nosocomial *Pseudomonas putida* strains. *Front. Microbiol.* 6, 1–11. doi:10.3389/fmicb.2015.00871.

Figueroa-Bustos, V., Palta, J. A., Chen, Y., Stefanova, K., Siddique, K. H. M. (2020). Wheat cultivars with contrasting root system size responded differently to terminal drought. *Front. Plant Sci.* 11, 1–12. doi:10.3389/fpls.2020.01285.

Finkel, O. M., Castrillo, G., Herrera Paredes, S., Salas González, I., Dangl, J. L. (2017). Understanding and exploiting plant beneficial microbes. *Curr. Opin. Plant Biol.* 38, 155–163. doi:10.1016/j.pbi.2017.04.018.

Finkel, O. M., Salas-González, I., Castrillo, G., Conway, J. M., Law, T. F., Teixeira, P. J. P. L., Wilson, E. D., Fitzpatrick, C. R., Jones, C. D., Dangl, J. L. (2020). A single bacterial genus maintains root growth in a complex microbiome. *Nature* 587, 103–108. doi:10.1038/s41586-020-2778-7.

Flemming, H. C., Wingender, J., Szewzyk, U., Steinberg, P., Rice, S. A., Kjelleberg, S. (2016). Biofilms: An emergent form of bacterial life. *Nat. Rev. Microbiol.* 14, 563–575. doi:10.1038/nrmicro.2016.94.

Foley, J. A., DeFries, R., Asner, G. P., Barford, C., Bonan, G., Carpenter, S. R., et al. (2005). Global consequences of land use. *Science* 309(5734), 570–574. doi:10.1126/science.1111772.

Francis, I. M., Stes, E., Zhang, Y., Rangel, D., Audenaert, K., Vereecke, D. (2016). Mining the genome of *Rhodococcus fascians*, a plant growth-promoting bacterium gone astray. *N. Biotechnol.* 33, 706–717. doi:10.1016/j.nbt.2016.01.009.

Francis, I. M., Vereecke, D. (2019). "Plant-Associated Rhodococcus species, for better and for worse," in *Biology of Rhodococcus*, ed. H. Alvarez (Switzerland: Springer), 359–377. doi: 10.1007/978-3-030-11461-9_13

Freilich, M. A., Wieters, E., Broitman, B. R., Marquet, P. A., Navarrete, S. A. (2018). Species co-occurrence networks: can they reveal trophic and non-trophic interactions in ecological communities? *Ecology* 99, 690–699. doi.org/10.1002/ecy.2142

French, E., Kaplan, I., Iyer-Pascuzzi, A., Nakatsu, C. H., Enders, L. (2021). Emerging strategies for precision microbiome management in diverse agroecosystems. *Nat. Plants* 7, 256–267. doi:10.1038/s41477-020-00830-9.

Fuqua, W. C., Winans, S. C., Greenberg, E. P. (1994). Quorum sensing in bacteria: The LuxR-LuxI family of cell density- responsive transcriptional regulators. *J. Bacteriol.* 176, 269–275. doi:10.1128/jb.176.2.269-275.1994.

Gantner, Isabella (March 2021) Master's thesis: Characterization of the rhizobacterium *Pseudomonas* sp. and its plant growth-promoting and biocontrol effect on *Arabidopsis thaliana* and wheat. (conducted at INET Helmholtz Center Munich and LMU Munich)

Garrett, K. A., Alcalá-Briseño, R. I., Andersen, K. F., Buddenhagen, C. E., Choudhury, R. A., Fulton, J. C., Hernandez Nopsa, J. F., Poudel, R., Xing, Y. (2018). Network analysis: A systems framework to address grand challenges in plant pathology. *Annu. Rev. Phytopathol.* 56, 559–580. doi:10.1146/annurev-phyto-080516-035326.

Gérard, F., Pradel, N., and Wu, L. F. (2005). Bactericidal activity of colicin V is mediated by an inner membrane protein, SdaC, of *Escherichia coli*. *J. Bacteriol.* 187, 1945–1950. doi:10.1128/JB.187.6.1945-1950.2005.

Gerlach, W., Sauthoff, W., Pag, H. (1958). Untersuchungen über die Fusariumwelke an *Aechmea fasciata* (Lindl.). *Bakt.Phytopathol.Z.* 32, 416–432. doi: 10.1111/j.1439-0434.1958.tb01784.x

Ghequire, M. G. K., De Mot, R. (2014). Ribosomally encoded antibacterial proteins and peptides from *Pseudomonas*. *FEMS Microbiol. Rev.* 38, 523–568. doi:10.1111/1574-6976.12079.

Giguère, S., Berghaus, L. J., Willingham-Lane, J. M. (2017). Antimicrobial resistance in *Rhodococcus equi*. *Acta Biochim. Pol.* 61, 633–638. doi:10.18388/abp.2014_1824.

Glick, B. R. (2012). Plant growth-promoting bacteria: mechanisms and applications. *Scientifica* 2012:963401. doi: 10.6064/2012/963401

Glick, B. R. (2014). Bacteria with ACC deaminase can promote plant growth and help to feed the world. *Microbiol. Res.* 169, 30–39. doi:10.1016/j.micres.2013.09.009.

Glick, B. R., Karaturovic, D. M., Newell, P. C. (1995). A novel procedure for rapid isolation of plant growth promoting pseudomonads. *Can. J. Microbiol.* 41, 533–536. doi:10.1139/m95-070.

Glickmann, E., Dessaux, Y. (1995). A critical examination of the specificity of the Salkowski reagent for indolic compounds produced by phytopathogenic bacteria. *Appl. Environ. Microbiol.*, 61(2): 793–796 doi: https://doi.org/10.1128/aem.61.2.793-796.1995

Gomila, M., Peña, A., Mulet, M., Lalucat, J., García-Valdés, E. (2015). Phylogenomics and systematics in *Pseudomonas*. *Front. Microbiol.* 6, 1–13. doi:10.3389/fmicb.2015.00214.

Gond, S. K., Bergen, M. S., Torres, M. S., White, J. F. (2015). Endophytic *Bacillus* spp . produce antifungal lipopeptides and induce host defence gene expression in maize. *Microbiol. Res.* 172, 79–87. doi:10.1016/j.micres.2014.11.004.

Gontia-Mishra, I., Sapre, S., Sharma, A., Tiwari, S. (2016). Amelioration of drought tolerance in wheat by the interaction of plant growth-promoting rhizobacteria. *Plant Biol.* 18, 992–1000. doi:10.1111/plb.12505.

Gorbunova, T. I., Egorova, D. O., Pervova, M. G., Kyrianova, T. D., Demakov, V. A., Saloutin, V. I., Chupakhin, O. N. (2020). Biodegradation of trichlorobiphenyls and their hydroxylated derivatives by *Rhodococcus*-strains. *J. Hazard. Mater.*, 124471. doi:10.1016/j.jhazmat.2020.124471.

Gordon, S. A., Weber, R. P. (1951). Colorimetric estimation of indoleacetic acid. *Plant Physiol.* 26, 192–195. doi: 10.1104/pp.26.1.192

Goris, J., Konstantinidis, K. T., Klappenbach, J. A., Coenye, T., Vandamme, P., Tiedje, J. M. (2007). DNA-DNA hybridization values and their relationship to whole-genome sequence similarities. *Int. J. Syst. Evol. Microbiol.* 57, 81–91. doi:10.1099/ijs.0.64483-0.

Goswami, G., Deka, P., Das, P., Bora, S. S., Samanta, R., Boro, R. C., Barooah, M. (2017). Diversity and functional properties of acid-tolerant bacteria isolated from tea plantation soil of Assam. *3 Biotech* 7, 1–16. doi:10.1007/s13205-017-0864-9.

Goyal, R.K., Tulpan, D., Chomistek, N., Fundora, D.G.P., West, C., Ellis, B.E., Frick, M., Laroche, A., Foroud, N.A. (2018). Analysis of MAPK and MAPKK gene families in wheat and related *Triticeae* species. *BMC Genomics*, 19, 178. doi.org/10.1186/s12864-018-4545-9

Greening, C., Biswas, A., Carere, C. R., Jackson, C. J., Taylor, M. C., Stott, M. B., Cook, G. M., Morales, S. E. (2016). Genomic and metagenomic surveys of hydrogenase distribution indicate H_2 is a widely utilised energy source for microbial growth and survival. *ISME J.* 10, 761–777. doi:10.1038/ismej.2015.153.

Grossmann, G., Guo, W. J., Ehrhardt, D. W., Frommer, W. B., Sit, R. V., Quake, S. R., Meier, M. (2011). The Rootchip: An integrated microfluidic chip for plant Science. *Plant Cell* 23, 4234–4240. doi:10.1105/tpc.111.092577.

Gu, S., Wei, Z., Shao, Z., Friman, V. P., Cao, K., Yang, T., et al. (2020). Competition for iron drives phytopathogen control by natural rhizosphere microbiomes. *Nat. Microbiol.* 5, 1002–1010. doi:10.1038/s41564-020-0719-8.

Guglielmetti S, Basilico R, Taverniti V, Arioli S, Piagnani C, Bernacchi A. (2013). *Luteibacter rhizovicinus* MIMR1 promotes root development in barley (*Hordeum vulgare* L.) under laboratory conditions. *World J Microbiol Biotechnol*. 29(11):2025-32. doi: 10.1007/s11274-013-1365-6.

Guo, X., Zhang, X., Qin, Y., Liu, Y. X., Zhang, J., Zhang, N., et al. (2020). Host-associated quantitative abundance profiling reveals the microbial load variation of root microbiome. *Plant Commun.* 1, 1–17. doi:10.1016/j.xplc.2019.100003.

Gupta, N., Skinner, K.A., Summers, Z.M., Edirisinghe, J.N., Faria, J.P., Marshall, C.W., Sharma, A., Gottel, N.R., Gilbert, J.A., Henry, C.S., O'Loughlin, E.J. (2019). Draft genome sequence of *Rhodococcus* sp. strain ATCC 49988, a quinoline-degrading bacterium. *Microbiol Resour Announc* 8:e00403-19. doi.org/10.1128/MRA.00403-19.

Hall, A. B., Tolonen, A. C., Xavier, R. J. (2017). Human genetic variation and the gut microbiome in disease. *Nat. Rev. Genet.* 18, 690–699. doi:10.1038/nrg.2017.63.

Hall, J. P. J., Harrison, E., Pärnänen, K., Virta, M., Brockhurst, M. A. (2020). The Impact of mercury selection and conjugative genetic elements on community structure and resistance gene transfer. *Front. Microbiol.* 11, 1–14. doi:10.3389/fmicb.2020.01846.

Hamonts, K., Trivedi, P., Garg, A., Janitz, C., Grinyer, J., Holford, P., Botha, F. C., Anderson, I. C., Singh, B. K. (2018). Field study reveals core plant microbiota and relative importance of their drivers. *Environ. Microbiol.* 20, 124–140. doi:10.1111/1462-2920.14031.

Han, S., Li, D., Trost, E., Mayer, K. F., Corina, V., Heller, W., Schmid, M., Hartmann, A., Rothballer, M. (2016). Systemic responses of barley to the 3-hydroxy-decanoyl-homoserine lactone producing plant beneficial endophyte *Acidovorax radicis* N35. *Front. Plant Sci.* 7, 1–14. doi:10.3389/fpls.2016.01868.

Harb, A., Krishnan, A., Ambavaram, M. M. R., Pereira, A. (2010). Molecular and physiological analysis of drought stress in Arabidopsis reveals early responses leading to acclimation in plant growth. *Plant Physiol.* 154, 1254–1271. doi:10.1104/pp.110.161752.

Harada, S., Kishi, T., Mizuno, K. (1971) Studies on T-2636 antibiotics. II. Isolation and chemical proteries of T-2636 antibiotics. *J Antibiot* 24 (1) 13-22, doi.org/10.7164/antibiotics.24.13

Hartman, K., van der Heijden, M. G. A., Roussely-Provent, V., Walser, J. C., Schlaeppi, K. (2017). Deciphering composition and function of the root microbiome of a legume plant. *Microbiome* 5, 1–13. doi:10.1186/s40168-016-0220-z.

Hartmann, A., Fischer, D., Kinzel, L., Chowdhury, S. P., Hofmann, A., Baldani, J. I., Rothballer, M. (2019). Assessment of the structural and functional diversities of plant microbiota: Achievements and challenges – A review. *J. Adv. Res.* 19, 3–13. doi:10.1016/j.jare.2019.04.007.

Hartmann, A., Hurek, T. (1988). Effect of carotenoid overproduction on oxygen tolerance of nitrogen fixation in *Azospirillum brasilense* Sp7. *Microbiology* 134, 2449–2455. doi:10.1099/00221287-134-9-2449.

Hartmann, A., Klink, S., Rothballer, M. (2021). Plant growth promotion and induction of systemic tolerance to drought and salt stress of plants by quorum sensing auto-inducers of the *N*-acyl-homoserine lactone type: Recent developments. *Front. Plant Sci.* 12, 1–6. doi:10.3389/fpls.2021.683546.

Hartmann, A., Rothballer, M., Schmid, M. (2008). Lorenz Hiltner, a pioneer in rhizosphere microbial ecology and soil bacteriology research. *Plant Soil* 312, 7–14. doi:10.1007/s11104-007-9514-z.

Hartmann, A., Singh, M., Klingmüller, W. (1983). Isolation and characterization of *Azospirillum* mutants excreting high amounts of indoleacetic acid . *Can. J. Microbiol.* 29, 916–923. doi:10.1139/m83-147.

Hashim, H. O., Al-Shuhaib, M. B. S. (2019). Exploring the potential and limitations of PCR-RFLP and PCR-SSCP for SNP detection: A review. *J. Appl. Biotechnol. Reports* 6, 137–144. doi:10.29252/JABR.06.04.02.

Haskett, T. L., Tkacz, A., Poole, P. S. (2021). Engineering rhizobacteria for sustainable agriculture. *ISME J.* 15, 949–964. doi:10.1038/s41396-020-00835-4.

Hasuty, A., Choliq, A., Hidayat, I. (2018). Production of indole acetic acid (IAA) by *Serratia marcescens* subsp. *marcescens* and *Rhodococcus* aff. *qingshengii*. *Int. J. Agric. Technol.* 14, 299–312.

Hernandez, D. J., David, A. S., Menges, E. S., Searcy, C. A., Afkhami, M. E. (2021). Environmental stress destabilizes microbial networks. *ISME J.* 15, 1722–1734. doi:10.1038/s41396-020-00882-x.

Hernández, I., Sant, C., Martínez, R., Fernández, C. (2020). Design of bacterial strain-specific qPCR assays using NGS data and publicly available resources and its application to track biocontrol strains. *Front. Microbiol.* 11, 1–11. doi:10.3389/fmicb.2020.00208.

Herrera Paredes, S., Gao, T., Law, T. F., Finkel, O. M., Mucyn, T., Teixeira, P. J. P. L., et al. (2018). Design of synthetic bacterial communities for predictable plant phenotypes. *PLoS Biol* 16(2): e2003962. doi.org/10.1371/journal.pbio.2003962

Herrmann, L., Lesueur, D. (2013). Challenges of formulation and quality of biofertilizers for successful inoculation. *Appl. Microbiol. Biotechnol.* 97, 8859–8873. doi:10.1007/s00253-013-5228-8.

Higdon, S. M., Pozzo, T., Kong, N., Huang, B. C., Yang, M. L., Jeannotte, R., Brown, T., Bennett, A. B., Weimer, B. C. (2020). Genomic characterization of a diazotrophic microbiota associated with maize aerial root mucilage. *PLoS One* 15, 1–26. doi:10.1371/journal.pone.0239677.

Hiltner L (1904) Über neuere Erfahrungen und Probleme auf dem Gebiete der Bodenbakteriologie unter besonderer Berücksichtigung der Gründüngung und Brache. *Arb DLG* 98:59–78

Hirt, H. (2020). Healthy soils for healthy plants for healthy humans. *EMBO Rep.* 21, 1–5. doi:10.15252/embr.202051069

Hone, H., Mann, R., Yang, G., Kaur, J., Tannenbaum, I., Li, T., Spangenberg, G., Sawbridge, T. (2021). Profiling, isolation and characterisation of beneficial microbes from the seed microbiomes of drought tolerant wheat. *Sci. Rep.* 11, 1–12. doi:10.1038/s41598-021-91351-8.

Hong, C. E., Jeong, H., Jo, S. H., Jeong, J. C., Kwon, S. Y., An, D., Park, J. M. (2016). A leaf-inhabiting endophytic bacterium, *Rhodococcus* sp. KB6, enhances sweet potato resistance to black rot disease caused by *Ceratocystis fimbriata*. *J. Microbiol. Biotechnol.* 26, 488–492. doi:10.4014/jmb.1511.11039.

Hu, J., Wei, Z., Friman, V. P., Gu, S. H., Wang, X. F., Eisenhauer, N., et al. (2016). Probiotic diversity enhances rhizosphere microbiome function and plant disease suppression. *MBio* 7. doi:10.1128/mBio.01790-16.

Hunt, M., Silva, N. De, Otto, T. D., Parkhill, J., Keane, J. A., Harris, S. R. (2015). Circlator: Automated circularization of genome assemblies using long sequencing reads. *Genome Biol.* 16, 1–10. doi:10.1186/s13059-015-0849-0.

Hutchins, D. A., Jansson, J. K., Remais, J. V., Rich, V. I., Singh, B. K., Trivedi, P. (2019). Climate change microbiology - problems and perspectives. *Nat. Rev. Microbiol.* 17, 391–396. doi:10.1038/s41579-019-0178-5.

Imran, A., Hakim, S., Tariq, M., Nawaz, M. S., Laraib, I., Gulzar, U., et al. (2021). Diazotrophs for lowering nitrogen pollution crises: Looking deep into the roots. *Front. Microbiol.* 12. doi:10.3389/fmicb.2021.637815.

Irawati, W., Soraya, Y. P., Baskoro, A. H. (2012). A study on mercury-resistant bacteria isolated from a gold mine in Pongkor Village, Bogor, Indonesia. *Hayati J. Biosci.* 19, 197–200. doi: 10.4308/hjb.19.4.197

Ismail, M. A., Amin, M. A., Eid, A. M., Hassan, S. E. D., Mahgoub, H. A. M., Lashin, I., et al. (2021). Comparative study between exogenously applied plant growth hormones versus metabolites of microbial endophytes as plant growth-promoting for *Phaseolus vulgaris* L. *Cells* 10, 1–26. doi:10.3390/cells10051059.

Iwatsuki, M., Uchida, R., Takakusagi, Y., Matsumoto, A., Jiang, C. L., Takahashi, Y., et al. (2007). Lariatins, novel anti-mycobacterial peptides with a lasso structure, produced by *Rhodococcus jostii* K01-B0171. *J. Antibiot.* 60, 357–363. doi:10.1038/ja.2007.48.

Jaiswal, S. K., Mohammed, M., Ibny, F. Y. I., Dakora, F. D. (2021). Rhizobia as a source of plant growth-promoting molecules: Potential applications and possible operational mechanisms. *Front. Sustain. Food Syst.* 4, 1–14. doi:10.3389/fsufs.2020.619676.

Jayakumar, A., Krishna, A., Nair, I. C., Radhakrishnan, E. K. (2020). Drought-tolerant and plant growth-promoting endophytic *Staphylococcus* sp. having synergistic effect with silicate supplementation. *Arch. Microbiol.* 202, 1899–1906. doi:10.1007/s00203-020-01911-1.

Jensen, L. J., Julien, P., Kuhn, M., von Mering, C., Muller, J., Doerks, T., Bork, P. (2008). eggNOG: Automated construction and annotation of orthologous groups of genes. *Nucleic Acids Res.* 36, 250–254. doi:10.1093/nar/gkm796.

Jochum, M. D., Mcwilliams, K. L., Borrego, E. J., Kolomiets, M. V, Niu, G., Pierson, E. A., Jo, Y.-K. (2019a). Bioprospecting plant growth-promoting rhizobacteria that mitigate drought stress in grasses. 10, 1–9. doi:10.3389/fmicb.2019.02106.

Jochum, M. D., McWilliams, K. L., Pierson, E. A., Jo, Y. K. (2019b). Host-mediated microbiome engineering (HMME) of drought tolerance in the wheat rhizosphere. *PLoS One* 14, 1–15. doi:10.1371/journal.pone.0225933.

Johnsson, L., Hökeberg, M., Gerhardson, B. (1998). Performance of the *Pseudomonas chlororaphis* biocontrol agent MA 342 against cereal seed-borne diseases in field experiments. *Eur. J. Plant Pathol.* 104, 701–711. doi:10.1023/A:1008632102747.

Jones, F. P., Clark, I. M., King, R., Shaw, L. J., Woodward, M. J., Hirsch, P. R. (2016). Novel European free-living, non-diazotrophic *Bradyrhizobium* isolates from contrasting soils that lack nodulation and nitrogen fixation genes - A genome comparison. *Sci. Rep.* 6, 1–10. doi:10.1038/srep25858.

Joshi, D., Chandra, R., Suyal, D. C., Kumar, S., Goel, R. (2019). Impacts of bioinoculants *Pseudomonas jesenii* MP1 and *Rhodococcus qingshengii* S10107 on chickpea (Cicer arietinum L.) yield and soil nitrogen status. Pedosphere 29, 388–399. doi: 10.1016/S1002-0160(19)60807-6

Junia, M. C., Carine, R. C., Bruno, S. V., Iara, da M. F., Robson, L. C. (2016). Use of *Bacillus* spp. as growth promoter in carrot crop. *African J. Agric. Res.* 11, 3355–3359. doi:10.5897/ajar2016.11316.

Juretschko S, Timmermann G, Schmid M, Schleifer KH, Pommerening-Röser A, Koops HP, Wagner M (1998) Combined molecular and conventional analyses of nitrifying bacterium diversity in activated sludge: *Nitrosococcus mobilis* and *Nitrospira*-like bacteria as dominant populations. *Appl Environ Microbiol* 64:3042–3051

Kai, M., Haustein, M., Molina, F., Petri, A., Scholz, B., Piechulla, B. (2009). Bacterial volatiles and their action potential. *Appl. Microbiol. Biotechnol.* 81, 1001–1012. doi:10.1007/s00253-008-1760-3.

Kamble, A. L., Banoth, L., Meena, V. S., Singh, A., Chisti, Y., Banerjee, U. C. (2013). Nitrile hydratase of *Rhodococcus erythropolis*: characterization of the enzyme and the use of whole cells for biotransformation of nitriles. *3 Biotech* 3, 319–330. doi:10.1007/s13205-012-0104-2.

Kang, S. M., Radhakrishnan, R., Khan, A. L., Kim, M. J., Park, J. M., Kim, B. R., Shin, D.-H., Lee, I.-J. (2014). Gibberellin secreting rhizobacterium, *Pseudomonas putida* H-2-3 modulates the hormonal and stress physiology of soybean to improve the plant growth under saline and drought conditions. *Plant Physiol. Biochem.* 84, 115–124. doi:10.1016/j.plaphy.2014.09.001.

Kanno, M., Constant, P., Tamaki, H., Kamagata, Y. (2016). Detection and isolation of plant-associated bacteria scavenging atmospheric molecular hydrogen. *Environ. Microbiol.* 18, 2495–2506. doi:10.1111/1462-2920.13162.

Kaufmann, M., and Michel, B. (1973). The osmotic potential of polyethylene glycol 6000. *Plant Physiol*. 51, 914–916. doi: 10.1104/pp.51.5.914

Kaul, S., Choudhary, M., Gupta, S., Dhar, M. K. (2021). Engineering host microbiome for crop improvement and sustainable agriculture. *Front. Microbiol.* 12, 1–10. doi:10.3389/fmicb.2021.635917.

Kaushal, M., Wani, S. P. (2016). Rhizobacterial-plant interactions: Strategies ensuring plant growth promotion under drought and salinity stress. *Agric. Ecosyst. Environ.* 231, 68–78. doi:10.1016/j.agee.2016.06.031.

Kavamura, V. N., Mendes, R., Bargaz, A., Mauchline, T. H. (2021). Defining the wheat microbiome: towards microbiome-facilitated crop production. *Comput. Struct. Biotechnol. J.* 19, 1200–1213. doi:10.1016/j.csbj.2021.01.045.

Kavamura, V. N., Robinson, R. J., Hughes, D., Clark, I., Rossmann, M., de Melo, I. S., Hirsch, P. R., Mendes, R., Mauchline, T. H. (2020). Wheat dwarfing influences selection of the rhizosphere microbiome. *Sci. Rep.* 10, 1–11. doi:10.1038/s41598-020-58402-y.

Kavamura, V. N., Santos, S. N., Silva, J. L. da, Parma, M. M., Ávila, L. A., Visconti, A., et al. (2013). Screening of Brazilian cacti rhizobacteria for plant growth promotion under drought. *Microbiol. Res.* 168, 183–191. doi:10.1016/j.micres.2012.12.002.

Khilyas, I. V., Sorokina, A. V., Markelova, M. I., Belenikin, M., Shafigullina, L., Tukhbatova, R. I., et al. (2020). Genomic and phenotypic analysis of siderophore-producing *Rhodococcus qingshengii* strain S10 isolated from an arid weathered serpentine rock environment. *Arch. Microbiol.*, 1–6. doi:10.1007/s00203-020-02057-w.

King, G. M., Weber, C. F. (2007). Distribution, diversity and ecology of aerobic CO-oxidizing bacteria. *Nat. Rev. Microbiol.* 5, 107–118. doi:10.1038/nrmicro1595.

Kirchhof, G., Eckert, B., Stoffels, M., Ivo Baldani, J., Reis, V. M., Hartmann, A. (2001). *Herbaspirillum frisingense* sp. nov., a new nitrogan-fixing bacterial species that occurs in C4-fibre plants. *Int. J. Syst. Evol. Microbiol.* 51, 157–168. doi:10.1099/00207713-51-1-157.

Kloepper, J., Schroth, M. . (1978). Plant growth-promoting rhizobacteria on radishes. *4th Int. Conf. Plant Pathog. Bact. Angers, Fr.* 2, 879–882.

Kloepper, J. W., Beauchamp, C. J. (1992). A review of issues related to measuring colonization of plant roots by bacteria. *Can. J. Microbiol.* 38, 1219–1232. doi:10.1139/m92-202.

Knights, H. E., Jorrin, B., Haskett, T. L., Poole, P. S. (2021). Deciphering bacterial mechanisms of root colonization. *Environ. Microbiol. Rep.* 13, 428–444. doi:10.1111/1758-2229.12934.

Kong, H. G., Song, G. C., Sim, H. J., Ryu, C. M. (2021). Achieving similar root microbiota composition in neighbouring plants through airborne signalling. *ISME J.* 15, 397–408. doi:10.1038/s41396-020-00759-z.

Kong, W., Meldgin, D. R., Collins, J. J., Lu, T. (2018). Designing microbial consortia with defined social interactions. *Nat. Chem. Biol.* 14, 821–829. doi:10.1038/s41589-018-0091-7.

Konstantinidis, K. T., Tiedje, J. M. (2005). Towards a genome-based taxonomy for prokaryotes. *J. Bacteriol.* 187, 6258–6264. doi:10.1128/JB.187.18.6258-6264.2005.

Kuhl, T., Chowdhury, S. P., Uhl, J., Rothballer, M. (2021). Genome-based characterization of plant-associated *Rhodococcus qingshengii* RL1 reveals stress tolerance and plant–microbe interaction traits. *Front. Microbiol.* 12, 1–22. doi:10.3389/fmicb.2021.708605.

Kuhl, T., Felder, M., Nussbaumer, T., Fischer, D., Kublik, S., Paul Chowdhury, S., Schloter, M., Rothballer, M. (2019). *De novo* genome assembly of a plant-associated *Rhodococcus qingshengii* strain (RL1) isolated from *Eruca sativa* Mill. and showing plant growth-promoting properties. *Microbiol. Resour. Announc.* 8, 14–16. doi:10.1128/MRA.01106-19.

Kumar, A., Patel, J. S., Meena, V. S., Srivastava, R. (2019). Recent advances of PGPR based approaches for stress tolerance in plants for sustainable agriculture. *Biocatal. Agric. Biotechnol.* 20, 101271. doi:10.1016/j.bcab.2019.101271.

Kumar, G.P., Mir Hassan Ahmed, S. K., Desai, S., Leo Daniel Amalraj, E., and Rasul, A. (2014). *In vitro* screening for abiotic stress tolerance in potent biocontrol and plant growth promoting strains of *Pseudomonas* and *Bacillus* spp. *Int. J. Bacteriol.* 2014, 1–6. doi:10.1155/2014/195946.

Kumar, S., Stecher, G., Li, M., Knyaz, C., Tamura, K. (2018). MEGA X: Molecular evolutionary genetics analysis across computing platforms. *Mol. Biol. Evol.* 35, 1547–1549. doi:10.1093/molbev/msy096.

Kumar, S., Suyal, D. C., Bhoriyal, M., Goel, R. (2018) Plant growth promoting potential of psychrotolerant *Dyadobacter* sp. for pulses and finger millet and impact of inoculation on soil chemical properties and diazotrophic abundance, *J. Plant Nutr.*, 41:8, 1035-1046, DOI: 10.1080/01904167.2018.1433211

Kwasiborski, A., Mondy, S., Beury-Cirou, A., Faure, D. (2014). Genome sequence of the quorum-quenching *Rhodococcus erythropolis* strain R138. *Genome Announc*. 2(2):e00224-14. doi:10.1128/genomeA.00224-14.

Kwasiborski, A., Mondy, S., Chong, T. M., Barbey, C., Chan, K. G., Beury-Cirou, A., Latour, X., Faure, D. (2015). Transcriptome of the quorum-sensing signal-degrading *Rhodococcus erythropolis* responds differentially to virulent and avirulent *Pectobacterium atrosepticum*. *Heredity (Edinb).* 114, 476–484. doi:10.1038/hdy.2014.121.

Lagkouvardos, I., Joseph, D., Kapfhammer, M., Giritli, S., Horn, M., Haller, D., Clavel, T. (2016). IMNGS: A comprehensive open resource of processed 16S rRNA microbial profiles for ecology and diversity studies. *Sci. Rep.* 6, 1–9. doi:10.1038/srep33721.

Lalucat, J., Mulet, M., Gomila, M., García-Valdés, E. (2020). Genomics in bacterial taxonomy: Impact on the genus pseudomonas. *Genes* 11(2):139. doi:10.3390/genes11020139.

Lane, D.J. (1991) 16S/23S rRNA Sequencing. In: Stackebrandt, E. and Goodfellow, M., Eds., *Nucleic Acid Techniques in Bacterial Systematic*, John Wiley and Sons, New York, 115-175.

Latour, X., Barbey, C., Chane, A., Groboillot, A., Burini, J.-F. (2013). *Rhodococcus erythropolis* and Its γ-Lactone catabolic pathway: An unusual biocontrol system that disrupts pathogen quorum sensing communication. *Agronomy* 3, 816–838. doi:10.3390/agronomy3040816.

Lau, C. K. Y., Krewulak, K. D., Vogel, H. J. (2016). Bacterial ferrous iron transport: The Feo system. *FEMS Microbiol. Rev.* 40, 273–298. doi:10.1093/femsre/fuv049.

Lebeis, S. L., Paredes, S. H., Lundberg, D. S., Breakfield, N., Gehring, J., McDonald, M., et al. (2015). Salicylic acid modulates colonization of the root microbiome by specific bacterial taxa. *Science,* 349, 860–864. doi:10.1126/science.aaa8764.

LeBlanc, J. C., Gonçalves, E. R., Mohn, W. W. (2008). Global response to desiccation stress in the soil actinomycete *Rhodococcus jostii* RHA1. *Appl. Environ. Microbiol.* 74, 2627–2636. doi:10.1128/AEM.02711-07.

Leigh, M. B., Prouzová, P., Macková, M., Macek, T., Nagle, D. P., Fletcher, J. S. (2006). Polychlorinated biphenyl (PCB)-degrading bacteria associated with trees in a PCB-contaminated site. *Appl. Environ. Microbiol.* 72, 2331–2342. doi:10.1128/AEM.72.4.2331-2342.2006.

Levy, A., Salas Gonzalez, I., Mittelviefhaus, M., Clingenpeel, S., Herrera Paredes, S., Miao, J., et al. (2018). Genomic features of bacterial adaptation to plants. *Nat. Genet.* 50, 138–150. doi:10.1038/s41588-017-0012-9.

Li, D., Rothballer, M., Schmid, M., Esperschütz, J., Hartmann, A. (2011). *Acidovorax radicis* sp. nov., a wheat-root-colonizing bacterium. *Int. J. Syst. Evol. Microbiol.* 61, 2589–2594. doi:10.1099/ijs.0.025296-0.

Li, Q., Li, L., Liu, Y., Lv, Q., Zhang, H., Zhu, J., Li, X. (2017). Influence of TaGW2-6A on seed development in wheat by negatively regulating gibberellin synthesis. *Plant Sci.* 263, 226–235. doi:10.1016/j.plantsci.2017.07.019.

Lincoln, S. A., Hamilton, T. L., Valladares Juárez, A. G., Schedler, M., Macalady, J. L., Müller, R., Freeman, K. H. (2015). Draft genome sequence of the piezotolerant and crude oil-degrading bacterium *Rhodococcus qingshengii* strain TUHH-12. *Genome Announc.* 3, e00268-15. doi:10.1128/genomeA.00268-15.

Liu, C.-H., Siew, W., Hung, Y.-T., Jiang, Y.-T., Huang, C.-H. (2021) 1-Aminocyclopropane-1-carboxylate (ACC) deaminase gene in *Pseudomonas azotoformans* is associated with the amelioration of salinity stress in tomato *J. Agric. Food Chem*. 69 (3), 913-921 doi: 10.1021/acs.jafc.0c05628

Liu, H., Brettell, L. E., Qiu, Z., Singh, B. K. (2020). Microbiome-mediated stress resistance in plants. *Trends Plant Sci.* 25, 733–743. doi:10.1016/j.tplants.2020.03.014.

Liu, W., Wang, Q., Hou, J., Tu, C., Luo, Y., Christie, P. (2016). Whole genome analysis of halotolerant and alkalotolerant plant growth-promoting rhizobacterium *Klebsiella* sp. D5A. *Sci. Rep.* 6, 20–22. doi:10.1038/srep26710.

Livak, K. J., Schmittgen, T. D. (2001). Analysis of relative gene expression data using real-time quantitative PCR and the 2-ΔΔCT method. *Methods* 25, 402–408. doi:10.1006/meth.2001.1262.

Loper, J. E., Schroth, M. N. (1986). Influence of bacterial sources of indole-3-acetic acid on root elongation of sugar beet. *Phytopathology* 76:386. doi:10.1094/phyto-76-386

Lozano, G. L., Bravo, J. I., Handelsman, J. (2017). Draft Genome Sequence of *Pseudomonas koreensis* CI12, a *Bacillus cereus* "Hitchhiker" from the Soybean Rhizosphere. *Genome Announc*. 29;5(26):e00570-17. doi: 10.1128/genomeA.00570-17.

Lundberg, D. S., Lebeis, S. L., Paredes, S. H., Yourstone, S., Gehring, J., Malfatti, S., et al. (2012). Defining the core *Arabidopsis thaliana* root microbiome. *Nature* 488, 86–90. doi:10.1038/nature11237.

Luo, Y., Wang, F., Huang, Y., Zhou, M., Gao, J., Yan, T., Sheng, H., An, L. (2019). *Sphingomonas* sp. Cra20 increases plant growth rate and alters rhizosphere microbial community structure of *Arabidopsis thaliana* under drought stress. *Front. Microbiol.* 10. doi:10.3389/fmicb.2019.01221.

Lynne, A. M., Haarmann, D., Louden, B. C. (2011). Use of blue agar CAS assay for siderophore detection. *J. Microbiol. Biol. Educ.* 12, 51–53. doi:10.1128/jmbe.v12i1.249.

Ma, Y. (2019). Editorial: Biotechnological potential of plant-microbe interactions in environmental decontamination. *Front. Plant Sci.* 10, 1–4. doi:10.3389/fpls.2019.01519.

Ma, Y., Oliveira, R. S., Freitas, H., Zhang, C. (2016a). Biochemical and molecular mechanisms of plant-microbe-metal interactions: Relevance for phytoremediation. *Front. Plant Sci.* 7, 1–19. doi:10.3389/fpls.2016.00918.

Ma, Y., Rajkumar, M., Zhang, C., Freitas, H. (2016b). Beneficial role of bacterial endophytes in heavy metal phytoremediation. *J. Environ. Manage.* 174, 14–25. doi:10.1016/j.jenvman.2016.02.047.

Madden T.L. (2002) The BLAST sequence analysis tool. In McEntyre, J. (ed.), *The NCBI Handbook* [Internet]. National Library of Medicine (US), National Center for Biotechnology Information, Bethesda, MD

Mahmoudi, T. R., Yu, J. M., Liu, S., Pierson, L. S., Pierson, E. A. (2019). Drought-stress tolerance in wheat seedlings conferred by phenazine-producing rhizobacteria. *Front. Microbiol.* 10, 1–14. doi:10.3389/fmicb.2019.01590.

Majeed, A., Kaleem Abbasi, M., Hameed, S., Imran, A., Rahim, N. (2015). Isolation and characterization of plant growth-promoting rhizobacteria from wheat rhizosphere and their effect on plant growth promotion. *Front. Microbiol.* 6, 1–10. doi:10.3389/fmicb.2015.00198.

Maldonado, S., Rodríguez, A., Ávila, B., Morales, P., González, M. P., Araya Angel, J. P. A., et al. (2020). Enhanced crop productivity and sustainability by using native phosphate solubilizing rhizobacteria in the agriculture of arid zones. *Front. Sustain. Food Syst.* 4, 1–14. doi:10.3389/fsufs.2020.607355.

Manker, D., presented for Bayer, Biologics (2020). The fascinating journey from discovery to product. Available online at: https://phytobiomesalliance.org/wp-content/uploads/2020/09/2020-09-24_Phytobiomes_webinar_Manker.pdf (accessed September 7, 2021)

Marín, O., González, B., Poupin, M. J. (2021). From microbial dynamics to functionality in the rhizosphere: A systematic review of the opportunities with synthetic microbial communities. *Front. Plant Sci.* 12, 1–12. doi:10.3389/fpls.2021.650609.

Martínez-García, P. M., López-Solanilla, E., Ramos, C., Rodríguez-Palenzuela, P. (2016). Prediction of bacterial associations with plants using a supervised machine-learning approach. *Environ. Microbiol.* 18, 4847–4861. doi:10.1111/1462-2920.13389.

Martiny, A. C. (2019). High proportions of bacteria are culturable across major biomes. *ISME* 13, 2125–2128. doi.org/10.1038/s41396-019-0410-3

Masmoudi, F., Tounsi, S., Dunlap, C. A., Trigui, M. (2021). Halotolerant *Bacillus spizizenii* FMH45 promoting growth, physiological, and antioxidant parameters of tomato plants exposed to salt stress. *Plant Cell Rep.* 40, 1199–1213. doi:10.1007/s00299-021-02702-8.

Mathur, S., Sutton, J. (2017). Personalized medicine could transform healthcare (Review). *Biomed. Reports* 7, 3–5. doi:10.3892/br.2017.922.

Mavrodi, D.V., Blankenfeldt, W., Thomashow, L.S. (2006). Phenazine compounds in fluorescent *Pseudomonas* spp. biosynthesis and regulation. *Annual Review of Phytopathology* 44:1, 417-445, doi.org/10.1146/annurev.phyto.44.013106.145710

Mayak, S., Tirosh, T., Glick, B.R. (2004) Plant growth-promoting bacteria confer resistance in tomato plants to salt stress. *Plant Physiol. Biochem*. 42, 565–572. doi.org/10.1016/j.plaphy.2004.05.009.

McNear Jr., D. H. (2013) The Rhizosphere - Roots, soil and everything in between. *Nature Education Knowledge* 4(3):1 www.nature.com/scitable/knowledge/library/the-rhizosphere-roots-soil-and-67500617/ (accessed 07.09.2021)

Meena, V. S., Mishra, P. K., Bisht, J. K., Pattanayak, A. (2017) Agriculturally important microbes for sustainable agriculture. Vol 2. Applications in crop production and protection. *Springer Nature Singapore* Pte Ltd, Singapore, 3–24 doi.org/10.1007/978-981-10-5343-6_1

Meier-Kolthoff, J. P., Göker, M. (2019). TYGS is an automated high-throughput platform for state-of-the-art genome-based taxonomy. *Nat. Commun.* 10. doi:10.1038/s41467-019-10210-3.

Mendes, L. W., Raaijmakers, J. M., De Hollander, M., Mendes, R., Tsai, S. M. (2018). Influence of resistance breeding in common bean on rhizosphere microbiome composition and function. *ISME J.* 12, 212–224. doi:10.1038/ismej.2017.158.

Mendes, R., Garbeva, P., Raaijmakers, J. M. (2013). The rhizosphere microbiome: Significance of plant beneficial, plant pathogenic, and human pathogenic microorganisms. *FEMS Microbiol. Rev.* 37, 634–663. doi:10.1111/1574-6976.12028.

Mendes, R., Raaijmakers, J. M. (2015). Cross-kingdom similarities in microbiome functions. *ISME J.* 9, 1905–1907. doi:10.1038/ismej.2015.7.

Mitter, B., Pfaffenbichler, N., Flavell, R., Compant, S., Antonielli, L., Petric, A., et al. (2017). A new approach to modify plant microbiomes and traits by introducing beneficial bacteria at flowering into progeny seeds. *Front. Microbiol.* 8, 1–10. doi:10.3389/fmicb.2017.00011.

Moccia, K., Willems, A., Papoulis, S., Flores, A., Forister, M. L., Fordyce, J. A., Lebeis, S. L. (2020). Distinguishing nutrient-dependent plant driven bacterial colonization patterns in alfalfa. *Environ. Microbiol. Rep.* 12, 70–77. doi:10.1111/1758-2229.12815.

Mohanty, P., Singh, P. K., Chakraborty, D., Mishra, S., Pattnaik, R. (2021). Insight into the role of PGPR in sustainable agriculture and environment. *Front. Sustain. Food Syst.* 5, 1–12. doi:10.3389/fsufs.2021.667150.

Mokhtari, R.B, Baluch, N., Homayouni, T. S., Morgatskaya, E., Kumar, S., Kazemi, P., Yeger, H. (2018). The role of Sulforaphane in cancer chemoprevention and health benefits: a mini-review. *J. Cell Commun. Signal.* 12, 91–101. doi:10.1007/s12079-017-0401-y.

Molina-Romero, D., Baez, A., Quintero-Hernández, V., Castañeda-Lucio, M., Fuentes-Ramírez, L. E., del RRocio Bustillos-Cristales, M., et al. (2017). Compatible bacterial mixture, tolerant to desiccation, improves maize plant growth. *PLoS One* 12, 1–21. doi:10.1371/journal.pone.0187913.

Moriya, Y., Itoh, M., Okuda, S., Yoshizawa, A. C., Kanehisa, M. (2007). KAAS: An automatic genome annotation and pathway reconstruction server. *Nucleic Acids Res.* 35, 182–185. doi:10.1093/nar/gkm321.

Mullaney, J. A., Ansell, J., Kelly, W. J., and Heyes, J. A. (2013a). Biotransformation of glucosinolates from a bacterial perspective. *CAB Rev*. 8, 1–15. doi: 10.1079/PAVSNNR20138034

Mullaney, J. A., Kelly, W. J., McGhie, T. K., Ansell, J., and Heyes, J. A. (2013b). Lactic acid bacteria convert glucosinolates to nitriles efficiently yet differently from enterobacteriaceae. *J. Agric. Food Chem.* 61, 3039–3046. doi:10.1021/jf305442j.

Müller, C., Birmes, F. S., Niewerth, H., Fetzner, S. (2014). Conversion of the *Pseudomonas aeruginosa* quinolone signal and related alkylhydroxyquinolines by *Rhodococcus* sp. strain BG43. *Appl. Environ. Microbiol.* 80, 7266–7274. doi:10.1128/AEM.02342-14.

Munna, M. S., Tahera, J., Mohibul Hassan Afrad, M., Nur, I. T., Noor, R. (2015). Survival of *Bacillus* spp. SUBB01 at high temperatures and a preliminary assessment of its ability to protect heat-stressed *Escherichia coli* cells. *BMC Res Notes* 8, 637 doi.org/10.1186/s13104-015-1631-9

Murugappan, R. M., Benazir, S., Usha, C., Lok, S. (2017). Growth promoting and probiotic potential of the endophytic bacterium *Rhodococcus globerulus* colonizing the medicinal plant *Plectranthus amboinicus* (Lour.) Spreng. *Int. J. Curr. Res. Rev.* 9, 7–13. doi:10.7324/ijcrr.2017.9143.

Nabti, E., Bensidhoum, L., Tabli, N., Dahel, D., Weiss, A., Rothballer, M., Schmid, M., Hartmann, A.(2014). Growth stimulation of barley and biocontrol effect on plant pathogenic fungi by a *Cellulosimicrobium* sp. strain isolated from salt-affected rhizosphere soil in northwestern Algeria. *Eur. J. Soil Biol.* 61, 20–26. doi:10.1016/j.ejsobi.2013.12.008.

Nabti, E., Sahnoune, M., Ghoul, M., Fischer, D., Hofmann, A., Rothballer, M., Schmid, M., Hartmann, A. (2010). Restoration of growth of durum wheat (*Triticum durum* var. *waha*) under saline conditions due to inoculation with the rhizosphere bacterium *Azospirillum brasilense* NH and extracts of the marine alga *Ulva lactuca*. *J. Plant Growth Regul.* 29, 6–22. doi:10.1007/s00344-009-9107-6.

Nagel, R., Bieber, J. E., Schmidt-Dannert, M. G., Nett, R. S., Peters, R. J. (2018). A third class: Functional gibberellin biosynthetic operon in beta-proteobacteria. *Front. Microbiol.* 9, 1–8. doi:10.3389/fmicb.2018.02916.

Nagel, R., Peters, R. J. (2017). Investigating the phylogenetic range of gibberellin biosynthesis in bacteria. *Mol. Plant-Microbe Interact.* 30, 343–349. doi:10.1094/MPMI-01-17-0001-R.

Nascimento, F. X., Hernández, A. G., Glick, B. R., Rossi, M. J. (2020). Plant growth-promoting activities and genomic analysis of the stress-resistant *Bacillus megaterium* STB1, a bacterium of agricultural and biotechnological interest. *Biotechnol. Reports* 25, 1–9. doi:10.1016/j.btre.2019.e00406.

Nautiyal, C. S. (1999). An efficient microbiological growth medium for screening phosphate solubilizing microorganisms. *FEMS Microbiol. Lett.* 170, 265–270. doi:10.1111/j.1574-6968.1999.tb13383.x.

Netzker, T., Shepherdson, E. M. F., Zambri, M. P., Elliot, M. A. (2020). Bacterial volatile compounds: Functions in communication, cooperation, and competition. *Annu. Rev. Microbiol.* 74, 409–430. doi:10.1146/annurev-micro-011320-015542.

Niu, B., Paulson, J. N., Zheng, X., Kolter, R. (2017). Simplified and representative bacterial community of maize roots. *Proc. Natl. Acad. Sci. U. S. A.* 114, E2450–E2459. doi:10.1073/pnas.1616148114.

Novinscak, A., Filion, M. (2020). Long term comparison of talc- and peat-based phytobeneficial *Pseudomonas fluorescens* and *Pseudomonas synxantha* bioformulations for promoting plant growth. *Front. Sustain. Food Syst.* 4, 1–10. doi:10.3389/fsufs.2020.602911.

Oger, P., Dessaux, Y., Petit, A., Gardan, L., Manceau, C., Chomel, C., Nesme, X. (1998). Validity, sensitivity and resolution limit of the PCR-RFLP analysis of the rrs (16S rRNA gene) as a tool to identify soil-borne and plant- associated bacterial populations. *Genet. Sel. Evol.* 30. doi:10.1051/gse:19980719.

Okazaki, K., Tsurumaru, H., Hashimoto, M., Takahashi, H., Okubo, T., Ohwada, T., Minamisawa, K., Ikeda, S. (2021). Community analysis-based screening of plant growth-promoting bacteria for sugar beet. *Microbes Environ.* 36, 1–11. doi:10.1264/jsme2.ME20137.

Omoboye, O. O., Oni, F. E., Batool, H., Yimer, H. Z., De Mot, R., Höfte, M. (2019). *Pseudomonas* cyclic lipopeptides suppress the rice blast fungus *Magnaporthe oryzae* by induced resistance and direct antagonism. *Front. Plant Sci.* 10, 1–17. doi:10.3389/fpls.2019.00901.

Osorio, H., Martínez, V., Nieto, P. A., Holmes, D. S., Quatrini, R. (2008). Microbial iron management mechanisms in extremely acidic environments: Comparative genomics evidence for diversity and versatility. *BMC Microbiol.* 8, 1–18. doi:10.1186/1471-2180-8-203.

O'Toole, G.A. (2011) Microtiter dish biofilm formation assay. *J Vis Exp*. 30;(47):2437. doi: 10.3791/2437.

Overbeek, R., Olson, R., Pusch, G. D., Olsen, G. J., Davis, J. J., Disz, T., et al. (2014). The SEED and the Rapid Annotation of microbial genomes using Subsystems Technology (RAST). *Nucleic Acids Res.* 42, 206–214. doi:10.1093/nar/gkt1226.

Pandit, A., Adholeya, A., Cahill, D., Brau, L., Kochar, M. (2020). Microbial biofilms in nature: Unlocking their potential for agricultural applications. *J. Appl. Microbiol.* 129, 199–211. doi:10.1111/jam.14609.

Panke-Buisse, K., Lee, S., Kao-Kniffin, J. (2017). Cultivated sub-populations of soil microbiomes retain early flowering plant trait. *Microb. Ecol.* 73, 394–403. doi:10.1007/s00248-016-0846-1.

Panke-Buisse, K., Poole, A. C., Goodrich, J. K., Ley, R. E., Kao-Kniffin, J. (2015). Selection on soil microbiomes reveals reproducible impacts on plant function. *ISME J.* 9, 980–989. doi:10.1038/ismej.2014.196.

Parada, A. E., Needham, D. M., Fuhrman, J. A. (2016). Every base matters: assessing small subunit rRNA primers for marine microbiomes with mock communities, time series and global field samples. *Environmental Microbiology*, 18(5), 1403–1414. http://doi.org/10.1111/1462-2920.13023

Park, Y.S., Dutta, S., Ann, M., Raaijmakers, J.M., Park, K. (2015). Promotion of plant growth by *Pseudomonas fluorescens* strain SS101 via novel volatile organic compounds. *Biochem Biophys Res Commun*. 461(2):361-5. doi: 10.1016/j.bbrc.2015.04.039.

Parte, A.C., Carbasse, J.S., Meier-Kolthoff, J.P., Reimer, L.C., Göker, M. (2020) List of prokaryotic names with standing in nomenclature. *Int. J. Syst. Evol. Microbiol*. 2020;70:5607–5612 DOI 10.1099/ijsem.0.004332

Pascale, A., Proietti, S., Pantelides, I. S., Stringlis, I. A. (2020). Modulation of the root microbiome by plant molecules: the basis for targeted disease suppression and plant growth promotion. *Front. Plant Sci.* 10, 1–23. doi:10.3389/fpls.2019.01741.

Passera, A., Compant, S., Casati, P., Maturo, M. G., Battelli, G., Quaglino, F., et al. (2019). Not just a pathogen? Description of a plant-beneficial *Pseudomonas syringae* strain. *Front. Microbiol.* 10. doi:10.3389/fmicb.2019.01409.

Pátek, M., Grulich, M., Nešvera, J. (2021). Stress response in *Rhodococcus* strains. *Biotechnol Adv.* 28:107698. doi: 10.1016/j.biotechadv.2021.107698

Paul, K., Nieto, V., Carlquist, W. C., Blair, D. F., Harshey, R. M. (2010). The c-di-GMP binding protein YcgR controls flagellar motor direction and speed to affect chemotaxis by a "backstop brake" mechanism. *Mol. Cell* 38, 128–139. doi:10.1016/j.molcel.2010.03.001.

Peralta, A. L., Sun, Y., McDaniel, M. D., Lennon, J. T. (2018). Crop rotational diversity increases disease suppressive capacity of soil microbiomes. *Ecosphere* 9. doi:10.1002/ecs2.2235.

Pérez-Miranda, S., Cabirol, N., George-Téllez, R., Zamudio-Rivera, L. S., Fernández, F. J. (2007). O-CAS, a fast and universal method for siderophore detection. *J. Microbiol. Methods* 70, 127–131. doi:10.1016/j.mimet.2007.03.023.

Pérez, J. M., Calderón, I. L., Arenas, F. A., Fuentes, D. E., Pradenas, G. A., Fuentes, E. L., et al. (2007). Bacterial toxicity of potassium tellurite: Unveiling an ancient enigma. *PLoS One* 2. doi:10.1371/journal.pone.0000211.

Pertot, I., Giovannini, O., Benanchi, M., Caffi, T., Rossi, V., Mugnai, L. (2017). Combining biocontrol agents with different mechanisms of action in a strategy to control *Botrytis cinerea* on grapevine. *Crop Prot.* 97, 85–93. doi:10.1016/j.cropro.2017.01.010.

Peschel, S., Müller, C. L., von Mutius, E., Boulesteix, A. L., Depner, M. (2021). NetCoMi: network construction and comparison for microbiome data in R. *Brief. Bioinform.* 22, 1–18. doi:10.1093/bib/bbaa290.

Pham, T. T. M., Rodriguez, N. J. P., Hijri, M., Sylvestre, M. (2015). Optimizing polychlorinated biphenyl degradation by flavonoid-induced cells of the rhizobacterium *Rhodococcus erythropolis* U23A. *PLoS One* 10, 1–17. doi:10.1371/journal.pone.0126033.

Philippot, L., Raaijmakers, J. M., Lemanceau, P., Van Der Putten, W. H. (2013). Going back to the roots: The microbial ecology of the rhizosphere. *Nat. Rev. Microbiol.* 11, 789–799. doi:10.1038/nrmicro3109.

Pieterse, C. M. J., Berendsen, R. L., de Jonge, R., Stringlis, I. A., Van Dijken, A. J. H., Van Pelt, J. A., Van Wees, S. C. M., Zamioudis, C., Bakker, P. A. H. M. (2020). *Pseudomonas simiae* WCS417: star track of a model beneficial rhizobacterium. *Plant Soil*. doi:10.1007/s11104-020-04786-9.

Pieterse, C.M.J., Van Pelt, J.A., Ton, J., Parchmann, S., Mueller, M.J., Buchala, A.J., Métraux, J.-P., Van Loon, L.C. (2000) Rhizobacteria-mediated induced systemic resistance (ISR) in Arabidopsis requires sensitivity to jasmonate and ethylene but is not accompanied by an increase in their production. *Physiol Mol Plant Pathol* 57:123–134 https://doi.org/10.1006/pmpp.2000.0291

Pieterse, C.M.J., Van Wees, S.C.M., Hoffland, E., Van Pelt, J.A., Van Loon, L.C. (1996) Systemic resistance in Arabidopsis induced by biocontrol bacteria is independent of salicylic acid accumulation and pathogenesis-related gene expression. *Plant Cell* 8:1225–1237 doi: 10.1105/tpc.8.8.1225

Pieterse, C. M. J., Zamioudis, C., Berendsen, R. L., Weller, D. M., Van Wees, S. C. M., Bakker, P. A. H. M. (2014). Induced systemic resistance by beneficial microbes. *Annu. Rev. Phytopathol.* 52, 347–375. doi:10.1146/annurev-phyto-082712-102340.

Płociniczak, T., Fic, E., Pacwa-Płociniczak, M., Pawlik, M., Piotrowska-Seget, Z. (2017). Improvement of phytoremediation of an aged petroleum hydrocarbon-contaminated soil by *Rhodococcus erythropolis* CD 106 strain. *Int. J. Phytoremediation* 19, 614–620. doi: 10.1080/15226514.2016.1278420

Pollak, S., Cordero, O. X. (2020). Rhizobiome shields plants from infection. *Nat. Microbiol.* 5, 978–979. doi:10.1038/s41564-020-0766-1.

Poly, F., Ranjard, L., Nazaret, S., Gourbière, F., Jocteur Monrozier, L. (2001). Comparison of *nifH* gene pools in soils and soil microenvironments with contrasting properties. *Appl. Environ. Microbiol.* 67, 2255–2262. doi:10.1128/AEM.67.5.2255-2262.2001.

Poudel, R., Jumpponen, A., Schlatter, D.C., Paulitz, T.C., Gardener, B.B., Kinkel, L.L., Garrett, K.A. (2016). Microbiome networks: A systems framework for identifying candidate microbial assemblages for disease management. *Phytopathology*. 106(10):1083-1096. doi: 10.1094/PHYTO-02-16-0058-FI.

Quiza, L., Lalonde, I., Guertin, C., Constant, P. (2014). Land-use influences the distribution and activity of high affinity CO-oxidizing bacteria associated to type I-*coxL* genotype in soil. *Front. Microbiol.* 5, 1–15. doi:10.3389/fmicb.2014.00271.

Raaijmakers, J. M., Paulitz, T. C., Steinberg, C., Alabouvette, C., Moënne-Loccoz, Y. (2009). The rhizosphere: A playground and battlefield for soilborne pathogens and beneficial microorganisms. *Plant Soil* 321, 341–361. doi:10.1007/s11104-008-9568-6.

Ramírez-Bahena, M. H., Cuesta, M. J., Flores-Félix, J. D., Mulas, R., Rivas, R., Castro-Pinto, J., Brañas, J., Mulas, D., González-Andrés, F., Velázquez, E., Peix, Á. (2014). *Pseudomonas helmanticensis* sp. nov., isolated from forest soil. *Int. J. Syst. Evol. Microbiol.* 64, 2338–2345. doi:10.1099/ijs.0.063560-0.

Rascovan, N., Carbonetto, B., Perrig, D., Díaz, M., Canciani, W., Abalo, M., et al. (2016). Integrated analysis of root microbiomes of soybean and wheat from agricultural fields. *Sci. Rep.* 6, 1–12. doi:10.1038/srep28084.

Rashid, U., Yasmin, H., Hassan, M. N., Naz, R., Nosheen, A., Sajjad, M., et al. (2021). Drought-tolerant *Bacillus megaterium* isolated from semi-arid conditions induces systemic tolerance of wheat under drought conditions. *Plant Cell Rep.* doi:10.1007/s00299-020-02640-x.

Rathi, M.S., Paul, S., Thakur, J.K. (2014). Response of wheat to inoculation with mycorrhizae alone and combined with selected rhizobacteria inccluding *Flavobacterium* sp. as a potential bioinoculant. *J. Plant Nutr.*, 37:1, 76-86, DOI: 10.1080/01904167.2013.848889

Raza, W., Ling, N., Liu, D., Wei, Z., Huang, Q., Shen, Q. (2016). Volatile organic compounds produced by *Pseudomonas fluorescens* WR-1 restrict the growth and virulence traits of *Ralstonia solanacearum*. *Microbiol. Res.* 192, 103–113. doi:10.1016/j.micres.2016.05.014.

Reid, T. E., Kavamura, V. N., Abadie, M., Torres-Ballesteros, A., Pawlett, M., Clark, I. M., Harris, J., Mauchline, T. H. (2021). Inorganic chemical fertilizer application to wheat reduces the abundance of putative plant growth-promoting rhizobacteria. *Front. Microbiol.* 12, 1–16. doi:10.3389/fmicb.2021.642587.

Reinhold-Hurek, B., Bünger, W., Burbano, C.S., Sabale, M., Hurek, T. (2015). Roots shaping their microbiome: Global hotspots for microbial activity. *Annu Rev Phytopathol*. 53:403-24. doi: 10.1146/annurev-phyto-082712-102342.

Rieusset, L., Rey, M., Muller, D., Vacheron, J., Gerin, F., Dubost, A., Comte, G., Prigent-Combaret, C. (2020). Secondary metabolites from plant-associated *Pseudomonas* are overproduced in biofilm. *Microb. Biotechnol.* 13, 1562–1580. doi:10.1111/1751-7915.13598.

Rodríguez, H., Fraga, R., Gonzalez, T., Bashan, Y. (2006). Genetics of phosphate solubilization and its potential applications for improving plant growth-promoting bacteria. *Plant Soil* 287, 15–21. doi:10.1007/s11104-006-9056-9.

Rodriguez, H., Gonzalez, T., Goire, I., Bashan, Y. (2004). Gluconic acid production and phosphate solubilization by the plant growth-promoting bacterium *Azospirillum* spp. *Naturwissenschaften* 91, 552–555. doi:10.1007/s00114-004-0566-0.

Rodríguez, M., Torres, M., Blanco, L., Béjar, V., Sampedro, I., Llamas, I. (2020). Plant growth-promoting activity and quorum quenching-mediated biocontrol of bacterial phytopathogens by *Pseudomonas segetis* strain P6. *Sci. Rep.* 10, 1–12. doi:10.1038/s41598-020-61084-1.

Rodriguez, P. A., Rothballer, M., Chowdhury, S. P., Nussbaumer, T., Gutjahr, C., Falter-Braun, P. (2019). Systems biology of plant-microbiome interactions. *Mol. Plant* 12, 804–821. doi:10.1016/j.molp.2019.05.006.

Roller, C., Wagner, M., Amann, R., Ludwig, W., Schleifer, K. (1994). *In situ* probing of Gram-positive bacteria with high DNA G + C content using 23s rRNAtargeted oligonucleotides. *Microbiology* 140, 2849–2858.

Romano, I., Ventorino, V., Pepe, O. (2020). Effectiveness of plant beneficial microbes: Overview of the methodological approaches for the assessment of root colonization and persistence. *Front. Plant Sci.* 11, 1–16. doi:10.3389/fpls.2020.00006.

Rothballer, M., Eckert, B., Schmid, M., Fekete, A., Schloter, M., Lehner, A., Pollmann, S., Hartmann, A. (2008). Endophytic root colonization of gramineous plants by *Herbaspirillum frisingense*. *FEMS Microbiol. Ecol.* 66, 85–95. doi:10.1111/j.1574-6941.2008.00582.x.

Rucká, L., Volkova, O., Pavlík, A., Kaplan, O., Kracík, M., Nešvera, J., Martínková, L., Pátek, M. (2014). Expression control of nitrile hydratase and amidase genes in *Rhodococcus erythropolis* and substrate specificities of the enzymes. *Antonie van Leeuwenhoek, Int. J. Gen. Mol. Microbiol.* 105, 1179–1190. doi:10.1007/s10482-014-0179-3.

Rückert, C., Birmes, F. S., Müller, C., Niewerth, H., Winkler, A., Fetzner, S., Kalinowski, J. (2015). Complete genome sequence of *Rhodococcus erythropolis* BG43 (DSM 46869), a degrader of *Pseudomonas aeruginosa* quorum sensing signal molecules. *J. Biotechnol.* 211, 99–100. doi:10.1016/j.jbiotec.2015.07.014.

Rungin, S., Indananda, C., Suttiviriya, P., Kruasuwan, W., Jaemsaeng, R., Thamchaipenet, A. (2012). Plant growth enhancing effects by a siderophore-producing endophytic streptomycete isolated from a Thai jasmine rice plant (*Oryza sativa* L. cv. KDML105). *Antonie van Leeuwenhoek, Int. J. Gen. Mol. Microbiol.* 102, 463–472. doi:10.1007/s10482-012-9778-z.

Saad, M. M., Eida, A. A., Hirt, H., Doerner, P. (2020). Tailoring plant-associated microbial inoculants in agriculture: A roadmap for successful application. *J. Exp. Bot.* 71, 3878–3901. doi:10.1093/jxb/eraa111.

Sacristán-Pérez-Minayo, G., López-Robles, D. J., Rad, C., Miranda-Barroso, L. (2020). Microbial inoculation for productivity improvements and potential biological control in sugar beet crops. *Front. Plant Sci.* 11, 1–10. doi:10.3389/fpls.2020.604898.

Salas-González, I., Reyt, G., Flis, P., Custódio, V., Gopaulchan, D., Bakhoum, N., Dew, T.P., Suresh, K., Franke, R.B., Dangl, J.L., Salt, D.E., Castrillo, G. (2021). Coordination between microbiota and root endodermis supports plant mineral nutrient homeostasis. *Science* 8;371(6525):eabd0695. doi: 10.1126/science.abd0695.

Salazar-Cerezo, S., Martínez-Montiel, N., García-Sánchez, J., Pérez-y-Terrón, R., Martínez-Contreras, R. D. (2018). Gibberellin biosynthesis and metabolism: A convergent route for plants, fungi and bacteria. *Microbiol. Res.* 208, 85–98. doi:10.1016/j.micres.2018.01.010.

Sangal, V., Goodfellow, M., Jones, A. L., Schwalbe, E. C., Blom, J., Hoskisson, P. A., Sutcliffe, I. C. (2016). Next-generation systematics: An innovative approach to resolve the structure of complex prokaryotic taxa. *Sci. Rep.* 6, 1–12. doi:10.1038/srep38392.

Santhanam, R., Menezes, R. C., Grabe, V., Li, D., Baldwin, I. T., Groten, K. (2019). A suite of complementary biocontrol traits allows a native consortium of root-associated bacteria to protect their host plant from a fungal sudden-wilt disease. *Mol. Ecol.* 28, 1154–1169. doi:10.1111/mec.15012.

Santos-Medellín, C., Edwards, J., Liechty, Z., Nguyen, B., Sundaresan, V. (2017). Drought stress results in a compartment-specific restructuring of the rice root-associated microbiomes. *mBio*;8(4):e00764-17. doi: 10.1128/mBio.00764-17.

Santos, A., Núñez-Montero, K., Lamilla, C., Pavez, M., Quezada-Solís, D., Barrientos, L. (2020). Antifungal activity screening of antarctic actinobacteria against phytopathogenic fungi. *Acta Biol. Colomb.* 25, 353–358. doi:10.15446/abc.v25n2.76405.

Santos, C. L., Correia-Neves, M., Moradas-Ferreira, P., Mendes, M. V. (2012). A walk into the LuxR regulators of actinobacteria: Phylogenomic distribution and functional diversity. *PLoS One* 7. doi:10.1371/journal.pone.0046758.

Santos, M. S., Nogueira, M. A., Hungria, M. (2019). Microbial inoculants: Reviewing the past, discussing the present and previewing an outstanding future for the use of beneficial bacteria in agriculture. *AMB Express* 9. doi:10.1186/s13568-019-0932-0.

Santoyo, G., Guzmán-Guzmán, P., Parra-Cota, F. I., de los Santos-Villalobos, S., Orozco-Mosqueda, M. del C., Glick, B. R. (2021). Plant growth stimulation by microbial consortia. *Agronomy* 11, 219. doi:10.3390/agronomy11020219.

Savary, S., Willocquet, L., Pethybridge, S. J., Esker, P., McRoberts, N., Nelson, A. (2019). The global burden of pathogens and pests on major food crops. *Nat. Ecol. Evol.* 3, 430–439. doi:10.1038/s41559-018-0793-y.

Scagliola, M., Valentinuzzi, F., Mimmo, T., Cesco, S., Crecchio, C., Pii, Y. (2021). Bioinoculants as promising complement of chemical fertilizers for a more sustainable agricultural practice. *Front. Sustain. Food Syst.* 4, 1–12. doi:10.3389/fsufs.2020.622169.

Schaefer, J. K., Yagi, J., Reinfelder, J. R., Cardona, T., Ellickson, K. M., Tel-Or, S., Barkay, T. (2004). Role of the bacterial organomercury lyase (MerB) in controlling methylmercury accumulation in mercury-contaminated natural waters. *Environ. Sci. Technol.* 38, 4304–4311. doi:10.1021/es049895w.

Schlaeppi, K., Bulgarelli, D. (2015). The plant microbiome at work. *Mol. Plant-Microbe Interact.* 28, 212–217. doi:10.1094/MPMI-10-14-0334-FI.

Schloss, P. D. Handelsman, J. (2005). Introducing DOTUR, a computer program for defining operational taxonomic units and estimating species richness. *Applied and environmental microbiology* 71, 1501–1506, doi: 10.1128/AEM.71.3.1501-1506.2005

Schmalenberger, A., Hodge, S., Bryant, A., Hawkesford, M.J., Singh, B.K. Kertesz, M.A. (2008), The role of *Variovorax* and other *Comamonadaceae* in sulfur transformations by microbial wheat rhizosphere communities exposed to different sulfur fertilization regimes. *Environmental Microbiology*, 10: 1486-1500. https://doi.org/10.1111/j.1462-2920.2007.01564.x

Schmerk, C. L., Bernards, M. A., Valvano, M. A. (2011). Hopanoid production is required for low-pH tolerance, antimicrobial resistance, and motility in *Burkholderia cenocepacia*. *J. Bacteriol.* 193, 6712–6723. doi:10.1128/JB.05979-11.

Schneider, L. (2021). When toxic chemicals refuse to die - An examination of the prolonged mercury pesticide use in Australia. *Elementa* 9, 1–18. doi:10.1525/elementa.2021.053.

Sessitsch, A., Kuffner, M., Kidd, P., Vangronsveld, J., Wenzel, W. W., Fallmann, K., Puschenreiter, M. (2013). The role of plant-associated bacteria in the mobilization and phytoextraction of trace elements in contaminated soils. *Soil Biol. Biochem.* 60, 182–194. doi:10.1016/j.soilbio.2013.01.012.

Shiferaw, B., Smale, M., Braun, H. J., Duveiller, E., Reynolds, M., Muricho, G. (2013). Crops that feed the world 10. Past successes and future challenges to the role played by wheat in global food security. *Food Secur.* 5, 291–317. doi:10.1007/s12571-013-0263-y.

Siddiqui, M. N., León, J., Naz, A. A., Ballvora, A. (2021). Genetics and genomics of root system variation in adaptation to drought stress in cereal crops. *J. Exp. Bot.* 72, 1007–1019. doi:10.1093/jxb/eraa487.

Simon, J. C., Marchesi, J. R., Mougel, C., Selosse, M. A. (2019). Host-microbiota interactions: From holobiont theory to analysis. *Microbiome* 7, 1–5. doi:10.1186/s40168-019-0619-4.

Singh, M., Kumar, J., Singh, S., Singh, V.P., Prasad, S.M. (2015). Roles of osmoprotectants in improving salinity and drought tolerance in plants: A review. *Rev. Environ. Sci. Biotechnol*. 14, 407–426 https://doi.org/10.1007/s11157-015-9372-8

Singh, D. P., Prabha, R., Gupta, V. K., Verma, M. K. (2018). Metatranscriptome analysis deciphers multifunctional genes and enzymes linked with the degradation of aromatic compounds and pesticides in the wheat rhizosphere. *Front. Microbiol.* 9, 1–15. doi:10.3389/fmicb.2018.01331.

Smith, P., House, J. I., Bustamante, M., Sobocká, J., Harper, R., Pan, G., et al. (2016). Global change pressures on soils from land use and management. *Glob. Chang. Biol.* 22, 1008–1028. doi:10.1111/gcb.13068.

Soltani, A.-A., Khavazi, K., Asadi-Rahmani, H., Omidavri, M., Dahaji, P. A., Mirhoseyni, H. (2010). Plant growth promoting characteristics in some *Flavobacterium* spp. isolated from soils of Iran. *J. Agric. Sci.* 2, 106–115. doi:10.5539/jas.v2n4p106

Sommermann, L., Geistlinger, J., Wibberg, D., Deubel, A., Zwanzig, J., Babin, D., Schlüter, A., Schellenberg, I. (2018). Fungal community profiles in agricultural soils of a long-term field trial under different tillage, fertilization and crop rotation conditions analyzed by high-throughput ITS-amplicon sequencing. *PLoS One*. 5;13(4):e0195345. doi: 10.1371/journal.pone.0195345.

Song, F., Han, X., Zhu, X., Herbert, S.J. (2012). Response to water stress of soil enzymes and root exudates from drought and non-drought tolerant corn hybrids at different growth stages. *Can J Soil Sci* 92:501–507. https://doi.org/10.4141/cjss2010-057.

Song, Y., Yin, H. Huang, W. E. (2016). Raman activated cell sorting. *Curr. Opin. Chem. Biol*. 33, 1–8 doi: 10.1016/j.cbpa.2016.04.002

Spaepen, S., Vanderleyden, J. (2011). Auxin and Plant-Microbe Interactions. *Cold Spring Harb Perspect Biol*. 1;3(4):a001438. doi: 10.1101/cshperspect.a001438

Spaepen, S., Vanderleyden, J., Remans, R. (2007). Indole-3-acetic acid in microbial and microorganism-plant signaling. *FEMS Microbiol. Rev.* 31, 425–448. doi:10.1111/j.1574-6976.2007.00072.x.

Steindler, L., Bertani, I., De Sordi, L., Schwager, S., Eberl, L., Venturi, V. (2009). LasI/R and RhlI/R quorum sensing in a strain of *Pseudomonas aeruginosa* beneficial to plants. *Appl. Environ. Microbiol.* 75, 5131–5140. doi:10.1128/AEM.02914-08.

Stevens, V., Thijs, S., McAmmond, B., Langill, T., Van Hamme, J., Weyens, N., Vangronsveld, J. (2017). Draft genome sequence of *Rhodococcus erythropolis* VSD3, a diesel fueldegrading and plant growth-promoting bacterium isolated from *Hedera helix* leaves. *Genome Announc.* 5, 12–13. doi:10.1128/genomeA.01680-16.

Stickler, D. J., Morris, N. S., Mclean, R. J. C., Fuqua, C. (1998). Biofilms on indwelling urethral catheters produce quorum sensing signal molecules *in situ* and *in vitro*. *Appl. Environ. Microbiol.* 64, 3486–3490. doi:10.1128/aem.64.9.3486-3490.1998.

Stringlis, I. A., Proietti, S., Hickman, R., Van Verk, M. C., Zamioudis, C., Pieterse, C. M. J. (2018). Root transcriptional dynamics induced by beneficial rhizobacteria and microbial immune elicitors reveal signatures of adaptation to mutualists. *Plant J.* 93, 166–180. doi:10.1111/tpj.13741.

Subramoni, S., Venturi, V. (2009). LuxR-family "solos": Bachelor sensors/regulators of signalling molecules. *Microbiology* 155, 1377–1385. doi:10.1099/mic.0.026849-0.

Sugiura, R., Tsuda,S., Tamiya, S., Itoh, A., Nishiwaki, K., Murakami, N., Shibuya, Y., Hirafuji, M., Nuske, S. (2016). Field phenotyping system for the assessment of potato late blight resistance using RGB imagery from an unmanned aerial vehicle. *Biosyst. Eng*. 148, 1–10 dx.doi.org/10.1016/j.biosystemseng.2016.04.010

Sun, S.L., Yang, W.L., Fang, W.W., Zhao, Y.X., Guo, L., Dai, Y.J. (2018). The plant growth-promoting rhizobacterium *Variovorax boronicumulans* CGMCC 4969 regulates the level of indole-3-acetic acid synthesized from indole-3-acetonitrile. *Appl Environ Microbiol*. 1;84(16):e00298-18. doi: 10.1128/AEM.00298-18.

Suyal, D. C., Yadav, A., Shouche, Y., Goel, R. (2014). Differential proteomics in response to low temperature diazotrophy of Himalayan psychrophilic nitrogen fixing *Pseudomonas migulae* S10724 strain. *Curr. Microbiol.* 68, 543–550. doi:10.1007/s00284-013-0508-1.

Tagele, S. B., Lee, H. G., Kim, S. W., Lee, Y. S. (2019). Phenazine and 1-undecene producing *Pseudomonas chlororaphis* subsp. *aurantiaca* strain KNU17Pc1 for growth promotion and disease suppression in Korean maize cultivars. *J. Microbiol. Biotechnol.* 29, 66–78. doi:10.4014/jmb.1808.08026.

Tan, I. S., Ramamurthi, K. S. (2014). Spore formation in *Bacillus subtilis*. *Environ. Microbiol. Rep.* 23, 1–7. doi:10.1111/1758-2229.12130.Spore.

Táncsics, A., Benedek, T., Farkas, M., Máthé, I., Márialigeti, K., Szoboszlay, S., Kukolya, J., Kriszt, B. (2014). Sequence analysis of 16S rRNA, gyrB and catA genes and DNA-DNA hybridization reveal that *Rhodococcus jialingiae* is a later synonym of *Rhodococcus qingshengii*. *Int. J. Syst. Evol. Microbiol.* 64, 298–301. doi:10.1099/ijs.0.059097-0.

Tatusov, R. L., Galperin, M. Y., Natale, D. A., Koonin, E. V. (2000). The COG database: A tool for genome-scale analysis of protein functions and evolution. *Nucleic Acids Res.* 28, 33–36. doi:10.1093/nar/28.1.33.

Textor, S., Gershenzon, J. (2009). Herbivore induction of the glucosinolate-myrosinase defense system: Major trends, biochemical bases and ecological significance. *Phytochem. Rev.* 8, 149–170. doi:10.1007/s11101-008-9117-1.

Thomas, F., Hehemann, J. H., Rebuffet, E., Czjzek, M., Michel, G. (2011). Environmental and gut Bacteroidetes: The food connection. *Front. Microbiol.* 2, 1–16. doi:10.3389/fmicb.2011.00093.

Thomloudi, E. E., Tsalgatidou, P. C., Douka, D., Spantidos, T. N., Dimou, M., Venieraki, A., Katinakis,P. (2019). Multistrain versus single-strain plant growth promoting microbial inoculants-The compatibility issue. *Hell. Plant Prot. J.* 12, 61–77. doi:10.2478/hppj-2019-0007.

Thompson, D., Cognat, V., Goodfellow, M., Koechler, S., Heintz, D., Carapito, C., Van Dorsselaer, A., Mahmoud, H., Sangal, V., Ismail, W. (2020). Phylogenomic classification and biosynthetic potential of the fossil fuel-biodesulfurizing *Rhodococcus* strain IGTS8. Frontiers in microbiology, 11, 1417. https://doi.org/10.3389/fmicb.2020.01417

Thompson, L. R., Sanders, J. G., McDonald, D., Amir, A., Ladau, J., Locey, K. J., et al. (2017). A communal catalogue reveals Earth's multiscale microbial diversity. *Nature* 551, 457–463. doi:10.1038/nature24621.

Tilman, D., Cassman, K. G., Matson, P. A., Naylor, R., Polasky, S. (2002). Agricultural sustainability and intensive production practices. *Nature* 418, 671–677. doi:10.1038/nature01014.

Timmermann, T., Armijo, G., Donoso, R., Seguel, A., Holuigue, L., González, B. (2017). *Paraburkholderia phytofirmans* PsJN protects *Arabidopsis thaliana* against a virulent strain of *Pseudomonas syringae* through the activation of induced resistance. *Mol. Plant-Microbe Interact.* 30, 215–230. doi:10.1094/MPMI-09-16-0192-R.

Tiwari, G., Duraivadivel, P., Sharma, S., Hariprasad, P. (2018). 1-Aminocyclopropane-1-carboxylic acid deaminase producing beneficial rhizobacteria ameliorate the biomass characters of *Panicum maximum* Jacq. by mitigating drought and salt stress. *Sci. Rep.* 8, 1–12. doi:10.1038/s41598-018-35565-3.

Toju, H., Abe, M. S., Ishii, C., Hori, Y., Fujita, H., Fukuda, S. (2020). Scoring species for synthetic community design: Network analyses of functional core microbiomes. *Front. Microbiol.* 11, 1–17. doi:10.3389/fmicb.2020.01361.

Toju, H., Peay, K. G., Yamamichi, M., Narisawa, K., Hiruma, K., Naito, K., Fukuda, S., Ushio, M., Nakaoka, S., Onoda, Y., Yoshida, K., Schlaeppi, K., Bai, Y., Sugiura, R., Ichihashi, Y., Minamisawa, K., Kiers, E.T. (2018). Core microbiomes for sustainable agroecosystems. *Nat. Plants* 4, 247–257. doi:10.1038/s41477-018-0139-4.

Torkamani, A., Andersen, K. G., Steinhubl, S. R., Topol, E. J. (2017). High-Definition Medicine. *Cell* 170, 828–843. doi:10.1016/j.cell.2017.08.007.

Torres-Cortés, G., Garcia, B. J., Compant, S., Rezki, S., Jones, P., Préveaux, A., Briand, M., Roulet, A., Bouchez, O., Jacobson, D., Barret, M. (2019). Differences in resource use lead to coexistence of seed-transmitted microbial populations. *Sci. Rep.* 9, 1–13. doi:10.1038/s41598-019-42865-9.

Trivedi, P., Delgado-Baquerizo, M., Trivedi, C., Hamonts, K., Anderson, I.C,, Singh, B.K. (2017). Keystone microbial taxa regulate the invasion of a fungal pathogen in agro-ecosystems. *Soil Biology and Biochemistry*, 111, 10-14, doi.org/10.1016/j.soilbio.2017.03.013.

Trivedi, P., Leach, J. E., Tringe, S. G., Sa, T., and Singh, B. K. (2020). Plant–microbiome interactions: from community assembly to plant health. *Nat. Rev. Microbiol.* 18, 607–621. doi:10.1038/s41579-020-0412-1.

Trivedi, P., Pandey, A., Sa, T. (2007). Chromate reducing and plant growth promoting activies of psychrotrophic *Rhodococcus erythropolis* MtCC 7905. *J. Basic Microbiol.* 47, 513–517. doi:10.1002/jobm.200700224.

Troncoso-Rojas, R., Tiznado-Hernández, M. E. (2014). Chapter 5: *Alternaria alternata* (Black Rot, Black Spot). In *Postharvest Decay*, Ed. Silvia Bautista-Baños, Academic Press, 147-187,doi.org/10.1016/B978-0-12-411552-1.00005-3.

Tsiafouli, M. A., Thébault, E., Sgardelis, S. P., de Ruiter, P. C., van der Putten, W. H., Birkhofer, K., et al. (2015). Intensive agriculture reduces soil biodiversity across Europe. *Glob. Chang. Biol.* 21, 973–985. doi:10.1111/gcb.12752.

Turkovskaya, O. V., Golubev, S. N. (2020). The collection of rhizosphere microorganisms: Its importance for the study of associative plant-bacterium interactions. *Vavilovskii Zhurnal Genet. Selektsii* 24, 315–324. doi:10.18699/VJ20.623.

Ujvári, G., Turrini, A., Avio, L., Agnolucci, M. (2021). Possible role of arbuscular mycorrhizal fungi and associated bacteria in the recruitment of endophytic bacterial communities by plant roots. *Mycorrhiza*. 31(5):527-544 doi:10.1007/s00572-021-01040-7.

Uroz, S., D'Angelo-Picard, C., Carlier, A., Elasri, M., Sicot, C., Petit, A., Oger, P., Faure, D., Dessaux, Y. (2003). Novel bacteria degrading N-acylhomoserine lactones and their use as quenchers of quorum-sensing-regulated functions of plant-pathogenic bacteria. *Microbiology* 149, 1981–1989. doi:10.1099/mic.0.26375-0.

Van Overbeek, L. S., Van Doorn, J., Wichers, J. H., Van Amerongen, A., Van Roermund, H. J. W., Willemsen, P. T. J. (2014). The arable ecosystem as battleground for emergence of new human pathogens. *Front. Microbiol.* 5, 1–17. doi:10.3389/fmicb.2014.00104.

Van Peer, R., Niemann, G.J., Schippers, B. (1991). Induced resistance and phytoalexin accumulation in biological control of *Fusarium* wilt of carnation by *Pseudomonas* sp. strain WCS417r. *Phytopathology* 81:728–34 *The American Phytopathological Society*. DOI: 10.1094/Phyto-81-728

Vandenkoornhuyse, P., Quaiser, A., Duhamel, M., Le Van, A., Dufresne, A. (2015). The importance of the microbiome of the plant holobiont. *New Phytol.* 206, 1196–1206. doi:10.1111/nph.13312.

Vereecke, D., Zhang, Y., Francis, I. M., Lambert, P. Q., Venneman, J., Stamler, R. A., Kilcrease, J., Randall, J. J. (2020). Functional genomics insights into the pathogenicity, habitat fitness, and mechanisms modifying plant development of *Rhodococcus* sp. PBTS1 and PBTS2. *Front. Microbiol.* 11, 1–23. doi:10.3389/fmicb.2020.00014.

Verginer, M., Siegmund, B., Cardinale, M., Müller, H., Choi, Y., Míguez, C. B., Leitner, E., Berg, G. (2010). Monitoring the plant epiphyte *Methylobacterium extorquens* DSM 21961 by real-time PCR and its influence on the strawberry flavor. *FEMS Microbiol. Ecol.* 74, 136–145. doi:10.1111/j.1574-6941.2010.00942.x.

Vishwakarma, K., Kumar, N., Shandilya, C., Mohapatra, S., Bhayana, S., Varma, A. (2020). Revisiting plant–microbe interactions and microbial consortia application for enhancing sustainable agriculture: A review. *Front. Microbiol.* 11, 1–21. doi:10.3389/fmicb.2020.560406.

Von Stetten, F., Mayr, R., Scherer, S. (1999). Climatic influence on mesophilic *Bacillus cereus* and psychrotolerant *Bacillus weihenstephanensis* populations in tropical, temperate and alpine soil. , 1(6), 503–515. doi:10.1046/j.1462-2920.1999.t01-1-00070.x

Vorholt, J. A. (2012). Microbial life in the phyllosphere. *Nat. Rev. Microbiol.* 10, 828–840. doi:10.1038/nrmicro2910.

Wagacha, J. M., Muthomi, J. W. (2007). *Fusarium culmorum*: Infection process, mechanisms of mycotoxin production and their role in pathogenesis in wheat. *Crop Prot.* 26, 877–885. doi:10.1016/j.cropro.2006.09.003.

Wagg, C., Schlaeppi, K., Banerjee, S., Kuramae, E. E., van der Heijden, M. G. A. (2019). Fungal-bacterial diversity and microbiome complexity predict ecosystem functioning. *Nat. Commun.* 10, 1–10. doi:10.1038/s41467-019-12798-y.

Walter, A., Finger, R., Huber, R., Buchmann, N. (2017). Smart farming is key to developing sustainable agriculture. *Proc. Natl. Acad. Sci. U. S. A.* 114, 6148–6150. doi:10.1073/pnas.1707462114.

Wang, J., Tao, F., Tian, W., Guo, Z., Chen, X., Xu, X., Shang, H., Hu, X. (2017). The wheat WRKY transcription factors TaWRKY49 and TaWRKY62 confer differential high-temperature seedling-plant resistance to *Puccinia striiformis* f. sp. *tritici*. *PloS one*, 12(7), p.e0181963.

Wang, Q., Ge, C., Xu, S., Wu, Y., Sahito, Z. A., Ma, L., et al. (2020). The endophytic bacterium *Sphingomonas* SaMR12 alleviates Cd stress in oilseed rape through regulation of the GSH-AsA cycle and antioxidative enzymes. *BMC Plant Biol.* 20, 1–14. doi:10.1186/s12870-020-2273-1.

Wang, X., Zhou, X., Cai, Z., Guo, L., Chen, X., Chen, X., Liu, J., Feng, M., Qiu, Y., Zhang, Y., Wang, A. (2021a). A biocontrol strain of *Pseudomonas aeruginosa* CQ-40 promote growth and control *Botrytis cinerea* in tomato. *Pathogens* 10, 1–17. doi:10.3390/pathogens10010022.

Wang, Y., Peng, S., Hua, Q., Qiu, C., Wu, P., Liu, X., Lin, X. (2021b). The long-term effects of using phosphate-solubilizing bacteria and photosynthetic bacteria as biofertilizers on peanut yield and soil bacteria community. *Front. Microbiol.* 12, 1–14. doi:10.3389/fmicb.2021.693535.

Wang, Z., Xu, J., Li, Y., Wang, K., Wang, Y., Hong, Q., Li, W.-J., Li, S.-P. (2010). *Rhodococcus jialingiae* sp. nov., an actinobacterium isolated from sludge of a carbendazim wastewater treatment facility. *Int. J. Syst. Evol. Microbiol.* 60, 378–381. doi:10.1099/ijs.0.013219-0.

Wassermann, B., Rybakova, D., Müller, C., Berg, G. (2017). Harnessing the microbiomes of *Brassica* vegetables for health issues. *Sci. Rep.* 7, 17649 doi:10.1038/s41598-017-17949-z.

Wei, Q., Luo, Q., Wang, R., Zhang, F., He, Y., Zhang, Y., Qiu, D., Li, K., Chang, J., Yang, G., He, G. (2017). A wheat R2R3-type MYB transcription factor TaODORANT1 positively regulates drought and salt stress responses in transgenic tobacco plants. *Frontiers in plant science,* 8, p.1374. doi: 10.3389/fpls.2017.01374

Weyens, N., Beckers, B., Schellingen, K., Ceulemans, R., Croes, S., Janssen, J., Haenen, S., Witters, N., Vangronsveld, J. (2013). Plant-associated bacteria and their role in the success or failure of metal phytoextraction projects: First observations of a field-related experiment. *Microb. Biotechnol.* 6, 288–299. doi:10.1111/1751-7915.12038.

Windisch, S., Sommermann, L., Babin, D., Chowdhury, S. P., Grosch, R., Moradtalab, N., Walker, F., Höglinger, B., El-Hasan, A., Armbruster, W., Nesme, J., Sørensen, S.J., Schellenberg, I., Geistlinger, J., Smalla, K., Rothballer, M., Ludewig, U., Neumann, G. (2021). Impact of long-term organic and mineral fertilization on rhizosphere metabolites, root–microbial interactions and plant health of lettuce. *Front. Microbiol.* 11. doi:10.3389/fmicb.2020.597745.

Winston, M. E., Hampton-Marcell, J., Zarraonaindia, I., Owens, S. M., Moreau, C. S., Gilbert, J. A., Hartsel, J.A., Kennedy, S.J., Gibbons, S.M. (2014). Understanding cultivar-specificity and soil determinants of the Cannabis microbiome. *PLoS One* 9(6):e99641. doi:10.1371/journal.pone.0099641.

Wippel, K., Tao, K., Niu, Y., Zgadzaj, R., Kiel, N., Guan, R., Dahms, E., Zhang, P., Jensen, D.B., Logemann, E., Radutoiu, S., Schulze-Lefert, P., Garrido-Oter, R. (2021). Host preference and invasiveness of commensal bacteria in the *Lotus* and *Arabidopsis* root microbiota. *Nat Microbiol*. 6(9):1150-1162. doi: 10.1038/s41564-021-00941-9.

Xie, S. S., Wu, H. J., Zang, H. Y., Wu, L. M., Zhu, Q. Q., Gao, X. W. (2014). Plant growth promotion by spermidine-producing *Bacillus subtilis* OKB105. *Mol. Plant-Microbe Interact.* 27, 655–663. doi:10.1094/MPMI-01-14-0010-R.

Xin, X. F., He, S. Y. (2013). *Pseudomonas syringae* pv. *tomato* DC3000: A model pathogen for probing disease susceptibility and hormone signaling in plants. *Annu. Rev. Phytopathol.* 51, 473–498. doi:10.1146/annurev-phyto-082712-102321.

Xu, J. L., He, J., Wang, Z. C., Wang, K., Li, W. J., Tang, S. K., Li, S. P. (2007). *Rhodococcus qingshengii* sp. nov., a carbendazim-degrading bacterium. *Int. J. Syst. Evol. Microbiol.* 57, 2754–2757. doi:10.1099/ijs.0.65095-0.

Xu, R., Lu, R., Zhang, T., Wu, Q., Cai, W., Han, X., Wan, Z., Jin, X., Zhang, Z., Zhang, C. (2021). Temporal association between human upper respiratory and gut bacterial microbiomes during the course of COVID-19 in adults. *Commun. Biol.* 4, 1–11. doi:10.1038/s42003-021-01796-w.

Yadav, S., Khan, M. A., Sharma, R., Malik, A., Sharma, S. (2021). Potential of formulated *Dyadobacter jiangsuensis* strain 12851 for enhanced bioremediation of chlorpyrifos contaminated soil. *Ecotoxicol. Environ. Saf.* 213, 112039. doi:10.1016/j.ecoenv.2021.112039.

Yang, G., Li, C. (2012). "General description of Rhizoctonia species complex," in *Plant Pathology*, ed. C. J. Cumagun (China: InTech), 41–52. doi: 10.5772/39026

Yang, L., Schröder, P., Vestergaard, G., Schloter, M., Radl, V. (2020). Response of barley plants to drought might be associated with the recruiting of soil-borne endophytes. *Microorganisms* 8, 1–18. doi:10.3390/microorganisms8091414.

Yin, C., Casa Vargas, J. M., Schlatter, D. C., Hagerty, C. H., Hulbert, S. H., Paulitz, T. C. (2021). Rhizosphere community selection reveals bacteria associated with reduced root disease. *Microbiome* 9, 1–18. doi:10.1186/s40168-020-00997-5.

Yin, S., Zhou, S., Kong, X., Han, Y., Wang, W. (2017). Altered gibberellin content affects growth and development in transgenic tobacco lines overexpressing a wheat gene encoding F-box protein. *Biol. Plant.* 61, 349–358. doi:10.1007/s10535-017-0707-x.

Yu, J. M., Wang, D., Ries, T. R., Pierson, L. S., Pierson, E. A. (2018). An upstream sequence modulates phenazine production at the level of transcription and translation in the biological control strain *Pseudomonas chlororaphis* 30-84. *PLoS One* 13, 1–23. doi:10.1371/journal.pone.0193063.

Zhang, J., Van Der Heijden, M. G. A., Zhang, F., Bender, S. F. (2020). Soil biodiversity and crop diversification are vital components of healthy soils and agricultural sustainability. *Front. Agric. Sci. Eng*. 7, 236–242. doi:10.15302/J-FASE-2020336.

Zhang, N., Yin, Y., Liu, X., Tong, S., Xing, J., Zhang, Y., et al. (2017). The E3 ligase TaSAP5 alters drought stress responses by promoting the degradation of DRIP proteins. *Plant Physiol.* 175, 1878–1892. doi:10.1104/pp.17.01319.

Zhang, S., Gan, Y., Xu, B., (2016). Application of plant-growth-promoting fungi *Trichoderma longibrachiatum* T6 enhances tolerance of wheat to salt stress through improvement of antioxidative defense system and gene expression. *Frontiers in plant science*, 7, p.1405. doi: 10.3389/fpls.2016.01405

Zhao, H., Liu, Y. P., Zhang, L. Q. (2019). *In silico* and genetic analyses of cyclic lipopeptide synthetic gene clusters in *Pseudomonas* sp. 11K1. *Front. Microbiol.* 10, 1–11. doi:10.3389/fmicb.2019.00544.

Zhao, Y. (2010). Auxin biosynthesis and its role in plant development. *Annu Rev Plant Biol.* 2, 49–64. doi:10.1146/annurev-arplant-042809-112308.Auxin.

Zhao, Y., Tian, X., Wang, F., Zhang, L., Xin, M., Hu, Z., Yao, Y., Ni, Z., Sun, Q. Peng, H., (2017). Characterization of wheat MYB genes responsive to high temperatures. *BMC plant biology*, 17(1), pp.1-14. doi.org/10.1186/s12870-017-1158-4

Zimin, A. V., Marçais, G., Puiu, D., Roberts, M., Salzberg, S. L., Yorke, J. A. (2013). The MaSuRCA genome assembler. *Bioinformatics* 29, 2669–2677. doi:10.1093/bioinformatics/btt476.

A. Supplementary data

Supplementary Figures

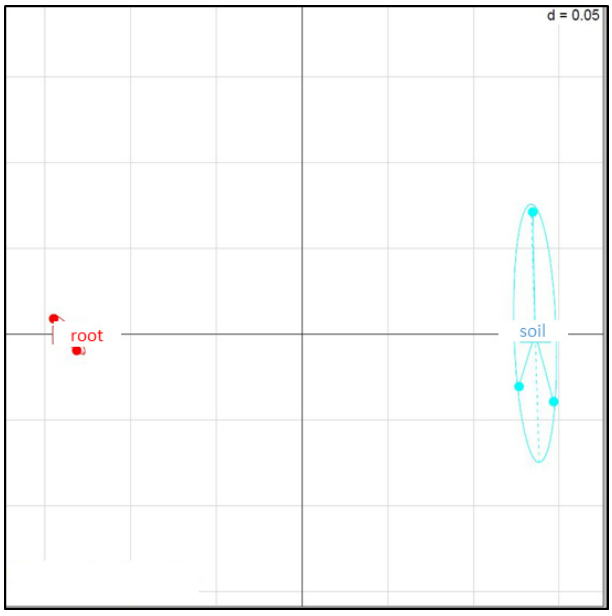

Figure S1: ß-diversity Scheyern separated by the factor compartment. Low sample size allowed no statistical analysis for significance. Data of root and rhizosphere microbiota of the Scheyern sampling site are presented in a two-dimensional MDS plot.

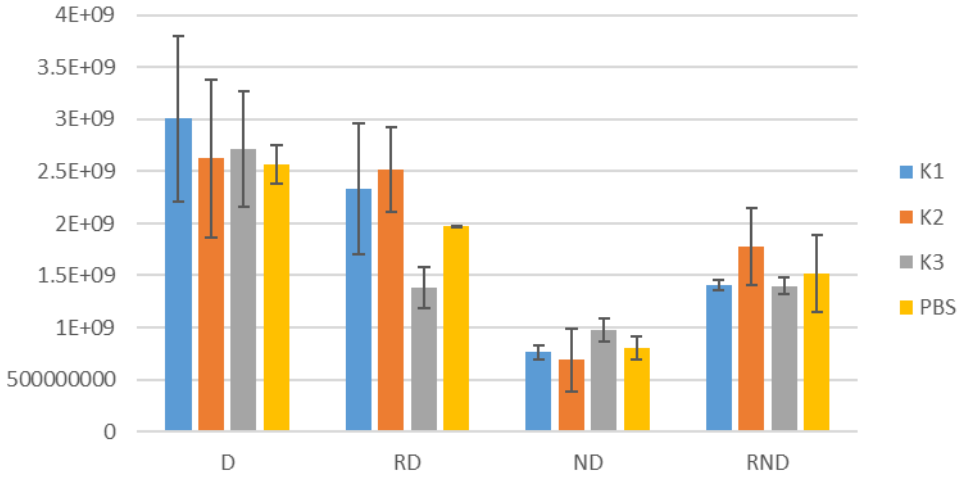

Figure S2: Bacterial load on wheat roots (separated). Number of bacteria per 1 g root and rhizosphere of consortium experiment 3. Error bars indicate standard deviation. D, ND: N = 3; RD, RND: N = 2.

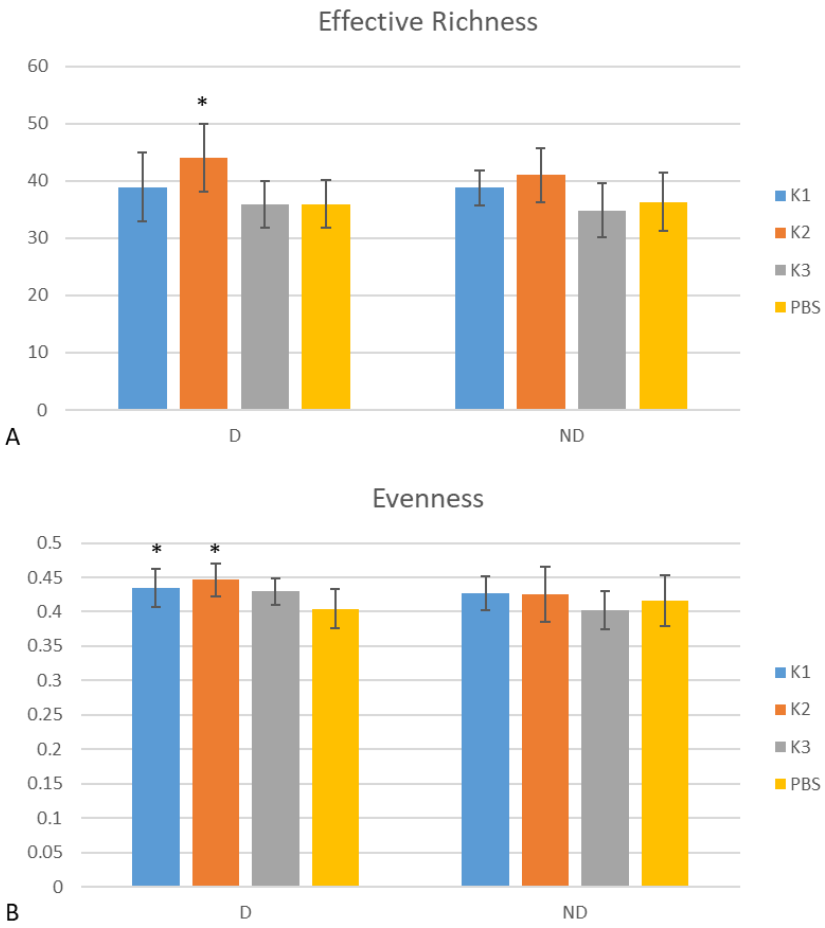

Figure S3: α-diversity in consortium experiments. Data obtained from root and rhizosphere microbiota of consortium experiments 1 and 3 under drought and non-drought conditions indicated by effective richness (**A**) and evenness (**B**). Error bars indicate standard deviation. Significant differences are indicated by $P < 0.05$.

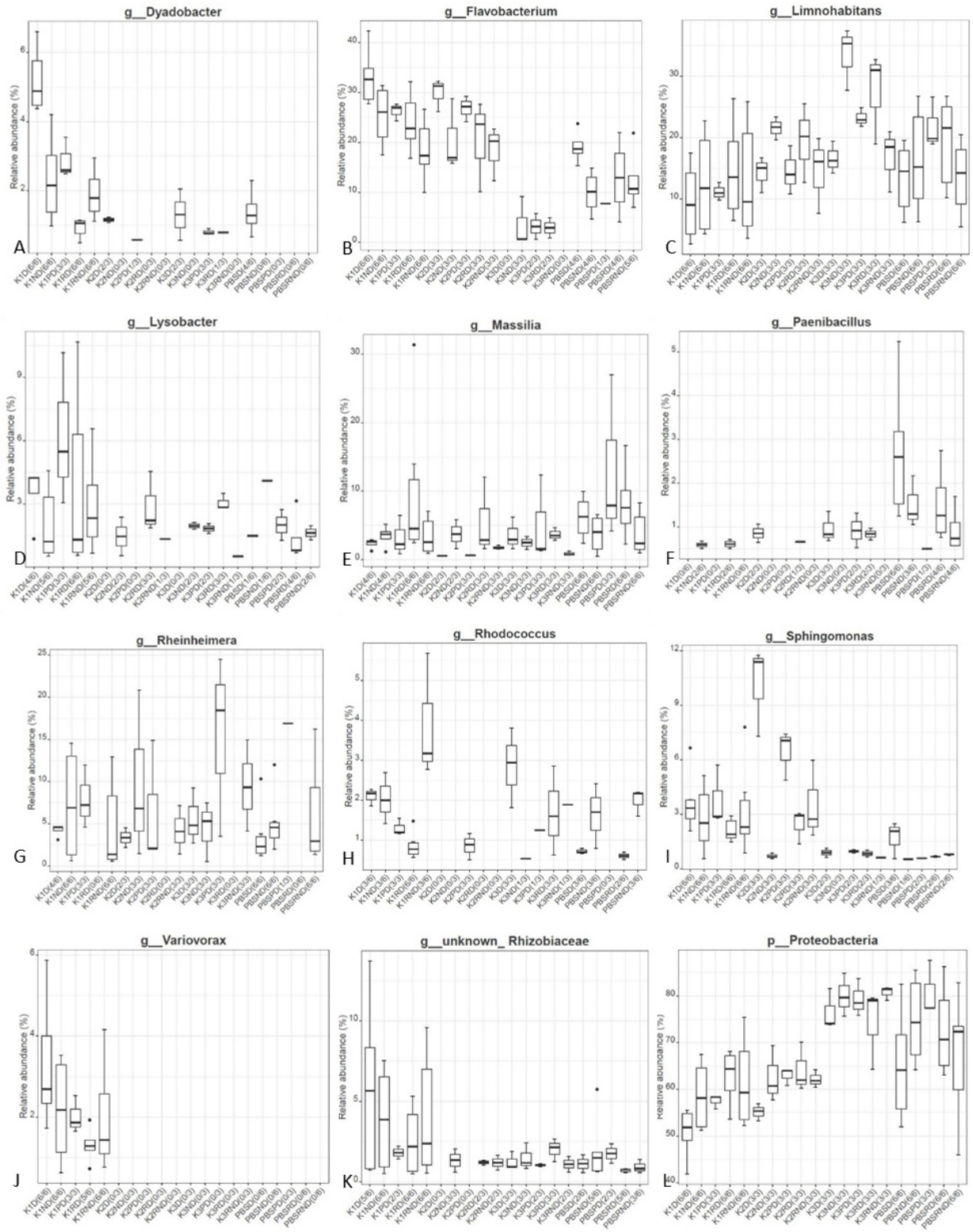

Figure S4: Microbial abundances of most differing taxa in consortium experiments. *Dyadobacter* (**A**), *Flavobacterium* (**B**), *Limnohabitans* (**C**), *Lysobacter* (**D**), *Massilia* (**E**), *Paenibacillus* (**F**), *Rheinheimera* (**G**), *Rhodococcus* (**H**), *Sphingomonas* (**I**), *Variovorax* (**J**), *Rhizobiaceae* (**K**) and Proteobacteria (**L**) in consortium experiments 1 and 3 at the different sampling points.

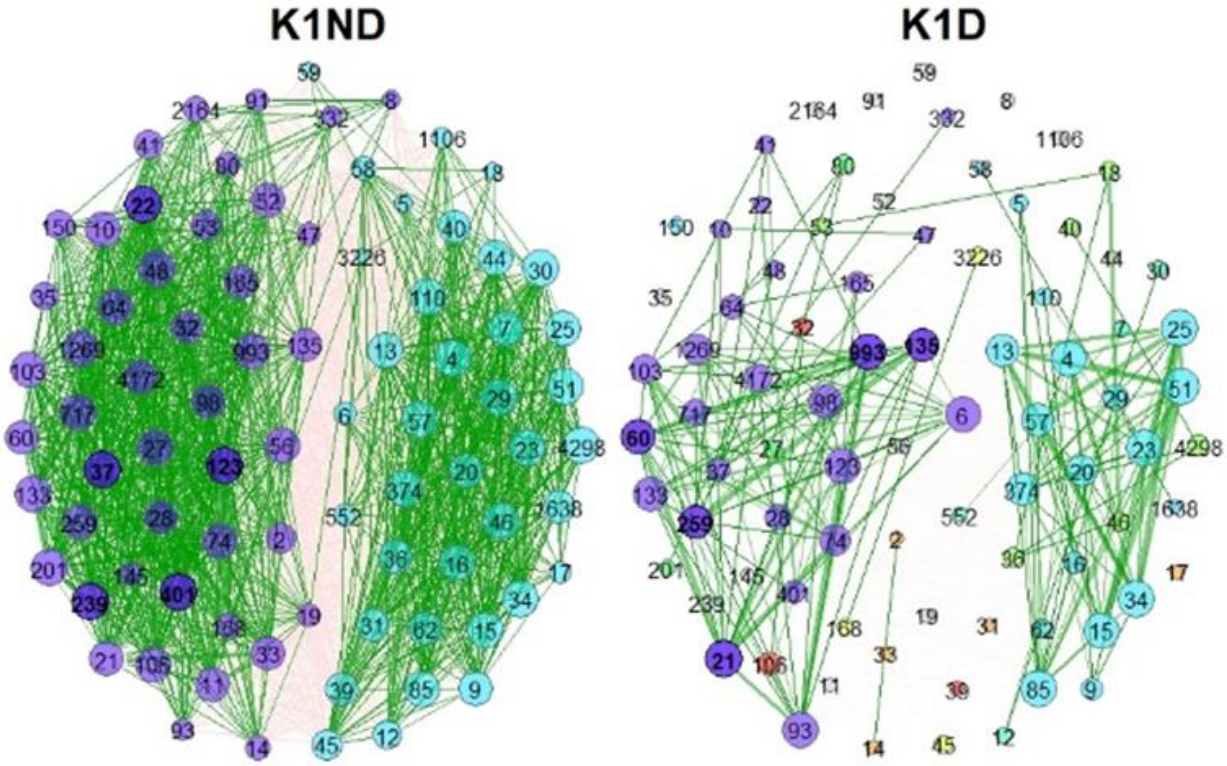

Figure S5: Co-occurrence networks of bacterial OTUs present in K1. Data of consortium experiment 1 and 3 were combined under drought (D) and non-drought conditions (ND). The correlation coefficient was calculated for pairwise relative abundance of bacterial genera using Pearson correlation implemented in the R-package NetCOMI (Peschel 2020), N = 6.

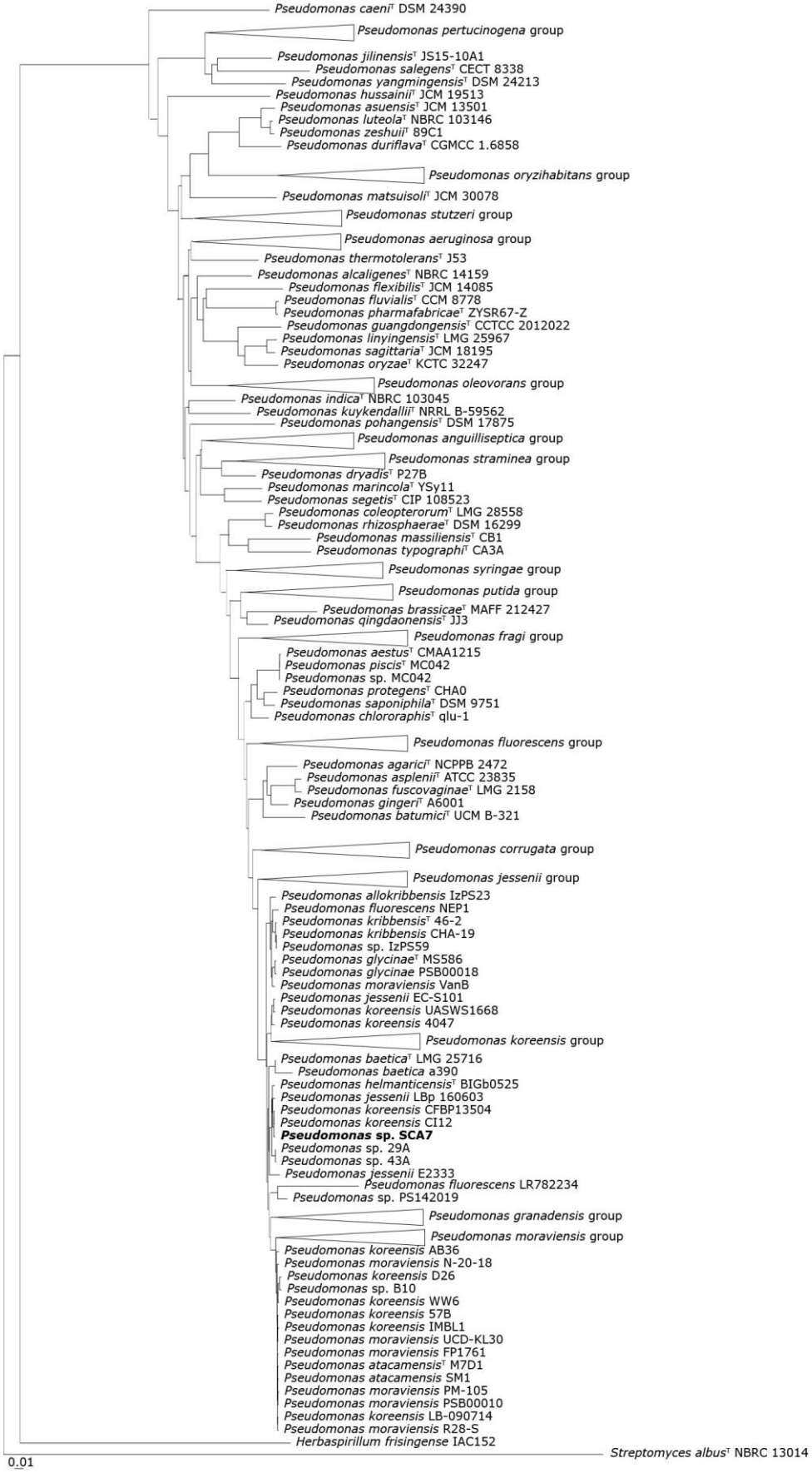
Pseudomonas caeni^T DSM 24390
Pseudomonas pertucinogena group
Pseudomonas jilinensis^T JS15-10A1
Pseudomonas salegens^T CECT 8338
Pseudomonas yangmingensis^T DSM 24213
Pseudomonas hussainii^T JCM 19513
Pseudomonas asuensis^T JCM 13501
Pseudomonas luteola^T NBRC 103146
Pseudomonas zeshuii^T 89C1
Pseudomonas duriflava^T CGMCC 1.6858
Pseudomonas oryzihabitans group
Pseudomonas matsuisoli^T JCM 30078
Pseudomonas stutzeri group
Pseudomonas aeruginosa group
Pseudomonas thermotolerans^T J53
Pseudomonas alcaligenes^T NBRC 14159
Pseudomonas flexibilis^T JCM 14085
Pseudomonas fluvialis^T CCM 8778
Pseudomonas pharmafabricae^T ZYSR67-Z
Pseudomonas guangdongensis^T CCTCC 2012022
Pseudomonas linyingensis^T LMG 25967
Pseudomonas sagittaria^T JCM 18195
Pseudomonas oryzae^T KCTC 32247
Pseudomonas oleovorans group
Pseudomonas indica^T NBRC 103045
Pseudomonas kuykendallii^T NRRL B-59562
Pseudomonas pohangensis^T DSM 17875
Pseudomonas anguilliseptica group
Pseudomonas straminea group
Pseudomonas dryadis^T P27B
Pseudomonas marincola^T YSy11
Pseudomonas segetis^T CIP 108523
Pseudomonas coleopterorum^T LMG 28558
Pseudomonas rhizosphaerae^T DSM 16299
Pseudomonas massiliensis^T CB1
Pseudomonas typographi^T CA3A
Pseudomonas syringae group
Pseudomonas putida group
Pseudomonas brassicae^T MAFF 212427
Pseudomonas qingdaonensis^T JJ3
Pseudomonas fragi group
Pseudomonas aestus^T CMAA1215
Pseudomonas piscis^T MC042
Pseudomonas sp. MC042
Pseudomonas protegens^T CHA0
Pseudomonas saponiphila^T DSM 9751
Pseudomonas chlororaphis^T qlu-1
Pseudomonas fluorescens group
Pseudomonas agarici^T NCPPB 2472
Pseudomonas asplenii^T ATCC 23835
Pseudomonas fuscovaginae^T LMG 2158
Pseudomonas gingeri^T A6001
Pseudomonas batumici^T UCM B-321
Pseudomonas corrugata group
Pseudomonas jessenii group
Pseudomonas allokribbensis IzPS23
Pseudomonas fluorescens NEP1
Pseudomonas kribbensis^T 46-2
Pseudomonas kribbensis CHA-19
Pseudomonas sp. IzPS59
Pseudomonas glycinae^T MS586
Pseudomonas glycinae PSB00018
Pseudomonas moraviensis VanB
Pseudomonas jessenii EC-S101
Pseudomonas koreensis UASWS1668
Pseudomonas koreensis 4047
Pseudomonas koreensis group
Pseudomonas baetica^T LMG 25716
Pseudomonas baetica a390
Pseudomonas helmanticensis^T BIGb0525
Pseudomonas jessenii LBp 160603
Pseudomonas koreensis CFBP13504
Pseudomonas koreensis CI12
Pseudomonas sp. SCA7
Pseudomonas sp. 29A
Pseudomonas sp. 43A
Pseudomonas jessenii E2333
Pseudomonas fluorescens LR782234
Pseudomonas sp. PS142019
Pseudomonas granadensis group
Pseudomonas moraviensis group
Pseudomonas koreensis AB36
Pseudomonas moraviensis N-20-18
Pseudomonas koreensis D26
Pseudomonas sp. B10
Pseudomonas koreensis WW6
Pseudomonas koreensis 57B
Pseudomonas koreensis IMBL1
Pseudomonas moraviensis UCD-KL30
Pseudomonas moraviensis FP1761
Pseudomonas atacamensis^T M7D1
Pseudomonas atacamensis SM1
Pseudomonas moraviensis PM-105
Pseudomonas moraviensis PSB00010
Pseudomonas koreensis LB-090714
Pseudomonas moraviensis R28-S
Herbaspirillum frisingense IAC152
Streptomyces albus^T NBRC 13014
0.01

Figure S6: Maximum-likelihood phylogenetic tree of the *Pseudomonas* genus generated with FastTree from 70 genes of the core genome. Triangles represent species groups according to Gomila *et al*. (2015). The scale bar represents nucleotide substitutions per site (0.01 scale = 1% nucleotide substitutions per site).

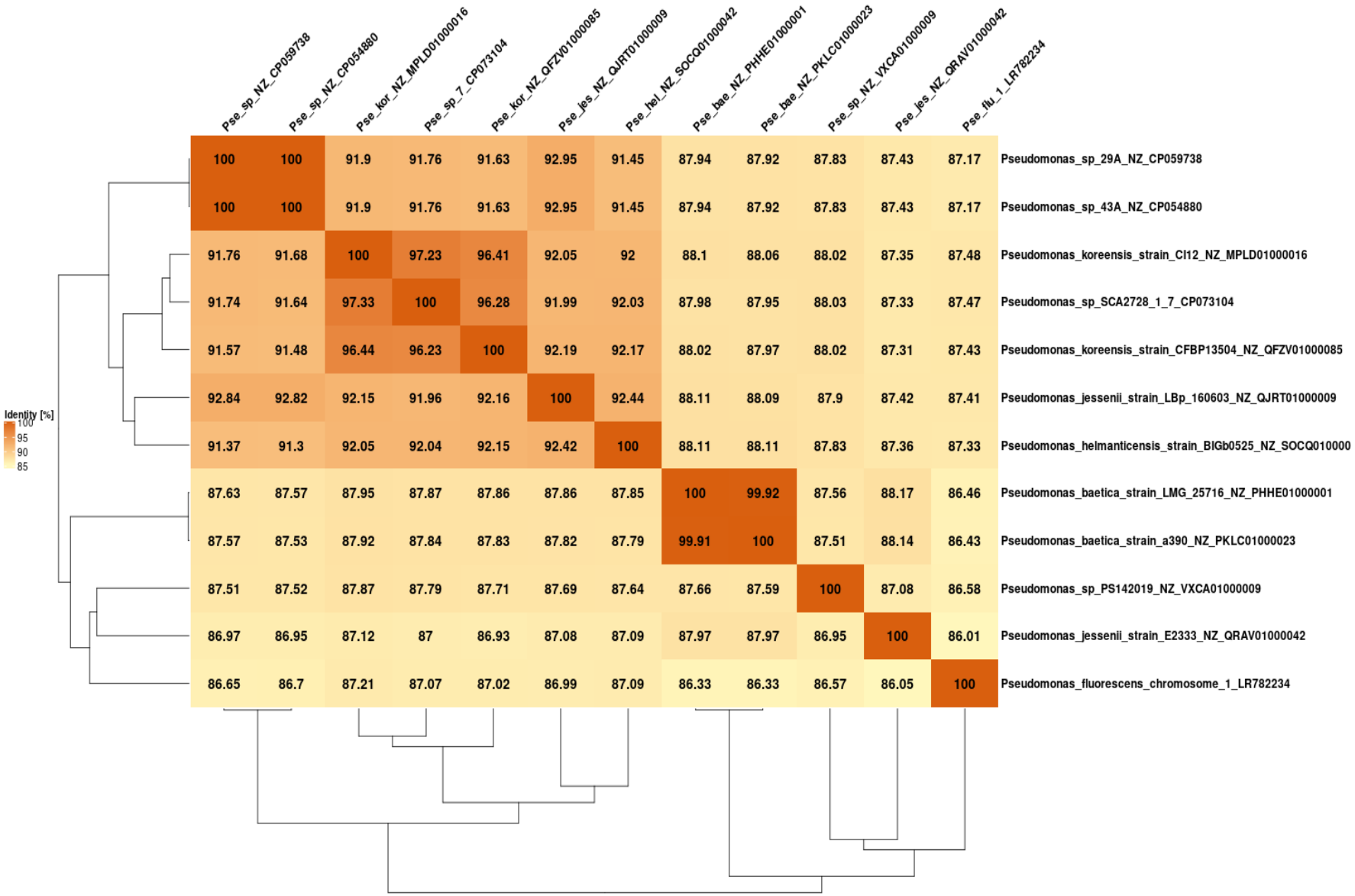
Pse_sp_NZ_CP059738
Pse_sp_NZ_CP054880
Pse_kor_NZ_MPLD01000016
Pse_sp_7_CP073104
Pse_kor_NZ_QFZV01000085
Pse_jes_NZ_QJRT01000009
Pse_hel_NZ_SOCQ01000042
Pse_bae_NZ_PHHE01000001
Pse_bae_NZ_PKLC01000023
Pse_sp_NZ_VXCA01000009
Pse_jes_NZ_QRAV01000042
Pse_flu_1_LR782234
100 100 91.9 91.76 91.63 92.95 91.45 87.94 87.92 87.83 87.43 87.17 Pseudomonas_sp_29A_NZ_CP059738
100 100 91.9 91.76 91.63 92.95 91.45 87.94 87.92 87.83 87.43 87.17 Pseudomonas_sp_43A_NZ_CP054880
91.76 91.68 100 97.23 96.41 92.05 92 88.1 88.06 88.02 87.35 87.48 Pseudomonas_koreensis_strain_CI12_NZ_MPLD01000016
91.74 91.64 97.33 100 96.28 91.99 92.03 87.98 87.95 88.03 87.33 87.47 Pseudomonas_sp_SCA2728_1_7_CP073104
91.57 91.48 96.44 96.23 100 92.19 92.17 88.02 87.97 88.02 87.31 87.43 Pseudomonas_koreensis_strain_CFBP13504_NZ_QFZV01000085
92.84 92.82 92.15 91.96 92.16 100 92.44 88.11 88.09 87.9 87.42 87.41 Pseudomonas_jessenii_strain_LBp_160603_NZ_QJRT01000009
91.37 91.3 92.05 92.04 92.15 92.42 100 88.11 88.11 87.83 87.36 87.33 Pseudomonas_helmanticensis_strain_BIGb0525_NZ_SOCQ010000
87.63 87.57 87.95 87.87 87.86 87.86 87.85 100 99.92 87.56 88.17 86.46 Pseudomonas_baetica_strain_LMG_25716_NZ_PHHE01000001
87.57 87.53 87.92 87.84 87.83 87.82 87.79 99.91 100 87.51 88.14 86.43 Pseudomonas_baetica_strain_a390_NZ_PKLC01000023
87.51 87.52 87.87 87.79 87.71 87.69 87.64 87.66 87.59 100 87.08 86.58 Pseudomonas_sp_PS142019_NZ_VXCA01000009
86.97 86.95 87.12 87 86.93 87.08 87.09 87.97 87.97 86.95 100 86.01 Pseudomonas_jessenii_strain_E2333_NZ_QRAV01000042
86.65 86.7 87.21 87.07 87.02 86.99 87.09 86.33 86.33 86.57 86.05 100 Pseudomonas_fluorescens_chromosome_1_LR782234
Identity [%]
100
95
90
85

Figure S7: ANI of SCA7 (=SCA2728.1_7) and closest related *Pseudomonas* strains. Data obtained from 11 complete genomes with EDGAR Software.

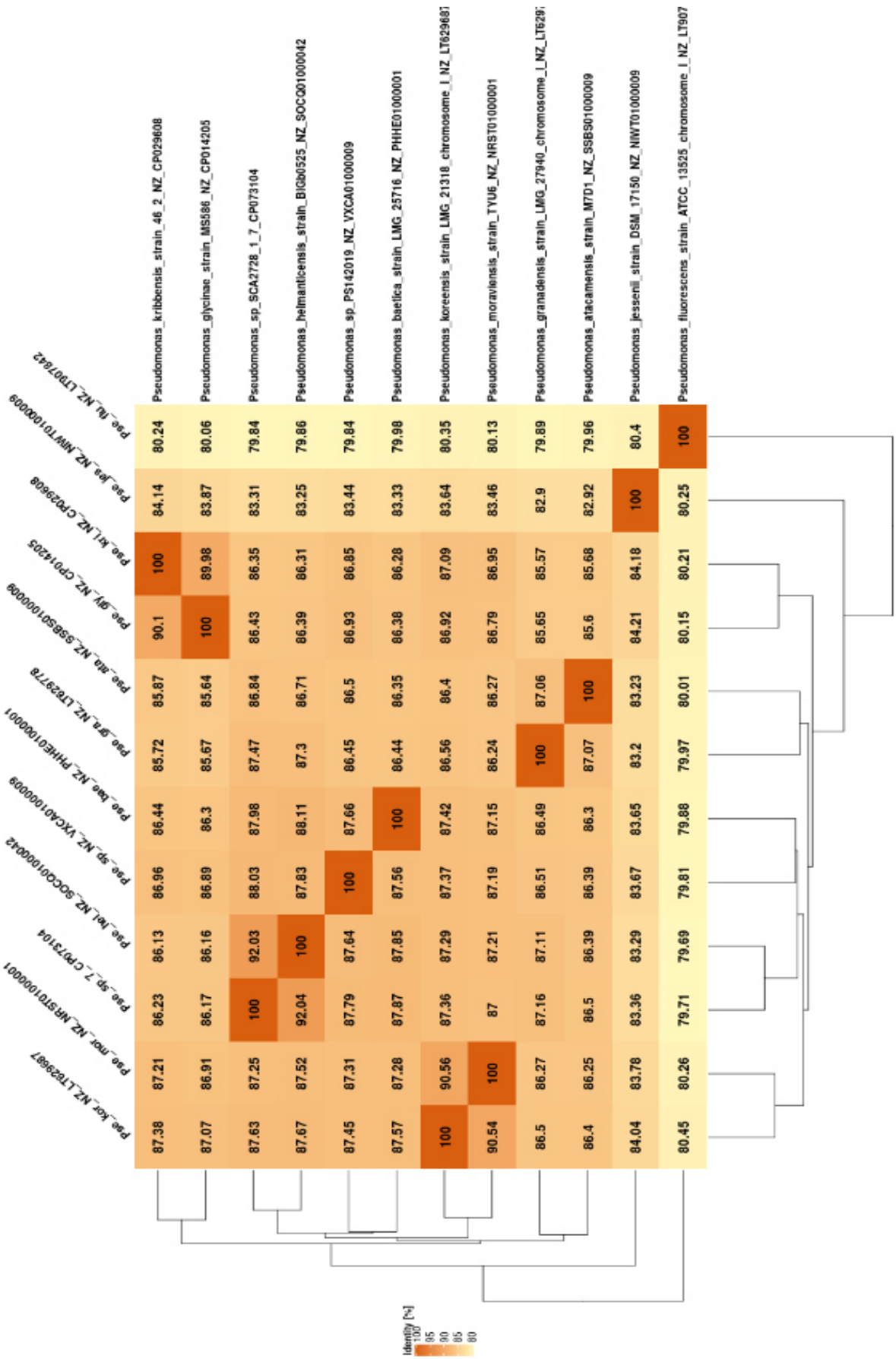
Pseudomonas_kribbensis_strain_46_2_NZ_CP029608
Pseudomonas_glycinae_strain_MS586_NZ_CP014205
Pseudomonas_sp_SCA2728_1_7_CP073104
Pseudomonas_helmanticensis_strain_BIGb0525_NZ_SOCQ01000042
Pseudomonas_sp_P5142019_NZ_VXCA01000009
Pseudomonas_baetica_strain_LMG_25716_NZ_PHHE01000001
Pseudomonas_koreensis_strain_LMG_21318_chromosome_I_NZ_LT629681
Pseudomonas_moraviensis_strain_TYU6_NZ_NRST01000001
Pseudomonas_granadensis_strain_LMG_27940_chromosome_I_NZ_LT629
Pseudomonas_atacamensis_strain_M7D1_NZ_SSBS01000009
Pseudomonas_jesseni_strain_DSM_17150_NZ_NIWT01000009
Pseudomonas_fluorescens_strain_ATCC_13525_chromosome_I_NZ_LT907
pse_flu_NZ_LT907842
pse_jes_NZ_NIWT01000009
pse_kri_NZ_CP029608
pse_gly_NZ_CP014205
pse_ata_NZ_SSBS01000009
pse_gra_NZ_LT629778
pse_bae_NZ_PHHE01000001
pse_sp_NZ_VXCA01000009
pse_hol_NZ_SOCQ01000042
pse_sp_7_CP073104
pse_mor_NZ_NRST01000001
pse_kor_NZ_LT629687
87.38 87.21 86.23 86.13 86.96 86.44 85.72 85.87 90.1 100 84.14 80.24
87.07 86.91 86.17 86.16 86.89 86.3 85.67 85.64 100 89.98 83.87 80.06
87.63 87.25 100 92.03 88.03 87.98 87.47 86.84 86.43 86.35 83.31 79.84
87.67 87.52 92.04 100 87.83 88.11 87.3 86.71 86.39 86.31 83.25 79.86
87.45 87.31 87.79 87.64 100 87.66 86.45 86.5 86.93 86.85 83.44 79.84
87.57 87.28 87.87 87.85 87.56 100 86.44 86.35 86.38 86.28 83.33 79.98
100 90.56 87.36 87.29 87.37 87.42 86.56 86.4 86.92 87.09 83.64 80.35
90.54 100 87 87.21 87.19 87.15 86.24 86.27 86.79 86.95 83.46 80.13
86.5 86.27 87.16 87.11 86.51 86.49 100 87.06 85.65 85.57 82.9 79.89
86.4 86.25 86.5 86.39 86.39 86.3 87.07 100 85.6 85.68 82.92 79.96
84.04 83.78 83.36 83.29 83.67 83.65 83.2 83.23 84.21 84.18 100 80.4
80.45 80.26 79.71 79.69 79.81 79.88 79.97 80.01 80.15 80.21 80.25 100
identity [%]
100
95
90
85
80

Figure S8: ANI of SCA7 (=SCA2728.1_7) and closest related *Pseudomonas* type strains. Data obtained from 11 available genomes with EDGAR Software.

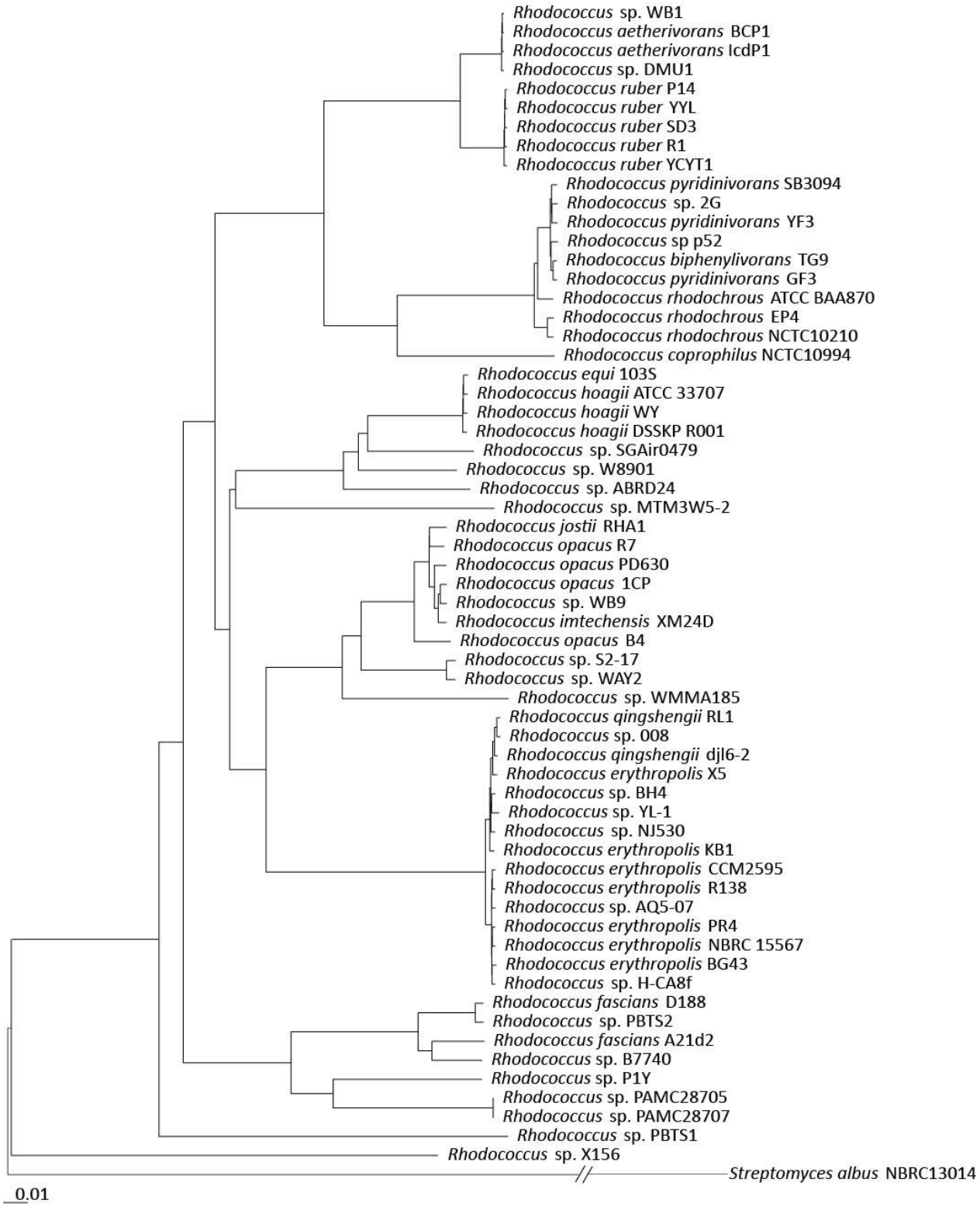

Figure S9: Maximum-likelihood phylogenetic tree of the *Rhodococcus* genus generated with FastTree from 633 genes of the core genome. The scale bar represents nucleotide substitutions per site (0.01 scale = 1% nucleotide substitutions per site).

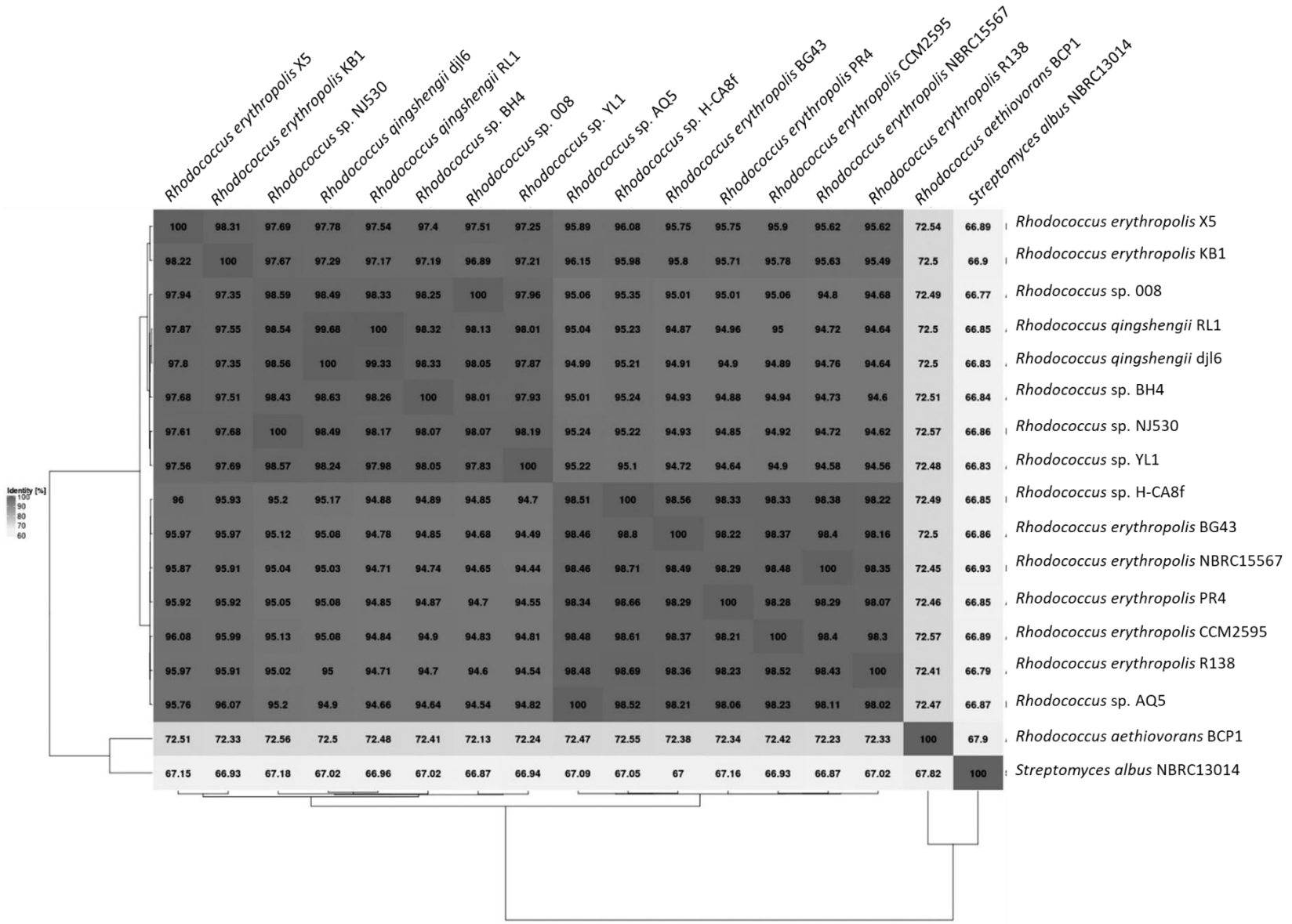
Rhodococcus erythropolis X5
Rhodococcus erythropolis KB1
Rhodococcus sp. NJ530
Rhodococcus qingshengii djl6
Rhodococcus qingshengii RL1
Rhodococcus sp. BH4
Rhodococcus sp. 008
Rhodococcus sp. YL1
Rhodococcus sp. AQ5
Rhodococcus sp. H-CA8f
Rhodococcus erythropolis BG43
Rhodococcus erythropolis PR4
Rhodococcus erythropolis CCM2595
Rhodococcus erythropolis NBRC15567
Rhodococcus erythropolis R138
Rhodococcus aethiovorans BCP1
Streptomyces albus NBRC13014
Identity [%]
100
90
80
70
60
100 98.31 97.69 97.78 97.54 97.4 97.51 97.25 95.89 96.08 95.75 95.75 95.9 95.62 95.62 72.54 66.89 Rhodococcus erythropolis X5
98.22 100 97.67 97.29 97.17 97.19 96.89 97.21 96.15 95.98 95.8 95.71 95.78 95.63 95.49 72.5 66.9 Rhodococcus erythropolis KB1
97.94 97.35 98.59 98.49 98.33 98.25 100 97.96 95.06 95.35 95.01 95.01 95.06 94.8 94.68 72.49 66.77 Rhodococcus sp. 008
97.87 97.55 98.54 99.68 100 98.32 98.13 98.01 95.04 95.23 94.87 94.96 95 94.72 94.64 72.5 66.85 Rhodococcus qingshengii RL1
97.8 97.35 98.56 100 99.33 98.33 98.05 97.87 94.99 95.21 94.91 94.9 94.89 94.76 94.64 72.5 66.83 Rhodococcus qingshengii djl6
97.68 97.51 98.43 98.63 98.26 100 98.01 97.93 95.01 95.24 94.93 94.88 94.94 94.73 94.6 72.51 66.84 Rhodococcus sp. BH4
97.61 97.68 100 98.49 98.17 98.07 98.07 98.19 95.24 95.22 94.93 94.85 94.92 94.72 94.62 72.57 66.86 Rhodococcus sp. NJ530
97.56 97.69 98.57 98.24 97.98 98.05 97.83 100 95.22 95.1 94.72 94.64 94.9 94.58 94.56 72.48 66.83 Rhodococcus sp. YL1
96 95.93 95.2 95.17 94.88 94.89 94.85 94.7 98.51 100 98.56 98.33 98.33 98.38 98.22 72.49 66.85 Rhodococcus sp. H-CA8f
95.97 95.97 95.12 95.08 94.78 94.85 94.68 94.49 98.46 98.8 100 98.22 98.37 98.4 98.16 72.5 66.86 Rhodococcus erythropolis BG43
95.87 95.91 95.04 95.03 94.71 94.74 94.65 94.44 98.46 98.71 98.49 98.29 98.48 100 98.35 72.45 66.93 Rhodococcus erythropolis NBRC15567
95.92 95.92 95.05 95.08 94.85 94.87 94.7 94.55 98.34 98.66 98.29 100 98.28 98.29 98.07 72.46 66.85 Rhodococcus erythropolis PR4
96.08 95.99 95.13 95.08 94.84 94.9 94.83 94.81 98.48 98.61 98.37 98.21 100 98.4 98.3 72.57 66.89 Rhodococcus erythropolis CCM2595
95.97 95.91 95.02 95 94.71 94.7 94.6 94.54 98.48 98.69 98.36 98.23 98.52 98.43 100 72.41 66.79 Rhodococcus erythropolis R138
95.76 96.07 95.2 94.9 94.66 94.64 94.54 94.82 100 98.52 98.21 98.06 98.23 98.11 98.02 72.47 66.87 Rhodococcus sp. AQ5
72.51 72.33 72.56 72.5 72.48 72.41 72.13 72.24 72.47 72.55 72.38 72.34 72.42 72.23 72.33 100 67.9 Rhodococcus aethiovorans BCP1
67.15 66.93 67.18 67.02 66.96 67.02 66.87 66.94 67.09 67.05 67 67.16 66.93 66.87 67.02 67.82 100 Streptomyces albus NBRC13014

Figure S10: ANI of *Rhodococcus erythropolis* clade. Average Nucleotide Identity (ANI) Matrix was based on 15 full *Rhodococcus* genomes + *Rhodococcus aethiovorans* BCP1 and *Streptomyces alba* NBRC13014 as outgroups. Data obtained with EDGAR Software.

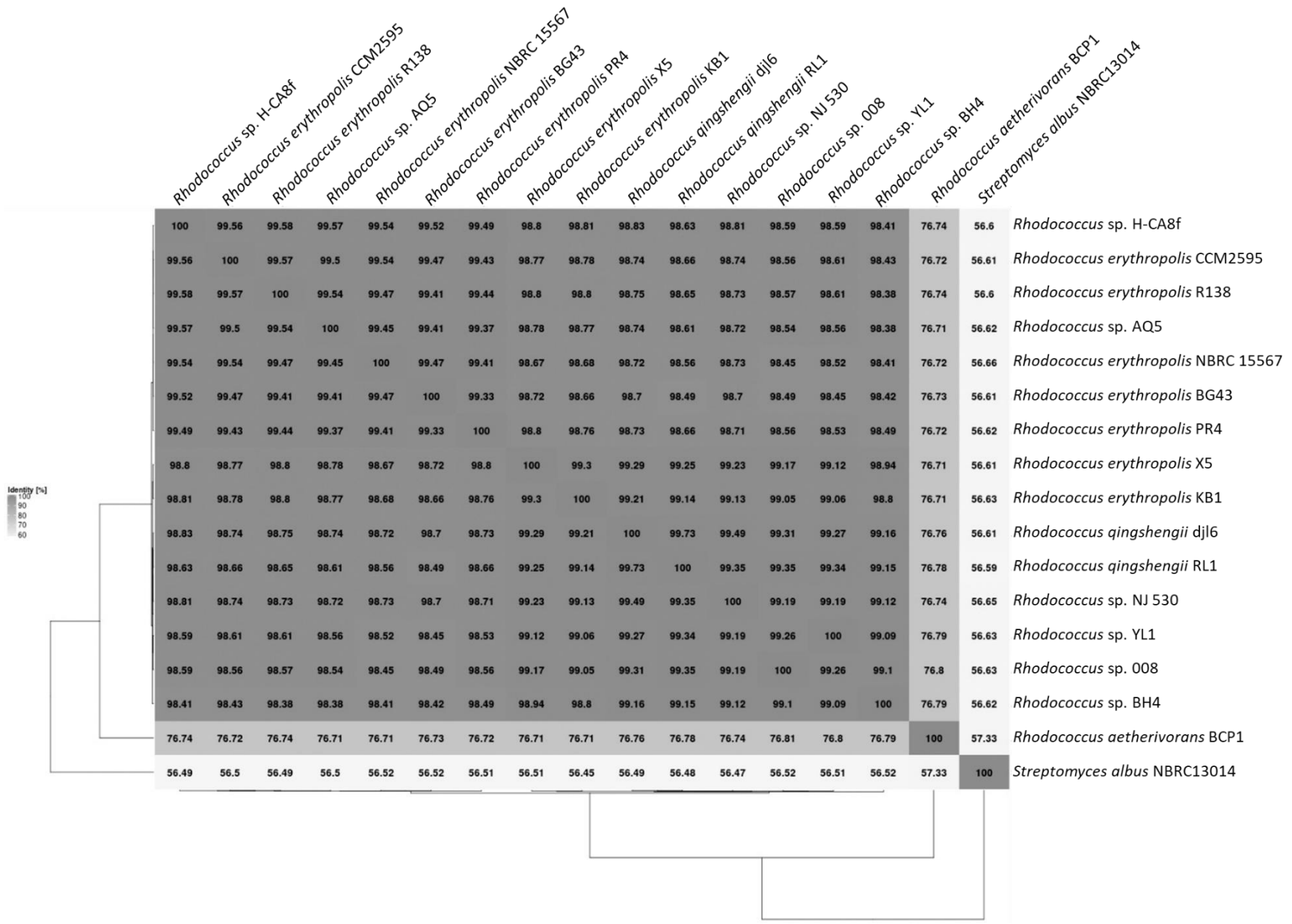
Rhodococcus sp. H-CA8f
Rhodococcus erythropolis CCM2595
Rhodococcus erythropolis R138
Rhodococcus sp. AQ5
Rhodococcus erythropolis NBRC 15567
Rhodococcus erythropolis BG43
Rhodococcus erythropolis PR4
Rhodococcus erythropolis X5
Rhodococcus erythropolis KB1
Rhodococcus qingshengii djl6
Rhodococcus qingshengii RL1
Rhodococcus sp. NJ 530
Rhodococcus sp. 008
Rhodococcus sp. YL1
Rhodococcus sp. BH4
Rhodococcus aetherivorans BCP1
Streptomyces albus NBRC13014
Identity [%]
100
90
80
70
60
100 99.56 99.58 99.57 99.54 99.52 99.49 98.8 98.81 98.83 98.63 98.81 98.59 98.59 98.41 76.74 56.6 Rhodococcus sp. H-CA8f
99.56 100 99.57 99.5 99.54 99.47 99.43 98.77 98.78 98.74 98.66 98.74 98.56 98.61 98.43 76.72 56.61 Rhodococcus erythropolis CCM2595
99.58 99.57 100 99.54 99.47 99.41 99.44 98.8 98.8 98.75 98.65 98.73 98.57 98.61 98.38 76.74 56.6 Rhodococcus erythropolis R138
99.57 99.5 99.54 100 99.45 99.41 99.37 98.78 98.77 98.74 98.61 98.72 98.54 98.56 98.38 76.71 56.62 Rhodococcus sp. AQ5
99.54 99.54 99.47 99.45 100 99.47 99.41 98.67 98.68 98.72 98.56 98.73 98.45 98.52 98.41 76.72 56.66 Rhodococcus erythropolis NBRC 15567
99.52 99.47 99.41 99.41 99.47 100 99.33 98.72 98.66 98.7 98.49 98.7 98.49 98.45 98.42 76.73 56.61 Rhodococcus erythropolis BG43
99.49 99.43 99.44 99.37 99.41 99.33 100 98.8 98.76 98.73 98.66 98.71 98.56 98.53 98.49 76.72 56.62 Rhodococcus erythropolis PR4
98.8 98.77 98.8 98.78 98.67 98.72 98.8 100 99.3 99.29 99.25 99.23 99.17 99.12 98.94 76.71 56.61 Rhodococcus erythropolis X5
98.81 98.78 98.8 98.77 98.68 98.66 98.76 99.3 100 99.21 99.14 99.13 99.05 99.06 98.8 76.71 56.63 Rhodococcus erythropolis KB1
98.83 98.74 98.75 98.74 98.72 98.7 98.73 99.29 99.21 100 99.73 99.49 99.31 99.27 99.16 76.76 56.61 Rhodococcus qingshengii djl6
98.63 98.66 98.65 98.61 98.56 98.49 98.66 99.25 99.14 99.73 100 99.35 99.35 99.34 99.15 76.78 56.59 Rhodococcus qingshengii RL1
98.81 98.74 98.73 98.72 98.73 98.7 98.71 99.23 99.13 99.49 99.35 100 99.19 99.19 99.12 76.74 56.65 Rhodococcus sp. NJ 530
98.59 98.61 98.61 98.56 98.52 98.45 98.53 99.12 99.06 99.27 99.34 99.19 99.26 100 99.09 76.79 56.63 Rhodococcus sp. YL1
98.59 98.56 98.57 98.54 98.45 98.49 98.56 99.17 99.05 99.31 99.35 99.19 100 99.26 99.1 76.8 56.63 Rhodococcus sp. 008
98.41 98.43 98.38 98.38 98.41 98.42 98.49 98.94 98.8 99.16 99.15 99.12 99.1 99.09 100 76.79 56.62 Rhodococcus sp. BH4
76.74 76.72 76.74 76.71 76.71 76.73 76.72 76.71 76.71 76.76 76.78 76.74 76.81 76.8 76.79 100 57.33 Rhodococcus aetherivorans BCP1
56.49 56.5 56.49 56.5 56.52 56.52 56.51 56.51 56.45 56.49 56.48 56.47 56.52 56.51 56.52 57.33 100 Streptomyces albus NBRC13014

Figure S11: AAI of *Rhodococcus erythropolis clade*. Average Aminoacid Identity (AAI) Matrix was based on 15 full genomes + *Rhodococcus aethiovorans* BCP1 and *Streptomyces alba* NBRC13014 as outgroups. Data obtained with EDGAR Software.

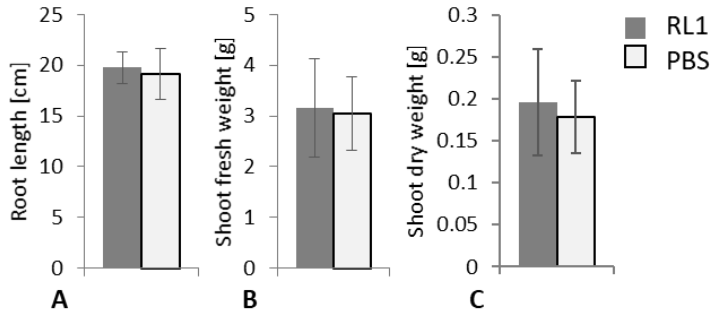

Figure S12: Rucola plants inoculated with RL1 grown in soil. Evaluated parameters were (**A**) root length, (**B**) shoot fresh weight and (**C**) shoot dry weight. Due to attached soil particles roots were not analyzed. Experiment was performed under non-drought conditions. Error bars indicate standard deviation.

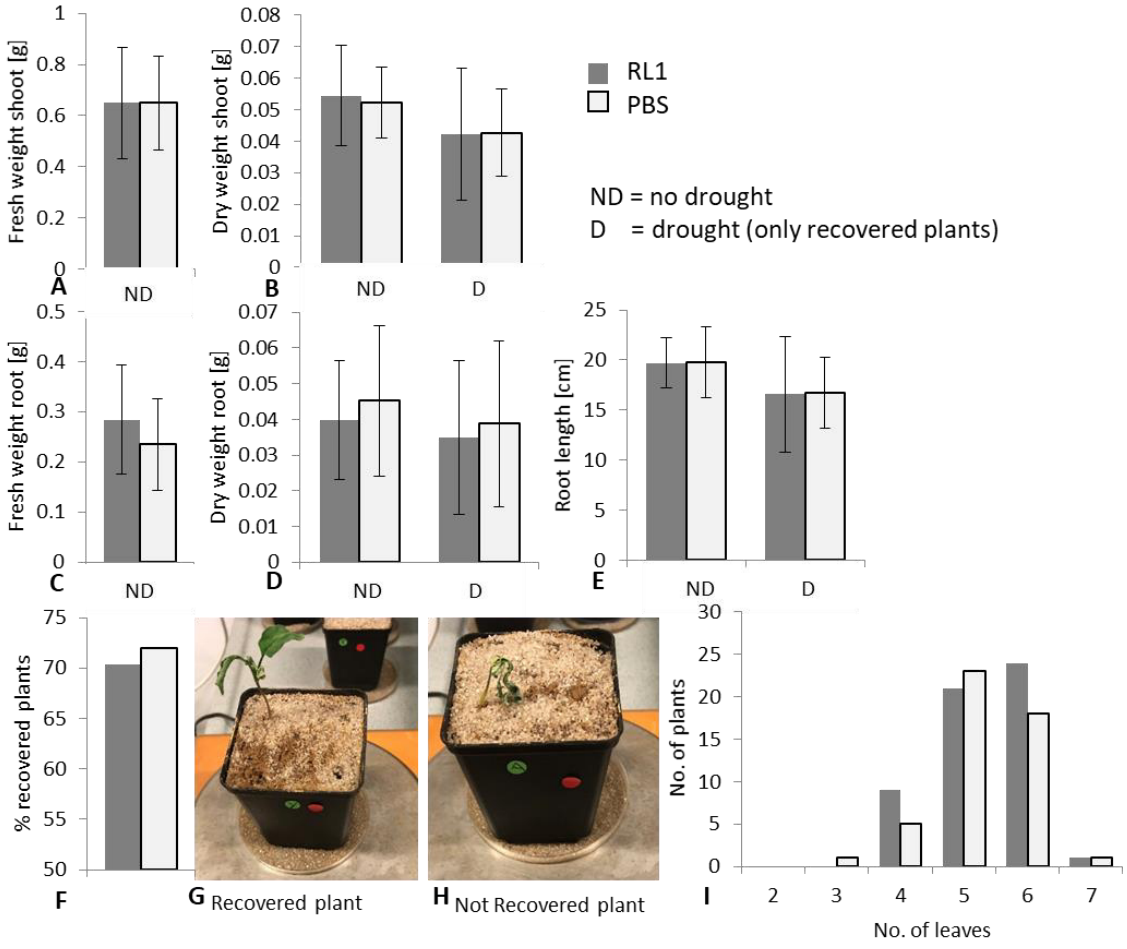

Figure S13: Rucola plants inoculated with RL1 under drought stress. Plants were grown in sand-clay pot system under drought (D) and non-drought conditions (ND). Evaluated plant parameters were shoot fresh weight (**A**), shoot dry weight (**B**), root fresh weight (**C**), root dry weight (**D**), root length (**E**), percent recovered plants (**F**) and number of leaves (**I**). Depicted are examples of recovered (**G**) and not recovered plants (**H**). Error bars indicate standard deviation. Significant difference is indicated by asterisks representing * = $P < 0.05$. RL1 N = 55, PBS N = 48

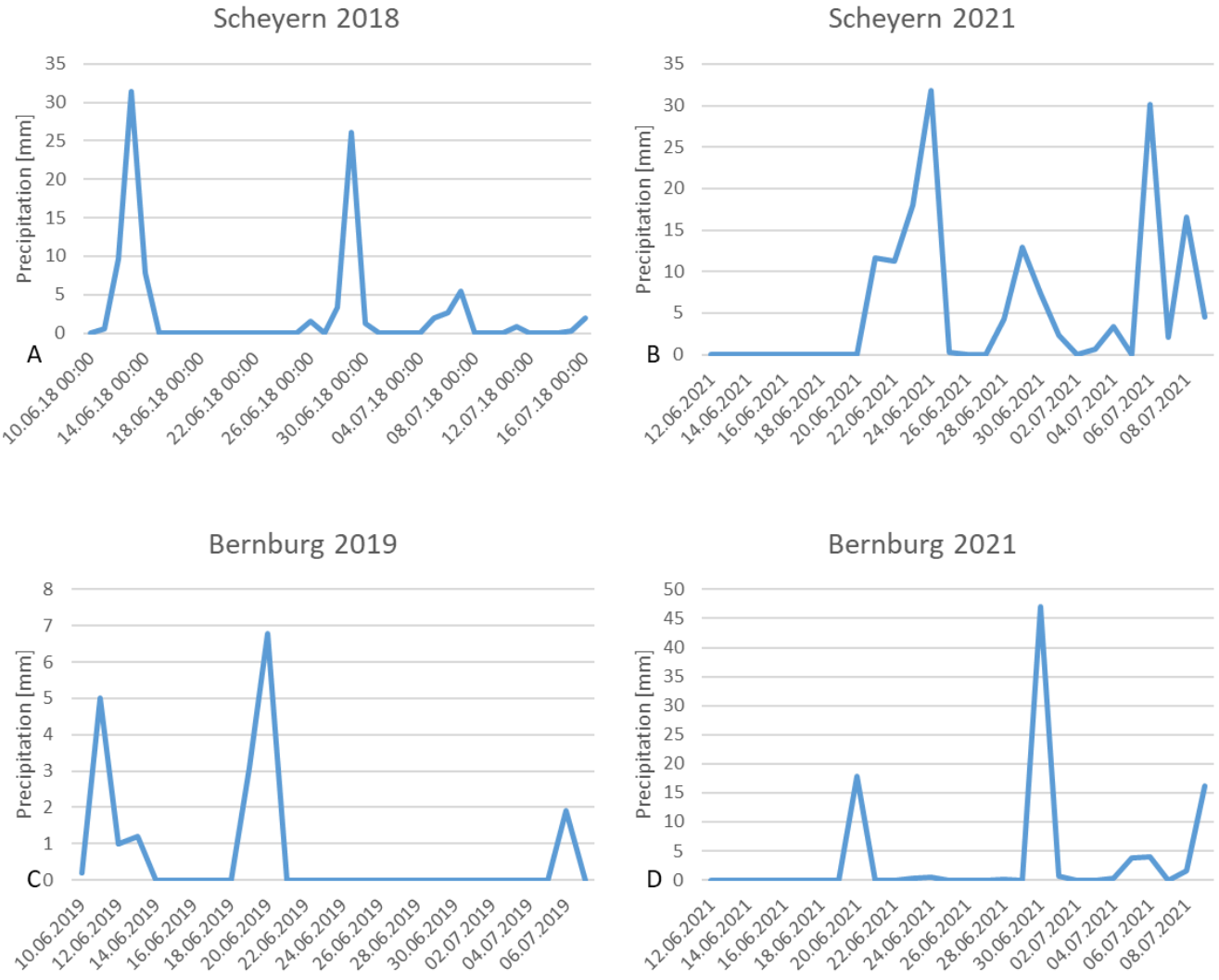

Figure S14: Precipitation rate in mm in Scheyern and Bernburg. Scheyern 2018 (**A**), Scheyern 2021 (**B**), Bernburg 2019 (**C**) and Bernburg 2021 (**D**).

Supplementary Tables

Table S1: List of annotated genes in *Pseudomonas* sp. SCA7 with the Software antiSMASH.

	Type	From (bp)	To (bp)	Most similar known cluster	Class of secondary metabolites	Similarity	comment/category
1	NRPS	60,885	137,783	lokisin	NRP	85%	Antifungal compounds
2	sidero-phore	1,322,522	1,334,372				siderophore
3	RiPP-like	1,537,456	1,547,441				multiple functions
4	NRPS	1,816,323	1,888,411	pyoverdin	NRP	18%	Siderophore/Antifungal com-pounds
5	RiPP-like	2,669,750	2,680,637				multiple functions
6	arylpoly-ene	3,653,220	3,696,824	APE Vf	Other	40%	biocontrol in general, most com-mon group of BGC in proteobac-teria, biofilm formation
7	NRPS-like	4,008,341	4,038,506	fragin	NRP	37%	Antifungal compounds
8	redox-co-factor	4,743,426	4,765,582	lankacidin C	NRP + Polyketide	13%	antibiotic
9	NAGGN	5,960,677	5,975,567				osmotic stress
10	NRPS	6,115,849	6,168,847	pyoverdin	NRP	17%	Siderophore/Antifungal com-pounds
11	betalactone	6,507,383	6,530,646	fengycin	NRP	13%	Antifungal compounds

Table S2: List of annotated genes in *Pseudomonas* sp. SCA7. Functional annotation of the genome was performed with RAST and antiSMASH software.

category/function	Annotated Genes and Cluster	SCA2728.1_7 gene ID
Auxin biosynthesis	Tryptophan synthase alpha chain (EC 4.2.1.20)	KBP52_17925
	Tryptophan synthase beta chain (EC 4.2.1.20)	KBP52_17930
	Anthranilate phosphoribosyltransferase (EC 2.4.2.18)	KBP52_21430
	Phosphoribosylanthranilate isomerase (EC 5.3.1.24)	KBP52_07890
Volatile production		
Butanediol metabolism/synthesis	Acetolactate synthase large subunit (EC 2.2.1.6)	KBP52_23150
	Acetolactate synthase small subunit (EC 2.2.1.6)	KBP52_23155
	BarA sensory histidine kinase (= VarS = GacS)	KBP52_26130
1-Undecene	Putative 1-Undecene synthesis gene undA: Pyrroloquinoline quinone (Coenzyme PQQ) biosynthesis protein C	KBP52_26850
Siderophore production		
Siderophore Pyoverdine biosynthetic gene cluster	Pyoverdine chromophore precursor synthetase PvdL	KBP52_27520
	Pyoverdine efflux carrier and ATP binding protein	KBP52_08140
	FIG049111: Hypothetical protein in pyoverdin gene cluster	KBP52_27595
	Outer membrane pyoverdine eflux protein	KBP52_08145
	FIG006220: Hypothetical MbtH-like protein	KBP52_27570
	Outer membrane porin, coexpressed with pyoverdine biosynthesis regulon	KBP52_23820
	Outer membrane ferripyoverdine receptor	KBP52_01340
	ABC transporter in pyoverdin gene cluster, periplasmic component	KBP52_27575

	Sigma-70 factor FpvI (ECF subfamily), controling pyoverdin biosynthesis	KBP52_28410
	Putative dipeptidase, pyoverdin biosynthesis PvdM	KBP52_08155
	PvdO, pyoverdine responsive serine/threonine kinase (predicted by OlgaV)	KBP52_08165
	Non-ribosomal peptide synthetase modules, pyoverdine	KBP52_08185, KBP52_08195
	Pyoverdine sidechain non-ribosomal peptide synthetase PvdD	KBP52_08190
	FIG014801: Cation ABC transporter, periplasmic cation-binding protein	KBP52_27590
	pyoverdine-specific efflux macA-like protein	KBP52_08135
	Sigma factor PvdS, controling pyoverdin biosynthesis	KBP52_27515
	ABC transporter in pyoverdin gene cluster, permease component	KBP52_27580
	Hypothetical protein PvdY	KBP52_27510
	Pyoverdin biosynthesis protein PvdH, L-2,4-diaminobutyrate:2-oxoglutarate aminotransferase (EC 2.6.1.76)	KBP52_27565
	FIG139991: Putative thiamine pyrophosphate-requiring enzyme	KBP52_27605
	L-ornithine 5-monooxygenase (EC 1.13.12.-), PvdA of pyoverdin biosynthesis	KBP52_08125
	PvdE, pyoverdine ABC export system, fused ATPase and permease components	KBP52_08170
	ABC transporter in pyoverdin gene cluster, ATP-binding component	KBP52_27580
	FIG137877: Hypothetical protein in pyoverdin gene cluster	KBP52_27600
	Pyoverdine biosynthesis related protein PvdP	KBP52_08150
	Pyoverdin biosynthesis protein PvdN, putative aminotransferase, class V	KBP52_08160
siderophore Achromobactin biosynthetic gene cluster	TonB-dependent ferric achromobactin receptor protein	KBP52_03145
Iron siderophore sensor and receptor system	FIG006045: Sigma factor, ECF subfamily	KBP52_08130, KBP52_13560, KBP52_13580, KBP52_18480, KBP52_25340, KBP52_28410
	Iron siderophore receptor protein	KBP52_13590, KBP52_28420
	Iron siderophore sensor protein	KBP52_02535, KBP52_05035, KBP52_13555, KBP52_13585, KBP52_25335, KBP52_28415
Quorum quenching	Acyl-homoserine lactone acylase PvdQ (EC 3.5.1.-), quorum-quenching	KBP52_02530
Antibiotic compounds		
Colicin V and Bacteriocin Production cluster	Amidophosphoribosyltransferase (EC 2.4.2.14)	KBP52_07865
	Colicin V production protein	KBP52_07870
	Dihydrofolate synthase (EC 6.3.2.12)	KBP52_07880
	Acetyl-coenzyme A carboxyl transferase beta chain (EC 6.4.1.2)	KBP52_07885
	DedA protein	KBP52_22090, KBP52_22200
	DedD protein	KBP52_07875
	tRNA pseudouridine synthase A (EC 4.2.1.70)	KBP52_07895, KBP52_12230
Antifungal compounds		
Putative Phenanzine biosynthetic cluster	PhnB protein	KBP52_02315
	Alkylphosphonate utilization operon protein PhnA	KBP52_22750
	PhnB protein; putative DNA binding 3-demethylubiquinone-9 3-methyltransferase domain protein	KBP52_27640
	Uncharacterized isomerase yddE, PhzC-PhzF family	KBP52_24585
Stress resistance	Osmotic stress (36) (Choline and betaine uptake, Glucans and sacrosine biosynthesis)	multiple genes
	Oxidative stress (95)	multiple genes

	Cold shock (6)	multiple genes
	Heat shock (17)	multiple genes
	Detoxification (28)	multiple genes
	Stress Response - no subcategory (36)	multiple genes
	Periplasmic Stress (6)	multiple genes

Table S3: List of annotated KEGG pathways in *Rhodococcus qingshengii* RL1. Number of identified genes of the respective pathway in RL1 in brackets.

Pathways KAAS (No. of identified Genes in RL1)			
00010 Glycolysis / Gluconeogenesis (36)	00571 Lipoarabinomannan (LAM) biosynthesis (11)	03050 Proteasome (3)	04976 Bile secretion (1)
00020 Citrate cycle (TCA cycle) (24)	00572 Arabinogalactan biosynthesis - Mycobacterium (10)	03018 RNA degradation (15)	04975 Fat digestion and absorption (1)
00030 Pentose phosphate pathway (18)	00730 Thiamine metabolism (12)	03030 DNA replication (14)	04979 Cholesterol metabolism (2)
00040 Pentose and glucuronate interconversions (10)	00740 Riboflavin metabolism (10)	03410 Base excision repair (12)	04978 Mineral absorption (1)
00051 Fructose and mannose metabolism (17)	00750 Vitamin B6 metabolism (7)	03420 Nucleotide excision repair (8)	04964 Proximal tubule bicarbonate reclamation (2)
00052 Galactose metabolism (10)	00760 Nicotinate and nicotinamide metabolism (17)	03430 Mismatch repair (11)	04724 Glutamatergic synapse (3)
00053 Ascorbate and aldarate metabolism (3)	00770 Pantothenate and CoA biosynthesis (14)	03440 Homologous recombination (20)	04727 GABAergic synapse (3)
00500 Starch and sucrose metabolism (25)	00780 Biotin metabolism (7)	03450 Non-homologous end-joining (2)	04728 Dopaminergic synapse (1)
00520 Amino sugar and nucleotide sugar metabolism (32)	00785 Lipoic acid metabolism (3)	02010 ABC transporters (96)	04726 Serotonergic synapse (1)
00620 Pyruvate metabolism (38)	00790 Folate biosynthesis (18)	02060 Phosphotransferase system (PTS) (5)	04730 Long-term depression (1)
00630 Glyoxylate and dicarboxylate metabolism (31)	00670 One carbon pool by folate (13)	03070 Bacterial secretion system (13)	04723 Retrograde endocannabinoid signaling (1)
00640 Propanoate metabolism (29)	00830 Retinol metabolism (4)	02020 Two-component system (77)	04211 Longevity regulating pathway (2)
00650 Butanoate metabolism (31)	00860 Porphyrin and chlorophyll metabolism (37)	04014 Ras signaling pathway (1)	04212 Longevity regulating pathway - worm (6)
00660 C5-Branched dibasic acid metabolism (8)	00130 Ubiquinone and other terpenoid-quinone biosynthesis (12)	04013 MAPK signaling pathway - fly (1)	04213 Longevity regulating pathway - multiple species (5)
00562 Inositol phosphate metabolism (11)	00900 Terpenoid backbone biosynthesis (13)	04016 MAPK signaling pathway - plant (3)	04713 Circadian entrainment (1)
00190 Oxidative phosphorylation (41)	00909 Sesquiterpenoid and triterpenoid biosynthesis (1)	04011 MAPK signaling pathway - yeast (1)	04714 Thermogenesis (3)
00195 Photosynthesis (8)	00906 Carotenoid biosynthesis (4)	04371 Apelin signaling pathway (1)	04626 Plant-pathogen interaction (5)
00710 Carbon fixation in photosynthetic organisms (11)	00981 Insect hormone biosynthesis (2)	04630 Jak-STAT signaling pathway (1)	05200 Pathways in cancer (6)
00720 Carbon fixation pathways in prokaryotes (25)	00908 Zeatin biosynthesis (2)	04066 HIF-1 signaling pathway (7)	05202 Transcriptional misregulation in cancer (1)
00680 Methane metabolism (26)	00903 Limonene and pinene degradation (5)	04068 FoxO signaling pathway (3)	05206 MicroRNAs in cancer (3)
00910 Nitrogen metabolism (17)	00281 Geraniol degradation (5)	04020 Calcium signaling pathway (1)	05205 Proteoglycans in cancer (2)
00920 Sulfur metabolism (28)	01051 Biosynthesis of ansamycins (1)	04070 Phosphatidylinositol signaling system (2)	05204 Chemical carcinogenesis (2)
00061 Fatty acid biosynthesis (12)	00523 Polyketide sugar unit biosynthesis (4)	04072 Phospholipase D signaling pathway (1)	05203 Viral carcinogenesis (2)
00062 Fatty acid elongation (2)	01054 Nonribosomal peptide structures (2)	04071 Sphingolipid signaling pathway (3)	05230 Central carbon metabolism in cancer (7)

00071 Fatty acid degradation (24)	01053 Biosynthesis of siderophore group nonribosomal peptides (4)	04024 cAMP signaling pathway (2)	05231 Choline metabolism in cancer (1)
00072 Synthesis and degradation of ketone bodies (6)	01055 Biosynthesis of vancomycin group antibiotics (1)	04151 PI3K-Akt signaling pathway (4)	05212 Pancreatic cancer (1)
00100 Steroid biosynthesis (3)	00940 Phenylpropanoid biosynthesis (2)	04152 AMPK signaling pathway (1)	05225 Hepatocellular carcinoma (2)
00120 Primary bile acid biosynthesis (2)	00950 Isoquinoline alkaloid biosynthesis (3)	04075 Plant hormone signal transduction (1)	05211 Renal cell carcinoma (1)
00140 Steroid hormone biosynthesis (4)	00960 Tropane, piperidine and pyridine alkaloid biosynthesis (2)	04080 Neuroactive ligand-receptor interaction (1)	05219 Bladder cancer (1)
00561 Glycerolipid metabolism (13)	00232 Caffeine metabolism (1)	04144 Endocytosis (1)	05215 Prostate cancer (1)
00564 Glycerophospholipid metabolism (15)	00965 Betalain biosynthesis (1)	04145 Phagosome (1)	05223 Non-small cell lung cancer (1)
00565 Ether lipid metabolism (3)	00966 Glucosinolate biosynthesis (2)	04142 Lysosome (2)	05340 Primary immunodeficiency (3)
00600 Sphingolipid metabolism (3)	00332 Carbapenem biosynthesis (2)	04146 Peroxisome (15)	05010 Alzheimer disease (3)
00590 Arachidonic acid metabolism (1)	00261 Monobactam biosynthesis (8)	04138 Autophagy - yeast (1)	05014 Amyotrophic lateral sclerosis (ALS) (4)
00591 Linoleic acid metabolism (1)	00521 Streptomycin biosynthesis (9)	04112 Cell cycle - Caulobacter (9)	05016 Huntington disease (3)
00592 alpha-Linolenic acid metabolism (5)	00524 Neomycin, kanamycin and gentamicin biosynthesis (1)	04113 Meiosis - yeast (2)	05020 Prion diseases (1)
01040 Biosynthesis of unsaturated fatty acids (6)	00525 Acarbose and validamycin biosynthesis (2)	04214 Apoptosis - fly (2)	05030 Cocaine addiction (1)
00230 Purine metabolism (54)	00401 Novobiocin biosynthesis (4)	04216 Ferroptosis (2)	05031 Amphetamine addiction (1)
00240 Pyrimidine metabolism (26)	00405 Phenazine biosynthesis (4)	04217 Necroptosis (5)	05034 Alcoholism (1)
00250 Alanine, aspartate and glutamate metabolism (30)	00333 Prodigiosin biosynthesis (2)	04550 Signaling pathways regulating pluripotency of stem cells (1)	05418 Fluid shear stress and atherosclerosis (5)
00260 Glycine, serine and threonine metabolism (30)	00998 Biosynthesis of various secondary metabolites - part 2 (2)	02024 Quorum sensing (35)	04930 Type II diabetes mellitus (1)
00270 Cysteine and methionine metabolism (30)	00997 Biosynthesis of various secondary metabolites - part 3 (1)	05111 Biofilm formation - Vibrio cholerae (7)	04940 Type I diabetes mellitus (2)
00280 Valine, leucine and isoleucine degradation (28)	00362 Benzoate degradation (23)	02025 Biofilm formation - Pseudomonas aeruginosa (9)	04931 Insulin resistance (4)
00290 Valine, leucine and isoleucine biosynthesis (12)	00627 Aminobenzoate degradation (10)	02026 Biofilm formation - Escherichia coli (11)	04934 Cushing syndrome (2)
00300 Lysine biosynthesis (14)	00364 Fluorobenzoate degradation (9)	02030 Bacterial chemotaxis (3)	05120 Epithelial cell signaling in Helicobacter pylori infection (1)
00310 Lysine degradation (13)	00625 Chloroalkane and chloroalkene degradation (10)	02040 Flagellar assembly (1)	05130 Pathogenic Escherichia coli infection (1)
00220 Arginine biosynthesis (24)	00361 Chlorocyclohexane and chlorobenzene degradation (6)	04621 NOD-like receptor signaling pathway (2)	05132 Salmonella infection (3)
00330 Arginine and proline metabolism (23)	00623 Toluene degradation (3)	04622 RIG-I-like receptor signaling pathway (1)	05134 Legionellosis (4)
00340 Histidine metabolism (19)	00622 Xylene degradation (7)	04612 Antigen processing and presentation (1)	05150 Staphylococcus aureus infection (1)
00350 Tyrosine metabolism (16)	00633 Nitrotoluene degradation (3)	04658 Th1 and Th2 cell differentiation (1)	05152 Tuberculosis (5)
00360 Phenylalanine metabolism (26)	00642 Ethylbenzene degradation (1)	04659 Th17 cell differentiation (2)	05166 Human T-cell leukemia virus 1 infection (2)
00380 Tryptophan metabolism (22)	00643 Styrene degradation (7)	04657 IL-17 signaling pathway (1)	05162 Measles (1)
00400 Phenylalanine, tyrosine and tryptophan biosynthesis (22)	00791 Atrazine degradation (5)	04666 Fc gamma R-mediated phagocytosis (1)	05161 Hepatitis B (1)
00410 beta-Alanine metabolism (11)	00930 Caprolactam degradation (5)	04062 Chemokine signaling pathway (1)	05169 Epstein-Barr virus infection (1)
00430 Taurine and hypotaurine metabolism (6)	00621 Dioxin degradation (4)	04910 Insulin signaling pathway (3)	05165 Human papillomavirus infection (1)
00440 Phosphonate and phosphinate metabolism (1)	00626 Naphthalene degradation (6)	04922 Glucagon signaling pathway (7)	05146 Amoebiasis (1)

00450 Selenocompound metabolism (11)	00624 Polycyclic aromatic hydrocarbon degradation (3)	04920 Adipocytokine signaling pathway (3)	05145 Toxoplasmosis (1)
00460 Cyanoamino acid metabolism (4)	00984 Steroid degradation (12)	03320 PPAR signaling pathway (6)	05142 Chagas disease (American trypanosomiasis) (1)
00471 D-Glutamine and D-glutamate metabolism (5)	00980 Metabolism of xenobiotics by cytochrome P450 (6)	04912 GnRH signaling pathway (1)	05143 African trypanosomiasis (1)
00472 D-Arginine and D-ornithine metabolism (3)	00982 Drug metabolism - cytochrome P450 (5)	04913 Ovarian steroidogenesis (1)	01501 beta-Lactam resistance (8)
00473 D-Alanine metabolism (2)	00983 Drug metabolism - other enzymes (8)	04915 Estrogen signaling pathway (1)	01502 Vancomycin resistance (6)
00480 Glutathione metabolism (11)	03020 RNA polymerase (4)	04914 Progesterone-mediated oocyte maturation (1)	01503 Cationic antimicrobial peptide (CAMP) resistance (5)
00510 N-Glycan biosynthesis (1)	03022 Basal transcription factors (1)	04917 Prolactin signaling pathway (1)	01524 Platinum drug resistance (1)
00515 Mannose type O-glycan biosynthesis (1)	03040 Spliceosome (1)	04926 Relaxin signaling pathway (1)	01523 Antifolate resistance (5)
00514 Other types of O-glycan biosynthesis (1)	03010 Ribosome (52)	04918 Thyroid hormone synthesis (1)	04970 Salivary secretion (1)
00531 Glycosaminoglycan degradation (1)	00970 Aminoacyl-tRNA biosynthesis (23)	04919 Thyroid hormone signaling pathway (1)	04122 Sulfur relay system (7)
00563 Glycosylphosphatidylinositol (GPI)-anchor biosynthesis (1)	03008 Ribosome biogenesis in eukaryotes (2)	04928 Parathyroid hormone synthesis, secretion and action (1)	04927 Cortisol synthesis and secretion (1)
00550 Peptidoglycan biosynthesis (19)	03060 Protein export (16)	04614 Renin-angiotensin system (1)	04141 Protein processing in endoplasmic reticulum (3)
00511 Other glycan degradation (1)			

Table S4: List of annotated genes in *Rhodococcus qingshengii* RL1 with the Software PIFAR.

geneID	Start	End	Input sequence	Strand	Factor type	Factor name	method	evalue
orf_0058	51003	53306	SEQ_1	1	Detoxification	Copper resistance cueAR	BLAST	3.00E-141
orf_0951	261253	262119	SEQ_3	1	EPS	galU	BLAST	6.00E-59
orf_1207	517884	519362	SEQ_3	1	Protease	htrA	BLAST	7.00E-44
orf_1345	683003	684058	SEQ_3	-1	Volatiles	2-3 butanediol	BLAST	3.00E-76
orf_1592	944117	944566	SEQ_3	1	Metabolism	aroQ	BLAST	8.00E-36
orf_1754	1106778	1107761	SEQ_3	-1	Detoxification	pip	BLAST	3.00E-108
orf_1787	1136730	1137740	SEQ_3	-1	PCWDE	lipA	BLAST	2.00E-84
orf_1806	1154072	1155997	SEQ_3	-1	Metabolism	asnB	BLAST	1.00E-20
orf_2029	1412833	1413642	SEQ_3	1	Metabolism	trpCG	BLAST	5.00E-51
orf_2042	1429614	1430231	SEQ_3	1	MAMP	Chemotaxis protein CheY	BLAST	3.00E-19
orf_2391	1835245	1835754	SEQ_3	-1	Metabolism	aroK	BLAST	4.00E-28
orf_2392	1835768	1836955	SEQ_3	-1	Metabolism	aroC	BLAST	2.00E-59
orf_2653	2104070	2104717	SEQ_3	-1	Siderophore	Bacillibactin	BLAST	3.00E-90
orf_2654	2104754	2106418	SEQ_3	-1	Siderophore	Bacillibactin	BLAST	0
orf_2655	2106460	2107260	SEQ_3	-1	Siderophore	Bacillibactin	BLAST	1.00E-50
orf_2682	2130292	2131755	SEQ_3	1	PCWDE	Cellulase	HMMER	2.40E-33
orf_2717	2167343	2168746	SEQ_3	-1	MDRs	MatE	HMMER	3.90E-26
orf_2752	2200229	2201767	SEQ_3	-1	Metabolism	mqo	BLAST	1.00E-159
orf_2765	2211876	2212226	SEQ_3	1	MDRs	Multi Drug Res	HMMER	2.40E-19
orf_2766	2212223	2212549	SEQ_3	1	MDRs	Multi Drug Res	HMMER	2.10E-23

orf_2889	2339906	2341711	SEQ_3	-1	Volatiles	budB	BLAST	6.00E-49
orf_3167	2631250	2632842	SEQ_3	1	Biofilm	Phosphoglucomutase protein yhxB	BLAST	3.00E-60
orf_3396	2869121	2882941	SEQ_3	-1	Siderophore	Bacillibactin	BLAST	0
orf_3396	2869121	2882941	SEQ_3	-1	Antibiotic	Fusaricidin	BLAST	0
orf_4078	3555729	3557951	SEQ_3	-1	Detoxification	katG	BLAST	0
orf_4220	3687531	3688619	SEQ_3	1	Siderophore	Bacillibactin	BLAST	8.00E-71
orf_4305	3774138	3775031	SEQ_3	-1	Metabolism	Purine biosynthesis purC	BLAST	6.00E-89
orf_4325	3800304	3801560	SEQ_3	-1	Metabolism	Purine biosynthesis purD	BLAST	9.00E-98
orf_4352	3829477	3829866	SEQ_3	1	MDRs	Multi_Drug_Res	HMMER	2.00E-22
orf_4701	4188558	4190246	SEQ_3	-1	Hormone	IAA_2	BLAST	5.00E-57
orf_4828	4326220	4327251	SEQ_3	1	Siderophore	arthrobactin	BLAST	1.00E-51
orf_4839	4337734	4339185	SEQ_3	-1	Detoxification	katB	BLAST	6.00E-101
orf_5046	4544094	4544936	SEQ_3	1	LPS	wzt	BLAST	1.00E-51
orf_5159	4671968	4673068	SEQ_3	-1	Hormone	Salycilic hydroxylase	BLAST	1.00E-18
orf_5253	4770921	4772372	SEQ_3	-1	Metabolism	Glutamate synthase gltBD	BLAST	1.00E-88
orf_5254	4772365	4776882	SEQ_3	-1	Metabolism	Glutamate synthase gltBD	BLAST	0
orf_5283	4800775	4801440	SEQ_3	-1	Metabolism	trpCG	BLAST	7.00E-65
orf_5404	4932161	4933726	SEQ_3	-1	Hormone	IAA_2	BLAST	5.00E-29
orf_5601	5128592	5130760	SEQ_3	1	Detoxification	katE	BLAST	0
orf_5672	5196732	5198201	SEQ_3	-1	PCWDE	Cellulase	HMMER	4.80E-57
orf_5860	5394494	5395975	SEQ_3	1	Metabolism	Citrate transporter	BLAST	4.00E-122
orf_6113	5621154	5621996	SEQ_3	-1	Antibiotic	Bacilysocin	BLAST	1.00E-23
orf_6476	5982132	5982755	SEQ_3	1	Biofilm	Signal peptidase I W sipW	BLAST	4.00E-20
orf_3991	3485966	3487453	SEQ_3	1	type_III_effector	RipTPS	BLAST	4.00E-68
orf_4368	3861937	3863472	SEQ_3	1	type_III_effector	RipTPS	BLAST	2.00E-64

Table S5: List of annotated genes in *Rhodococcus qingshengii* RL1 with the Software antiSMASH.

	Type	**From (bp)**	**To (bp)**	**Most similar known cluster**	**Class of secondary metabolites**	**Similarity**
1	ectoine	965,135	975,533	ectoine	Other	75%
2	terpene	1,174,497	1,194,805	isorenieratene	Terpene	25%
3	NRPS	1,274,976	1,329,636	monensin	Polyketide	5%
4	NRPS	1,332,756	1,415,066	rifamorpholine A / rifamorpholine B / rifamorpholine C / rifamorpholine D / rifamorpholine E	Polyketide	4%
5	NRPS	1,634,393	1,697,371	coelichelin	NRP	27%
6	NRPS,terpene	1,730,598	1,783,490	SF2575	Polyketide:Type II + Saccharide:Hybrid/tailoring	6%
7	NRPS	2,071,856	2,126,033	heterobactin A / heterobactin S2	NRP	100%
8	NRPS-like	2,390,492	2,432,746	thiolutin	NRP	8%
9	NRPS	2,824,057	2,931,597	chloramphenicol	NRP	17%

10	NRPS	3,572,754	3,618,512	hygromycin A	Saccharide	9%
11	NRPS	3,815,523	3,872,232	erythrochelin	NRP	57%
12	NRPS-like	4,205,438	4,249,331			
13	T1PKS	4,378,613	4,424,648	kirromycin	NRP + Polyketide:Modular type I + Polyketide:Trans-AT type I	8%
14	T1PKS	4,557,040	4,601,965			
15	LAP	4,692,380	4,722,476	diisonitrile antibiotic SF2768	NRP	11%
16	bacteriocin	4,882,807	4,894,737	branched-chain fatty acids	Other	75%
17	lanthipeptide	5,270,044	5,292,626			
18	butyrolactone	5,522,805	5,533,692			

Table S6: List of annotated genes in *Rhodococcus qingshengii* RL1. Functional annotation of the genome was performed with RAST, PIFAR and antiSMASH softwares.

Category	Annotated Genes and Cluster	RL1 gene ID
Osmotic stress		
	hydroxyacid dehydrogenase	D6M20_07215
	L-ectoine synthase	D6M20_07220
	Diaminobutyrate--2-oxoglutarate transaminase (EC 2.6.1.76)	D6M20_07225
	glycerol uptake facilitator protein (aquaporine family)	D6M20_03015
	Glycine betaine transporter OpuD	D6M20_04180
	L-Proline/Glycine betaine transporter ProP	D6M20_07250, D6M20_20860
	High-affinity choline uptake protein BetT	D6M20_22060
Salt stress	Na+/H+ antiporter A and Na+/H+ antiporter B	D6M20_17510
	Na+/H+ antiporter C	D6M20_17515
	Na+/H+ antiporter D	D6M20_17520
	Na+/H+ antiporter E	D6M20_17525
	Na+/H+ antiporter F	D6M20_17530
	Na+/H+ antiporter G	D6M20_17535
Oxidative stress	Catalase KatE-intracellular protease (EC 1.11.1.6)	D6M20_26210
	Catalase-peroxidase KatG (EC 1.11.1.21)	D6M20_19015
	Catalase KatE (EC 1.11.1.6)	D6M20_22570
	superoxide dismutase [Mn]	D6M20_23995
	sigmafactor SigB , SigF	D6M20_00855 (plasmid), D6M20_01170 (plasmid), D6M20_11750, D6M20_17130, D6M20_18680
	bacterial hemoglobin gene	D6M20_07015
pH tolerance	squalene cyclase	D6M20_23450
	Arginine deiminase (arcA)	D6M20_04155
	ornithine carbamoyltransferase (arcB)	D6M20_09510
	ornithine/arginine antiporter (arcD)	D6M20_24210
	arginine pathway regulatory protein of the ArgR-AhrC family (argR)	D6M20_09515
DNA phosphorothio-ation	Cysteine desulfurase *DndA*	D6M20_05845
	DNA sulfur modification protein *DndB*	D6M20_05850

	DNA phosphorothioation system sulfutransferase *DndC*	D6M20_05855
	DNA sulphur modification protein *DndD*	D6M20_05860
	DndE	D6M20_05865
	DNA phosphorothioation-associated putative methyltransferase	D6M20_05870
	DNA phosphorothioation-associated protein 4	D6M20_05875
Multidrug resistance	Multi_Drug_Res (PF00893) family	D6M20_06295
	DAED/DEAH box helicase family protein	D6M20_05885
	GIY-YIG nuclease family protein	D6M20_05895
	plasmid pRiA4b ORF-3 family protein	D6M20_05905
Antibiotic resistance	vancomycin resistance protein	D6M20_19620
	beta-lactamase	D6M20_27815
	Metal-dependent hydrolases of the beta-lactamase superfamily III	D6M20_06650
	Beta-lactamase class C-like and penicillin binding proteins (PBPs) superfamily	D6M20_07770, D6M20_12855, D6M20_15185, D6M20_15195, D6M20_20105, D6M20_21115
	rifampicin monooxygenase	D6M20_14905
Tellurite resistance	Tellurium ion resistance protein TerA	D6M20_04715
	Tellurite resistance TerB	D6M20_21770
	tellurium ion resistance protein TerD	D6M20_21785, **D6M20_21815**, D6M20_30505, **D6M20_05745**
Heavy metal resistance/detoxification	copper-translocating protein	D6M20_04250
	Cytoplasmic copper homeostasis protein CutC	D6M20_06255
	ATPase:Heavy metal (Lead, cadmium, zinc, mercury) translocating P-type ATPase	D6M20_04240, D6M20_00235
	heavy-metal-associated domain-containing protein/heavy metal transport/detoxification protein	D6M20_04250
	Copper resistance protein CopD	D6M20_06885
	Arsenical pump-driving ATPase (EC 3.6.3.16) TEMP	D6M20_00060
	Arsenical resistance operon trans-acting repressor ArsD	D6M20_00065
	lead, cadmium, zinc, arsenical resistance proteins	D6M20_19920, D6M20_00050,
	IS110 family transposase	D6M20_28370
	alkylmercury lyase	D6M20_28375
	merR family DNA-binding protein	D6M20_28380
CO degradation	CoxL, large subunit, Xanthine dehydrogenase, molybdenum binding subunit (EC 1.17.1.4)	D6M20_09010
	CoxM, middle subunit, Xanthine dehydrogenase, FAD binding subunit (EC 1.17.1.4)	D6M20_09015
	CoxS, small subunit, carbon monoxide dehydrogenase	D6M20_09005
	Carbon monoxide oxidation accessory protein CoxD	D6M20_07265, D6M20_16125
	Carbon monoxide oxidation accessory protein CoxE	D6M20_07270, D6M20_16120
	Xanthine and CO dehydrogenases maturation factor, XdhC/CoxF family	D6M20_25450
Hydrogen utilization	[NiFe] hydrogenase metallocenter assembly protein HypE	D6M20_12420
	[NiFe] hydrogenase metallocenter assembly protein HypD	D6M20_12425
	[NiFe] hydrogenase metallocenter assembly protein HypC	D6M20_12430
	[NiFe] hydrogenase metallocenter assembly protein HypF	D6M20_12435
	Hydrogenase assembly chaperone HypC/HupF	D6M20_12440
	Hydrogenase maturation protease	D6M20_12445
Degradation of hydrocarbons and organic	Alkane-1 monooxygenase (alkB)	D6M20_00720 (plasmid), D6M20_13355, D6M20_14305, D6M20_18855,

compounds		D6M20_21045, D6M20_27785
	Catechol 1,2-dioxygenase (catA)	D6M20_27935
	Dibenzothiophene desulfurization enzyme B (dszB)	D6M20_25605
Glucosinolate metabolism	branched-chain amino acid aminotransferase	D6M20_08100
	3-isopropylmalate/(R)-2-methylmalate dehydratase large subunit	D6M20_13320
	3-isopropylmalate dehydratase small subunit (EC 4.2.1.33)	D6M20_13315
	ß-glucosidase (myrosinase)	D6M20_11475
	Peptide-methionine (S)-S-oxide reductase/methionine sulfoxide reductase A *msrA*	D6M20_23985
	Peptide-methionine (S)-S-oxide reductase/mehionine sulfoxide reductase B *msrB*	D6M20_11510
	aldoxime dehydratase *oxd*	D6M20_25300
	Alkyl sulfatase and related hydrolases, MBL-fold metallo-hydrolase superfamily	D6M20_19070
	cobalt-containing nitrile hydratase subunit beta	D6M20_25275
	cobalt-containing nitrile hydratase subunit alpha	D6M20_25280
	amidase clustered with urea ABC transporter and nitrile hydratase functions	D6M20_25285
	formamidase	D6M20_17170
	5-aminopentanamidase	D6M20_21895
Bile acid degradation	Bile acid 7-alpha dehydratase BaiE	D6M20_04375
Indole acetic acid production	tryptophan synthase alpha chain	D6M20_09210
	tryptophan synthase beta chain	D6M20_09205
	anthranilate phosphoribosyltransferase	D6M20_08200
	Indole-3-glycerol phosphate synthase	D6M20_09200
	amidase *amiE*	D6M20_30045
	amine oxidase *iaaM* (identified as iaaM in PIFAR, blastP 56% identity with Psyr_1536)	D6M20_13780
Salicylic acid	salicylate hydroxylase	D6M20_24110
Gibberelin production	SDR family oxidoreductase	D6M20_09080
	Lanosterol 14-alpha demethylase @ Cytochrome P450 51	D6M20_09085
	ferredoxin	D6M20_09090
	Geranylgeranyl diphosphate synthase	D6M20_08310
Cytokinin	Phosphoribohydrolase (homolog of plant cytokinin-activating enzyme LOG)	D6M20_05240
Glutamate biosynthesis	glutamate synthase large subunit *gltB*	D6M20_09230, D6M20_24575
	glutamate synthase small subunit	D6M20_09235, D6M20_24570
Spermidine	arginine decarboxylase SpeA	D6M20_01150 (plasmid)
	agmtinase (agmatine deiminase) SpeB	D6M20_03950
	spermidine synthase SpeE	D6M20_07935, D6M20_29000
Siderophore production	chorsimate synthase	D6M20_10990
	class I SAM-dependent methyltransferase	D6M20_12200
	amino acid adenylation domain-containing protein	D6M20_12245
	isochorismatase	D6M20_12255
	2,3-dihydroxybenzoate-AMP ligase	D6M20_12260
	2,3-dihydro-2,3-dihydroxybenzoate dehydrogenase	D6M20_12265
	isochorismatase	D6M20_12270

	isochorismatase synthase	D6M20_12275
	ABC transporter ATP-binding protein	D6M20_12210
	MFS transporter	D6M20_12225
	enterobactin transporter EntS	D6M20_12235
	ABC transporter substrate-binding protein	D6M20_12240
	ATP-binding cassette domain-containing protein	D6M20_12305
	sigma-70 family RNA polymerase sigma factor	D6M20_12190
	TipAS antibiotic-recognition domain-containing protein	D6M20_12335
	TetR/AcrR family transcriptional regulator	D6M20_12350
	o-succinylbenzoate synthase	D6M20_20205
	M20 family metallopeptidase	D6M20_20215
	MbtH family protein	D6M20_20290
	lysine N(6)-hydroxylase/L-ornithine N(5)-oxygenase family protein	D6M20_20295
	non-ribosomal peptide synthetase	D6M20_20300
	MMPL family transporter	D6M20_20310
	alpha/beta hydrolase	D6M20_20325
	methionyl-tRNA formyltransferase	D6M20_20330
	MFS transporter	D6M20_20225
	ATP-binding cassette domain-containing protein	D6M20_20335
	ABC transporter ATP-binding protein	D6M20_20340
	HAMP domain-containing histidine kinase	D6M20_20245
	response regulator transcription factor	D6M20_20250
Iron acquisition	ferrous iron transport peroxidase EfeB	D6M20_04645
	ferrous iron transport permease EfeU	D6M20_04655
	ferrous iron transport periplasmic protein EfeO	D6M20_04650
Organic acid production	6-phosphogluconate dehydrogenase	D6M20_10425, D6M20_24825
	L-lactate dehydrogenase	D6M20_05005
Phosphate metabolism	alkaline phosphatase	D6M20_15135
	inorganic pyrophosphatase	D6M20_21710
	Phosphate ABC transporter, periplasmic phosphate-binding protein PstS	D6M20_30820
	Phosphate transport system permease protein PstC	D6M20_30825
	Phosphate transport system permease protein PstA	D6M20_30830
	Phosphate transport ATP-binding protein PstB	D6M20_30835
Aromatic carbon metabolism	enoyl-CoA hydratase	D6M20_19280
	fumarylacetoacetate hydrolase	D6M20_19325
Nitrogen metabolism	uncharacterized NifU-like protein (MSMEG_2718)	D6M20_12465
	Respiratory nitrate reductase gamma chain (EC 1.7.99.4)	D6M20_00810
	Respiratory nitrate reductase delta chain (EC 1.7.99.4), nitrate reductase molybdenum cofactor assembly chaperone	D6M20_00815
	Respiratory nitrate reductase beta chain (EC 1.7.99.4)	D6M20_00820
	Respiratory nitrate reductase alpha chain (EC 1.7.99.4)	D6M20_00825
	FdhF/YdeP family oxidoreductase	D6M20_00830
Carbon metabolism	LacI transcription regulator	D6M20_14825, D6M20_21260, D6M20_30610

	aldo-keto reductase	D6M20_03265, D6M20_03280, D6M20_05680, D6M20_09925, D6M20_13825, D6M20_14655, D6M20_29790
Volatiles	acetolactate synthase small subunit *budB*	D6M20_13380
	acetolactate synthase large subunit *budB*	D6M20_13385
	(R,R)-butanediol dehydrogenase	D6M20_05945, D6M20_29895
	lipoyl synthase *lipA*	D6M20_08065, D6M20_29915
Exopolysaccharides	UTP--glucose-1-phosphate uridylyltransferase *galU*	D6M20_04080, D6M20_18535
Proteases	periplasmic serine endoprotease DegP-like *htrA*	D6M20_05305
Biofilm formation	phosphoglucomutase	D6M20_13745
	signal peptidase I W	D6M20_27405, D6M20_13075, D6M20_17775
MAMP	chemotaxis protein CheY	D6M20_26160
Antibiotic production	dTDP-glucose 4,6-dehydratase	D6M20_23600
Quorum sensing	two-component transcriptional response regulator from the LuxR family	D6M20_29615
Quorum quenching	*qsdA* Aryldialkylphosphatase (phosphotriester-ase/paraoxonase/putative php); putative N-Acyl homoserine lac-tonase	D6M20_27580

Table S7: Singleton genes RL1. Analysis was based on genome comparison with BG43 and djl6 in EDGAR.

Category	Annotated Gene	Gene locus tag RL1
Aromatic carbon metabolism	enoyl-CoA hydratase/isomerase family protein	D6M20_RS19280
	fumarylacetoacetate hydrolase	D6M20_RS19325
pH tolerance	squalene cyclase	D6M20_RS23450
DNA phosphorothioation	Cysteine desulfurase *DndA*	D6M20_RS05845
	DNA sulfur modification protein *DndB*	D6M20_RS05850
	DNA phosphorothioation system sulfutransferase *DndC*	D6M20_RS05855
	DNA sulphur modification protein *DndD*	D6M20_RS05860
	DndE	D6M20_RS05865
	DNA phosphorothioation-associated putative methyltransferase	D6M20_RS05870
	DNA phosphorothioation-associated protein 4	D6M20_RS05875
Multidrug resistance	DAED/DEAH box helicase family protein	D6M20_RS05885
	GIY-YIG nuclease family protein	D6M20_RS05895
	plasmid pRiA4b ORF-3 family protein	D6M20_RS05905
Heavy metal resistance	IS110 family transposase	D6M20_RS28370
	alkylmercury lyase	D6M20_RS28375
	merR family DNA-binding protein	D6M20_RS28380
Other	AAA family ATPase	D6M20_RS05880

	bifunctional 3-(3-hydroxy-phenyl)propionate/3-hydroxycinnamic acid hydroxylase	D6M20_RS19290
	MFS transporter	D6M20_RS19300
	helix-turn-helix domain-containing protein	D6M20_RS19305
	DUF3500 domain-containing protein	D6M20_RS19315
	FCD domain-containing protein	D6M20_RS19320
Hypothetical proteins		D6M20_RS05890, D6M20_RS06865, D6M20_RS09680, D6M20_RS09985, D6M20_RS10445, D6M20_RS17155, D6M20_RS17400, D6M20_RS17770, D6M20_RS17780, D6M20_RS18200, D6M20_RS19225, D6M20_RS19295, D6M20_RS19310, D6M20_RS21385, D6M20_RS23515, D6M20_RS23590, D6M20_RS28335

Table S8: Similarities of consortium strains with OTUs in consortium experiments.

Consortium strain ID	highest similarity OTUs	Query (%)	Identity (%)
Cha2930_14	1002	29	99.5
M92526_32	11, 3920	27, 27	99.25, 99.24
R2A20_2	1021, 478, 2	100	95.68
Cha2324a_1	1002, 642, 112	75, 76, 76	97.78, 91.97, 91.97
Cha2324a_4	Low quality sequence		
Cha2324b_23	Low quality sequence		
Cha2324b_3	46	56	100
Cha2324a_8	1002, 160	33, 33	98.8, 97.6
Cha2324b_12	Low quality sequence		
Cha2324b_30	Low quality sequence		
Cha2324a_16	56	33	98.8
M92526_27	33, 736	56	98.02
Cha2324a_18	8, 1338	34, 35	98.41, 98.02
SCA27_61	33, 736	32,32	100, 97.23
SCA27_60	153, 1315	33, 48	100, 92.76
M92526_31	14, 161	32, 32	100, 96.05
NB17_5	21, 53	30, 30	100, 95.65
2xTY356_6	53, 21	32, 32	99.6, 95.29
2xTY356_27	21, 53	32, 32	98.81, 94.47
R2A20_29M	552, 259, 1328, 4	32, 33, 33, 33	98.79, 98.42, 98.02, 98.02

R2A20_29R	Low quality sequence		
M92526_34	4172, 237, 4339	58, 58, 80	98.81, 98.42, 93.66
2xTY356_31	1315, 37, 45	100, 96, 96	97.98, 98.75, 95.42
M925_13	37,1315, 45	31, 45, 31	100, 99.16, 96.84
2xTY356_21	37, 1315, 45	33, 46, 33	98.81, 98.32, 95.65
2xT56_7	37, 1315, 45	32, 46, 32	100, 99.16, 96.84
M925_14	45, 1315, 37	32, 46, 32	99.6, 96.65, 96.44
NB17_19	37, 1315, 45	34, 48, 34	100, 99.16, 96.84

Table S9: Composition of growth media used in this study. All media were prepared with MilliQ water and autoclaved for sterilization. Unless further specified 1.7% agar-agar granulated (Carl Roth, Karlsruhe, Germany) was added for solid media.

Medium	**Composition per liter**
Nutrient Broth (NB)	8 g Nutrient Broth (Carl Roth, Germany) pH 6.8 *Components: beef extract 3 g/l, gelatin peptone 5 g/l)*
Tryptic Soy Broth (TSB)	30 g Tryptic Soy Broth (Sigma, USA) pH 7.3 *Components: casein peptone (pancreatic), 17 g/L, dipotassium hydrogen phosphate, 2.5 g/L, glucose, 2.5 g/L, sodium chloride, 5 g/L, soya peptone (papain digest.), 3 g/L*
M9 Minimal Medium (M9)	33.1 mM Na2HPO4 22 mM KH2PO4 8.55 mM NaCl 9.35 mM NH4Cl 0.4 % glucose 1 mM MgSO4 0.3 mM CaCl2 Preparation: Autoclave stock solutions (M9 salt solution 10X, glucose 20%, CaCl2 1M, MgSO4 1M) separately and mix afterwards: 100 mL M9 salt solution 10X 20 mL glucose solution 20% 0.3 mL $CaCl_2$ solution 1 M 2 ml $MgSO_4$ solution 1 M
2x Tryptone Yeast medium (2xTY) (nutrient enriched medium)	16 g Tryptone 10 g Yeast extract 5 g NaCl pH 7 +/- 0.2
King's B	33 g King Agar B (Fluka Analytical) 10 mL glycerol Agar included pH 7.2 +/- 0.2 *Components: mixed peptone 20 g/L, dipotassium hydrogen phosphate 1.5 g/L, magnesium sulfate 1.5 g/L, agar 10 g/L*

Starch Casein agar (SCA) (selective for actinomycetes, because of complex substrates and high carbon/nitrogen ratio)	10 g starch 0.3 g casein 2 g Kaliumnitrat (KNO_3) 2 g Natriumchloride (NaCl) 2 g K2HPO4 0.05 g MgSO4*7H2O 0.02 g Calciumcarbonate (CaCO3) 0.01 g Ironsulfate (FeSO4*7H2O)
R2A	18.2 g BD™ Difco™ R2A agar (BD Biosciences) agar included pH 7.2 +/- 0.2 *components: yeast extract 0.5 g/L, proteose peptone No.3 0.5 g/L, casamino acids 0.5 g/L, dextrose 0.5 g/L, soluble starch 0.5 g/L, sodium pyruvate 0.3 g/L, dipotassium phosphate 0.3 g/L, magnesium sulfate 0.05 g/L, agar 15 g/L*
Cha agar (selective for sulfur-oxidizing bacteria)	4 g Di-Potassiumhydrogenphosphate (K2HPO4) 4 g Potassium-di-hydrogenphosphate (KH2PO4) 0.8 g Magnesiumsulfate (MgSO4) 0.5 g Na2EDTA-di-sodium-di-hydrate 0.22 g zinc sulfate (ZnSO4) 0.05 g Calciumchloride (CaCl2) 0.01 g Manganchloride (MnCl2) 0.001 g iron sulfate (FeSO4) 0.01 g Ammonium-Hepta-Molybdat-Tetrahydrat ((NH4)6Mo7O24) 0.01 g copper sulfate (CuSO4) 10 g sodiumthiosulfate (Na2S2O3*5H2O) 0.2 g yeast extract
Jensen	20 g Sucrose 1 g K2HPO4 0.5 g MgSO4*5H2O 0.5 g NaCl 0.5 0.1 g FeSO4 0.005 g Na2MoO4 2 g CaCO3
Ashby	20 g Mannitol 0.2 g K2HPO4 0.2 g MgSO4*5H2O 0.2 g NaCl 0.2 0.1 g K2SO4 5 g CaCO3
Nfb medium, semisolid (nitrogen fixation) Döbereiner 1995	5 g L-malic acid 0.5 g K2HPO4 0.2 g MgSO4*7H20 0.1 g NaCl 0.02 g CaCl2 * H2O 2 mL trace element solution (see below) 4 mL Fe-EDTA 1.64% 1 mL Vitamin solution (see below) 1.75 g agar

	pH 6.8 (adjust with KOH) cook in microwave and distribute in culture tubes 5 mL Trace element solution (1 L): 0.4 g CuSO4 x 5 H2O 0.12 g ZnSO4 x 7 H2O 1.4 g H3BO3 0.2 g MnSO4 x H2O 1 g Na2MoO4 x 2 H2O Vitamin solution (1L): 0.1 g Biotin 0.2 g Pyridoxol-HCl
NBRIP (Phosphate solubilization) Nautiyal 1999	10 g glucose 5 g tricalcium phosphate ($Ca_3(PO_4)_2$) 5 g magnesium chloride hexahydrate (MgCl2*6H2O) 0.25 g magnesium sulphate heptahydrate (MgSO4*7H2O) 0.2 g Potassium chloride (KCl) 0.1 g Ammonium sulphate ((NH4)2SO4)
Potato Dextrose agar (PDA)	24 g Potato dextrose agar (Sigma, USA) *Components: potato extract 4.0 g/L, glucose 20.0 g/L*
½ X Murashige Skoog (MS)	2.16 g MS including B5 vitamins (Duchefa Biochemie) 8 g plant agar (Duchefa Biochemie) adjusted to pH 5.7 with KOH
Hoagland's solution	1.6 g Hoagland's No. 2 Basal Salt (Sigma, USA)
Salkowski reagent	0.01 M FeCl3 anhydrous (Fluka Biochemika, Germany) in perchloric acid (HClO4) 35% (Merck, Germany)

B. Publications

AMERICAN SOCIETY FOR MICROBIOLOGY | Microbiology Resource Announcements

GENOME SEQUENCES

De Novo Genome Assembly of a Plant-Associated *Rhodococcus qingshengii* Strain (RL1) Isolated from *Eruca sativa* Mill. and Showing Plant Growth-Promoting Properties

Theresa Kuhl,[a] Marius Felder,[b]* Thomas Nussbaumer,[a,d] Doreen Fischer,[c] Susanne Kublik,[c] Soumitra Paul Chowdhury,[a] Michael Schloter,[c] Michael Rothballer[a]

[a]Institute for Network Biology (INET), Helmholtz Center Munich, Neuherberg, Germany
[b]Research Unit for Plant Genome and Systems Biology (PGSB), Helmholtz Center Munich, Neuherberg, Germany
[c]Research Unit for Comparative Microbiome Analysis (COMI), Helmholtz Center Munich, Neuherberg, Germany
[d]Institute for Environmental Medicine (IEM), UNIKA-T, Augsburg, Germany

ABSTRACT *Rhodococcus qingshengii* RL1 was isolated from surface-sterilized leaves of *Eruca sativa* Mill. and shows plant growth-promoting (PGP) properties. The *de novo* genome assembly consists of one chromosome with 6,253,838 bp and two plasmids with 144,038 bp and 448,745 bp. Many genes could be identified reflecting its PGP potential.

The genus *Rhodococcus* belongs to the phylum *Actinobacteria* and includes aerobic, Gram-positive, nonsporulating bacteria isolated from a broad variety of environments (1–3). Some of these bacteria have large genomes (>5 Mb) with high G+C content (1–4). Their ability to degrade a large spectrum of environmentally problematic compounds (2, 5) or perform quorum quenching (4) makes them suitable for bioremediation or agricultural applications.

RL1 was isolated from leaves of *Eruca sativa* Mill. Leaves were surface sterilized with 12% NaOCl, washed with sterile water, and macerated with sterile saline. The extract was plated on R2 agar and allowed to grow at 22°C for 5 days. Selected colonies were picked and allowed to grow on tryptic soy agar (TSA) and R2 agar at 28°C. For sequencing genomic DNA from RL1, a single colony picked from an agar plate was grown overnight in tryptic soy broth at 28°C. DNA was isolated via standard phenol-chloroform extraction with previous lysis with 600 μg/ml ampicillin for 3 h before extraction. For the PacBio Sequel system, the library was prepared with the SMRTbell template prep kit 1.0-SPv3 and SMRTbell barcoded adapter complete prep kit-96. PacBio sequencing was performed with the Sequel sequencing kit 2.0 (8 reactions) and single-molecule real-time (SMRT) cell 1 M v2 tray. For Illumina MiSeq sequencing, the library was prepared using the TruSeq DNA PCR-free library preparation kit (Illumina, San Diego, CA, USA). Genomic DNA was fragmented by applying the Covaris E220 system according to the manufacturer's protocol for a 550-bp average insert size and sequenced using MiSeq reagent kit v3 (600 cycles) (Illumina).

A total of 376,794 PacBio long reads (average read lengths of 15,245 bp, 16,813 bp, and 34,341 bp [3 SMRT cells]; 209× coverage) and a total of 1,068,580 Illumina short reads (read length, 300 bp; 49× coverage), quality checked with FastQC 0.11.8 (6), were included in the *de novo* assembly of the RL1 genome using the hybrid assembler MaSuRCA 3.2.1_01032017 (7). Sequence assembly produced three contigs representing one chromosome and two plasmids (chromosome, 6,253,838 bp; plasmid 1, 144,038 bp; plasmid 2, 448,745 bp) with a G+C content of 62.4%. The chromosome and plasmid 1 were circularized with Circlator version 1.5.5 (8). A total of 6,652 coding sequences were predicted with Rapid Annotations using Subsystems Technology (RAST) 2.0 (9), and

Citation Kuhl T, Felder M, Nussbaumer T, Fischer D, Kublik S, Paul Chowdhury S, Schloter M, Rothballer M. 2019. *De novo* genome assembly of a plant-associated *Rhodococcus qingshengii* strain (RL1) isolated from *Eruca sativa* Mill. and showing plant growth-promoting properties. Microbiol Resour Announc 8:e01106-19. https://doi.org/10.1128/MRA.01106-19.

Editor Vincent Bruno, University of Maryland School of Medicine

Copyright © 2019 Kuhl et al. This is an open-access article distributed under the terms of the Creative Commons Attribution 4.0 International license.

Address correspondence to Theresa Kuhl, theresa.kuhl@helmholtz-muenchen.de.

* Present address: Marius Felder, Department of Biology, Ludwig-Maximilians-University, Munich, Germany.

Received 7 September 2019
Accepted 22 October 2019
Published 14 November 2019

Downloaded from http://mra.asm.org/ on November 14, 2019 at GSF/ZENTRALBIBLIOTHEK

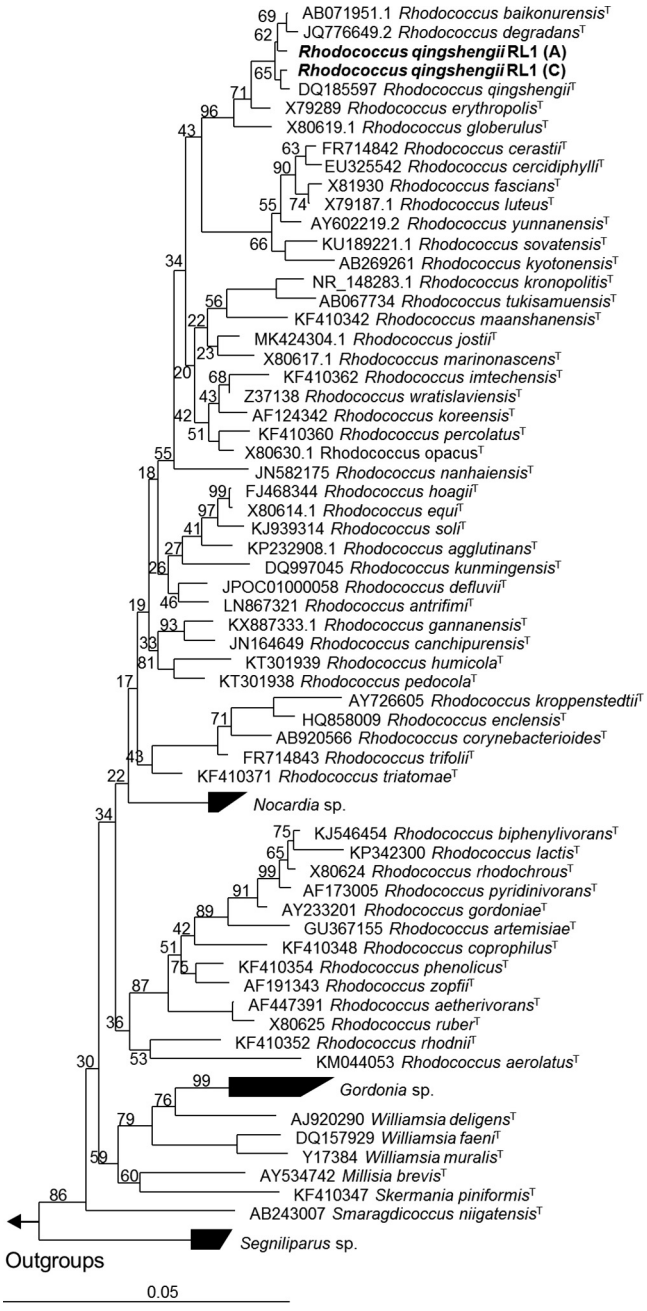

FIG 1 Neighbor-joining phylogenetic tree based on 16S rRNA sequences showing the phylogenetic relationship between *Rhodococcus qingshengii* RL1 and other members of the genus *Rhodococcus* and the family *Nocardiaceae*. Bootstrap values (%) for 1,000 resamplings are given at the nodes. Two versions of the 16S rRNA gene in the RL1 genome are included, differing at position 1074 (A or C) of the complete 16S rRNA gene.

gene clusters were identified with antiSMASH 4.2.0 (10) and Plant-bacteria Interaction Factors Resource (PIFAR) (11). All tools were used with their default settings. Many identified gene clusters were associated with traits relevant for (beneficial) microbe-plant interactions, including siderophore production, indole acetic acid (IAA) production, osmoregulation (ectoine), glucosinolate metabolism (β-glucosidase and *msrB*), quorum quenching (*qsdA*), antibiotic production, biofilm formation, lipopolysaccharide production, multidrug resistance, microbe-associated molecular patterns (MAMPs), heavy metal tolerance, and reactive oxygen species resistance.

The *de novo* assembly of the RL1 genome showed the highest similarity of >99%

Downloaded from http://mra.asm.org/ on November 14, 2019 at GSF/ZENTRALBIBLIOTHEK

sequence identity with over 90% of the *Rhodococcus qingshengii* djl-6^T genome, and the 16S rRNA genes of RL1 were 99.9% identical to those of djl-6^T. In a 16S rRNA gene-based phylogenetic neighbor-joining tree (12) calculated with ARB 5.3 (13), RL1 was placed within a cluster (bootstrap support, 99%) consisting of *Rhodococcus erythropolis*^{T}, *Rhodococcus qingshengii* djl-6^T, *Rhodococcus degradans* CCM 4446^T, and *Rhodococcus baikonurensis*^{T} (Fig. 1). Further phylogenetic analysis of the *gyrB* gene verified the taxonomic classification of RL1 as *Rhodococcus qingshengii* (data not shown).

Data availability. This whole-genome sequencing project was deposited in GenBank under accession no. CP042915, CP042916, and CP042917 and in SRA (raw data) under accession no. SRR10070368 and SRR10070367.

REFERENCES

1. Xu JL, He J, Wang ZC, Wang K, Li WJ, Tang SK, Li SP. 2007. Rhodococcus qingshengii sp. nov., a carbendazim-degrading bacterium. Int J Syst Evol Microbiol 57:2754–2757. https://doi.org/10.1099/ijs.0.65095-0.
2. Lincoln SA, Hamilton TL, Valladares Juárez AG, Schedler M, Macalady JL, Müller R, Freeman KH. 2015. Draft genome sequence of the piezotolerant and crude oil-degrading bacterium *Rhodococcus qingshengii* strain TUHH-12. Genome Announc 3:e00268-15. https://doi.org/10.1128/genomeA.00268-15.
3. Bala M, Kumar S, Raghava GP, Mayilraj S. 2013. Draft genome sequence of Rhodococcus qingshengii strain BKS 20-40. Genome Announc 1:e00128-13. https://doi.org/10.1128/genomeA.00128-13.
4. Rückert C, Birmes FS, Müller C, Niewerth H, Winkler A, Fetzner S, Kalinowski J. 2015. Complete genome sequence of Rhodococcus erythropolis BG43 (DSM 46869), a degrader of Pseudomonas aeruginosa quorum sensing signal molecules. J Biotechnol 211:99–100. https://doi.org/10.1016/j.jbiotec.2015.07.014.
5. Kamble AL, Banoth L, Meena VS, Singh A, Chisti Y, Banerjee UC. 2013. Nitrile hydratase of Rhodococcus erythropolis: characterization of the enzyme and the use of whole cells for biotransformation of nitriles. 3 Biotech 3:319–330. https://doi.org/10.1007/s13205-012-0104-2.
6. Andrew S. 2010. FastQC: a quality control tool for high throughput sequence data. https://www.bioinformatics.babraham.ac.uk/projects/fastqc/.
7. Zimin AV, Marçais G, Puiu D, Roberts M, Salzberg SL, Yorke JA. 2013. The MaSuRCA genome assembler. Bioinformatics 29:2669–2677. https://doi.org/10.1093/bioinformatics/btt476.
8. Hunt M, De Silva N, Otto TD, Parkhill J, Keane JA, Harris SR. 2015. Circlator: automated circularization of genome assemblies using long sequencing reads. Genome Biol 16:1–10. https://doi.org/10.1186/s13059-015-0849-0.
9. Overbeek R, Olson R, Pusch GD, Olsen GJ, Davis JJ, Disz T, Edwards RA, Gerdes S, Parrello B, Shukla M, Vonstein V, Wattam AR, Xia F, Stevens R. 2014. The SEED and the Rapid Annotation of microbial genomes using Subsystems Technology (RAST). Nucleic Acids Res 42:D206–D214. https://doi.org/10.1093/nar/gkt1226.
10. Blin K, Wolf T, Chevrette MG, Lu X, Schwalen CJ, Kautsar SA, Suarez Duran HG, De Los Santos ELC, Kim HU, Nave M, Dickschat JS, Mitchell DA, Shelest E, Breitling R, Takano E, Lee SY, Weber T, Medema MH. 2017. antiSMASH 4.0—improvements in chemistry prediction and gene cluster boundary identification. Nucleic Acids Res 45:W36–W41. https://doi.org/10.1093/nar/gkx319.
11. Martínez-García PM, López-Solanilla E, Ramos C, Rodríguez-Palenzuela P. 2016. Prediction of bacterial associations with plants using a supervised machine-learning approach. Environ Microbiol 18:4847–4861. https://doi.org/10.1111/1462-2920.13389.
12. Saitou N, Nei M. 1987. The neighbor-joining method: a new method for reconstructing phylogenetic trees. Mol Biol Evol 4:406–425. https://doi.org/10.1093/oxfordjournals.molbev.a040454.
13. Ludwig W, Strunk O, Westram R, Richter L, Meier H, Yadhukumar A, Buchner A, Lai T, Steppi S, Jacob G, Förster W, Brettske I, Gerber S, Ginhart AW, Gross O, Grumann S, Hermann S, Jost R, König A, Liss T, Lüßmann R, May M, Nonhoff B, Reichel B, Strehlow R, Stamatakis A, Stuckmann N, Vilbig A, Lenke M, Ludwig T, Bode A, Schleifer KH. 2004. ARB: a software environment for sequence data. Nucleic Acids Res 32:1363–1371. https://doi.org/10.1093/nar/gkh293.

Downloaded from http://mra.asm.org/ on November 14, 2019 at GSF/ZENTRALBIBLIOTHEK

frontiers in Microbiology

ORIGINAL RESEARCH
published: 18 August 2021
doi: 10.3389/fmicb.2021.708605

Genome-Based Characterization of Plant-Associated *Rhodococcus qingshengii* RL1 Reveals Stress Tolerance and Plant–Microbe Interaction Traits

*Theresa Kuhl[1], Soumitra Paul Chowdhury[1], Jenny Uhl[2] and Michael Rothballer[1]**

[1] Institute for Network Biology, Helmholtz Zentrum München – German Research Center for Environmental Health (GmbH), Neuherberg, Germany, [2] Research Unit Analytical Biogeochemistry, Helmholtz Zentrum München – German Research Center for Environmental Health (GmbH), Neuherberg, Germany

OPEN ACCESS

Edited by:
Frank T. Robb, University of Maryland, Baltimore, United States

Reviewed by:
Samina Mehnaz, Forman Christian College, Pakistan
Daniel Van Der Lelie, Gusto Global LLC, United States

***Correspondence:**
Michael Rothballer
rothballer@helmholtz-muenchen.de

Specialty section:
This article was submitted to Evolutionary and Genomic Microbiology, a section of the journal Frontiers in Microbiology

Received: *12 May 2021*
Accepted: *26 July 2021*
Published: *18 August 2021*

Citation:
Kuhl T, Chowdhury SP, Uhl J and Rothballer M (2021) Genome-Based Characterization of Plant-Associated Rhodococcus qingshengii RL1 Reveals Stress Tolerance and Plant–Microbe Interaction Traits. Front. Microbiol. 12:708605. doi: 10.3389/fmicb.2021.708605

Stress tolerant, plant-associated bacteria can play an important role in maintaining a functional plant microbiome and protecting plants against various (a)biotic stresses. Members of the stress tolerant genus *Rhodococcus* are frequently found in the plant microbiome. *Rhodococcus qingshengii* RL1 was isolated from *Eruca sativa* and the complete genome was sequenced, annotated and analyzed using different bioinformatic tools. A special focus was laid on functional analyses of stress tolerance and interactions with plants. The genome annotation of RL1 indicated that it contains a repertoire of genes which could enable it to survive under different abiotic stress conditions for e.g., elevated mercury concentrations, to interact with plants via root colonization, to produce phytohormones and siderophores, to fix nitrogen and to interact with bacterial signaling via a LuxR-solo and quorum quenching. Based on the identified genes, functional analyses were performed *in vitro* with RL1 under different growth conditions. The *R. qingshengii* type strain djl6 and a closely related *Rhodococcus erythropolis* BG43 were included in the experiments to find common and distinct traits between the strains. Genome based phylogenetic analysis of 15 available and complete *R. erythropolis* and *R. qingshengii* genome sequences revealed a separation of the *R. erythropolis* clade in two subgroups. First one harbors only *R. erythropolis* strains including the *R. erythropolis* type strain. The second group consisted of the *R. qingshengii* type strain and a mix of *R. qingshengii* and *R. erythropolis* strains indicating that some strains of the second group should be considered for taxonomic re-assignment. However, BG43 was clearly identified as *R. erythropolis* and RL1 clearly as *R. qingshengii* and the strains had most tested traits in common, indicating a close functional overlap of traits between the two species.

Keywords: *Rhodococcus qingshengii*, plant–microbe interaction, quorum quenching, mercury tolerance, nitrogen fixation

INTRODUCTION

Anthropogenic activities over the past decades, including pollution with heavy metals, pesticides and chemical fertilizer, as well as improper soil exploitation coupled with climate change have led to immense global soil degradation (Smith et al., 2016). This has resulted in loss of soil biodiversity, increase in pathogens and has created harsh biotic and abiotic conditions for plants and their associated microbes (Foley et al., 2005; Brevik and Burgess, 2014; Tsiafouli et al., 2015; Banerjee et al., 2019; Wagg et al., 2019). To survive difficult environmental conditions and maintain a functional plant holobiont (stress resistant) beneficial bacteria are important. Over the last decades, several mechanisms have been identified which are involved in beneficial associations between plant and microbes. They either involve plant growth promotion based on production of plant hormones and providing enhanced nutrients to the plants (Glick, 2012) or plant protection against plant pathogens by producing antimicrobial compounds (Chowdhury et al., 2015a,b) or acting indirectly by inducing host systemic resistance (Kloepper and Beauchamp, 1992; Pieterse et al., 2014; Bahramisharif and Rose, 2019). Apart from that, beneficial bacteria have been shown to support plants as stress protecting agents under abiotic stress conditions like salt and drought stress (Alavi et al., 2013; Berg et al., 2013; Kaushal and Wani, 2016; Bhat et al., 2020) or by supporting plant growth in contaminated soils (Sessitsch et al., 2013; Ma et al., 2016a,b). However, not only plant-microbe interactions, but also microbe-microbe interactions influence the functionality of the plant holobiont. For example, it has been shown that members of the genus *Variovorax* play a major role in shaping the microbiome and with this influence root growth in *Arabidopsis* by balancing auxin production (Finkel et al., 2020). This report emphasizes the importance to understand the role of all relevant members in the plant holobiont. The multifaceted interactions of plants and several plant-associated bacteria have been widely studied to understand the underlying molecular mechanisms and to exploit plant beneficial traits for sustainable agriculture (Berg et al., 2017; Rodriguez et al., 2019; Babin et al., 2021; Windisch et al., 2021). In this context it is important to further the knowledge of the functional repertoire also of yet lesser known members of the plant microbiome such as *Rhodococcus* to understand what enables them to interact with the plant as well as other microbes and which traits could be useful for an application in specifically demanding agricultural scenarios.

Members of the genus *Rhodococcus* are resistant to various stresses (Dabrock et al., 1994; Weyens et al., 2013; Pátek et al., 2021) and are able to degrade and metabolize a large spectrum of toxic compounds (Kamble et al., 2013; Lincoln et al., 2015; Pham et al., 2015; Ceniceros et al., 2017; Gupta et al., 2019; Gorbunova et al., 2020). These traits make the genus *Rhodococcus* interesting for bioremediation applications (Leigh et al., 2006; Płociniczak et al., 2017). Moreover, in metagenomic and microbiome analyses the genus *Rhodococcus* has been frequently reported as an established member of the plant microbiome (Francis and Vereecke, 2019; Vereecke et al., 2020). Many plant associated *Rhodococci* also show plant beneficial traits *in vitro* (Trivedi et al., 2007; Abbamondi et al., 2016; Murugappan et al., 2017) and *in planta* (Belimov et al., 2001).

The here studied closely plant associated *Rhodococcus qingshengii* RL1 was isolated from surface sterilized Rucola (*Eruca sativa* L.) leaves and the genome was recently sequenced (Kuhl et al., 2019). The type strain of species *R. qingshengii* djl-6 was isolated from a carbendazim polluted soil (Xu et al., 2007). Other *R. qingshengii* isolates have been shown to possess nitrogen fixing capacity improving growth of chick pea plants (Joshi et al., 2019) and to produce high amounts of IAA *in vitro* (Hasuty et al., 2018). In combination with the genetic traits for bioremediation, stress resistance, and biocontrol on plants widely distributed across the whole *Rhodococcus* genus these reports clearly warrant a characterization of our new isolate *R. qingshengii* RL1.

We were able to assess the genomic potential of RL1 by characterizing beneficial traits in the genome (Levy et al., 2018) and found that RL1 is well equipped with genes essential for survival under different abiotic stress conditions and for microbial interactions with other microbes and plants. *In vitro* assays were used to assess if these genomic potential was actually transferred into functional traits. To our knowledge, this is the first report of a *R. qingshengii*, which survives under mercury stress and degrades quorum quenching signals (AHLs). Additionally, for the first time we could identify a potential gibberellin producing operon in an actinobacterial genus as well as indications for existence of alternative nitrogen fixation pathways. For establishment of the taxonomic position of RL1 we performed a whole genome based phylogenetic analysis of 15 available and complete *R. erythropolis* and *R. qingshengii* genome sequences and included the *R. qingshengii* type strain djl6 and a closely related *R. erythropolis* BG43 in the *in vitro* experiments. Thus, this work contributes to the elucidation of molecular mechanisms and underlying genetic determinants of plant–microbe interactions and possible functions in the plant holobiont of *R. qingshengii* RL1 and closely related strains.

MATERIALS AND METHODS

Bacterial Strains and Growth Conditions

Rhodococcus qingshengii RL1, named hereafter RL1, is a gram-positive Actinobacterium and was isolated from Rucola (*Eruca sativa* L.) leaves. Colonies appear in off-white, beige colors. The overnight grown culture corresponds with OD_{600} = 0.42 representing approximately 4×10^7 CFU (colony forming units). *Rhodococcus qingshengii* djl6 DSM 45222 (type strain), named hereafter djl6 (Xu et al., 2007) and *Rhodococcus erythropolis* BG43 DSM 46869, named hereafter BG43 (Müller et al., 2014) were obtained from German Collection of Microorganisms and Cell Cultures (DSMZ, Braunschweig). The overnight grown cultures correspond with OD_{600} = 0.5 representing approximately 5×10^7 CFU and OD_{600} = 0.92 representing approximately 5×10^8 CFU, respectively. *Rhodococcus* strains were cultivated in tryptic soy broth (TSB, Sigma, United States) [casein peptone (pancreatic), 17 g/L, dipotassium hydrogen phosphate, 2.5 g/L, glucose, 2.5 g/L, sodium chloride, 5 g/L, soya peptone (papain digest.), 3 g/L] or

solid tryptic soy agar (1.7% agar) with pH 7.3, unless further specified, at 28°C and 180 rpm.

Control strains for the conducted experiments were: the strain *Bacillus velezensis* FZB42 DSM 23117, producing fungal antagonistic compounds like surfactin, fengycin and iturin (Chowdhury et al., 2015a), the AHL biosensor strain *Agrobacterium tumefaciens* A136 ATCC 51350 (Stickler et al., 1998; Han et al., 2016), the AHL producer strain *Acidovorax radicis* N35 DSM 23535 (Li et al., 2011) the non-AHL-producing mutant strain *Acidovorax radicis* N35 AHL- *araI::tet* (Han et al., 2016), the AHL-degrading mutant strain *Rhizobium radiobacter* F4 AHL- expressing an AHL lactonase (AiiA) (Alabid et al., 2020) and able to grow on potassium tellurite trihydrate ($K2TeO_3*3H_2O$) 100 μg/ml, the phosphate solubilizing strain *Luteibacter* sp. Cha2324a_16 and the ACC utilizing strain *Variovorax* sp. M92526_27 isolated from wheat roots (this study), the nitrogen-fixing and IAA producing *Herbaspirillum frisingense* GSF30 DSM 1328 (Kirchhof et al., 2001), the nitrogen-fixing *Azospirillum brasilense* Sp7 DSM 1690 (Tarrand et al., 1978; Hartmann and Hurek, 1988), the biofilm-producing *Pseudomonas simiae* WCS417r (Pieterse et al., 2020) and the non-biofilm-producing *Escherichia coli* DH5α (Anton and Raleigh, 2016). Strains were cultivated in liquid nutrient broth (NB, Roth, Germany) (beef extract 3 g/l, gelatin peptone 5 g/l) or solid nutrient agar (with 1.7% agar) with pH 6.8, unless further specified, at 28°C at 180 rpm.

Genome Comparison

The genome of *Rhodococcus qingshengii* RL1 (Kuhl et al., 2019) was compared to the genomes of the type strain *Rhodococcus qingshengii* djl6 (Xu et al., 2007; Wang et al., 2010; Táncsics et al., 2014), as well as the closely related soil isolate *Rhodococcus erythropolis* BG43 (Rückert et al., 2015). The genome djl6 is based on the species *R. jialingiae* (Wang et al., 2010) which was later identified as a synonym of the type strain *R. qingshengii* (Táncsics et al., 2014). For the genome comparison and the identification of orthologous and unique genes in the three different genomes the efficient database framework for comparative Genome Analyses using BLAST score Ratios – EDGAR (Blom et al., 2016) was used.

Functional Annotation of RL1 Genome

The RL1 genome was annotated upon submission to NCBI with the NCBI prokaryotic Genome Annotation Pipeline (PGAP) with the annotation method best-placed reference protein set with GeneMarkS-2+ and the Rapid Annotation using Subsystem Technology 2.0 (RAST) with default parameter of the classicRAST annotation scheme plus frameshift fixing and backfilling of gaps allowed, where the annotated genome was browsed afterward in the SEED environment (Aziz et al., 2008; Overbeek et al., 2014). Functional annotation by grouping genes in clusters of orthologous groups (COG) of proteins according to Tatusov et al. (2000) was performed with eggNOG v5.0 (Jensen et al., 2008). Genes were annotated with the KEGG (Kyoto Encyclopedia of Genes and Genomes) orthology (KO) identifiers, or the K numbers, and directly linked to the KEGG pathways with the KEGG automatic annotation server (KAAS) (Moriya et al., 2007) and KEGG Mapper. Further functional annotation was performed by identifying plant microbe interaction factors and gene clusters for biosynthesis of secondary metabolites with Plant–bacteria Interaction Factors Resource (PIFAR) (Martínez-García et al., 2016) and the antibiotics and secondary metabolite analysis shell – antiSMASH (Blin et al., 2017) using the default parameters.

Phylogenetic Analysis

Sixty-one complete genomes of the genus *Rhodococcus* and the genome of the out-group *Streptomyces albus* NBRC 13014 (type strain), were used for the full-genome approximately maximum-likelihood phylogenetic tree build in EDGAR. 15 genomes identified in the phylogenetic tree as members of the *Rhodococcus erythropolis* clade and two out-group genomes were used for the approximately maximum-likelihood phylogenetic tree calculated in EDGAR using FastTree Software with the Shimodaira–Hasegawa test for bootstrap values. Average nucleotide identity (ANI) and Average amino acid identity (AAI) was calculated in EDGAR (Blom et al., 2016) as described in Konstantinidis and Tiedje (2005) and Goris et al. (2007).

Evaluation of Growth and Tolerance to Different Stress Factors

If not indicated otherwise all *Rhodococcus* strains were pre-cultured in liquid TSB overnight.

Mercury Tolerance

Overnight grown cultures were transferred to fresh TSB medium with increasing mercury levels 0.001, 0.01, 0.1, and 1 mM adjusted with mercury-II-chloride ($HgCl_2$, Roth, Germany) according to Dziewit et al. (2013) and incubated at 28°C. Growth rates were evaluated by spectrophotometric measurement of optical density at 600 nm (OD_{600}) after 24 and 48 h. For treatments without detectable growth (=0.1 mM and 1 mM mercury), the recovery of cells was evaluated by the ability to form colonies on TSB agar plates without mercury. Hundred microliter of cultures from the treatments with 0.1 and 1 mM mercury were plated on TSB without mercury and incubated at 28°C for 24 and 48 h. Experiment was repeated three times. Non-mercury-tolerant strains *Herbaspirillum frisingense* GSF30 and *Bacillus velezensis* FZB42 served as negative controls.

Salt Stress Tolerance

Overnight grown cultures were transferred to fresh TSB medium with increasing sodium chloride (NaCl, Merck, Germany) levels 0, 1, 2.5, 3.5, 5.5, 7.5, 12, and 15% according to De Carvalho et al. (2014) and incubated at 28°C. Growth rates were evaluated by spectrophotometric measurement of optical density at 600 nm (OD_{600}) after 24 and 48 h. For treatments without detectable growth (12 and 15% NaCl), the recovery of cells was evaluated by the ability to form colonies on TSB agar plates without NaCl. Hundred microliter of cultures from the treatments 12 and 15% were plated on TSB agar without NaCl and incubated at 28°C for 24 and 48 h. Experiment was repeated three times. Less salt tolerant *Herbaspirillum frisingense* GSF30 and *Bacillus velezensis* FZB42 served as negative controls.

pH Tolerance

Overnight grown cultures were transferred to fresh TSB medium with pH values 8, 7, 6, 5, 4, 3, 2 adjusted with hydrochloric acid (HCl, Merck, Germany) or sodium hydroxide (NaOH, Sigma, United States) and incubated at 28°C. Growth rates were evaluated by spectrophotometric measurement optical density at 600 nm (OD_{600}) after 24 and 48 h. Recovery was evaluated by the ability to form colonies on TSB agar plates at pH 7.3 after 48 h in treatments without detectable growth (pH 4, 3 and 2). Hundred microliter of medium from the treatments pH 4, 3, and 2 were plated on TSB and incubated at 28°C for 24 and 48 h. The experiment was repeated three times. *Herbaspirillum frisingense* GSF30 and *Bacillus velezensis* FZB42 which did not grow in low pH (below 5) served as negative controls.

Osmotic Stress Tolerance

Overnight grown cultures were transferred to fresh TSB medium with increasing osmotic stress levels 0, −0.25, −0.5, −0.75, −1, −1.25, and −1.5 MPa and incubated at 28°C. Increasing osmotic stress was adjusted with polyethylene glycol 6000 (PEG6000, Serva Electrophoresis GmbH, Heidelberg, Germany) based on decreasing water potential with the formula of Kaufmann and Michel (1973), according to Kumar et al. (2014) and Jayakumar et al. (2020). −1.5 MPa is the water potential plants in regular soil start to wilt irreversibly. Growth rates were evaluated by spectrophotometric measurement optical density at 600 nm (OD_{600}) after 24 and 48 h. Experiment was repeated three times. Gram-negative *Herbaspirillum frisingense* GSF30 and gram-positive *Bacillus velezensis* FZB42 served as controls.

Antibiotic Resistance

Overnight grown cultures were diluted 1:10 with fresh TSB medium. Two hundred microliter of the diluted overnight cultures were spread on TSB agar plates and antimicrobial susceptibility test stripes (Himedia Laboratories, India) for kanamycin (0.016–256 μg/ml), ampicillin (0.016–256 μg/ml), rifampicin (0.002–32 μg/ml), and vancomycin (0.016–256 μg/ml) were placed according to manufacturer's protocol. The inhibition zone was evaluated after 24 and 48 h.

Bacterial strains were streaked on a fresh TSB or NB plate from glycerol stocks and grown overnight. A single colony of RL1 was picked and streaked on nutrient broth (NB) agar plates with 100 μg/ml potassium tellurite trihydrate (K_2TeO_3 * $3H_2O$, Sigma, United States) for 48 h. Dark gray colony growth was evaluated as positive growth. The strain *Rhizobium radiobacter* F4 AHL- aiiA- genetically modified to tolerate a tellurite concentration of 100 μg/ml served as positive control.

Characterization of Traits Involved in Microbe–Plant Interactions

If not indicated otherwise all *Rhodococcus* strains were pre-cultured in liquid TSB overnight.

Indole-Acetic Acid Production

Indole-acetic acid (IAA) production was determined by the colorimetric method of Gordon and Weber (1951). Overnight grown cultures were transferred to fresh TSB medium with and without the IAA precursor 5 mM tryptophan (1 mg/mL, Sigma) and grown for 48 h. Liquid cultures were centrifuged for 2 min at 5000 × *g*. Hundred microliter of supernatant were mixed with 100 μl of Salkowski reagent [0.01 M $FeCl_3$ anhydrous (Fluka Biochemika, Germany) in perchloric acid ($HClO_4$) 35% (Merck, Germany)] (Loper and Schroth, 1986) and 1 μl of orthophosphoric acid (Sigma, United States). After incubation in the dark for 30 min amounts of IAA in the supernatant were analyzed in a plate reader (Spectra Max iD3, Molecular Devices) at 530 nm wavelength. A standard curve was prepared from commercial indole-3-acetic acid (Fluka Biochemika, Germany) in TSB with concentrations ranging from 0 to 100 μg/ml and *Herbaspirillum frisingense* GSF30 was used as positive control. Supernatant measurements were performed in triplicates. Evaluation was based on the amount of produced IAA normalized to an $OD_{600} = 1$.

Siderophore Production

Siderophore production was analyzed according to Pérez-Miranda et al. (2007) and Lynne et al. (2011) with modifications. Twenty-five microliter of overnight grown cultures were spotted on TSB agar plate and grown for 48 h. Dye solutions [chrome azurol blue S (Sigma, United States), $FeCl_3$ (Fluka Biochemika, Germany), HDTMA (Hexadecyltrimethylammonium bromide, Sigma, United States)] were prepared and mixed according to Lynne et al. (2011). Piperazin-*N,N*'-bis-(2-ethanesulfonic acid) (Pipes, Roth, Germany) was added to H_2O with 0.9 % agar and pH was adjusted to 6.8. After autoclaving separately, the dye solution was slowly mixed with the Pipes-Agar mix. Cooled but still liquid overlay agar (10 ml) was poured on plates with bacteria. After 2 h siderophore production was analyzed by detection of color change from blue to orange. The experiment was repeated three times.

Phosphate Solubilization

Overnight grown cultures were washed twice in 1x PBS and 25 μl were spotted on National Botanical Research Institute's phosphate growth medium (NBRIP) according to Nautiyal (1999) and incubated at 28°C. After 6 days, phosphate solubilization activity was determined according to the formation of a clear halo surrounding the spotted colony using the Phosphate Solubilization Index (SI): (Colony diameter + Halo zone diameter)/colony diameter). The phosphate-solubilizing *Luteibacter* sp. Cha2324a_16 served as positive control. The experiment was repeated three times.

1-Aminocyclopropane-1-Carboxylate Utilization

1-Aminocyclopropane-1-carboxylate (ACC, Biozol Diagnostica GmbH, Germany) utilization as nitrogen source was analyzed with M9 minimal medium [Na_2HPO_4 33.1 mM, KH_2PO_4 22 mM, NaCl 8.55 mM (NH_4Cl 9.35 mM), glucose 0.4%, $MgSO_4$ 1 mM, $CaCl_2$ 0.3 mM] containing NH_4Cl 9.35 mM (Roth, Germany) or ACC 3 mM as nitrogen source or no nitrogen source. Overnight grown cultures were washed twice in 1x PBS and 25 μl were spotted on each plate. After 10 days, ACC utilization as nitrogen source was analyzed by comparing bacterial growth on M9, M9 with ACC and nitrogen-free

M9 plates. ACC utilizing *Variovorax* sp. M92526_27 served as positive control. The experiment was repeated three times.

Nitrogen Fixation

Nitrogen fixation was analyzed with nitrogen-free semi-solid Nfb-medium according to Döbereiner (1995), on Ashby's mannitol medium (Mannitol 20 g/l, K_2HPO_4 0.2 g/l, $MgSO_4*5H_2O$ 0.2 g/l, NaCl 0.2 g/l, K_2SO_4 0.1 g/l, $CaCO_3$ 5 g/l, Agar 15 g/l) and on Jensen's medium (Sucrose 20 g/l, K_2HPO_4 1 g/l, $MgSO_4*5H_2O$ 0.5 g/l, NaCl 0.5 g/l, $FeSO_4$ 0.1 g/l, Na_2MoO_4 0.005 g/l, $CaCO_3$ 2 g/l, Agar 15 g/l). Overnight grown cultures were washed twice in 1x PBS and 10 μl were spotted on nitrogen-free semi-solid Nfb-medium and incubated at 28°C. Pellicle formation was evaluated after 48 h. Ten microliter of washed overnight cultures were streaked on Ashby's mannitol agar. Bacterial strains were streaked on a fresh TSB or NB plate from glycerol stocks and grown overnight. A single colony of each strain was picked and streaked on Jensen's agar. Bacteria on Ashby's medium and Jensen's medium were incubated at 28°C and growth was evaluated after 3 days. The experiments were repeated three times. Nitrogen-fixing *Azospirillum brasilense* Sp7 served as positive control.

Biofilm Formation

Biofilm formation was analyzed according to O'Toole (2011). Overnight grown cultures were washed in 1xPBS and OD_{600} was adjusted to 0.1. Bacterial strains were cultivated in a microtiter plate in 100 μl modified M9 minimal medium with 0.5% casamino acids (Biozol Diagnostica Vertrieb GmbH, Germany) without shaking at 28°C. After incubation OD_{600} was measured in the plate reader (SpectraMax iD3, Molecular Devices). After 24 h OD_{600} was measured and unattached cells were dumped out of the plate. The plate was washed twice by submerging it in MilliQ water to further remove unattached cells. Hundred and twenty-five microliter of 0.1% crystal violet (Roth, Germany) solution was added to each well. After 15 min the plate was rinsed three times in MilliQ water and dried for 1.5 h before visual inspection of biofilm production. For quantification of the biofilm 125 μl of 30% acetic acid (Roth, Germany) was added to each well and incubated for 15 min at room temperature. The solution was transferred to a new microtiter plate and color intensity was quantified at the plate reader (SpectraMax iD3, Molecular Devices) with absorbance at 550 nm and 30% acetic acid as blank. Biofilm-forming *Pseudomonas simiae* WCS417 served as positive control and non-biofilm-producing *Escherichia coli* DH5α served as negative control. The experiment was repeated three times with 6–12 replicates per strain.

Interactions With Other Organisms

Confrontation Assay Against Plant–Pathogenic Fungi

The interaction of RL1 with the well-known plant pathogenic fungi *Rhizoctonia solani*, *Fusarium culmorum*, and *Fusarium oxysporum* was investigated with an *in vitro* confrontation assay. The following pathogenic fungi were used: *Rhizoctonia solani*, causing potato stem cancer and black scurf (Yang and Li, 2012), wheat pathogenic fungus *Fusarium culmorum* G2191 causing seedling blight, foot rot, and head blight (Wagacha and Muthomi, 2007) and the wilt-causing *Fusarium oxysporum* DSM62297 (Gerlach et al., 1958). Fungi were cultivated on potato dextrose agar (PDA, Sigma, United States) (potato extract 4.0 g/L, glucose 20.0 g/L) at room temperature in the dark and stored at 4°C until further use.

RL1 was pre-grown in TSB. Overnight grown culture was diluted to OD_{600} = 0.1 with fresh TSB medium and 10 μl were dripped on the plate. Approximately 1 mm^3 PDA pieces grown with fungi were aseptically transferred to TSB plates at a distance of approximately 3 cm. After 9 days of growth the zone of inhibition formation was visually analyzed and documented photographically. Sterile water served as negative control and *Bacillus velezensis* FZB42, a known fungal antagonistic strain served as positive control. Confrontation assays were performed in triplicates.

Degradation of Synthetic and Bacterial *N*-Acyl-Homoserine Lactones (AHLs)

The identified *qsdA* gene sequence of the RL1 genome encoding the AHL lactonase was used to construct a phylogenetic tree with nearest relatives with MEGA X (Kumar et al., 2018). *Rhodococcus* strains were analyzed with a well diffusion agar-plate assay (Rodríguez et al., 2020) and a V-shaped assay (Berendsen et al., 2018) with modifications.

Well diffusion plate assay

For the experiments with synthetic AHL *Rhodococcus* strains were pre-grown in TSB. Overnight grown cultures were transferred to fresh TSB liquid medium supplemented with 10 μM C12-HSL (Biomol GmbH, Germany) and incubated at 28°C 180 rpm. Cell-free TSB medium supplemented with 10 μM C12-HSL served as control. For the co-cultivation experiment RL1 and *Acidovorax radicis* N35e overnight cultures were adjusted to OD_{600} = 0.2 and co-cultured in fresh liquid NB medium. Pure culture of *Acidovorax radicis* N35e served as control.

The well diffusion plates were prepared as follows: The AHL biosensor strain *Agrobacterium tumefaciens* A136 was pre-grown in NB. NB plates were overlaid with soft NB agar (0.5% agar) supplemented with the biosensor strain A136 and 80 μg/ml 5-bromo-4-chloro-3-indolyl-β-D-galactopyranoside (X-gal, Life Technologies GmbH, Germany). Twenty microliter of each supernatant from the co-cultivation or synthetic AHL experiment were filled in wells prepared in the soft agar and incubated at 28°C for 30 h. Remaining AHLs were detected by color change. Pure NB was used as negative control for presence of AHLs.

V-shaped plate assay

The AHL biosensor strain *Agrobacterium tumefaciens* A136 was pre-grown in NB. *Agrobacterium tumefaciens* A136 and 80 μg/ml 5-bromo-4-chloro-3-indolyl-β-D-galactopyranoside (X-gal, Life Technologies GmbH, Germany) were spread on NB plates. *Rhodococcus* strains were pre-grown in TSB. The AHL producing strains *Acidovorax radicis* N35e was pre-grown in NB, non-AHL-producing mutant strain *Acidovorax radicis* N35 AHL- *araI::tet* was pre-grown in NB with tetracyclin 20 μg/ml and kanamycin 50 μg/ml. Overnight grown cultures were washed in 1x PBS and

optical density was adjusted to OD_{600} = 0.1. Eight times 1 µl of each culture was dripped in a diagonal row on the prepared NB plates in V-shape with increasingly closer inoculation sites. Plates were incubated for 30 h at 28°C. AHL degradation was detected by color change.

Evaluation of Rhizosphere Competence

Root Inoculation in Axenic System

Rucola (*Eruca sativa* L.) seeds were washed in Tween 80 1% (Sigma, United States) for 2 min, surface sterilized with sodium hypochlorite 12% (NaOCl, Roth, Germany) for 8 min and washed three times in sterile deionized water for 2 min. Sterilized seeds were placed on Hoagland's solution (Sigma, United States) with 0.8% agar to germinate 4 days. *Rhodococcus* strains were pre-grown in TSB. Overnight grown cultures were washed two times in 1x PBS (AppliChem, Germany) and diluted to a concentration of 10^7 CFUs. Seedlings were inoculated in the prepared bacterial solution of RL1, BG43, and djl6 for 1 h under shaking at 160 rpm at 28°C. Seedlings inoculated in 1x PBS served as negative control. Inoculated seedlings were transferred to an axenic system with 80 ml sterile quartz sand and 20 ml Hoagland's solution in a sterile Phytatray II (Sigma, United States). Seedlings inoculated with RL1 were additionally transferred on plates with 0.5x Murashige and Skoog Medium (0.5x MS) including vitamins (Duchefa Biochemie, Netherlands); pH was adjusted to 5.7 with 2N KOH. No additional sucrose was added to 0.5x MS. The axenic system was placed in a Phytochamber (Weiss Technik, Modell SGC120PG2, Germany) with 23°C, 55% humidity, day-night-cycle 12 h : 12 h. After seven and 14 days freshly harvested roots were washed in 1x PBS, fixed in 55% EtOH and 1x PBS mix and stored at –20°C until further use.

Fluorescence *in situ* Hybridization (FISH)

Fluorescence *in situ* hybridization was performed following the protocol of Alquéres et al. (2013). Chemicals were obtained from AppliChem, Germany. After an increasing ethanol series [(50, 80, and 96% [vol/vol] for 3 min each] for fixation and desiccation, roots were incubated in 50 µl hybridization buffer [0.9 M NaCl, 0.01% sodium dodecyl sulfate (SDS), 10 mM Tris-HCl (pH 8.0), 35% deionized formamide] with 15 pmol of the fluorescently labeled probes EUB338, specific for eubacteria (Amann et al., 1990; Daims et al., 1999) and labeled with fluorescein (FITC, Thermo Scientific, Germany), and HGC69a (Roller et al., 1994), specific for bacteria with high G + C content in their 16S rRNA and labeled with Cy3 (Thermo Scientific, Germany) or ATTO550. Hybridization was performed for 1.5 h at 46°C.

Confocal Laser Scanning Microscopy (CLSM)

FISH stained roots and bacterial cells were investigated at the Zeiss confocal laser scanning microscope LSM880 (Zeiss, Oberkochen, Germany) with argon ion laser and helium neon laser for excitation of FITC (488 nm), Cy3 (561 nm) and an unlabeled control channel (633 nm). Cells were observed with a 64x C-Apochromat water immersion objective. Micrographs were recorded using the software Zen Black Edition (Zeiss, Oberkochen, Germany).

Quantitative Evaluation

Rhizosphere competence of the investigated bacterial strains were estimated via counting of colony forming units (CFU). Sterilized Rucola (*Eruca sativa* L.) seedlings were inoculated in bacterial solution and planted in the axenic system as described above. After 7 days three roots per treatment were harvested, weighed and ground in a sterilized mortar with 1 ml 1x PBS. Ground roots were diluted three times (10^{-3}), 100 µl of each dilution was plated in triplicates on TSB plates and incubated at 28°C. After 48 h CFUs of dilution 10^{-3} were counted and mean values were compared between treatments. Plating of dilutions 10^{-1} and 10^{-2} resulted in too many CFUs for counting.

Statistical Analysis

Sample size was not predetermined using statistical methods. Statistical analysis was performed with RStudio 3.6.1. Data were tested for normal distribution with Shapiro–Wilk-Test and analyzed with the non-parametric Fligner-Killeen-Test or with analysis of variances (ANOVA) followed by the post-hoc analysis with Tukey's test. Significance level was 5% marked in the graphs by asterisks.

RESULTS

Phylogenetic Analysis

The full genome based phylogenetic tree of *Rhodococcus* was constructed on a core genome of 633 genes from 39246 genes in total (**Supplementary Figure 1**). Based on this phylogenetic tree 15 genomes of the *R. erythropolis* clade were chosen to calculate the full genome based phylogenetic tree of the *R. erythropolis* clade. It was built on a core genome of 1211 genes from 20587 genes in total and revealed that the clade can be separated into two groups (**Figure 1**). The first group includes *R. erythropolis* strains only. The second group harbors a mix of *R. erythropolis* and *R. qingshengii* strains. ANI values between all analyzed *R. erythropolis* or *R. qingshengii* genomes were higher than 94% (**Supplementary Figure 2**). The ANI value within the first group was 98.02–98.8% and within the second group 97.17–99.3%. The outgroups *Rhodococcus aethiovorans* and *Streptomyces albus* had ANI values of 72.13–72.57% and 66.79–67.9%, compared to the first group and the second group, respectively. AAI values between the first and the second group of the *R. erythropolis* clade were all above 98% (**Supplementary Figure 3**), and between both groups and the outgroups *R. aethiovorans* and *S. albus* AAI values were 56.45–57.33% and 76.71–76.81, respectively. *R. qingshengii* djl6 and RL1 grouped together in the second group. *R. erythropolis* BG43 was allocated to the first group.

Comparing the RL1 genome with the genomes of *R. qingshengii* djl6 and *R. erythropolis* BG43, 5293 genes could be identified that were shared between all three strains (**Figure 2**). RL1 and djl6 shared more genes (294) than each

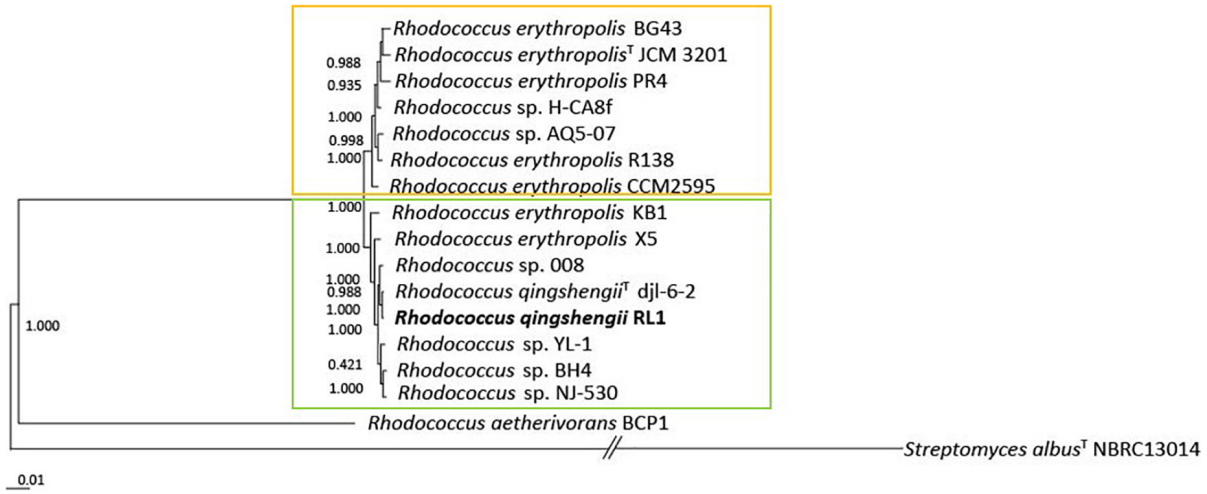

FIGURE 1 | Maximum-likelihood phylogenetic tree of 15 genomes of the *Rhodococcus erythropolis* clade generated with FastTree 2.1 from 1211 nucleotide sequences of the core genome. Values represent local support values based on Shimodaira–Hasegawa test (1 SH = 100% bootstrap). The scale bar represents nucleotide substitutions per site (0.01 scale = 1% nucleotide substitutions per site). The *Rhodococcus erythropolis* subgroup is marked in orange and the *Rhodococcus qingshengii* subgroup in green.

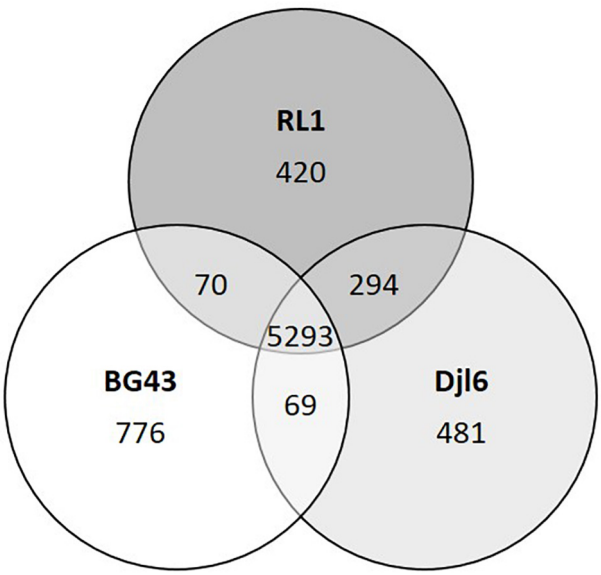

FIGURE 2 | Venn-diagram representing comparative distribution of shared genes between the genomes of RL1, djl6, and BG43. Data obtained with EDGAR Software. Unique genes or singletons are here genes without any hit (BLAST) against any other genome.

of them with BG43 (69; 70). For RL1 39 singleton genes could be identified of which 17 were annotated as hypothetical proteins (**Table 1**).

Functional Annotation of RL1 Genome

A total of 6,554 protein coding sequences were predicted from the genome of RL1 with (RAST) and 6,328 genes with PGAP (**Table 2**). 5918 of the predicted genes could be annotated to an assigned function and 92.4% of them were classified into 21 clusters of orthologous groups (COG) identified with eggNOG (**Figure 3**). Genes involved in metabolism represented the largest fraction (37.1%), followed by information and storage processing (19.2%), and cellular processes and signaling (12.7%) (**Figure 3**). In more details, the highest number of genes could be assigned to be involved in transcription (K, 11.5%), followed by amino acid transport and metabolism (E, 7.5%) and energy production and conversion (C, 6.9%). 3.6% of the genes could be assigned to the category of secondary metabolites biosynthesis, transport, and catabolism (Q). 9.4% of the genes were assigned to more than one category (>1 cat.). 21.4% of the genes could not be assigned to a known function (S). 35% of the coding sequences in the RL1 genome were sorted in 23 main RAST subsystems and 424 subsystems (subsystem coverage). With KEGG pathway analysis genes involved in 273 pathways were identified (**Supplementary Table 1**). The genome was further analyzed for presence of genes known to be involved in interactions with plants using the web-based tool PIFAR and 45 genes representing 14 categories could be identified (**Supplementary Table 2**). Using the tool antiSMASH 17 biosynthetic gene clusters (BGC) with the potential to produce secondary metabolites, such as ectoine, erythrochelin, and heterobactin A/heterobactin S2, could be identified (**Supplementary Table 3**). In this study we focused on the cluster with highest similarity (>50%) to known secondary metabolite biosynthesis pathways.

The genome annotation of RL1 revealed several genes which have been previously identified to be involved in stress tolerance under different abiotic stress conditions, bioremediation of toxic compounds, rhizosphere colonization and (beneficial) plant-microbe interactions and were partly verified by manual annotation with blastp alignment (**Supplementary Table 4**). In more details, the RL1 genome harbors many genes, which

TABLE 1 | Singleton genes RL1 based on genome comparison with BG43 and djl6 in EDGAR.

Category	Annotated gene	Gene locus tag RL1	
Aromatic carbon metabolism	Enoyl-CoA hydratase/isomerase family protein	D6M20_RS19280	
	Fumarylacetoacetate hydrolase	D6M20_RS19325	
pH tolerance	Squalene cyclase	D6M20_RS23450	
DNA phosphorothioation	Cysteine desulfurase *DndA*	D6M20_RS05845	
	DNA sulfur modification protein *DndB*	D6M20_RS05850	
	DNA phosphorothioation system sulfutransferase *DndC*	D6M20_RS05855	
	DNA sulfur modification protein *DndD*	D6M20_RS05860	
	DndE	D6M20_RS05865	
	DNA phosphorothioation-associated putative methyltransferase	D6M20_RS05870	
	DNA phosphorothioation-associated protein 4	D6M20_RS05875	
Multidrug resistance	DAED/DEAH box helicase family protein	D6M20_RS05885	
	GIY-YIG nuclease family protein	D6M20_RS05895	
	Plasmid pRiA4b ORF-3 family protein	D6M20_RS05905	
Heavy metal resistance	IS110 family transposase	D6M20_RS28370	
	Alkylmercury lyase	D6M20_RS28375	
	merR family DNA-binding protein	D6M20_RS28380	
Other	AAA family ATPase	D6M20_RS05880	
	Bifunctional 3-(3-hydroxy-phenyl)propionate/3-hydroxycinnamic acid hydroxylase	D6M20_RS19290	
	MFS transporter	D6M20_RS19300	
	Helix-turn-helix domain-containing protein	D6M20_RS19305	
	DUF3500 domain-containing protein	D6M20_RS19315	
	FCD domain-containing protein	D6M20_RS19320	
Hypothetical proteins		D6M20_RS05890, D6M20_RS09680, D6M20_RS10445, D6M20_RS17400, D6M20_RS17780, D6M20_RS19225, D6M20_RS19310, D6M20_RS23515, D6M20_RS28335	D6M20_RS06865, D6M20_RS09985, D6M20_RS17155, D6M20_RS17770, D6M20_RS18200, D6M20_RS19295, D6M20_RS21385, D6M20_RS23590,

TABLE 2 | Overview of general genome properties of the isolates used in this study.

Genome properties	RL1	Djl6	BG43
Chromosome size (Mbp)	6.25	6.52	6.33
No. plasmids (size in kbp)	2 (144, 448.7)	3 (84.6, 80.9, 15.8)	3 (240.1, 266.7, 30)
GC content (%)	62.4%	62.4%	62.3%
Total genes (PGAP)	6.328	6.332	6.394
RNAs	72	77	71
NCBI Accession Numbers	NZ_CP042917, NZ_CP042916, NZ_CP042915	NZ_CP025959, NZ_CP025960, NZ_CP025961, NZ_CP025962	NZ_CP011295, NZ_CP011296, NZ_CP011297, NZ_CP011298
References	Kuhl et al., 2019	Xu et al., 2007; Wang et al., 2010; Táncsics et al., 2014	Rückert et al., 2015

can be expressed to withstand osmotic, salt, oxidative and acidic stress and are relevant for heavy metal tolerance (mercury, lead, cadmium, arsenic) and bioremediation of aromatic hydrocarbons (*alkB*, *catA*) and fossil fuels (*dszB*). Moreover, genes potentially involved in multiple drug resistance, DNA repair by phosphorothioation, antibiotic resistance and degradation of CO and hydrogen could be identified, for example the complete carbon monoxide dehydrogenase (CODH) and a [NiFe]-hydrogenase cluster. The RL1 genome annotation indicated that it is equipped with several genes which could enable it to interact with the plant and survive in the plant environment via plant hormone and siderophore production of the siderophores enterobactin, bacillibactin, arthrobactin, and heterobactin as well

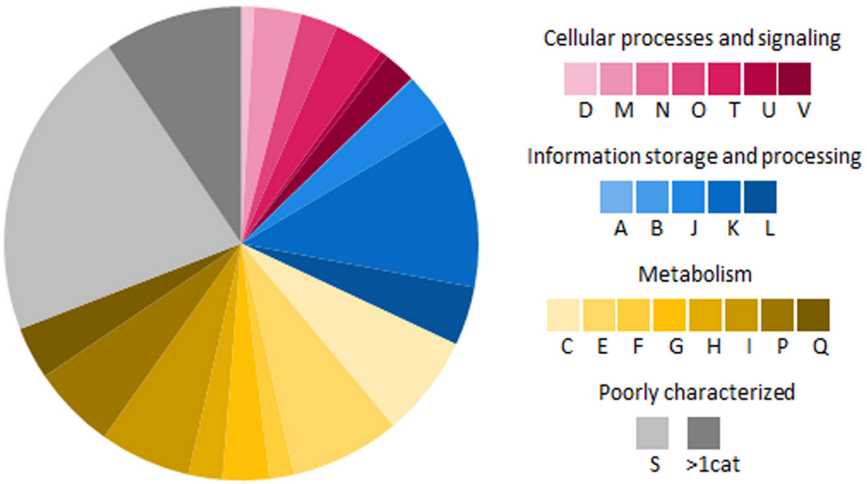

FIGURE 3 | Functional classification of genes encoding proteins in RL1 based on cluster of orthologous groups (COG) (Tatusov et al., 2000). All alphabets represent different COG functional classes: **A**, RNA processing and modification; **B**, Chromatin structure and dynamics; **C**, energy production and conversion; **D**, cell cycle control, cell division, and chromosome partitioning; **E**, amino acid transport and metabolism; **F**, nucleotide transport and metabolism; **G**, carbohydrate transport and metabolism; **H**, coenzyme transport and metabolism; **I**, lipid transport and metabolism; **J**, translation, ribosomal structure, and biogenesis; **K**, transcription; **L**, replication, recombination, and repair; **M**, cell wall, cell membrane, and cell envelope biogenesis; **N**, cell motility; **O**, posttranslational modification, protein turnover, and chaperones; **P**, inorganic ion transport and metabolism; **Q**, secondary metabolites biosynthesis, transport, and catabolism; **S**, no functional prediction; **T**, signal transduction mechanisms; **U**, intracellular trafficking, secretion, and vesicular transport; and **V**, defense mechanisms; **>1 cat**, classified in more than 1 category.

as nitrogen fixation, iron acquisition, phosphate solubilization, biofilm formation, and stress protection. Additionally, the RL1 genome harbors genes involved in quorum quenching, glucosinolate metabolism, aldoxime, isothiocyanate (ITC) and nitrile degradation, as well as genes important for the production of volatiles, exopolysaccharides (EPS), proteases and microbe-associated molecular patterns (MAMP). Therefore, we analyzed functional traits with focus on stress tolerance and plant–microbe interactions.

Evaluation of Growth and Tolerance to Different Stress Factors

Mercury Tolerance

The RL1 genome harbors genes for alkylmercury lyase and *merR* family DNA-binding protein (**Supplementary Table 4**). Active growth determined by optical density was detectable in the medium with 0.001 mM mercury for djl6 and BG43. RL1 was able to grow in the medium with up to 0.01 mM mercury. RL1 and BG43 could recover from up to 1 mM mercury in the medium, whereas djl6 recovered from up to 0.1 mM mercury. The gram-positive control strain *Bacillus velezensis* FZB42 could grow in the medium with up to 0.01 mM mercury and the gram-negative control strain *Herbaspirillum frisingense* GSF30 only in medium with 0.001 mM mercury. Both control strains did not recover from medium containing 0.1 mM mercury.

Salt Stress Tolerance

The RL1 genome harbors genes for the complete Na+/H+ antiporter operon (**Supplementary Table 4**). RL1 and BG43 were able to grow in medium with 7.5% NaCl, whereas djl6 could grow up to 5.5% NaCl in the medium. Although there was no visible growth, all tested *Rhodococcus* strains were able to recover from salt stress of 15% NaCl in the medium. The gram-positive control strain *Bacillus velezensis* FZB42 could grow up to 7.5% NaCl in the medium and did not recover from medium with 15% NaCl. The gram-negative control strain *Herbaspirillum frisingense* GSF30 could grow in medium with up to 3.5% NaCl and could not recover from 7.5% NaCl in the medium.

pH Tolerance

Genes encoding for squalene cyclase and the ADI cluster were identified in the RL1 genome (**Supplementary Table 4**). The *Rhodococcus* strains were able to grow up to pH 5 and recovered after 48 h in pH 3 and 4 h in pH 2. Control strains *Herbaspirillum frisingense* GSF30 and *Bacillus velezensis* FZB42 were able to grow up to pH 5 and recovered from pH 4.

Osmotic Stress Tolerance

The gene cluster for ectoine biosynthesis was identified in RL1 with 75% identity to the ectoine biosynthetic cluster of *Streptomyces anulatus*. The *Rhodococcus* strains RL1, djl6, BG43, and the control strains FZB42 and GSF30 were able to grow under PEG_{6000} induced osmotic stress of –1.5 MPa, which was the tested maximum.

Antibiotic Resistance

Genes involved in antibiotic resistance and tellurite resistance were identified in the RL1 genome (**Supplementary Table 4**). RL1 was tolerant to Kanamycin up to the concentration of 96 μg/ml, Ampicillin up to 6 μg/ml, Rifampicin up to 0.025 μg/ml, but not tolerant to Vancomycin. Djl6 was tolerant to Kanamycin up to 12 μg/mL, Ampicillin up to 3 μg/mL, Rifampicin up to 0.047 μg/ml and Vancomycin up to 0.023 μg/ml. BG43

was tolerant to Kanamycin up to 48 μg/ml, Ampicillin up to 2 μg/ml, Rifampicin up to 0.023 μg/ml and Vancomycin up to 0.5 μg/ml. RL1 was able to grow on NB plates containing 100 μg/ml potassium tellurite trihydrate. The other strains were not tested for this trait.

Traits Involved in Microbe–Plant Interactions

Indole-Acetic Acid Production

The genes encoding for amidase *amiE* and amine oxidase *iaaM* as well as genes involved in tryptophan metabolism were identified in the RL1 genome (**Supplementary Table 4**). RL1 produced 16 ± 2.6 μg/ml of IAA which is the highest amount compared to djl6 and BG43 with 10.7 ± 2.4 μg/ml and 10.9 ± 3.8 μg/ml, respectively. The positive control strain *Herbaspirillum frisingense* GSF30 produced 41 ± 9.8 μ g/ml IAA.

Siderophore Production

In the RL1 genome, biosynthesis cluster for erythrochelin was identified with 57% identity and heterobactinA/heterobactin S2 identified with 100% identity compared to the heterobactin BGC of *R. erythropolis* PR4 (**Figure 4A**). Genes encoding for relevant proteins of the heterobactin BGC are isochorismate synthase, isochorismatase, 2,3-dihydro-2,3-dihydroxybenzoate dehydrogenase, 2,3-dihydroxybenzoate-AMP ligase, amino acid adenylation domain-containing protein and related transporter (**Supplementary Table 4**). RL1 produced siderophores indicated by the color change of the overlay agar from blue to orange (**Figure 4B**). BG43 and djl6 did not produce siderophores.

Phosphate Solubilization

The RL1 genome harbors genes involved in organic acid production (**Supplementary Table 4**). *Rhodococcus qingshengii* strains RL1 and djl6 were able to solubilize phosphate indicated by clear halo formation and SI values of 2.3 and 2.4 respectively. BG43 showed no halo formation and SI value was 2, which indicates no phosphate solubilization. Positive control *Luteibacter* sp. Cha2324a_16 showed halo formation and SI values of 2.7.

1-Aminocyclopropane-1-Carboxylate Utilization

Growth on M9 and M9 with ACC and no growth on nitrogen-free M9 indicate ACC utilization. RL1, BG43, and djl6 could grow on plates with ACC, on regular M9 medium and on nitrogen-free medium. The positive control *Variovorax* sp. M92526_27 grew on M9 and M9 with ACC, but not on M9 without nitrogen (**Figure 5A**). ACC deaminase activity remained unclear, because *Rhodococcus* strains could also grow on M9 without nitrogen. The gene *acdS* was not present in the RL1 genome.

Nitrogen Fixation

The RL1 genome harbors an uncharacterized nifU-like protein (**Supplementary Table 4**). The strains RL1, djl6, and BG43 could grow on all tested nitrogen free media, which were nitrogen-free M9 medium (**Figure 5A**), Ashby's medium, Jensen's medium (**Figure 5B**) and Nfb-medium (**Figure 5C**). Pellicle formation in Nfb-medium was smaller compared to positive control *Azospirillum brasilense* Sp7.

Biofilm Formation

Genes encoding for a phosphoglucomutase and a signal peptidase I were identified in the RL1 genome (**Supplementary Table 4**). The strains RL1, djl6 and BG43 were able to produce biofilms in varying intensities (**Figure 6**), but stronger than the negative control *Escherichia coli* DH5α. Djl6 showed the strongest biofilm formation. Positive

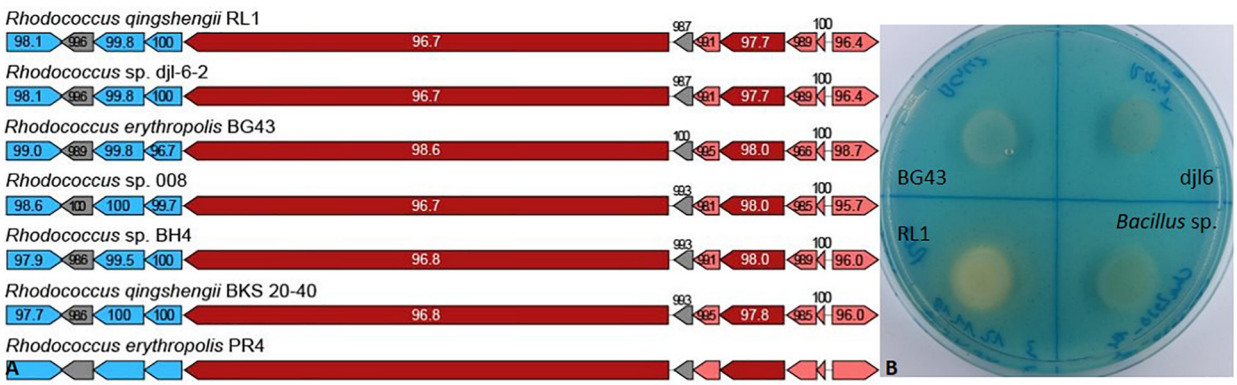

FIGURE 4 | Siderophore biosynthetic gene clusters and *in vitro* assay. **(A)** Heterobactin biosynthetic gene cluster based on antiSMASH results of *Rhodococcus qingshengii* RL1 compared to the reference genome of *R. erythropolis* PR4 and other *Rhodococcus* strains. Depicted as arrows are the core biosynthetic genes in dark red, additional biosynthetic genes in light red, transport-related genes in blue and additional genes in gray. The biosynthetic genes (dark and light red) are presented in order of their appearance from right to left encoding for isochorismate synthase, isochorismatase, 2,3-dihydro-2,3-dihydroxybenzoate dehydrogenase, 2,3-dihydroxybenzoate-AMP ligase, isochorismatase, and an amino acid adenylation domain-containing protein. Numbers indicate percentage of similarity to PR4. **(B)** *In vitro* assay for siderophore production of RL1, BG43, djl6 and *Bacillus* sp. detected with Chrome Azurol Blue overlay agar. Siderophore production is indicated by color change of the medium from blue to orange.

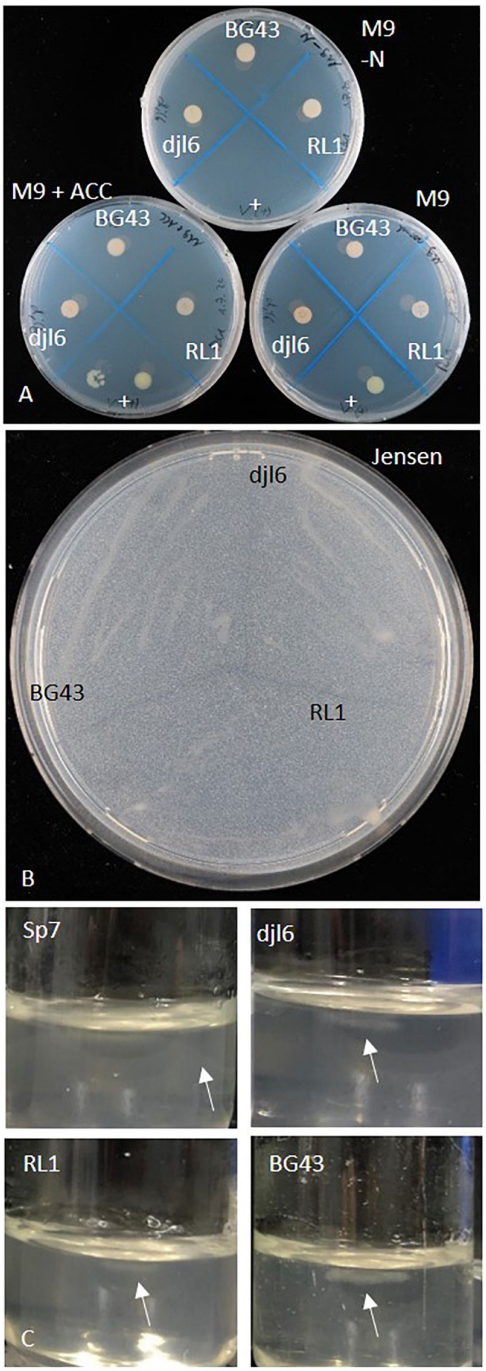

FIGURE 5 | Growth characterization of *Rhodococcus* strains RL1, djl6, and BG43 on various nitrogen-free media. **(A)** M9-N, M9 (control) and M9 + ACC, **(B)** Jensen's medium, and **(C)** Nfb-semisolid medium (Döbereiner, 1995) Sp7 = *Azospirillum brasilense* Sp7 (positive control for nitrogen fixation), + = *Variovorax* sp. (positive control for ACC deaminase activity). Arrows mark pellicle formation.

control *Pseudomonas simiae* WCS417 normalized biofilm formation was lower compared to djl6, but stronger compared to RL1 and BG43.

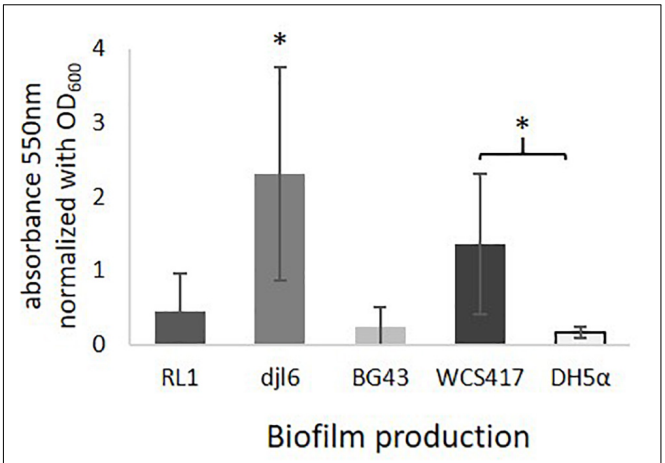

FIGURE 6 | Ability to produce Biofilms with averaged results from 3 experiments normalized to OD600 = 1. Significant difference is indicated by asterisks representing $^*P < 0.05$.

Interaction With Other Microbes

Confrontation Assay Against Plant–Pathogenic Fungi

RL1 inhibited the plant-pathogenic fungus *Fusarium oxysporum in vitro*. The positive biocontrol strain FZB42 inhibited the plant–pathogenic fungi *Rhizoctonia solani*, *Fusarium oxysporum*, and *Fusarium culmorum* indicated by inhibition zones (**Supplementary Figure 4**).

Degradation of Synthetic and Bacterial *N*-Acyl-Homoserinelactones (AHLs)

A *qsdA* gene (QEM30276) could be identified in the RL1 genome, which belongs to a class of large-spectrum quorum-quenching lactonases also present in other *Rhodococcus* sp. (**Figure 7A**). Therefore, AHL degradation ability was tested in RL1, djl6 and BG43 using the sensor strain A136. In this set-up it could be clearly shown that RL1, djl6 and BG43 were able to degrade synthetic C12-HSL (**Figures 7B–D**). Additionally, co-culturing of *Acidovorax radicis* N35e with RL1 resulted in no visible blue color formation by the sensor strain, indicating degradation of produced AHL (**Figure 7B**). Finally, V-shaped spotting of *Acidovorax radicis* N35e and RL1, djl6 and BG43 showed an inhibition of blue color formation where strains were in direct contact (**Figures 7E–H**).

Rhizosphere Competence

Root Colonization in Axenic System

Root colonization was analyzed with fluorescence *in situ* hybridization using probes EUB Mix Fluos and HGC69A Atto550 or HGC69A Cy3. Single cells of RL1 could be found on the root surface of its host plant Rucola (*Eruca sativa* L.) when grown in the axenic system (**Figures 8A–C**), while dense cell patches were identified on roots from MS agar plates (**Figure 8D**). Similar colonization patterns were found for strains djl6 and BG43. All strains were localized rather in the basal mature part of the root in areas of emergence of root hairs. No endophytic colonization was observed.

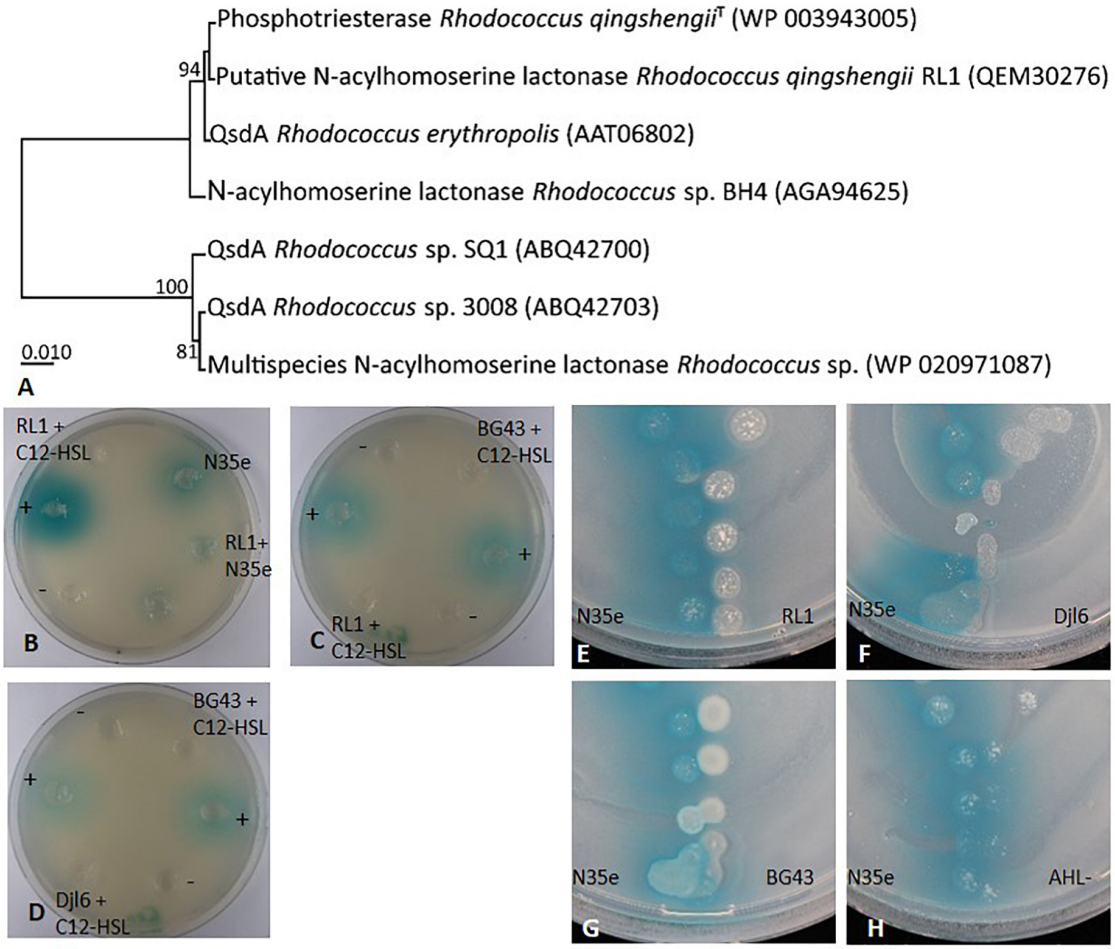

FIGURE 7 | AHL degradation and quorum quenching by *Rhodococcus* strains RL1, djl6, and BG43. **(A)** UPGMA phylogenetic tree of translated *qsdA* (quorum-sensing signal degradation) gene of RL1 and related sequences from *Rhodococcus* strains. The percentage of replicate trees in which the associated taxa clustered together in the bootstrap test (1000 replicates) are shown next to the branches. The evolutionary distances were computed using the Poisson correction method. All ambiguous positions were removed for each sequence pair (pairwise deletion option). There were a total of 323 positions in the final dataset. Evolutionary analyses were conducted in MEGA X (Kumar et al., 2018). **(B–D)** Well-diffusion plate assays on NB plates all supplemented with the sensor strain A136 and X-Gal. Except for the cultures containing AHL producing strain *A. radicis* N35e, C12-HSL was added during cultivation of all bacteria. Supernatants of these cultures were added to the wells and blue color formation by the sensor strain indicated remaining AHL in the tested supernatant. NB with C12-HSL (+) served as positive control, and NB without C12-HSL (–) as negative control. **(E–H)** V-shaped assays on NB after 30 h supplemented with the sensor strain A136 and X-Gal. AHL negative mutant *A. radicis* N35e AHL- served as control. Presence of AHLs is detected by the sensor strain *Agrobacterium tumefaciens* A136 indicated by blue color change of X-Gal.

Quantitative estimation based on CFU/mg root mass (**Figure 8E**) showed significantly higher colonization numbers for RL1 and djl6 (p-value = 0.012) than BG43. Djl6 showed a trend toward higher root colonization compared to RL1. All strains were significantly higher than the uninoculated control.

DISCUSSION

The genus *Rhodococcus* is frequently found in the plant microbiome (Francis and Vereecke, 2019; Vereecke et al., 2020). Therefore, it is important to analyze and understand functions of the plant-associated members of this genus, such as RL1 isolated from *Eruca sativa* leaves. Additionally, as mentioned in the introduction, the genus *Rhodococcus* is well-known for stress tolerant strains (Pátek et al., 2021). For these reasons, we wanted to elucidate genomic properties with a special focus on functional analyses of stress tolerance and interaction with plants to understand the possible functions that the plant-associated *R. qingshengii* RL1 could provide within the plant holobiont and also compare it to the closely related strains djl6 and BG43.

RL1 Genome Harbors Several Genes Involved in Survival and Tolerance to Different Stress Conditions

Genes involved in acidic pH tolerance were identified in RL1, either involved in the production of the compound squalene,

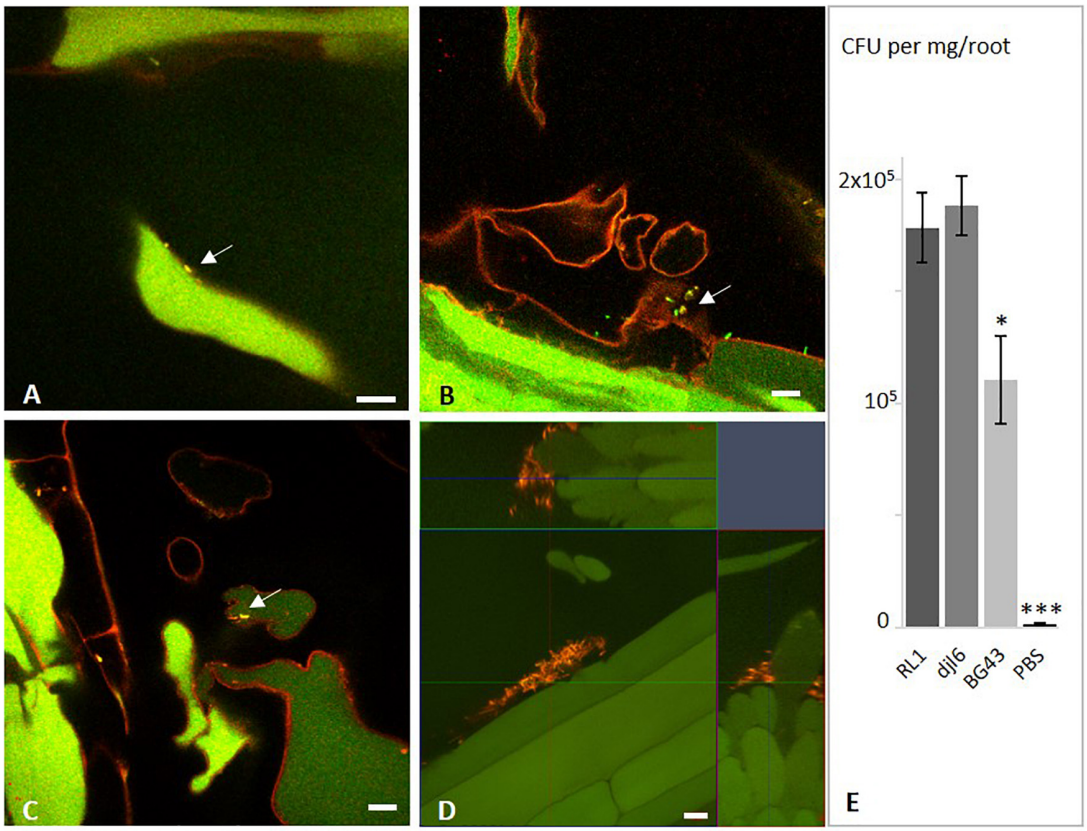

FIGURE 8 | Interaction of *Rhodococcus* strains RL1, BG43, and djl6 with *Eruca sativa* roots. *In situ* detection of root colonization of *Eruca sativa* by *Rhodococcus* strains visualized by fluorescence *in situ* hybridization (FISH). **(A)** RL1, **(B)** BG43, and **(C)** djl6 on 1 week old *Eruca sativa* roots grown in axenic quartz-sand system. **(D)** RL1 on 2 weeks old *Eruca sativa* roots grown on MS agar without additional sucrose. **(E)** Quantification of root colonization 1 week after inoculation. Arrows indicate bacterial cells identified by yellow color from overlaying channels of probes EUB (green) and HGC (red). Root autofluorescence is assigned in green and red. Scale bar represents 10 μm. Significant difference is indicated by asterisks representing $^{*}P < 0.05$ and $^{***}P < 0.001$.

such as squalene cyclase, a precursor of hopanoid (Schmerk et al., 2011) or based on the expression of the ADI cluster (in the presence of arginine). The latter is a mechanism to overcome acidic stress often found in gram-positive bacteria (Cotter and Hill, 2003). The experimental evidence proved the ability of *Rhodococcus* strain RL1 to survive and recover from acidic pH conditions. This trait was also shared by the closely related strains djl6 and BG43, indicating that this trait may be widespread amongst the genus *Rhodococcus*. In the genus *Rhodococcus* tolerance to acidic pH was reported for *R. qingshengii* BBG1 (Benedek et al., 2012) and for the mammalian pathogen *Rhodococcus equi*, which can withstand a pH of 4 (Benoit et al., 2000). Conventional agricultural practices and soil exploitation can lead to increased soil acidity (Goswami et al., 2017). Therefore, acidic pH tolerance is an important trait of plant-associated and soil bacteria to maintain a functional plant microbiome also under acidic soil conditions.

Ectoine is a compound associated with osmoregulation in bacteria (Bremer and Krämer, 2019) and important for survival during osmotic stress. The gene cluster for ectoine biosynthesis and transporters were identified in RL1, indicating the ability of RL1 to synthesize ectoine under osmotic stress. Alternative to biosynthesis, bacteria can take up compatible solutes, such as proline or betaine from their environment (Bremer and Krämer, 2019). Genes encoding the respective transporters were found in the RL1 genome. Additionally, the full operon of Na+/H+ antiporter was identified in the RL1 genome, which could play a role in salt stress tolerance (Liu et al., 2016; Bhat et al., 2020). Results of the *in vitro* experiments of the tested *Rhodococcus* strains growing under high salt and osmotic stress confirmed previous reports of osmotic and salt stress tolerant members of the genus *Rhodococcus*. For example, an upregulation of genes involved in ectoine biosynthesis was observed in *Rhodococcus jostii* RHA1 under desiccation (LeBlanc et al., 2008) and rapid adaptation to salt stress was described for *R. erythropolis* DSM 1069 (De Carvalho et al., 2014). Moreover, plant associated bacteria tolerant to osmotic and salt stress could also be beneficial for the plant via support of ion homeostasis (Bhat et al., 2020; Salas-González et al., 2021) and upregulation of osmoprotective compound biosynthesis in the plant. For example, *Bacillus* sp. can directly influence proline biosynthesis in plants to improve osmotolerance (Kaushal and Wani, 2016; Bhat et al., 2020).

Heavy metals, such as mercury, are highly persistent environmental pollutants and a threat to all living organisms

(Boyd and Barkay, 2012). Organomercury compounds were used in several agricultural applications, for example as common pest control agent in the 1900's. Although its use has been banned in several countries, it is still used in Australia to treat the plant pathogenic fungus *Ceratocystis paradoxa* (Schneider, 2021). Mercury resistant bacteria can convert organomercury compounds or Hg(II) to gaseous Hg(0) to reduce the mercury concentration in their environment (Boyd and Barkay, 2012). Mercury resistance was described in *R. erythropolis* BD2 and *Pseudomonas fluorescens* SBW25 to be located and transferred on a plasmid (Dabrock et al., 1994; Hall et al., 2020) containing the *mer*-operon (Boyd and Barkay, 2012). Loss of this plasmid caused a loss of mercury resistance (Dabrock et al., 1994; Hall et al., 2020). However, in RL1 the identified mercury resistance genes, such as a transcriptional regulator *MerR* and a unique alkylmercury lyase involved in the degradation of toxic organomercury compounds (e.g., MeHg) (Schaefer et al., 2004), are located in the chromosome. We report for the first time that mercury tolerance is also present in an isolate of *R. qingshengii* based on the results of the *in vitro* experiment. BG43 and RL1 were both able to survive up to 1 mM of mercury in the growth medium. Survival and detoxification of heavy metals have been reported for other members of the genus *Rhodococcus* (Trivedi et al., 2007; Irawati et al., 2012), emphasizing the exceptional stress tolerance of this genus. Heavy metal resistance in bacteria in combination with a close association with plants could indicate the adaptation to toxic heavy metal residues of such compounds previously used as pesticides.

Apart from tolerance to heavy metals, we could identify several operons in the genome of RL1 which show that this bacterium has the ability to survive under selective environmental conditions by metabolizing trace gasses like CO and H_2. Comparison of deduced amino acid sequences revealed that the identified CODH belongs to the functional type1-CODH enzymes, which catalyze the unidirectional conversion of CO to CO_2 (King and Weber, 2007). This type of enzyme has been extensively studied in aerobic CO-oxidizers, or carboxydotrophic Actinobacteria (Quiza et al., 2014). Sequence similarity revealed that the identified [NiFe]-hydrogenase cluster belongs to the high-affinity group 1 h/5 Actinobacteria type of hydrogenases which have been shown to scavenge electrons from tropospheric H_2 to sustain aerobic respiration during starvation (Constant et al., 2011; Greening et al., 2016). Interestingly, less is known about plant associated atmospheric H_2-oxidizing bacteria. Atmospheric H_2 may serve as the maintenance energy during starvation and sporulation of high-affinity H_2-oxidizing Actinobacteria, providing them the advantage of survival in plant tissues, as was shown for endophytic *Streptomyces* spp. (Greening et al., 2016; Kanno et al., 2016). The simultaneous presence of the carbon monoxide dehydrogenase (CODH) genes and the [NiFe]-hydrogenase cluster indicate that RL1 can use CO and H_2 as energy source.

The functional annotation of RL1 genome also revealed that it harbors genes involved in multidrug resistance, tellurite resistance and antibiotic resistance. Tellurite is a metalloid often used as antibiotic compound in *in vitro* experiments and is toxic to eukaryotic and prokaryotic cells (Chien and Han, 2009). Resistance against tellurite can be mediated by a reduction of tellurite (TeO_3^{2-}) to elemental tellurium, indicated by the color change of the colonies, which was also observed in RL1. Moreover, the RL1 genome harbors genes potentially involved in protection against oxidative stress. These genes could be involved in detoxification of tellurite, because the toxicity of tellurite is eventually caused through intracellular generation of reactive oxygen species (ROS) (Pérez et al., 2007).

In vitro tests with antibiotics revealed resistance of RL1 against kanamycin and ampicillin, whereas djl6 and BG43 are more resistant to rifampicin and vancomycin respectively. Antibiotic resistance was mainly investigated and is widespread in the horse pathogen *Rhodococcus equi* (Giguère et al., 2017), because of its relevance in livestock animal infections. Antibiotic resistance in plant-associated *Rhodococcus* species was not intensively studied yet and could confer them a competitive advantage in surviving against other antibiotic-producing microbes in specialized niches like the rhizosphere (Raaijmakers et al., 2009; Mendes et al., 2013).

RL1 Genome Reveals Successful Interaction and Survival Strategies in Association With Plants

The genome annotation of RL1 and functional analysis revealed a large repertoire of traits involved in plant–microbe and microbe–microbe interactions, which can be relevant for the role of RL1 in the plant microbiome.

An important trait of plant-associated bacteria is the ability to colonize plant roots to facilitate, e.g., the exchange of metabolites (Kloepper and Beauchamp, 1992; Pandit et al., 2020). For successful root colonization it can be beneficial for the bacteria to be able to produce biofilms (Pandit et al., 2020), which was demonstrated for RL1, djl6, and BG43. Accordingly, the RL1 genome harbors genes encoding for enzymes involved in biofilm formation. Qualitative evaluation of rhizosphere competence revealed that all three strains were able to colonize the roots of *E. sativa* epiphytically. However, quantitative evaluation revealed that RL1 and djl6 had significantly more CFUs per mg *E. sativa* root than BG43, which indicates a better root colonization ability of *R. qingshengii* species. Verification of endo- or epiphytic leaf colonization of RL1 analyzed with FISH (data not shown) did not deliver clear results due to high auto-fluorescence of the leaves and transformation of fluorescent markers in RL1 was not successful. Therefore, final conclusions upon leaf colonization of RL1 cannot be drawn.

The leaves of *Brassicacea*, such as Rucola (*Eruca sativa* L.) contain glucosinolates (GSLs), which are sulfur-containing secondary metabolites involved in the protection of plants against herbivores (Textor and Gershenzon, 2009; Bell et al., 2015). Since RL1 was isolated from the leaves of Rucola (*Eruca sativa* L.), we were interested if the genome reveals some interesting information about its ability to metabolize glucosinolates. Our results showed that the genome harbors genes potentially involved in the metabolic pathways of GSLs, such as myrosinase, methionine sulfoxide reductase (*msrA*, *msrB*) or aldoxime dehydratase *oxd* (**Supplementary Table 4**). Degradation of GSLs

was investigated for gut microbes regarding beneficial effects of ITC production as a chemoprotective function against cancer (Mullaney et al., 2013a,b; Bessler and Djaldetti, 2018; Mokhtari et al., 2018). An *in vitro* experiment with Rucola (*Eruca sativa* L.) leaf extract and pure GSLs (data not shown) did not reveal clear and consistent results on GSL synthesis, bioconversion or degradation by RL1, djl6, and BG43.

The RL1 genome harbors genes related to the production of volatiles, exopolysaccharides and proteases, which are important in microbial communication, plant colonization and microbial detection by the host (Flemming et al., 2016; Netzker et al., 2020). The chemotaxis protein CheY relevant for the transmission of sensory signals from the chemoreceptors to the flagella motors, which is additionally a microbe-associated molecular pattern (MAMP) (Paul et al., 2010) was identified in the RL1 genome. As *Rhodococcus* is a non-motile genus CheY has a rather different function, e.g., in sensory signal transduction in another pathway or interaction with the plant. Additionally, in the RL1 genome genes encoding for a LacI transcription regulator and an aldo-keto reductase were identified, which were found to be enriched in genomes of plant beneficial microbes (Levy et al., 2018).

Plant associated bacteria in general can influence root growth, germination, flowering and developmental stages via balancing or producing plant hormones, such as gibberellin (Kang et al., 2014; Panke-Buisse et al., 2017; Salazar-Cerezo et al., 2018) or indole-3-acetic acid (IAA) (Finkel et al., 2020). In the *in vitro* assay RL1 produced a higher amount of IAA in comparison to the strains djl6 and BG43. The best-known pathway for IAA production includes the enzyme indolepyruvate decarboxylase (*ipdC*), which is not present in the RL1 genome. Instead genes of the alternative indole-3-acetamide pathway for IAA production (Spaepen et al., 2007) were identified in the RL1 genome. The ability to produce IAA *in vitro* was not only shown for RL1 but also in another *R. qingshengii* strain (Hasuty et al., 2018) and other members of the genus *Rhodococcus* (Francis and Vereecke, 2019). Bacterial production of IAA can be beneficial for the plant by increasing the root system (Spaepen and Vanderleyden, 2011) and balancing IAA production is an important function of the root microbiome (Finkel et al., 2020). Gibberellin production is encoded by a conserved operon, which was characterized in α- and β-proteobacteria (Nagel et al., 2018). Essential parts of the gibberellin operon were identified in the RL1 genome. To our knowledge, this is the first report about the presence of genes of the gibberellin operon in any Actinobacteria. Some plant-pathogenic bacteria produce bioactive GA4, which can have a detrimental effect on seedling development. Beneficial bacteria only produce the precursor GA9 as they lack the cytochrome P450 (CYP115) for the final step in the production of the bioactive GA4 (Nagel and Peters, 2017). As RL1 also lacks the cytochrome P450 (CYP115) this indicates its allocation to the plant beneficial bacteria. Verification of the production of gibberellin by RL1 with gas chromatography was beyond the scope of this work.

The bacterially produced polyamine spermidine increases biofilm formation and overall bacterial fitness (Xie et al., 2014; Liu et al., 2016). Additionally, it is the plant growth-promoting compound in strains such as *B. subtilis* OKB105 or *Klebsiella* sp. D5A (Xie et al., 2014; Liu et al., 2016) and the upregulation of spermidine export proteins in *Stenotrophomonas rhizophila* DSM14405 upon salt stress in combination with exposure to root exudates emphasizes the role of spermidine as key substance in stress protection in roots (Alavi et al., 2013). Presence of genes encoding for the enzymes involved in the biosynthesis of spermidine, such as arginine decarboxylase, agmatinase, spermidine synthase in the RL1 genome indicate the ability of RL1 to function as stress-protecting agent and support plants under abiotic stress.

The degradation of 1-amino-cyclopropane-1-carboxylate (ACC), the precursor of the plant hormone ethylene, by bacterial ACC deaminase can protect the plant from detrimental effects of long exposure to ethylene (Glick, 2012; Dubois et al., 2018). In a standard *in vitro* assay RL1, djl6, and BG43 were able to grow on nitrogen-free M9 plates with ACC in the medium, indicating ACC deaminase activity (**Figure 5A**). However, the essential gene *acdS* encoding for ACC deaminase is missing in the RL1 genome. Additionally, all three tested *Rhodococcus* strains were able to grow on all tested nitrogen free media. The results indicate that the isolates grow on N-free media through utilization of atmospheric nitrogen rather than using ACC as a nitrogen source. Biological nitrogen fixation is defined as the bacterial conversion of dinitrogen to ammonia through the expression of canonical *nif* gene products (Dos Santos et al., 2012; Higdon et al., 2020). In the RL1 genome the SUF system FeS assembly protein of the *nifU* family was identified (MSMEG_2718, **Supplementary Table 4**), which stabilizes the nitrogenase complex and is relevant for diazotrophy especially under low temperature conditions (Suyal et al., 2014). The *nifH* gene was previously identified in a diazotrophic *R. qingshengii* strain (Suyal et al., 2014; Joshi et al., 2019) and used as molecular marker to directly link to a diazotrophic lifestyle. However, no *nifH* gene was identified in the RL1 genome. In a large scale genome analysis Higdon et al. (2020) identified three distinct groups of diazotrophic bacteria defined by *nif* gene content and structural variation. The genus *Rhodococcus* was classified as DS-negative (=no Dos Santos model *nif* gene homolog present in genome). This implies the presence of alternative *nif* genes and metabolic pathways relevant for nitrogen fixation in *Rhodococcus* genomes beyond the currently known models. Transcriptome analysis and mutant construction would reveal insights to alternative nitrogen fixation mechanisms in RL1 as representative of the genus *Rhodococcus*.

Siderophores not only chelate iron and have beneficial effects in plant growth, they are also involved in bioremediation, function as biosensors and are relevant in microbial competition and defense against other microbes, which can lead to a beneficial biocontrol effect for the plant (Ahmed and Holmström, 2014; Gu et al., 2020; Pollak and Cordero, 2020). Genes involved in iron acquisition and siderophore production were identified in the RL1 genome, for example for the siderophore heterobactin, which is unique to the *Rhodococcus* genus (Carrano et al., 2001; Bosello et al., 2013; Khilyas et al., 2020). The *in vitro* assay for siderophore production was positive for RL1, corroborating that the identified genes were actually expressed. These results were

in contrast to djl6 and BG43, where the functional analysis was negative. Iron acquisition and ferrous iron transport can occur via two systems, the FeoABC and EfeUOB transporters (Lau et al., 2016). The EfeUOB was reported to be low-pH-induced (Cao et al., 2007) and was predicted in the genome of a *Leptospirillum* sp. tolerant to acidic pH (Osorio et al., 2008). RL1 harbors the genes encoding for the EfeUOB operon, which could contribute to the low pH tolerance of RL1, because it allows iron acquisition also under low pH.

The RL1 genome harbors genes relevant for organic acid production, which are involved in phosphate solubilization and genes potentially relevant for phosphate metabolism and transport. However, genes involved in gluconic acid production, which is the main driver in phosphate solubilization could not be identified (Rodríguez et al., 2006). Despite of that, the *in vitro* assay for this trait was positive for RL1 which suggests the presence of alternative organic acids involved in phosphate solubilization. Phosphate solubilization capacity was previously reported for *Rhodococcus globerulus* isolated from *Plectranthus amboinicus* (Murugappan et al., 2017).

RL1 Genome Reveals Competitive Potential Against Other Microorganisms

Members of the genus *Rhodococcus* have been reported to show antifungal activity *in vitro* against plant-pathogenic fungi (Chiba et al., 1999; Iwatsuki et al., 2007; Santos et al., 2020) and RL1 reduced growth of *F. oxysporum in vitro,* but showed no inhibition against *R. solani* and *F. culmorum* (**Supplementary Figure 4**). Further studies using model plants will reveal the full potential of RL1 as biocontrol agent against plant pathogenic fungi.

Degradation or interference with quorum sensing molecules can disturb bacterial communication and is called quorum quenching (Dong et al., 2001). The *qsdA* gene, encoding for a *N*-acyl-HSL lactonase was first described by Uroz et al. (2003) for the strain *R. erythropolis* W2 and could also be identified in the RL1 genome (**Figure 7A**). Moreover, the RL1 genome harbors a two-component transcriptional AHL responsive regulator from the LuxR family. However, as RL1 is not producing AHLs this regulator is likely a so-called LuxR-solo, which allows bacteria to respond to quorum sensing signals from neighboring cells without itself contributing to signal synthesis. This was also previously described for the genus *Rhodococcus* and other gram-positive bacteria (Subramoni and Venturi, 2009; Santos et al., 2012). *In vitro* experiments showed the ability of RL1 to degrade AHLs. To our knowledge, this is the first report of an AHL-degrading *R. qingshengii*. Also it is the first description of functional AHL degradation by BG43, which was previously reported only to interfere with the quinolone signal of *Pseudomonas aeruginosa* (Müller et al., 2014). Quorum quenching ability was intensively studied in *R. erythropolis* R138 (Cirou et al., 2007; Barbey et al., 2013; Latour et al., 2013; Kwasiborski et al., 2015), which was able to reduce the soft-rot pathogen *Pectobacterium* in potatoes and most likely use the degraded AHLs as carbon source. Quorum quenching can also be a beneficial trait in other crop-pathogen systems as reported for example in *Pseudomonas segetis* (Rodríguez et al., 2020) or *Bacillus thuringensis* (Dong et al., 2004). Further analysis of RL1 quorum quenching abilities, e.g., against plant pathogens such as *Pectobacterium* or *Pseudomonas syringae*, would reveal its full potential as plant biocontrol agent.

Genome Comparison of Related *R. erythropolis* and *R. qingshengii* Isolates Show Potential for Re-classification of Clade Members

Rhodococcus is a genus well-known for its high potential to produce versatile secondary metabolites and the RL1 genome annotation confirms previous studies (Ceniceros et al., 2017; Thompson et al., 2020). The number of genes from the genome of RL1, which were assigned to the COG group for secondary metabolites, were higher compared to other bacteria, for example *Stenotrophomonas* or *Enterobacter* (Alavi et al., 2014; Andrés-Barrao et al., 2017). Additionally, 17 BGC for secondary metabolites were identified in RL1. The average number of BGCs in the *R. erythropolis* clade are 13–24 BGCs and are mostly shared by *R. erythropolis* and *R. qingshengii* strains (Thompson et al., 2020). Four BGC cluster were highly conserved among the *R. erythropolis* clade and three of them were also identified in RL1 (**Supplementary Table 3**). The remaining unknown BGCs in the RL1 genome are potentially capable of producing novel compounds which could be analyzed in future studies.

Rhodococcus is a heterogeneous genus with eight identified phylogenetic clades (Alvarez, 2019). Phylogenetic analysis based on complete genome sequences of the *R. erythropolis* clade reveals a clear separation into two subgroups at an ANI value of 97% (**Figure 1** and **Supplementary Figure 2**). The first one includes sequences belonging to only *R. erythopolis*, the second includes *R. qingshengii* and *R. erythropolis* strains. Based on the clear separation we can confirm previous recommendations to separate the *R. erythropolis* clade into the two groups consisting of the species *R. qingshengii* and *R. erythropolis* respectively (Sangal et al., 2016; Khilyas et al., 2020; Thompson et al., 2020). We also suggest that the *R. erythropolis* strains assigned to the *R. qingshengii* group should be re-named as previously recommended (Sangal et al., 2016; Thompson et al., 2020). The genomes of RL1 and djl6 were clearly identified as belonging to the *R. qingshengii* cluster (Xu et al., 2007; Kuhl et al., 2019) and had more genes in common with each other than with BG43 (**Figure 2**), whereas the BG43 genome was classified as *R. erythropolis* (Müller et al., 2014; Rückert et al., 2015). Despite the clear separation the strains RL1 and BG43 had many functional traits in common, indicating a close functional overlap between the species. At the same time, djl6 and RL1 showed different results in the *in vitro* experiment for siderophore production and mercury tolerance, indicating differences on the genetic and functional level also within the species *R. qingshengii* (**Figure 4**). RL1 showed overall the best performance in the tested traits. This emphasizes the importance of RL1 and the necessity to analyze the genetic and functional potential of individual strains to understand the role also of lesser known members of the plant microbiome.

CONCLUSION AND OUTLOOK

The study shows the remarkable genomic potential of the isolate *R. qingshengii* RL1 for tolerating various abiotic stresses, plant–microbe and microbe–microbe interactions, many of which could be confirmed by functional analysis *in vitro*. By this thorough characterization we aim to contribute to a better understanding of relevant attributes for interactions in the plant holobiont as well as provide selection criteria for using strains, such as RL1, in specific agricultural or biotechnological applications. Furthermore, we provided phylogenetic evidence based on whole genome comparisons to justify a taxonomic separation of the *R. erythropolis* and *R. qingshengii* cluster and re-name some members of the *R. erythropolis* cluster. However, the functional analysis also indicates many shared traits between the two species *R. qingshengii* and *R. erythropolis*, some of them also described for the first time for the strains djl6 and BG43, but also different traits within the same species. Further experiments involving inoculation of different plants with RL1 under various conditions, which were beyond the scope of this study, would reveal insights into its plant beneficial functions. This could be coupled with transcriptome analysis of RL1 to reveal such intriguing aspects as an alternative nitrogen fixation pathway. Further investigation of the quorum quenching ability against various plant–pathogenic bacteria could advance the understanding of the role of RL1 in biological control.

DATA AVAILABILITY STATEMENT

The datasets presented in this study can be found in the NCBI database. Accession numbers are for *Rhodococcus qingshengii* RL1 NZ_CP042917, NZ_CP042916, NZ_CP042915, for *Rhodococcus qingshengii* djl6 NZ_CP025959, NZ_CP025960, NZ_CP025961, NZ_CP025962, and for *Rhodococcus erythropolis* BG43 NZ_CP011295, NZ_CP011296, NZ_CP011297, and NZ_CP011298.

AUTHOR CONTRIBUTIONS

TK, SC, and MR contributed to conception and design of the study. TK performed the experiments and wrote the first draft of the manuscript. JU contributed parts of the experimental data. SC and TK analyzed the data. SC and MR wrote sections of the manuscript. All authors contributed to manuscript revision, read, and approved the submitted version.

ACKNOWLEDGMENTS

We thank the Institute of Biochemical Plant Pathology (BIOP) at Helmholtz Center Munich for providing *Fusarium culmorum* G2191, *Fusarium oxysporum* DSM62297 and Dr. Rita Grosch [Leibniz Institute of Vegetable and Ornamental Crops (IGZ), Großbeeren, Germany] for providing *Rhizoctonia solani* for our experiments. Thank you to S. Klink, F. Tunc, and A. Sabunchi for technical support.

SUPPLEMENTARY MATERIAL

The Supplementary Material for this article can be found online at: https://www.frontiersin.org/articles/10.3389/fmicb.2021.708605/full#supplementary-material

REFERENCES

Abbamondi, G. R., Tommonaro, G., Weyens, N., Thijs, S., Sillen, W., Gkorezis, P., et al. (2016). Plant growth-promoting effects of rhizospheric and endophytic bacteria associated with different tomato cultivars and new tomato hybrids. *Chem. Biol. Technol. Agric.* 3, 1–10. doi: 10.1186/s40538-015-0051-3

Ahmed, E., and Holmström, S. J. M. (2014). Siderophores in environmental research: roles and applications. *Microb. Biotechnol.* 7, 196–208. doi: 10.1111/1751-7915.12117

Alabid, I., Hardt, M., Imani, J., Hartmann, A., Rothballer, M., Li, D., et al. (2020). The N-acyl homoserine-lactone depleted Rhizobium radiobacter mutant RrF4NM13 shows reduced growth-promoting and resistance-inducing activities in mono- and dicotyledonous plants. *J. Plant Dis. Prot.* 127, 769–781. doi: 10.1007/s41348-020-00360-8

Alavi, P., Starcher, M. R., Thallinger, G. G., Zachow, C., Müller, H., and Berg, G. (2014). *Stenotrophomonas* comparative genomics reveals genes and functions that differentiate beneficial and pathogenic bacteria. *BMC Genomics* 15:482. doi: 10.1186/1471-2164-15-482

Alavi, P., Starcher, M. R., Zachow, C., Müller, H., and Berg, G. (2013). Root-microbe systems: the effect and mode of interaction of Stress Protecting Agent (SPA) *Stenotrophomonas* rhizophila DSM14405T. *Front. Plant Sci.* 4:141. doi: 10.3389/fpls.2013.00141

Alquéres, S., Meneses, C., Rouws, L., Rothballer, M., Baldani, I., Schmid, M., et al. (2013). The bacterial superoxide dismutase and glutathione reductase are crucial for endophytic colonization of rice roots by Gluconacetobacter diazotrophicus PAL5. *MPMI* 26, 937–945. doi: 10.1094/MPMI-12-12-0286-R

Alvarez, H. M. (2019). *Biology of Rhodococcus*. Switzerland: Springer.

Amann, R. I., Krumholz, L., and Stahl, D. A. (1990). Fluorescent-oligonucleotide probing of whole cells for determinative and environmental studies in microbiology. *J. Bacteriol.* 172, 762–770. doi: 10.1128/jb.172.2.762-770.1990

Andrés-Barrao, C., Lafi, F. F., Alam, I., de Zélicourt, A., Eida, A. A., Bokhari, A., et al. (2017). Complete genome sequence analysis of *Enterobacter* sp. SA187, a plant multi-stress tolerance promoting endophytic bacterium. *Front. Microbiol.* 8:2023. doi: 10.3389/fmicb.2017.02023

Anton, B. P., and Raleigh, E. A. (2016). Complete Genome Sequence of NEB 5-alpha, a Derivative of *Escherichia coli* K-12 DH5α. *Genome Announc.* 4, 6–7. doi: 10.1128/genomeA.01245-16

Aziz, R. K., Bartels, D., Best, A., DeJongh, M., Disz, T., Edwards, R. A., et al. (2008). The RAST Server: Rapid annotations using subsystems technology. *BMC Genomics* 9:75. doi: 10.1186/1471-2164-9-75

Babin, D., Sommermann, L., Chowdhury, S. P., Behr, J. H., Sandmann, M., Neumann, G., et al. (2021). Distinct rhizomicrobiota assemblages and plant performance in lettuce grown in soils with different agricultural management histories. *FEMS Microbiol. Ecol.* 97:fiab027. doi: 10.1093/femsec/fiab027

Bahramisharif, A., and Rose, L. E. (2019). Efficacy of biological agents and compost on growth and resistance of tomatoes to late blight. *Planta* 249, 799–813. doi: 10.1007/s00425-018-3035-2

Banerjee, S., Walder, F., Büchi, L., Meyer, M., Held, A. Y., Gattinger, A., et al. (2019). Agricultural intensification reduces microbial network complexity and the abundance of keystone taxa in roots. *ISME* 13, 1722–1736. doi: 10.1038/s41396-019-0383-2

Barbey, C., Crépin, A., Bergeau, D., Ouchiha, A., Mijouin, L., Taupin, L., et al. (2013). In Planta biocontrol of *Pectobacterium atrosepticum* by *Rhodococcus erythropolis* involves silencing of pathogen communication by the rhodococcal gamma-lactone catabolic pathway. *PLoS One* 8:e66642. doi: 10.1371/journal.pone.0066642

Belimov, A. A., Safronova, V. I., Sergeyeva, T. A., Egorova, T. N., Matveyeva, V. A., Tsyganov, V. E., et al. (2001). Characterization of plant growth promoting rhizobacteria isolated from polluted soils and containing 1-aminocyclopropane-1-carboxylate deaminase. *Can. J. Microbiol.* 47, 642–652. doi: 10.1139/w01-062

Bell, L., Oruna-Concha, M. J., and Wagstaff, C. (2015). Identification and quantification of glucosinolate and flavonol compounds in rocket salad (*Eruca sativa*, *Eruca vesicaria* and *Diplotaxis tenuifolia*) by LC-MS: highlighting the potential for improving nutritional value of rocket crops. *Food Chem.* 172, 852–861. doi: 10.1016/j.foodchem.2014.09.116

Benedek, T., Máthé, I., Salamon, R., Rákos, S., Pásztohy, Z., Márialigeti, K., et al. (2012). Potential bacterial soil inoculant made up by Rhodococcus sp. and *Pseudomonas* sp. for remediation in situ of hydrocarbon - and heavy metal polluted soils. *Stud. Univ. Babes-Bolyai Chem.* 2012, 199–211.

Benoit, S., Taouji, S., Benachour, A., and Hartke, A. (2000). Resistance of *Rhodococcus* equi to acid pH. *Int. J. Food Microbiol.* 55, 295–298. doi: 10.1016/S0168-1605(00)00172-0

Berendsen, R. L., Vismans, G., Yu, K., Song, Y., de Jonge, R., Burgman, W. P., et al. (2018). Disease-induced assemblage of a plant-beneficial bacterial consortium. *ISME J.* 12, 1496–1507. doi: 10.1038/s41396-018-0093-1

Berg, G., Alavi, M., and Schmidt, C. S. (2013). "Biocontrol and osmoprotection for plants under salinated conditions," in *Molecular Microbial Ecology of the Rhizosphere 2*, ed. F. J. de Bruijn (Hoboken, NJ: John Wiley and Sons, Inc), 587–592. doi: 10.1002/9781118297674.ch55

Berg, G., Rybakova, D., Grube, M., Köberl, M., and Price, A. (2017). The plant microbiome explored: implications for experimental botany. *J. Exp. Bot.* 67, 995–1002. doi: 10.1093/jxb/erv466

Bessler, H., and Djaldetti, M. (2018). Broccoli and human health: immunomodulatory effect of sulforaphane in a model of colon cancer. *Int. J. Food Sci. Nutr.* 69, 946–953. doi: 10.1080/09637486.2018.1439901

Bhat, M. A., Kumar, V., Wani, I. A., Dar, F. L., Farooq, I., Bhatti, F., et al. (2020). Mechanistic insights of the interaction of plant growth-promoting rhizobacteria (PGPR) with plant roots toward enhancing plant productivity by alleviating salinity stress. *Front. Microbiol.* 11:1952. doi: 10.3389/fmicb.2020.01952

Blin, K., Wolf, T., Chevrette, M. G., Lu, X., Schwalen, C. J., Kautsar, S. A., et al. (2017). AntiSMASH 4.0 - improvements in chemistry prediction and gene cluster boundary identification. *Nucleic Acids Res.* 45, W36–W41. doi: 10.1093/nar/gkx319

Blom, J., Kreis, J., Spänig, S., Juhre, T., Bertelli, C., Ernst, C., et al. (2016). EDGAR 2.0: an enhanced software platform for comparative gene content analyses. *Nucleic Acids Res.* 44, W22–W28. doi: 10.1093/nar/gkw255

Bosello, M., Zeyadi, M., Kraas, F. I., Linne, U., Xie, X., and Marahiel, M. A. (2013). Structural characterization of the *heterobactin siderophores* from *Rhodococcus erythropolis* PR4 and elucidation of their biosynthetic machinery. *J. Nat. Prod.* 76, 2282–2290. doi: 10.1021/np4006579

Boyd, E. S., and Barkay, T. (2012). The mercury resistance operon: from an origin in a geothermal environment to an efficient detoxification machine. *Front. Microbiol.* 3:349. doi: 10.3389/fmicb.2012.00349

Bremer, E., and Krämer, R. (2019). Responses of microorganisms to osmotic stress. *Annu. Rev. Microbiol.* 73, 313–334. doi: 10.1146/annurev-micro-020518-115504

Brevik, E. C., and Burgess, L. C. (2014). The influence of soils on human health. *Nat. Educ. Knowl.* 5:1.

Cao, J., Woodhall, M. R., Alvarez, J., Cartron, M. L., and Andrews, S. C. (2007). EfeUOB (YcdNOB) is a tripartite, acid-induced and CpxAR-regulated, low-pH Fe2+ transporter that is cryptic in *Escherichia coli* K-12 but functional in E. coli O157:H7. *Mol. Microbiol.* 65, 857–875. doi: 10.1111/j.1365-2958.2007.05802.x

Carrano, C. J., Jordan, M., Drechsel, H., Schmid, D. G., and Winkelmann, G. (2001). Heterobactins: a new class of siderophores from *Rhodococcus erythropolis* IGTS8 containing both hydroxamate and catecholate donor groups. *BioMetals* 14, 119–125. doi: 10.1023/A:1016633529461

Ceniceros, A., Dijkhuizen, L., and Petrusma, M. (2017). Molecular characterization of a *Rhodococcus jostii* RHA1 γ-butyrolactone(-like) signalling molecule and its main biosynthesis gene gblA. *Sci. Rep.* 7:17743. doi: 10.1038/s41598-017-17853-6

Chiba, H., Agematu, H., Sakai, K., Dobashi, K., and Yoshioka, T. (1999). Rhodopeptins, novel cyclic tetrapeptides with antifungal activities from Rhodococcus sp. *J. Antibiot. (Tokyo)* 52, 710–720. doi: 10.7164/antibiotics.52.710

Chien, C. C., and Han, C. T. (2009). Tellurite resistance and reduction by a Paenibacillus sp. isolated from heavy metal-contaminated sediment. *Environ. Toxicol. Chem.* 28, 1627–1632. doi: 10.1897/08-521.1

Chowdhury, S. P., Hartmann, A., Gao, X. W., and Borriss, R. (2015a). Biocontrol mechanism by root-associated Bacillus amyloliquefaciens FZB42 - A review. *Front. Microbiol.* 6:780. doi: 10.3389/fmicb.2015.00780

Chowdhury, S. P., Uhl, J., Grosch, R., Alquéres, S., Pittroff, S., Dietel, K., et al. (2015b). Cyclic lipopeptides of Bacillus amyloliquefaciens subsp. plantarum colonizing the lettuce rhizosphere enhance plant defense responses toward the bottom rot pathogen *Rhizoctonia solani*. *MPMI* 28, 984–995. doi: 10.1094/MPMI-03-15-0066-R

Cirou, A., Diallo, S., Kurt, C., Latour, X., and Faure, D. (2007). Growth promotion of quorum-quenching bacteria in the rhizosphere of *Solanum tuberosum*. *Environ. Microbiol.* 9, 1511–1522. doi: 10.1111/j.1462-2920.2007.01270.x

Constant, P., Chowdhury, S. P., Hesse, L., Pratscher, J., and Conrad, R. (2011). Genome data mining and soil survey for the novel group 5 [NiFe]-hydrogenase to explore the diversity and ecological importance of presumptive high-affinity H 2-oxidizing bacteria. *Appl. Environ. Microbiol.* 77, 6027–6035. doi: 10.1128/AEM.00673-11

Cotter, P. D., and Hill, C. (2003). Surviving the acid test: responses of gram-positive bacteria to low pH. *Microbiol. Mol. Biol. Rev.* 67, 429–453. doi: 10.1128/mmbr.67.3.429-453.2003

Dabrock, B., Kesseler, M., Averhoff, B., and Gottschalk, G. (1994). Identification and characterization of a transmissible linear plasmid from *Rhodococcus erythropolis* BD2 that encodes isopropylbenzene and trichloroethene catabolism. *Appl. Environ. Microbiol.* 60, 853–860. doi: 10.1128/aem.60.3.853-860.1994

Daims, H., Bruhl, A., Amann, R. I., Schleifer, K.-H., and Wagner, M. (1999). The domainspecific probe EUB-338 is insufficient for the detection of all bacteria: development and evaluation of a more comprehensive probe set. *Syst. Appl. Microbiol.* 22, 434–444. doi: 10.1016/s0723-2020(99)80053-8

De Carvalho, C. C. C. R., Marques, M. P. C., Hachicho, N., and Heipieper, H. J. (2014). Rapid adaptation of *Rhodococcus erythropolis* cells to salt stress by synthesizing polyunsaturated fatty acids. *Appl. Microbiol. Biotechnol.* 98, 5599–5606. doi: 10.1007/s00253-014-5549-2

Döbereiner, J. (1995). "Isolation and identification of aerobic nitrogen-fixing bacteria from soil and plants," in *Methods in Applied Soil Microbiology and Biochemistry*, eds K. Alef and P. Nannipieri (London: Academic Press), 134–141.

Dong, Y.-H., Wang, L.-H., Xu, J.-L., Zhang, H.-B., Zhang, X.-F., and Zhang, L.-H. (2001). Quenching quorum-sensing- dependent bacterial infection by an N-acyl *homoserine lactonase*. *Nature* 411, 813–817. doi: 10.1038/35081101

Dong, Y. H., Zhang, X. F., Xu, J. L., and Zhang, L. H. (2004). Insecticidal Bacillus *thuringiensis* silences *Erwinia carotovora* virulence by a new form of microbial antagonism, signal interference. *Appl. Environ. Microbiol.* 70, 954–960. doi: 10.1128/AEM.70.2.954-960.2004

Dos Santos, P. C., Fang, Z., Mason, S. W., Setubal, J. C., and Dixon, R. (2012). Distribution of nitrogen fixation and nitrogenase-like sequences amongst microbial genomes. *BMC Genomics* 13:162. doi: 10.1186/1471-2164-13-162

Dubois, M., Van den Broeck, L., and Inzé, D. (2018). The pivotal role of ethylene in plant growth. *Trends Plant Sci.* 23, 311–323. doi: 10.1016/j.tplants.2018.01.003

Dziewit, L., Pyzik, A., Matlakowska, R., Baj, J., Szuplewska, M., and Bartosik, D. (2013). Characterization of Halomonas sp. ZM3 isolated from the Zelazny most post-flotation waste reservoir, with a special focus on its mobile DNA. *BMC Microbiol.* 13:59. doi: 10.1186/1471-2180-13-59

Finkel, O. M., Salas-González, I., Castrillo, G., Conway, J. M., Law, T. F., Teixeira, P. J. P. L., et al. (2020). A single bacterial genus maintains root growth in a complex microbiome. *Nature* 587, 103–108. doi: 10.1038/s41586-020-2778-7

Flemming, H. C., Wingender, J., Szewzyk, U., Steinberg, P., Rice, S. A., and Kjelleberg, S. (2016). Biofilms: an emergent form of bacterial life. *Nat. Rev. Microbiol.* 14, 563–575. doi: 10.1038/nrmicro.2016.94

Foley, J. A., DeFries, R., Asner, G. P., Barford, C., Bonan, G., Carpenter, S. R., et al. (2005). Global consequences of land use. *Science (80-.)* 309, 570–574. doi: 10.1126/science.1111772

Francis, I. M., and Vereecke, D. (2019). "Plant-Associated Rhodococcus species, for better and for worse," in *Biology of Rhodococcus*, ed. H. Alvarez (Switzerland: Springer), 359–377. doi: 10.1007/978-3-030-11461-9_13

Gerlach, W., Sauthoff, W., and Pag, H. (1958). Untersuchungen über die fusariumwelke an Aechmea fasciata (Lindl.). *Bakt.Phytopathol.Z.* 32, 416–432. doi: 10.1111/j.1439-0434.1958.tb01784.x

Giguère, S., Berghaus, L. J., and Willingham-Lane, J. M. (2017). Antimicrobial resistance in *Rhodococcus equi*. *Acta Biochim. Pol.* 61, 633–638. doi: 10.18388/abp.2014_1824

Glick, B. R. (2012). Plant growth-promoting bacteria: mechanisms and applications. 2012. *Scientifica* 2012:963401. doi: 10.6064/2012/963401

Gorbunova, T. I., Egorova, D. O., Pervova, M. G., Kyrianova, T. D., Demakov, V. A., Saloutin, V. I., et al. (2020). Biodegradation of *trichlorobiphenyls* and their hydroxylated derivatives by *Rhodococcus*-strains. *J. Hazard. Mater.* 409:124471. doi: 10.1016/j.jhazmat.2020.124471

Gordon, S. A., and Weber, R. P. (1951). Colorimetric estimation of indoleacetic acid. *Plant Physiol.* 26, 192–195. doi: 10.1104/pp.26.1.192

Goris, J., Konstantinidis, K. T., Klappenbach, J. A., Coenye, T., Vandamme, P., and Tiedje, J. M. (2007). DNA-DNA hybridization values and their relationship to whole-genome sequence similarities. *Int. J. Syst. Evol. Microbiol.* 57, 81–91. doi: 10.1099/ijs.0.64483-0

Goswami, G., Deka, P., Das, P., Bora, S. S., Samanta, R., Boro, R. C., et al. (2017). Diversity and functional properties of acid-tolerant bacteria isolated from tea plantation soil of Assam. *3 Biotech* 7:229. doi: 10.1007/s13205-017-0864-9

Greening, C., Biswas, A., Carere, C. R., Jackson, C. J., Taylor, M. C., Stott, M. B., et al. (2016). Genomic and metagenomic surveys of hydrogenase distribution indicate H 2 is a widely utilised energy source for microbial growth and survival. *ISME J.* 10, 761–777. doi: 10.1038/ismej.2015.153

Gu, S., Wei, Z., Shao, Z., Friman, V. P., Cao, K., Yang, T., et al. (2020). Competition for iron drives phytopathogen control by natural *rhizosphere microbiomes*. *Nat. Microbiol.* 5, 1002–1010. doi: 10.1038/s41564-020-0719-8

Gupta, N., Skinner, K. A., Summers, Z. M., Edirisinghe, J. N., Faria, J. P., Marshall, C. W., et al. (2019). Draft genome sequence of *Rhodococcus* sp. strain ATCC 49988, a quinoline-degrading bacterium. *Microbiol. Resour. Announc.* 8, e403–e419.

Hall, J. P. J., Harrison, E., Pärnänen, K., Virta, M., and Brockhurst, M. A. (2020). The impact of mercury selection and conjugative genetic elements on community structure and resistance gene transfer. *Front. Microbiol.* 11:1846. doi: 10.3389/fmicb.2020.01846

Han, S., Li, D., Trost, E., Mayer, K. F., Corina, V., Heller, W., et al. (2016). Systemic responses of barley to the 3-hydroxy-decanoyl-homoserine lactone producing plant beneficial endophyte Acidovorax radicis N35. *Front. Plant Sci.* 7:1868. doi: 10.3389/fpls.2016.01868

Hartmann, A., and Hurek, T. (1988). Effect of carotenoid overproduction on oxygen tolerance of nitrogen fixation in *Azospirillum brasilense* Sp7. *Microbiology* 134, 2449–2455. doi: 10.1099/00221287-134-9-2449

Hasuty, A., Choliq, A., and Hidayat, I. (2018). Production of indole acetic acid (IAA) by *Serratia marcescens* subsp. marcescens and *Rhodococcus aff. qingshengii*. *Int. J. Agric. Technol.* 14, 299–312.

Higdon, S. M., Pozzo, T., Kong, N., Huang, B. C., Yang, M. L., Jeannotte, R., et al. (2020). Genomic characterization of a *diazotrophic microbiota* associated with maize aerial root mucilage. *PLoS One* 15:e239677. doi: 10.1371/journal.pone.0239677

Irawati, W., Soraya, Y. P., and Baskoro, A. H. (2012). A study on mercury-resistant bacteria isolated from a gold mine in Pongkor Village, Bogor, Indonesia. *HAYATI J. Biosci.* 19, 197–200. doi: 10.4308/hjb.19.4.197

Iwatsuki, M., Uchida, R., Takakusagi, Y., Matsumoto, A., Jiang, C. L., Takahashi, Y., et al. (2007). Lariatins, novel anti-mycobacterial peptides with a lasso structure, produced by Rhodococcus jostii K01-B0171. *J. Antibiot. (Tokyo)* 60, 357–363. doi: 10.1038/ja.2007.48

Jayakumar, A., Krishna, A., Nair, I. C., and Radhakrishnan, E. K. (2020). Drought-tolerant and plant growth-promoting endophytic Staphylococcus sp. having synergistic effect with silicate supplementation. *Arch. Microbiol.* 202, 1899–1906. doi: 10.1007/s00203-020-01911-1

Jensen, L. J., Julien, P., Kuhn, M., von Mering, C., Muller, J., Doerks, T., et al. (2008). eggNOG: automated construction and annotation of orthologous groups of genes. *Nucleic Acids Res.* 36, 250–254. doi: 10.1093/nar/gkm796

Joshi, D., Chandra, R., Suyal, D. C., Kumar, S., and Goel, R. (2019). Impacts of bioinoculants *Pseudomonas* jesenii MP1 and *Rhodococcus qingshengii* S10107 on chickpea (*Cicer arietinum* L.) yield and soil nitrogen status. *Pedosphere* 29, 388–399. doi: 10.1016/S1002-0160(19)60807-6

Kamble, A. L., Banoth, L., Meena, V. S., Singh, A., Chisti, Y., and Banerjee, U. C. (2013). Nitrile hydratase of Rhodococcus erythropolis: characterization of the enzyme and the use of whole cells for biotransformation of nitriles. *Biotech* 3, 319–330. doi: 10.1007/s13205-012-0104-2

Kang, S. M., Radhakrishnan, R., Khan, A. L., Kim, M. J., Park, J. M., Kim, B. R., et al. (2014). Gibberellin secreting rhizobacterium, *Pseudomonas* putida H-2-3 modulates the hormonal and stress physiology of soybean to improve the plant growth under saline and drought conditions. *Plant Physiol. Biochem.* 84, 115–124. doi: 10.1016/j.plaphy.2014.09.001

Kanno, M., Constant, P., Tamaki, H., and Kamagata, Y. (2016). Detection and isolation of plant-associated bacteria scavenging atmospheric molecular hydrogen. *Environ. Microbiol.* 18, 2495–2506. doi: 10.1111/1462-2920.13162

Kaufmann, M., and Michel, B. (1973). The osmotic potential of polyethylene glycol 6000. *Plant Physiol.* 51, 914–916. doi: 10.1104/pp.51.5.914

Kaushal, M., and Wani, S. P. (2016). Rhizobacterial-plant interactions: strategies ensuring plant growth promotion under drought and salinity stress. *Agric. Ecosyst. Environ.* 231, 68–78. doi: 10.1016/j.agee.2016.06.031

Khilyas, I. V., Sorokina, A. V., Markelova, M. I., Belenikin, M., Shafigullina, L., Tukhbatova, R. I., et al. (2020). Genomic and phenotypic analysis of siderophore-producing *Rhodococcus qingshengii* strain S10 isolated from an arid weathered serpentine rock environment. *Arch. Microbiol.* 203, 855–860. doi: 10.1007/s00203-020-02057-w

King, G. M., and Weber, C. F. (2007). Distribution, diversity and ecology of aerobic CO-oxidizing bacteria. *Nat. Rev. Microbiol.* 5, 107–118. doi: 10.1038/nrmicro1595

Kirchhof, G., Eckert, B., Stoffels, M., Ivo Baldani, J., Reis, V. M., and Hartmann, A. (2001). *Herbaspirillum* frisingense sp. nov., a new nitrogan-fixing bacterial species that occurs in C4-fibre plants. *Int. J. Syst. Evol. Microbiol.* 51, 157–168. doi: 10.1099/00207713-51-1-157

Kloepper, J. W., and Beauchamp, C. J. (1992). A review of issues related to measuring colonization of plant roots by bacteria. *Can. J. Microbiol.* 38, 1219–1232. doi: 10.1139/m92-202

Konstantinidis, K. T., and Tiedje, J. M. (2005). Towards a genome-based taxonomy for prokaryotes. *J. Bacteriol.* 187, 6258–6264. doi: 10.1128/JB.187.18.6258-6264.2005

Kuhl, T., Felder, M., Nussbaumer, T., Fischer, D., Kublik, S., Paul Chowdhury, S., et al. (2019). De novo genome assembly of a plant-associated *Rhodococcus qingshengii* Strain (RL1) isolated from *Eruca sativa* Mill. and showing plant growth-promoting properties. *Microbiol. Resour. Announc.* 8, 14–16. doi: 10.1128/MRA.01106-19

Kumar, G. P., Mir Hassan Ahmed, S. K., Desai, S., Leo Daniel Amalraj, E., and Rasul, A. (2014). In vitro screening for abiotic stress tolerance in potent biocontrol and plant growth promoting strains of *Pseudomonas* and Bacillus spp. *Int. J. Bacteriol.* 2014:195946. doi: 10.1155/2014/195946

Kumar, S., Stecher, G., Li, M., Knyaz, C., and Tamura, K. (2018). MEGA X: Molecular evolutionary genetics analysis across computing platforms. *Mol. Biol. and Evol.* 35, 1547–1549. doi: 10.1093/molbev/msy096

Kwasiborski, A., Mondy, S., Chong, T. M., Barbey, C., Chan, K. G., Beury-Cirou, A., et al. (2015). Transcriptome of the quorum-sensing signal-degrading *Rhodococcus erythropolis* responds differentially to virulent and *avirulent Pectobacterium atrosepticum*. *Heredity (Edinb)* 114, 476–484. doi: 10.1038/hdy.2014.121

Latour, X., Barbey, C., Chane, A., Groboillot, A., and Burini, J.-F. (2013). *Rhodococcus erythropolis* and its γ-Lactone catabolic pathway: an unusual biocontrol system that disrupts pathogen quorum sensing communication. *Agronomy* 3, 816–838. doi: 10.3390/agronomy3040816

Lau, C. K. Y., Krewulak, K. D., and Vogel, H. J. (2016). Bacterial ferrous iron transport: the Feo system. *FEMS Microbiol. Rev.* 40, 273–298. doi: 10.1093/femsre/fuv049

LeBlanc, J. C., Gonçalves, E. R., and Mohn, W. W. (2008). Global response to desiccation stress in the soil *actinomycete Rhodococcus jostii* RHA1. *Appl. Environ. Microbiol.* 74, 2627–2636. doi: 10.1128/AEM.02711-07

Leigh, M. B., Prouzová, P., Macková, M., Macek, T., Nagle, D. P., and Fletcher, J. S. (2006). Polychlorinated biphenyl (PCB)-degrading bacteria associated with trees in a PCB-contaminated site. *Appl. Environ. Microbiol.* 72, 2331–2342. doi: 10.1128/AEM.72.4.2331-2342.2006

Levy, A., Salas Gonzalez, I., Mittelviefhaus, M., Clingenpeel, S., Herrera Paredes, S., Miao, J., et al. (2018). Genomic features of bacterial adaptation to plants. *Nat. Genet.* 50, 138–150. doi: 10.1038/s41588-017-0012-9

Li, D., Rothballer, M., Schmid, M., Esperschütz, J., and Hartmann, A. (2011). Acidovorax radicis sp. nov., a wheat-root-colonizing bacterium. *Int. J. Syst. Evol. Microbiol.* 61, 2589–2594. doi: 10.1099/ijs.0.025296-0

Lincoln, S. A., Hamilton, T. L., Valladares Juárez, A. G., Schedler, M., Macalady, J. L., Müller, R., et al. (2015). Draft genome sequence of the *piezotolerant* and crude oil-degrading bacterium *Rhodococcus qingshengii* strain TUHH-12. *Genome Announc.* 3:e268–15. doi: 10.1128/genomeA.00268-15

Liu, W., Wang, Q., Hou, J., Tu, C., Luo, Y., and Christie, P. (2016). Whole genome analysis of halotolerant and *alkalotolerant* plant growth-promoting *rhizobacterium Klebsiella* sp. *D5A. Sci. Rep.* 6, 20–22. doi: 10.1038/srep26710

Loper, J. E., and Schroth, M. N. (1986). Influence of bacterial sources of indole-3-acetic acid on root elongation of sugar beet. *Phytopathology* 76:386. doi: 10.1094/phyto-76-386

Lynne, A. M., Haarmann, D., and Louden, B. C. (2011). Use of blue agar CAS assay for siderophore detection. *J. Microbiol. Biol. Educ.* 12, 51–53. doi: 10.1128/jmbe.v12i1.249

Ma, Y., Oliveira, R. S., Freitas, H., and Zhang, C. (2016a). Biochemical and molecular mechanisms of plant-microbe-metal interactions: relevance for phytoremediation. *Front. Plant Sci.* 7:918. doi: 10.3389/fpls.2016.00918

Ma, Y., Rajkumar, M., Zhang, C., and Freitas, H. (2016b). Beneficial role of bacterial endophytes in heavy metal phytoremediation. *J. Environ. Manage.* 174, 14–25. doi: 10.1016/j.jenvman.2016.02.047

Martínez-García, P. M., López-Solanilla, E., Ramos, C., and Rodríguez-Palenzuela, P. (2016). Prediction of bacterial associations with plants using a supervised machine-learning approach. *Environ. Microbiol.* 18, 4847–4861. doi: 10.1111/1462-2920.13389

Mendes, R., Garbeva, P., and Raaijmakers, J. M. (2013). The *rhizosphere microbiome*: significance of plant beneficial, plant pathogenic, and human pathogenic microorganisms. *FEMS Microbiol. Rev.* 37, 634–663. doi: 10.1111/1574-6976.12028

Mokhtari, R. B., Baluch, N., Homayouni, T. S., Morgatskaya, E., Kumar, S., Kazemi, P., et al. (2018). The role of *Sulforaphane* in cancer chemoprevention and health benefits: a mini-review. *Cell Commun. Signal.* 12, 91–101. doi: 10.1007/s12079-017-0401-y

Moriya, Y., Itoh, M., Okuda, S., Yoshizawa, A. C., and Kanehisa, M. (2007). KAAS: an automatic genome annotation and pathway reconstruction server. *Nucleic Acids Res.* 35, 182–185. doi: 10.1093/nar/gkm321

Mullaney, J. A., Ansell, J., Kelly, W. J., and Heyes, J. A. (2013a). Biotransformation of glucosinolates from a bacterial perspective. *CAB Rev.* 8, 1–15. doi: 10.1079/PAVSNNR20138034

Mullaney, J. A., Kelly, W. J., McGhie, T. K., Ansell, J., and Heyes, J. A. (2013b). Lactic acid bacteria convert glucosinolates to nitriles efficiently yet differently from *enterobacteriaceae*. *J. Agric. Food Chem.* 61, 3039–3046. doi: 10.1021/jf305442j

Müller, C., Birmes, F. S., Niewerth, H., and Fetzner, S. (2014). Conversion of the *Pseudomonas aeruginosa* quinolone signal and related alkylhydroxyquinolines by Rhodococcus sp. strain BG43. *Appl. Environ. Microbiol.* 80, 7266–7274. doi: 10.1128/AEM.02342-14

Murugappan, R. M., Benazir, S., Usha, C., and Lok, S. (2017). Growth promoting and probiotic potential of the endophytic bacterium *Rhodococcus globerulus* colonizing the medicinal plant *Plectranthus amboinicus* (Lour.) Spreng. *Int. J. Curr. Res. Rev.* 9, 7–13. doi: 10.7324/ijcrr.2017.9143

Nagel, R., Bieber, J. E., Schmidt-Dannert, M. G., Nett, R. S., and Peters, R. J. (2018). A third class: Functional gibberellin biosynthetic operon in beta-*proteobacteria*. *Front. Microbiol.* 9:2916. doi: 10.3389/fmicb.2018.02916

Nagel, R., and Peters, R. J. (2017). Investigating the phylogenetic range of gibberellin biosynthesis in bacteria. *MPMI* 30, 343–349. doi: 10.1094/MPMI-01-17-0001-R

Nautiyal, C. S. (1999). An efficient microbiological growth medium for screening phosphate solubilizing microorganisms. *FEMS Microbiol. Lett.* 170, 265–270. doi: 10.1111/j.1574-6968.1999.tb13383.x

Netzker, T., Shepherdson, E. M. F., Zambri, M. P., and Elliot, M. A. (2020). Bacterial volatile compounds: functions in communication, cooperation, and competition. *Annu. Rev. Microbiol.* 74, 409–430. doi: 10.1146/annurev-micro-011320-015542

Osorio, H., Martínez, V., Nieto, P. A., Holmes, D. S., and Quatrini, R. (2008). Microbial iron management mechanisms in extremely acidic environments: comparative genomics evidence for diversity and versatility. *BMC Microbiol.* 8:203. doi: 10.1186/1471-2180-8-203

O'Toole, G. A. (2011). Microtiter dish biofilm formation assay. *J. Vis. Exp.* 47:2437.

Overbeek, R., Olson, R., Pusch, G. D., Olsen, G. J., Davis, J. J., Disz, T., et al. (2014). The SEED and the rapid annotation of microbial genomes using subsystems technology (RAST). *Nucleic Acids Res.* 42, 206–214. doi: 10.1093/nar/gkt1226

Pandit, A., Adholeya, A., Cahill, D., Brau, L., and Kochar, M. (2020). Microbial biofilms in nature: unlocking their potential for agricultural applications. *J. Appl. Microbiol.* 129, 199–211. doi: 10.1111/jam.14609

Panke-Buisse, K., Lee, S., and Kao-Kniffin, J. (2017). Cultivated sub-populations of soil microbiomes retain early flowering plant trait. *Microb. Ecol.* 73, 394–403. doi: 10.1007/s00248-016-0846-1

Pátek, M., Grulich, M., and Nešvera, J. (2021). Stress response in *Rhodococcus* strains. *Biotechnol Adv.* 28:107698. doi: 10.1016/j.biotechadv.2021.107698

Paul, K., Nieto, V., Carlquist, W. C., Blair, D. F., and Harshey, R. M. (2010). The c-di-GMP binding protein ycgR controls flagellar motor direction and speed to affect chemotaxis by a "backstop brake" mechanism. *Mol. Cell* 38, 128–139. doi: 10.1016/j.molcel.2010.03.001

Pérez, J. M., Calderón, I. L., Arenas, F. A., Fuentes, D. E., Pradenas, G. A., Fuentes, E. L., et al. (2007). Bacterial toxicity of potassium tellurite: unveiling an ancient enigma. *PLoS One* 2:e211. doi: 10.1371/journal.pone.0000211

Pérez-Miranda, S., Cabirol, N., George-Téllez, R., Zamudio-Rivera, L. S., and Fernández, F. J. (2007). O-CAS, a fast and universal method for siderophore detection. *J. Microbiol. Methods* 70, 127–131. doi: 10.1016/j.mimet.2007.03.023

Pham, T. T. M., Rodriguez, N. J. P., Hijri, M., and Sylvestre, M. (2015). Optimizing polychlorinated biphenyl degradation by flavonoid-induced cells of the *rhizobacterium Rhodococcus erythropolis* U23A. *PLoS One* 10:e126033. doi: 10.1371/journal.pone.0126033

Pieterse, C. M. J., Berendsen, R. L., de Jonge, R., Stringlis, I. A., Van Dijken, A. J. H., Van Pelt, J. A., et al. (2020). *Pseudomonas simiae* WCS417: star track of a model beneficial *rhizobacterium*. *Plant Soil.* 461, 245–263. doi: 10.1007/s11104-020-04786-9

Pieterse, C. M. J., Zamioudis, C., Berendsen, R. L., Weller, D. M., Van Wees, S. C. M., and Bakker, P. A. H. M. (2014). Induced systemic resistance by beneficial microbes. *Annu. Rev. Phytopathol.* 52, 347–375. doi: 10.1146/annurev-phyto-082712-102340

Płociniczak, T., Fic, E., Pacwa-Płociniczak, M., Pawlik, M., and Piotrowska-Seget, Z. (2017). Improvement of phytoremediation of an aged petroleum hydrocarbon-contaminated soil by *Rhodococcus erythropolis* CD 106 strain. *Int. J. Phytoremediation* 19, 614–620. doi: 10.1080/15226514.2016.1278420

Pollak, S., and Cordero, O. X. (2020). Rhizobiome shields plants from infection. *Nat. Microbiol.* 5, 978–979. doi: 10.1038/s41564-020-0766-1

Quiza, L., Lalonde, I., Guertin, C., and Constant, P. (2014). Land-use influences the distribution and activity of high affinity CO-oxidizing bacteria associated to type I-coxL genotype in soil. *Front. Microbiol.* 5:271. doi: 10.3389/fmicb.2014.00271

Raaijmakers, J. M., Paulitz, T. C., Steinberg, C., Alabouvette, C., and Moënne-Loccoz, Y. (2009). The rhizosphere: a playground and battlefield for soilborne pathogens and beneficial microorganisms. *Plant Soil* 321, 341–361. doi: 10.1007/s11104-008-9568-6

Rodríguez, H., Fraga, R., Gonzalez, T., and Bashan, Y. (2006). Genetics of phosphate solubilization and its potential applications for improving plant growth-promoting bacteria. *Plant Soil* 287, 15–21. doi: 10.1007/s11104-006-9056-9

Rodríguez, M., Torres, M., Blanco, L., Béjar, V., Sampedro, I., and Llamas, I. (2020). Plant growth-promoting activity and quorum quenching-mediated biocontrol of bacterial phytopathogens by *Pseudomonas segetis* strain P6. *Sci. Rep.* 10:4121. doi: 10.1038/s41598-020-61084-1

Rodriguez, P. A., Rothballer, M., Chowdhury, S. P., Nussbaumer, T., Gutjahr, C., and Falter-Braun, P. (2019). Systems biology of plant-microbiome interactions. *Mol. Plant* 12, 804–821. doi: 10.1016/j.molp.2019.05.006

Roller, C., Wagner, M., Amann, R., Ludwig, W., and Schleifer, K. H. (1994). In situ probing of gram-positive bacteria with high DNA G + C content using 23S rRNA-targeted oligonucleotides. *Microbiol-SGM* 140 (Pt 10), 2849–2858. doi: 10.1099/00221287-140-10-2849

Rückert, C., Birmes, F. S., Müller, C., Niewerth, H., Winkler, A., Fetzner, S., et al. (2015). Complete genome sequence of Rhodococcus erythropolis BG43 (DSM 46869), a degrader of *Pseudomonas aeruginosa* quorum sensing signal molecules. *J. Biotechnol.* 211, 99–100. doi: 10.1016/j.jbiotec.2015.07.014

Salas-González, I., Reyt, G., Flis, P., Custódio, V., Gopaulchan, D., Bakhoum, N., et al. (2021). Coordination between microbiota and root endodermis supports plant mineral nutrient homeostasis. *Science* 371:eabd0695. doi: 10.1126/science.abd0695

Salazar-Cerezo, S., Martínez-Montiel, N., García-Sánchez, J., Pérez-y-Terrón, R., and Martínez-Contreras, R. D. (2018). Gibberellin biosynthesis and metabolism: a convergent route for plants, fungi and bacteria. *Microbiol. Res.* 208, 85–98. doi: 10.1016/j.micres.2018.01.010

Sangal, V., Goodfellow, M., Jones, A. L., Schwalbe, E. C., Blom, J., Hoskisson, P. A., et al. (2016). Next-generation systematics: an innovative approach to resolve the structure of complex prokaryotic taxa. *Sci. Rep.* 6:38392. doi: 10.1038/srep38392

Santos, A., Núñez-Montero, K., Lamilla, C., Pavez, M., Quezada-Solís, D., and Barrientos, L. (2020). Antifungal activity screening of antarctic actinobacteria against *phytopathogenic* fungi. *Acta Biol. Colomb.* 25, 353–358. doi: 10.15446/abc.v25n2.76405

Santos, C. L., Correia-Neves, M., Moradas-Ferreira, P., and Mendes, M. V. (2012). A Walk into the LuxR Regulators of *Actinobacteria*: phylogenomic distribution and functional diversity. *PLoS One* 7:e46758. doi: 10.1371/journal.pone.0046758

Schaefer, J. K., Yagi, J., Reinfelder, J. R., Cardona, T., Ellickson, K. M., Tel-Or, S., et al. (2004). Role of the bacterial organomercury lyase (MerB) in controlling methylmercury accumulation in mercury-contaminated natural waters. *Environ. Sci. Technol.* 38, 4304–4311. doi: 10.1021/es049895w

Schmerk, C. L., Bernards, M. A., and Valvano, M. A. (2011). Hopanoid production is required for low-pH tolerance, antimicrobial resistance, and motility in *Burkholderia cenocepacia*. *J. Bacteriol.* 193, 6712–6723. doi: 10.1128/JB.05979-11

Schneider, L. (2021). When toxic chmicals refuse to die – An examination of the prolonged mercury pesticide use in Australia. *Elem. Sci. Anth.* 9:053. doi: 10.1525/elementa.2021.053

Sessitsch, A., Kuffner, M., Kidd, P., Vangronsveld, J., Wenzel, W. W., Fallmann, K., et al. (2013). The role of plant-associated bacteria in the mobilization and phytoextraction of trace elements in contaminated soils. *Soil Biol. Biochem.* 60, 182–194. doi: 10.1016/j.soilbio.2013.01.012

Smith, P., House, J. I., Bustamante, M., Sobocká, J., Harper, R., Pan, G., et al. (2016). Global change pressures on soils from land use and management. *Glob. Chang. Biol.* 22, 1008–1028. doi: 10.1111/gcb.13068

Spaepen, S., and Vanderleyden, J. (2011). Auxin and plant-microbe interactions. *Cold Spring Harb. Perspect. Biol.* 3:a001438. doi: 10.1101/cshperspect.a001438

Spaepen, S., Vanderleyden, J., and Remans, R. (2007). Indole-3-acetic acid in microbial and microorganism-plant signaling. *FEMS Microbiol. Rev.* 31, 425–448. doi: 10.1111/j.1574-6976.2007.00072.x

Stickler, D. J., Morris, N. S., Mclean, R. J. C., and Fuqua, C. (1998). Biofilms on indwelling urethral catheters produce quorum sensing signal molecules in situ and in vitro. *Appl. Environ. Microbiol.* 64, 3486–3490. doi: 10.1128/aem.64.9.3486-3490.1998

Subramoni, S., and Venturi, V. (2009). LuxR-family "solos": bachelor sensors/regulators of signalling molecules. *Microbiology* 155, 1377–1385. doi: 10.1099/mic.0.026849-0

Suyal, D. C., Yadav, A., Shouche, Y., and Goel, R. (2014). Differential proteomics in response to low temperature diazotrophy of Himalayan psychrophilic nitrogen fixing *Pseudomonas* migulae S10724 strain. *Curr. Microbiol.* 68, 543–550. doi: 10.1007/s00284-013-0508-1

Táncsics, A., Benedek, T., Farkas, M., Máthé, I., Márialigeti, K., Szoboszlay, S., et al. (2014). Sequence analysis of 16S rRNA, gyrB and catA genes and DNA-DNA hybridization reveal that *Rhodococcus jialingiae* is a later synonym of *Rhodococcus qingshengii*. *Int. J. Syst. Evol. Microbiol.* 64, 298–301. doi: 10.1099/ijs.0.059097-0

Tarrand, J. J., Krieg, N. R., and Döbereiner, J. (1978). A taxonomic study of the *Spirillum lipoferum* group, with descriptions of a new genus, *Azospirillum* gen. nov. and two species, *Azospirillum lipoferum* (Beijerinck) comb. nov. and *Azospirillum brasilense* sp. nov. *Can J Microbiol.* 24, 967–980. doi: 10.1139/m78-160

Tatusov, R. L., Galperin, M. Y., Natale, D. A., and Koonin, E. V. (2000). The COG database: A tool for genome-scale analysis of protein functions and evolution. *Nucleic Acids Res.* 28, 33–36. doi: 10.1093/nar/28.1.33

Textor, S., and Gershenzon, J. (2009). Herbivore induction of the glucosinolate-myrosinase defense system: major trends, biochemical bases and ecological significance. *Phytochem. Rev.* 8, 149–170. doi: 10.1007/s11101-008-9117-1

Thompson, D., Cognat, V., Goodfellow, M., Koechler, S., Heintz, D., Carapito, C., et al. (2020). Phylogenomic classification and biosynthetic potential of the fossil fuel-*biodesulfurizing Rhodococcus* strain IGTS8. *Front. Microbiol.* 11:1417. doi: 10.3389/fmicb.2020.01417

Trivedi, P., Pandey, A., and Sa, T. (2007). Chromate reducing and plant growth promoting activies of psychrotrophic *Rhodococcus erythropolis* MtCC 7905. *J. Basic Microbiol.* 47, 513–517. doi: 10.1002/jobm.200700224

Tsiafouli, M. A., Thébault, E., Sgardelis, S. P., de Ruiter, P. C., van der Putten, W. H., Birkhofer, K., et al. (2015). Intensive agriculture reduces soil biodiversity across Europe. *Glob. Chang. Biol.* 21, 973–985. doi: 10.1111/gcb.12752

Uroz, S., D'Angelo-Picard, C., Carlier, A., Elasri, M., Sicot, C., Petit, A., et al. (2003). Novel bacteria degrading N-acylhomoserine lactones and their use as quenchers of quorum-sensing-regulated functions of plant-pathogenic bacteria. *Microbiology* 149, 1981–1989. doi: 10.1099/mic.0.26375-0

Vereecke, D., Zhang, Y., Francis, I. M., Lambert, P. Q., Venneman, J., Stamler, R. A., et al. (2020). Functional genomics insights into the pathogenicity, habitat fitness, and mechanisms modifying plant development of Rhodococcus sp. PBTS1 and PBTS2. *Front. Microbiol.* 11:14. doi: 10.3389/fmicb.2020.00014

Wagacha, J. M., and Muthomi, J. W. (2007). *Fusarium culmorum*: infection process, mechanisms of mycotoxin production and their role in pathogenesis in wheat. *Crop Prot.* 26, 877–885. doi: 10.1016/j.cropro.2006.09.003

Wagg, C., Schlaeppi, K., Banerjee, S., Kuramae, E. E., and van der Heijden, M. G. A. (2019). Fungal-bacterial diversity and microbiome complexity predict ecosystem functioning. *Nat. Commun.* 10:4841. doi: 10.1038/s41467-019-12798-y

Wang, Z., Xu, J., Li, Y., Wang, K., Wang, Y., Hong, Q., et al. (2010). *Rhodococcus jialingiae* sp. nov., an actinobacterium isolated from sludge of a carbendazim wastewater treatment facility. *Int. J. Syst. Evol. Microbiol.* 60, 378–381. doi: 10.1099/ijs.0.013219-0

Weyens, N., Beckers, B., Schellingen, K., Ceulemans, R., Croes, S., Janssen, J., et al. (2013). Plant-associated bacteria and their role in the success or failure of metal phytoextraction projects: first observations of a field-related experiment. *Microb. Biotechnol.* 6, 288–299. doi: 10.1111/1751-7915.12038

Windisch, S., Sommermann, L., Babin, D., Chowdhury, S. P., Grosch, R., Moradtalab, N., et al. (2021). Impact of long-term organic and mineral fertilization on rhizosphere metabolites, root–microbial interactions and plant health of lettuce. *Front. Microbiol.* 11:597745. doi: 10.3389/fmicb.2020.597745

Xie, S. S., Wu, H. J., Zang, H. Y., Wu, L. M., Zhu, Q. Q., and Gao, X. W. (2014). Plant growth promotion by spermidine-producing Bacillus subtilis OKB105. *MPMI* 27, 655–663. doi: 10.1094/MPMI-01-14-0010-R

Xu, J. L., He, J., Wang, Z. C., Wang, K., Li, W. J., Tang, S. K., et al. (2007). Rhodococcus qingshengii sp. nov., a carbendazim-degrading bacterium. *Int. J. Syst. Evol. Microbiol.* 57, 2754–2757. doi: 10.1099/ijs.0.65095-0

Yang, G., and Li, C. (2012). "General description of Rhizoctonia species complex," in *Plant Pathology*, ed. C. J. Cumagun (China: InTech), 41–52. doi: 10.5772/39026

Conflict of Interest: The authors declare that the research was conducted in the absence of any commercial or financial relationships that could be construed as a potential conflict of interest.

Publisher's Note: All claims expressed in this article are solely those of the authors and do not necessarily represent those of their affiliated organizations, or those of the publisher, the editors and the reviewers. Any product that may be evaluated in this article, or claim that may be made by its manufacturer, is not guaranteed or endorsed by the publisher.

Copyright © 2021 Kuhl, Chowdhury, Uhl and Rothballer. This is an open-access article distributed under the terms of the Creative Commons Attribution License (CC BY). The use, distribution or reproduction in other forums is permitted, provided the original author(s) and the copyright owner(s) are credited and that the original publication in this journal is cited, in accordance with accepted academic practice. No use, distribution or reproduction is permitted which does not comply with these terms.

C. Acknowledgements

This work would not have been possible without the support of the following wonderful people.

Thank you very much…

… to my supervisor *Michael Rothballer* for his constant availability for feedback, his patient explanations and his trust in my skills, which gave me the confidence to deal also with difficult phases of the project. Without his guidance and expertise this project would not have been realized.

...to my doctor father *Pascal Falter-Braun* for the opportunity to conduct this thesis in his laboratory. I am thankful for challenging discussions and his helpful advices throughout the whole project, which made me grow professionally and personally.

…to the former INET-Members *Soumitra Paul Chowdhury* and *Patricia Rodriguez Coloma* for sharing their knowledge and enthusiasm about plants and microbes with me. I really enjoyed our personal and professional chats.

…to *the whole INET-Team.* I am grateful for having such amazing colleagues by my side.

…to my second examiner *Kirsten Jung and the members of the examination committee* for assessing my thesis and to *Peter Schröder* for providing helpful feedback as member of my TAC.

…to my master's students *Furkan Tunc* and *Isabella Gantner* for their contribution to this work and for improving my supervisory skills.

…to *Andrea Ghirardo, Rita Grosch, Silvia Gschwendtner, Doreen Fischer, Marius Felder, Susanne Kublik, Thomas Nussbaumer, Jenny Uhl* and *Fabian Weikl* for supporting me with their skills, knowledge or equipment during the thesis.

…to *my family and my friends* for their support and for making the time spent together so precious.

…to *Lucy*, my fluffy, hairy friend, for just being the dog you are.

…to my husband *Nico Nagel* for his unconditional love and his support during the thesis. You calmed me down during rough times and gave me the confidence to successfully finish this thesis.

Many thanks to all of you!